FINITE ELEMENT DYNAMIC ANALYSIS
OF
AXISYMMETRIC STRUCTURES

A THESIS

submitted in fulfilment of the
requirements for the award of the degree
of
DOCTOR OF PHILOSOPHY
in
EARTHQUAKE ENGINEERING

By

SURAJ PARKASH

DEPARTMENT OF EARTHQUAKE ENGINEERING
UNIVERSITY OF ROORKEE
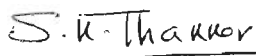ROORKEE – 247 667 (INDIA)

JUNE, 1997

CANDIDATE'S DECLARATION

I hereby certify that the work which is being presented in the thesis entitled **'Finite Element Dynamic Analysis of Axisymmetric Structures'** in fulfilment of the requirement for the award of the Degree of **Doctor of Philosophy** and submitted in the **Department of Earthquake Engineering** of the University is an authentic record of my own work carried out during a period from 01-08-91 to 10-06-97 under the supervision of **Dr.S.K.Thakkar** and **Dr.N.C.Singhal.**

The matter presented in this thesis has not been submitted by me for the award of any other degree of this or any other University.

Suraj Prakash
Signature of the Candidate

This is to certify that the above statement made by the Candidate is correct to the best of our knowledge.

S.K.Thakkar
11.6.97
Dr.S.K.Thakkar
Professor

NC Singhal
Dr.N.C.Singhal
Associate Professor

Department of Earthquake Engineering, University of Roorkee, Roorkee 247 667 (India)

The Ph.D. Viva-Voce examination of SURAJ PARKASH, Research Scholar, has been held on...19/1/98.........

S.K.Thakkar   NC Singhal   *19/1/98*
Signature of Supervisors   Signature of H.O.D.   Signature of External Examiner

i

ABSTRACT

In recent years analysis of axisymmetric structures, such as hyperbolic cooling towers, chimneys, reactor containment shells, etc., subjected to dynamic or seismic loading has attracted considerable attention, specially in the area of nuclear power plants. The structural safety of such structures during expected earthquake motion is of great importance in view of possibility of radiation hazards. Therefore, such structures are required to be analyzed and designed in most rational manner. Further due to rapid expansion in number and size of power plants in India and elsewhere in the world , there is great need for careful and detailed investigation of their behaviour under severe ground motions. In many countries, little consideration has been given to seismic forces in the design of structures because of infrequent occurrence of earthquakes in the past history. However, the potential damage exposure from an accident from a large power plant makes it imperative that ground motion effects be considered in the design of such structures, even in the areas that now appear to have low seismic activity. These important structures should not show any kind of distress under most severe motion expected in the life of the structure.

The design philosophy of these structures differ from that of conventional buildings. The conventional structures are designed to be ductile permitting inelastic deformations and some damages are accepted while in these important structures the system should behave elastically during the seismic event.

An axisymmetric structure resting on rock/soil subjected to an earthquake motions will develop additional stresses on the structure due to inertia effects. In general when a structure such as massive structure is embedded, it will interact with the surrounding and base soil.

The dynamic analysis of such structures involve consideration of several aspects such as characteristics of ground motion and its frequency content, soil structure interaction effect, energy dissipating characteristics of structure and foundation. The dynamic analysis of axisymmetric structures has been studied by many investigators in the past but many aspects like modelling of boundaries, modelling of reactor internals along with complete reactor building has not received sufficient attention with particular reference to reactor type containment

structures.

In this thesis, study has been made of the problems which are encountered in the seismic analysis of massive embedded axisymmetric structures subjected to strong ground motions.

The seismic response of two axisymmetric structures, that is, (i) Containment shell and (ii) Intake tower has been studied using beam and finite element methods of analysis considering the soil-structure interaction effects. The beam model does not represent real behaviour of soil-structure system because of one-dimensional idealization. To capture the real behaviour of soil-structure system subjected to horizontal ground motions, three-dimensional modelling of the system is required. The axisymmetric finite element method takes into account 3-dimensional nature of the system and is employed to carry out a detailed investigation of some of the aspects of dynamic analysis of axisymmetric structures.

The soil is assumed to be linearly elastic and its damping is higher as compared to that of structure. A single value of damping has been assigned to each mode which reflects both the low damping of the structure and the high damping of the soil. This has been done by calculating a weighted damping based on strain energy in various sub systems including soil.

The dimensions of the structure are finite while the soil mass around the structure is of infinite extent in horizontal and vertical directions. So the approximate dimensions of the soil are to be determined for dynamic analysis of soil-structure system. To do so, a parametric study of depth and width of soil has been done for the containment structure subjected to horizontal ground motion. The effect of considering soil mass on the seismic response of structure has also been studied.

Two massive embedded axisymmetric structures, containment shell alone and the complete reactor building with internals are analyzed by finite element model to study the effect of soil-structure interaction on overall seismic response of the structure.

These two structures with fixed base, and flexible base of different shear wave velocities of soil are subjected to horizontal ground motion and responses are computed. The responses of these structures fixed at base are compared to that of structures founded on soil having different elasticity properties.

Also the effect of depth of embedment of these two structure on seismic behaviour of soil-structure system has been investigated.

In order to study the effect of the characteristics of ground motion on these two structures, three real earthquake motions are normalized to common peak accelerations and elastic time history analysis has been carried out for containment and reactor building.

The structural behaviour of reactor building during earthquake is explained with the aid of mode shapes of the structure.

The six component of stresses are obtained from seismic analysis of a reactor building and are plotted along the height of outer shell. This showed that the stress pattern is significantly changed at the junction points such as junction of shell and raft.

The finite element seismic analysis of some axisymmetric structures has been carried out using timewise mode superposition and direct step-by-step time integration methods. The choice of one method over the other has been determined by studying seismic response of these structures.

The fixed soil boundaries in finite element mesh of soil-structure system under seismic event reflect the incoming waves and affect the response of the structure. In order to absorb the incoming waves and minimize their reflection at the boundary, the viscous boundaries in the form of dampers are employed . A study has been carried out to evaluate the effectiveness of these viscous boundaries in absorption of most of the incoming waves in relation to fixed boundaries. Also, study is made to determine the position of placing viscous boundaries in horizontal and vertical directions of soil medium.

Even with the sophisticated finite element analysis of reactor building, the reactor

internal being non-axisymmetric poses problems in its axisymmetric idealization. The various methods of modelling of reactor internals as equivalent axisymmetric body are employed. The two hypothetical reactor buildings of different size and type are selected and their internals are modelled by using various modelling methods. The seismic response of these two reactor buildings with their equivalent internal structure has been computed and examined. The study is made to determine the suitable method of modelling of internals for obtaining more realistic seismic response of a reactor building.

ACKNOWLEDGEMENTS

Suraj Prakash

(SURAJ PARKASH)

CONTENTS

LIST OF FIGURES

LIST OF TABLES

NOTATIONS AND SYMBOLS

A	Width of soil domain
a	Area of soil domain
B	Depth of soil domain
$\underline{B}$	Strain shape function matrix
$\underline{C}$	Damping matrix
$\underline{C}$	Normalized damping matrix
C_r, C_z, C_θ	Mode participation factors in radial, vertical and tangential directions, respectively
C_p, C_s	Damping coefficient for P and S waves
D	Depth of embedment
$\underline{D}$	Elasticity matrix
dV	Volume differential
E	Young's modulus of elasticity
EI	Flexural rigidity
f	Frequency of structure (Hertz)
G	Shear modulus
g	Acceleration due to gravity
H	Height of structure
I	Moment of inertia
$[\underline{J}]$	Jacobian matrix
$|\underline{J}|$	Jacobian determinant
$\underline{K}$	Stiffness matrix
$\underline{K}^{\bullet}$	Normalized stiffness matrix
$\underline{K}^{(\cdot)}$	Effective stiffness matrix
$K_{xb}, K_{\theta b}$	Stiffness constant of base springs
$K_{xs}, K_{\theta s}$	Stiffness constant of side springs
$\underline{L}$	Partial derivative matrix (strain operator)
l_1, l_2	Half of the distances between the node of lumped damping value and the adjacent nodes having dampers.
$\underline{M}$	Mass matrix
$\underline{M}^{\bullet}$	Normalized mass matrix
$\underline{N}$	Displacement shape function matrix
$\underline{P} = P_r, P_z, P_\theta$	Force vector (forces in radial, vertical and tangential directions, respectively

R	Radius of raft
$\underline{R}$	External load vector
$\underline{R}^{\Theta}$	Effective load vector
r	Radius of soil domain
S_a	Spectral acceleration
T	Time period of structure (sec)
t	Thickness, time
u	Horizontal/radial displacement
v	Vertical displacement
V	Volume
V_p	P-wave velocity
V_s	Shear wave velocity
W	Weight
w	Tangential displacement
$\underline{Z}$	Vector of nodal generalized displacements

Subscripts

g	Ground motion
gh	Horizontal ground motion
gv	Vertical ground motion
m,n	Order of Harmonics
r	Radial direction
z	Vertical/ axial/normal direction
θ	Tangential/circumferential direction
(r,z,θ)	Cylindrical coordinates

Superscripts

a	Antisymmetric component of displacement or load
e	Finite element
s	Symmetric component of displacement or load

Suffix

$i=1,N_d$	N_i = Interpolation or shape function at ith node

N_d = Total number of nodes in a finite element

$j = 1, M_a$ M_a = Total number of modes of vibration

$k = 1, N_m$ N_m = Total number of materials in the system

Greek Symbols

α	Coefficient to determine Rayleigh's damping
β & γ	Newmark's constants of direct integration of equations of motion
$\underline{\delta} = (u, v, w)^T$	Displacement vector
$\underline{\dot{\delta}} = d\underline{\delta}/dt, \quad \underline{\ddot{\delta}} = d^2\underline{\delta}/dt^2$	First and second derivatives of displacement vector with respect to time
$\underline{\varepsilon} = (\varepsilon_r, \varepsilon_z, \varepsilon_\theta, \gamma_{rz}, \gamma_{r\theta}, \gamma_{z\theta})^T$	Strain vector
$\underline{\sigma} = (\sigma_r, \sigma_z, \sigma_\theta, \tau_{rz}, \tau_{r\theta}, \tau_{z\theta})^T$	Stress vector
ρ	Mass density
ϕ	Column node shape vector
ω	Circular frequency (rad/sec)
ς	Weighted modal damping
(ξ, η)	Natural coordinates
$\tau = \theta \Delta t$	θ = Wilson's constant of direct integration of equations of motion, and also angle in degree Δt = Time increment, τ = Time
ψ	Energy

Chapter 1

INTRODUCTION

1.1 Background

Analysis of axisymmetric structures subjected to seismic forces has attracted considerable attention, especially, in the area of the nuclear power plants because such structures are required to be analysed and designed in most rational manner due to safety considerations. Further due to rapid expansion in number and size of nuclear power plants in India and elsewhere in the world, there is great need for careful and detailed investigation of their behaviour under seismic forces.

A prime concern of nuclear safety is to prevent the release of fission products to the environment. This aspect of safety distinguishes nuclear power plants from conventional plants in which hazards are relatively localized. In many countries, little consideration has been given to seismic forces in the design of structures because of infrequent occurrence of low magnitude earthquakes in the recorded past history. However, the occurrence of some devastating earthquakes in this century in India and the spectacular surge in the construction of large capacity nuclear power plants have provided an impetus for the detailed study of the effect of seismic forces on such structures. The potential damage exposure from an accident at a large nuclear power plant makes it imperative that ground motion effects be considered in the design of such structures, even in the areas that now appear to have low seismic activity. These important structures should not show any kind of distress under most severe motion expected in the life of structure.

The analysis of axisymmetric structures is not limited to nuclear power plants only. There are other practical applications like pressure vessels, domes, fluid containers, cooling towers, stacks, etc.

A ⟶ SOIL WIDTH
B ⟶ SOIL DEPTH
D ⟶ DEPTH OF EMBEDMENT
R ⟶ RADIUS OF RAFT
H ⟶ HEIGHT OF STRUCTURE
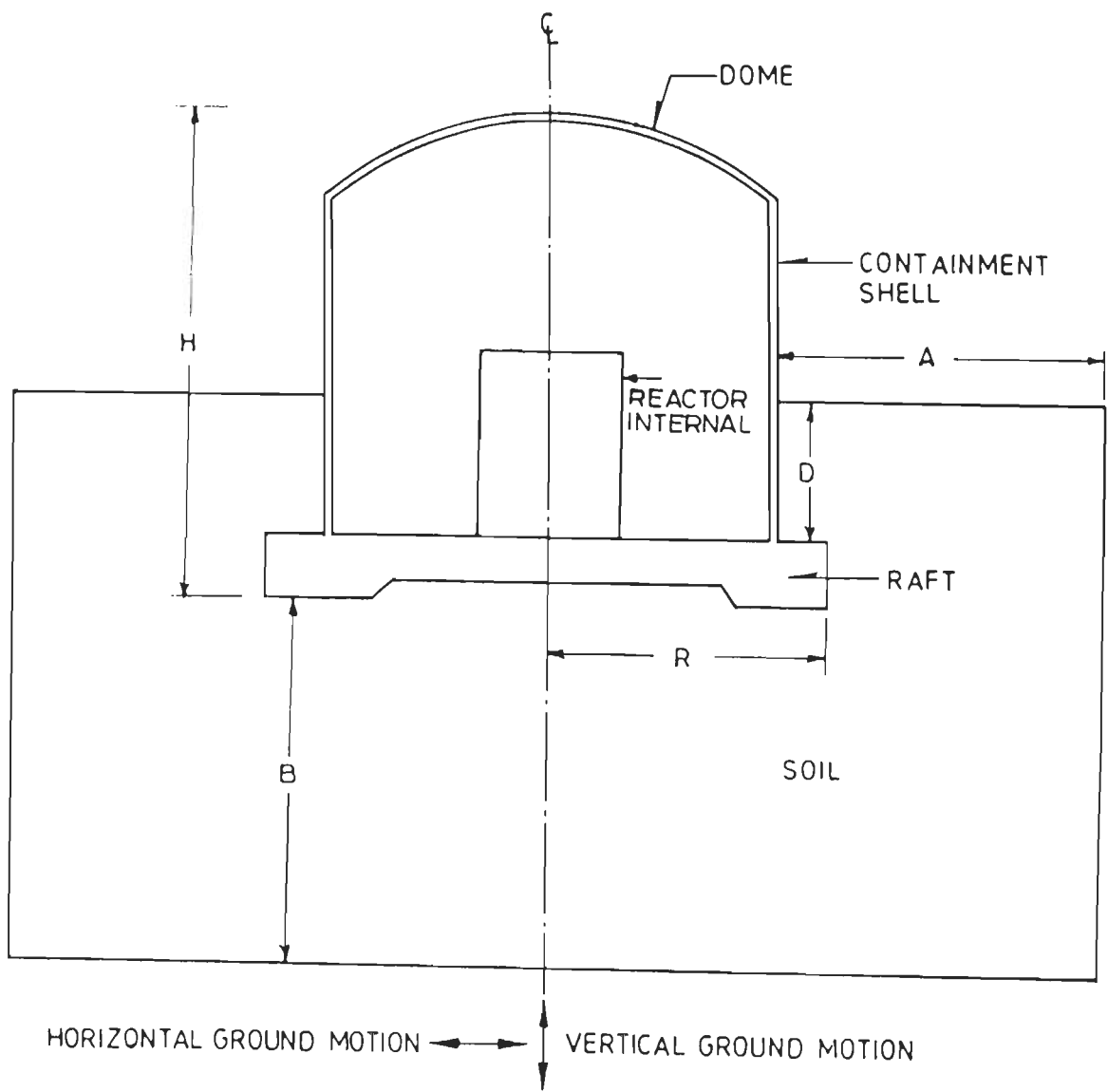
FIG. 1·1 AXI-SYMMETRIC STRUCTURE SUBJECTED TO EARTHQUAKE MOTIONS

Though the governing field equations for axisymmetric systems have been known for many years, yet their analytical solutions are available only for a limited class of problems. However, numerical solutions with the aid of digital computers have been obtained for arbitrary geometric configurations. One of the various numerical methods-the finite element method, has received extensive treatment in the technical literature in recent years.

The rational evaluation of forces and displacements in various locations of the structure and the foundation during strong ground motion is most important since additional forces are induced in the structure due to ground motions caused by earthquakes. A major portion of energy input to the structure from earthquake motion is transformed into strain energy and small portion of it is dissipated due to various types of damping effects. The strain energy causes deformations and stresses in the structure and if the structure is not designed for these effects, it may show cracking or various types of damage.

1.2 Statement of the Problem

An axisymmetric structure such as containment structure resting on rock/ soil, subjected to horizontal and vertical ground motions, (Fig.1.1), will develop additional stresses on the structure due to inertia effects. In general, when a structure is embedded, it will interact with the surrounding and base soil. To take this soil-structure interaction effect into account, the soil should also be modelled along with the structure. The soil is semi-infinite medium, an unbonded domain, so the infinite extent of foundation medium is to be properly modelled.

Following problems need attention while analysing massive embedded axisymmetric structures, such as nuclear containment, subjected to seismic forces :

(i)   Extent of foundation to be taken into account in seismic analysis of such structures, as fixed boundaries of finite mesh would reflect the waves and could affect the structural and soil response.

(ii) Effect of soil-structure interaction on seismic response of a structure.

3

(iii) Effect of different damping in different materials of structure and the foundation on overall response of the system.

(iv) Effect of modelling of non-axisymmetric internal structure of a nuclear reactor building on the response of containment shell and raft.

1.3 Objectives of the Study

The present study deals with the linear elastic analysis in the time domain of axisymmetric structures subjected to earthquake forces. The analysis is done by using the sophisticated finite element method. To find the maximum structural response, the timewise mode superposition and the direct step -by-step integration methods have been used. The damping in the structure has been assumed to be viscous.

The main objectives of this study are :

(i) Literature review and review of methodology of seismic analysis of axisymmetric structures.

(ii) To evaluate the significance of effects of soil-structure interaction on the seismic response of a reactor building of a nuclear power plant.

(iii) To compare the earthquake response of axisymmetric structures in time domain using two methods, namely, mode superposition and direct step-by-step integration; and to determine suitability of the method for seismic response computation.

(iv) To study the effect of viscous boundaries on seismic response of axisymmetric structure in relation to fixed boundaries.

(v) To study the effect of modelling of non-axisymmetric internal structure of nuclear reactor building as equivalent axisymmetric body on total seismic response.

1.4 Scope of the Study

The detailed description of work is as follows :

Literature Review and Review of Methodology of Seismic Analysis of Axisymmetric Structures

The work done by various investigators in past on seismic analysis of axisymmetric structures has been reviewed. Also, finite element methodology of axisymmetric structures subjected to non- axisymmetric loads like horizontal earthquake excitation has been presented.

Soil-Structure Interaction

The traditional method to analyze a soil-structure interaction system is to represent the system by a one-dimensional structure with lumping the mass at discrete points. The base is assumed to be supported by a set of horizontal, rotational and vertical frequency independent springs to represent the soil system. This model is commonly known as beam model which characterizes the interaction mechanism by using lumped parameters from the assumption of a rigid plate resting on an elastic half-space. It can not truly represent the dynamic interaction behaviour of the system because of being one dimensional. Another method of analysis, known as finite element method, involves modelling of structure as well as soil medium by using finite elements. Finite element method can take into account the three dimensional nature of the system.

The soil is assumed to be linearly elastic and its damping is higher as compared to the structural damping. A single value of damping has been assigned to each mode which reflects both the low damping of the structure and the high damping of the soil. This has been done by calculating a weighted damping based on weighted values of strain energy in various sub-systems including soil.

To obtain an understanding of the interaction phenomenon between soil and structure, an analytical parametric study involving shear wave velocity of soil as parameter has been attempted on a model of a reactor building.

To compare the seismic response of structure obtained by using mode superposition and direct step-by-step integration methods

The axisymmetric structure subjected to horizontal ground motion is analysed and seismic responses such as stresses and displacements obtained by mode superposition and direct step-by-step integration method are compared. Also, the

suitability of the method is determined for seismic response computation of axisymmetric structures.

To study the effects of viscous boundaries on seismic response of axisymmetric structure in relation to fixed boundaries

An approach of viscous boundaries to absorb the radiation energy of the axisymmetric structure subjected to horizontal ground motion is used and its effects are compared with the extended fixed boundaries.

Effects of modelling of non-axisymmetric internal structure of reactor building as equivalent axisymmetric body

As the reactor internal structure is not axisymmetric, so in order to model the complete reactor building as axisymmetric; the reactor internal structure is modelled as equivalent solid cylinder based on a parametric study. Thus, the finite element seismic analysis of whole of the reactor building is carried out and the seismic response are evaluated under severe ground motion which contributes significantly in designing of such important structures.

1.5 Factors Affecting Seismic Response of the Structure

Seismic analysis of a structure involves considerations of several aspects such as :

(i) Type of ground motion

(ii) Mathematical modelling of structure and foundation

(iii) Dynamic characteristics of structure

(iv) Effects of soil-structure interaction on seismic response of a structure

(v) Energy dissipating characteristics of structure and foundation.

1.6 Input Required for Seismic Analysis of the Structure

The following input parameters are required for dynamic analysis of structure :

Material Characteristics

(i) Elastic properties of different components of structure and foundation material such as modulus of elasticity, Poisson's ratio.

(ii) Mass density of different structural components and foundation soil.

(iii) Damping characteristics of various subsystems of structure and radiation damping of soil, i.e., equivalent damping for rocking and translational mode.

Structural Characteristics

(i) The structural size of different subsystems, that is, thickness, width, length, height, diameter, etc.

Loading Characteristics

(i) Weight of equipment and system, other dead and live loads on structure.

(ii) Ground motions: Response spectrum for horizontal and vertical ground motion for different damping factors, acceleration time history for various components of ground motion.

1.7 Uncertainties of Input Parameters

The elastic properties of structural components are usually known to a reasonably accuracy. The accuracy of elastic properties of soil/rock can not be obtained to that accuracy. This is because of heterogeneous character of foundation material and difficulties in accurately determining in-situ properties, particularly at great depth below ground [Ma, S. M. et al(1981)]. The damping properties of a structure are known to a better accuracy as compared to that of foundation. To overcome these difficulties, a range of elastic properties are chosen for foundation soil and response is determined for this range.

The uncertainties are also associated with design earthquake motion. The design response spectrum is established on the basis of seismological data, local geology and local soil characteristics. The basic data on which the design response spectrum is based, is not so accurate due to paucity of data. A good

deal of judgment is therefore necessary in establishing design response spectrum. The spectrum compatible time history is often used for analysis of structure. In the deterministic analysis currently in use, only one time history is used for each component of ground motion. It is necessary to use more than one time history to take care of possible variation in ground motion characteristics.

1.8 Layout of the Thesis

The thesis has been put in total of 8 chapters and the brief description about the chapters are described below :

In Chapter 1 the significance and importance of the problem has been highlighted along with objectives of the present study.

Chapter 2 covers the critical review of work related to seismic analysis of axisymmetric structures.

Chapter 3 describes the details of mathematical formulation of axisymmetric structure subjected to non-axisymmetric loading in general, and to earthquake loading in particular. The procedure of evaluating earthquake response using the proposed two methods, that is, mode superposition and direct step- by -step integration method, have been explained.

Chapter 4 presents the parametric study of the effects of soil-structure interaction on seismic response of a nuclear reactor building.

Chapter 5 compares the seismic behaviour of axisymmetric structures obtained by mode superposition and direct step -by -step integration methods of analysis. Suitability of the method for seismic response computation of axisymmetric structure has also been presented in this chapter.

Chapter 6 presents the effects of viscous boundaries on seismic response of axisymmetric structures in relation to fixed boundaries.

Chapter 7 presents the effects of modelling of non-axisymmetric internal structure of nuclear reactor building by a equivalent axisymmetric body.

Chapter 8 presents the summary of the investigation in the thesis and the conclusions drawn from the present study.

REVIEW OF LITERATURE

2.1 Introduction

Axisymmetric structures form a class of three-dimensional analysis problem which have various practical applications like pressure vessels, tanks, containment structures, etc. Though the governing field equations for axisymmetric systems have been known for many years, yet their analytical solutions are available only for a limited class of problems. However numerical solutions with the aid of digital computers have been obtained for arbitrary geometric configurations. One of the various numerical methods, the finite element method, has received extensive treatment in the technical literature in recent years.

An axisymmetric structure subjected to earthquake motions will develop additional stresses on the structure due to inertia effects. If the structure is not designed for these effects, it may show cracking or various types of damage. Therefore, the detailed seismic analysis of axisymmetric structures is required for rational evaluation of forces and displacements in various locations of the structure and foundation during strong ground motion.

Literature on the seismic behaviour of axisymmetric structures and its analytical procedures has been reviewed in this Chapter which takes into account several aspects such as characteristics of ground motion, soil-structure interaction effects, energy dissipating characteristics of structure and foundation, modelling of boundaries and modelling of non-axisymmetric internal structure of reactor building, etc.

2.2 Soil-Structure Interaction (SSI) Analysis

2.2.1 Background on SSI Analysis (Wolf, 1985 & 1987)

It is a common practice to assume that the structure is attached to a rigid foundation and the influence of local properties of the ground on the response of

structure are ignored. The earthquake motions are assumed to be introduced of specified quantities at the support and are not influenced by the structure (Richart, 1970). In general, however, the structure will interact with the surrounding soil. It must also be considered that in many important cases such as earthquake excitation, the loading is applied to the soil region around the structure. It is thus not permissible to analyse only the structure, the soil is also to be modelled in some way (Julio et al, 1977). The soil is a semi-infinite medium, an unbounded domain; so the infinite extent of foundation is to be properly modelled (Isenberg & Adham, 1972).

For static loading, a fictitious boundary (Fig. 2.1a) at a sufficient distance from the structure, where the response is expected to be died out from a practical point of view, can be introduced. This leads to a finite domain for the soil which can be modelled similar to the structure. The total discretized system thus, consisting of the structure and the soil; can be analyzed straightforwardly.

(a) FICTITIOUS BOUNDARY FOR STATIC
FINITE ELEMENT ANALYSIS

(b) TRANSMITTING BOUNDARY FOR DYNAMIC
FINITE ELEMENT ANALYSIS
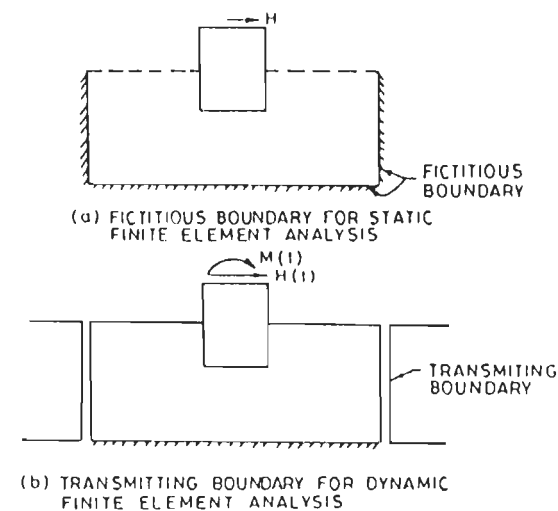
FIG. 2·1 BOUNDARY FOR STATIC AND
DYNAMIC LOADING

However, for dynamic loading, this procedure cannot be used. The fictitious boundary would reflect waves originating from the vibrating structure back into the discretized soil region instead of letting them pass through and propagate towards infinity (Smith, 1974). This needs to model the unbounded foundation medium taking care of its infinite extent through transmitting boundaries (Deek & Rondolph, 1994; Lysmer, 1974 & 1975; Tzung et al, 1981; Udaka, 1981), viscous boundaries, infinite elements (Medina, 1980; White, 1974), boundary elements (Van, 1984), etc., in dynamic problems (Fig. 2.1b). Dynamic problems

are thus more complicated in its mathematical modelling as compared to static problems. Stojko(1989) carried out soil-structure analysis in the time domain.

2.2.2 Objectives of SSI Analysis

The fundamental objective of soil-structure interaction analysis is illustrated in Fig.2.2. A specified time varying load acts on a structure embedded in layered soil. The dynamic response of the structure and, to a lesser extent, of the soil is calculated, taking into account the radiation energy of the waves propagating into the soil region. Many types of time varying loads acting directly on the structure can arise, such as impact loads, blast loading, periodic loads originating from rotatory machinery in buildings etc., the most important and most complicated loading to analyze, is earthquake excitation, which acts primarily on the soil (Seed et al, 1969, 1970, 1973, 1974, 1975 and 1977). Earthquakes are caused by a sudden energy release in a volume of rock laying on a fault. This source is normally located at a large distance away and at a significant depth from the site. Even if all details of how the source mechanism works and data of the travel path of the seismic waves to the site were available, it would still be impossible to model all aspects. In any event, the many uncertainties involved, make it meaningless to analyze the complete earthquake excitation problem.
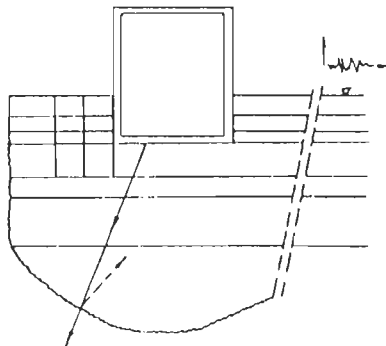
FIG. 2·2 FUNDAMENTAL OBJECTIVE OF ANALYSIS OF SOIL – STRUCTURE INTERACTION

Today's state of the art of earthquake engineering allows only the influence of the local soil conditions on the seismic input motion to be taken into account. To be able to do this, seismic hazard of the region is assessed and specifies the acceptable probability that the earthquake used for design will be exceeded during the life of the structure. In this evaluation, the type of the structure will

play an important role. For a potentially hazardous structure, such as a nuclear power plant this probability will be selected to be very small. This needs the determination of the important parameters of ground motion, such as peak ground acceleration, frequency content etc. All this allows the source mechanism, the transmission path, the local geology and the soil conditions at the site to be taken into account approximately (Valera, 1977; Vaish & Chopra, 1973 and 1974).

The seismic motion acting on the structure is thus not known before the soil-structure analysis is performed. In summary, for seismic excitation, analyzing soil-structure interaction analysis consists of two distinct parts; first, determining the free field response of the site, and second, calculating the modification of the seismic motion, the actual interaction, when the structure is inserted into the seismic environment of the free field. The loading applied directly to the structure are, however, contained as special case in the general formulation.

To illustrate the salient features of soil-structure interaction, two identical structures, one is founded on rock and another is rested on soil, subjected to same horizontal motion arriving from the source of earthquake into the underlying rock in the form of vertically propagated seismic waves (Fig.2.3a) are selected. The control point is chosen at the free surface of the rock (point 'A'). From a practical point of view, the motion throughout the rock (e.g. in point 'B') will be the same. For the structure on the rock this horizontal motion can be directly applied to the base of the structure. The input acceleration resulting in the applied horizontal inertia loads will be constant over the height of the structure. During the earthquake, an overturning moment and transverse shear at the base will develop. As the rock is very stiff, these two stress resultants will not lead to any additional deformation at the base. The resulting horizontal displacement of the base is thus equal to the control motion; no rocking motion arises at the base. For a given control motion, the seismic response of the structure depends only on the properties of the structure. For the structure founded on soft soil, the motion of the base of the structure in point 'O'(Fig.2.3a) will be different from the control motion in the control point, because of the coupling of the soil-structure system.

To gain insight into how the soil affects the dynamic response of the structure, it is convenient to distinguish between the following aspects :
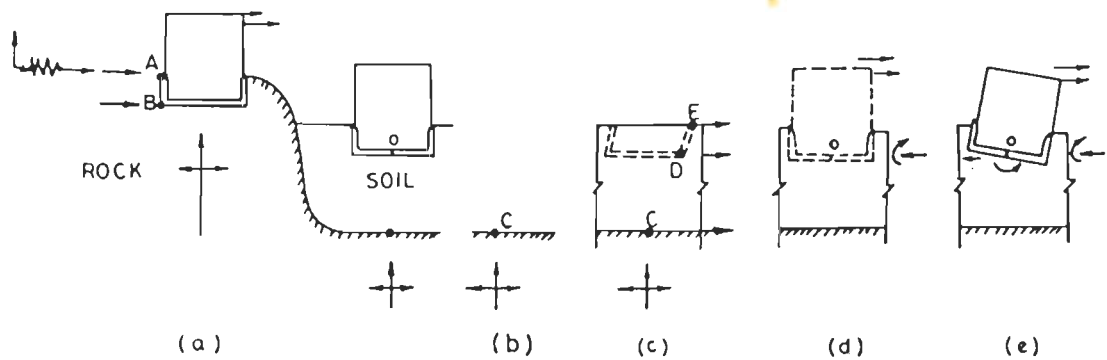
FIG. 2·3   SEISMIC RESPONSE OF STRUCTURE FOUNDED ON ROCK AND ON SOIL

2.2.3 Free Field Response

The motion of the site in the absence of the structure and without excavation, what is called the free field response is modified (Fig. 2.3c). If there were no soil on the top of the rock (point 'C' of Fig. 2.3c), the motion in this fictitious outcrop shown in Fig.2.3b, would hardly differ from the control motion of the rock in point 'A'. The presence of soil layer will reduce the motion in point 'C' (Fig. 2.3c). This wave will propagate vertically through the soil layer, resulting in motions in points 'D' and 'E' which differ from that in point 'C'. Points 'D' and 'E' are nodes in the free field which will subsequently lies on the structure-soil interface (the base) when the structure has been built. In general, the motion is amplified, but not always (depending upon its frequency content), thus resulting in horizontal displacements that increase towards the free surface on the site.

2.2.4 Kinematic Interaction

The excavation and insertion of rigid base into the site will modify the motion (Fig. 2.3d). The rigid base will experience some average horizontal displacement and a rocking component. This rigid motion will result in accelerations (leading to inertial loads) which will vary over the height of structure, in contrast to the applied accelerations in the case of structure founded on rock. The geometric averaging of the seismic response will be the result of the so called kinematic

interaction part of the analysis.

In embedded structure, the presence of the structure modifies the free field motion due to kinematic interaction. In kinematic interaction analysis for embedded structures, the soil above the base of the structure is assumed to be rigid.

2.2.5 Inertial Interaction Analysis

This approach is perfectly justified in the case of a surface structure on a linear elastic material since the kinematic interaction effects are zero in this case (if the input consists of vertically propagated body waves) and the motions in the structure are exactly equal to those produced by the control motion (free field motion). The inertial load applied to the structure will lead to an overturning moment and a transverse shear acting at point 'O'(Fig. 2.3e).

These will cause deformations in the soil and thus, once again modify the motion at the base. This part of analysis is called inertial interaction. Any correct mathematical modelling of inertial interaction effects only will provide good results for a surface structure whose validity depends only on the accuracy of the assumptions made in establishing the model.

2.2.6 Complete Soil-Structure Interaction Analysis

It includes both kinematic and inertial interaction. In fact the soil-structure system is subjected to earthquake ground motions which vary from point to point even in rock well below the structure and travel in some unknown way across the base of the soil-structure system.

To achieve a solution it is necessary to determine the motions at all points in the soil deposit as well as those in the structure. Such information can be obtained by assuming that the motions in the soil result from vertical propagation of shear waves. This is clearly an approximation of the actual condition and is justified only on the grounds that it is believed to be sufficiently accurate for engineering purposes.

On the basis of this approximation, there are several ways in which the ground distribution and response of the structure can be evaluated. One way is to deconvolve the control motion to some depth in the soil profile such as soil-rock interface (Schnabel,1972).

2.3 Computer Programs Available on Seismic Analysis of Axisymmetric Structures

A list of various publicly available computer programs for seismic analysis of axisymmetric structures is given in Table 2.1. This list is by no means complete but has been provided to indicate that there are several programs available for a designer to easily and effectively carry out a dynamic analysis of axisymmetric structures.

Table 2.1
Computer Programs for Seismic Analysis of Axisymmetric Structures

Program Acronym	Reference/documentation	Developer/author / contact person
ASHSD	Dynamic stress analysis of axisymmetric structures under arbitrary loading, EERC Report 69-10,Univ. of California,Berkeley,USA	S. Ghosh E.L. Wilson
LUSH	A computer program for complex response analysis of soil-structure system, EERC Report 74-4, Univ. of California, Berkeley, USA	J. Lysmer T. Udaka H.B. Seed R. Hwang
FLUSH	A computer program for approximate three dimensional soil-structure interaction problems, EERC Report 75-30, Univ. of California, Berkeley, USA	J. Lysmer T. Udaka C.F. Isai H.B. Seed
ALUSH	A computer program for seismic response analysis of axisymmetric soil-structure interaction systems, EERC Report 75-31, Univ. of California, Berkeley, USA	E. Berger J. Lysmer H.B. Seed R. Hwang
PLUSH	Probabilistic three-dimensional analysis with viscous and transmitting boundaries, 1977, Univ. of California, Berkeley, USA	P.R. Miguel J.L. Lysmer H.B. Seed

ASHSD

Ghosh and Wilson (1969) developed this computer code 'ASHD' on dynamic stress analysis of axisymmetric structures under arbitrary loading. The main features of this program are as under :

(i)   A finite element method is presented for the dynamic analysis of axisymmetric structures subjected to any arbitrary static or dynamic loading or base acceleration etc.

(ii)   The three-dimensional axisymmetric continuum is represented as an axisymmetric thin shell or as a solid of revolution or as a combination of both.

(iii)   The axisymmetric shell is descretized as a series of frustum of cones and the solid of revolution.

(iv)   Hamilton's variational principle is used to derive the equations of motion for this descretized structure.

(v)   The mass matrix, stiffness matrix, load vectors are consistent with the assumed displacement field, i.e., with the shape function.

(vi)   Diagonal mass matrix has been assumed to minimize computer storage and execution time.

(vii)   These equations of motion are solved numerically through the time domain either by direct integration or mode superposition method.

(viii) This method of analysis is applied to various practical cases like nuclear reactor containment, pressure vessel etc.

(ix)   The above formulation is also applied to investigate structure-foundation interaction effect.

LUSH

Lysmer et.al.(1974) developed this computer program 'LUSH' which is basically a

finite element program designed for earthquake analysis of plane structures. This program has following features :

(i) It provides a complete tool for seismic soil-structure interaction analysis by complex response method.

(ii) The mass distribution within the finite element model can be either distributed (consistent mass matrix) or concentrated at the nodal points (lumped mass matrix) or it can be any combination of these choices.

(iii) Many options are available for output which may consist of time histories or response spectra for selected nodal points.

FLUSH

Lysmer et.al.(1975) modified their earlier program 'LUSH' on an approximate three-dimensional analysis of soil-structure interaction problems. This program 'FLUSH' is faster than 'LUSH', so called as Fast LUSH . It includes large number of new features as under :

(i) Transmitting boundaries

(ii) Beam elements

(iii) An approximate three-dimensional analysis

(iv) Deconvolution within the program

(v) Out of core equation solver

(vi) New input/output features which improve the efficiency and utility of the program

(vii) A method of approximate three-dimensional analysis of dynamic soil-structure interaction problems which is similar to a two-dimensional finite element analysis. The three-dimensional effect being achieved by the addition of viscous forces to account for wave propagation.

ALUSH

Berger et.al.(1975) added some new features in their earlier programs LUSH and FLUSH which further improve efficiency and utility of the program. In this program 'ALUSH', seismic response analysis of axisymmetric soil-structure interaction systems using finite element method with extensive mesh and with transmitting boundaries has been compared.

PLUSH

Miguel, Lysmer and Seed (1977) developed a new probabilistic analysis procedure based on finite element analysis approach used in the program FLUSH, but incorporating in a probabilistic way, all possible time histories of motion having a power spectrum corresponding to the response spectrum of the design basis earthquake. The computer program for accomplishing this has been named PLUSH (Probabilistic LUSH). The procedure eliminates the need for generation of a time history of motion, it presents response data in probabilistic form in terms of confidence limits, and it permits the analysis to be made still more efficiently than following a deterministic procedure.

2.4 Review of Past Work

The work carried out by the various investigators on seismic analysis of axisymmetric structures including effects of soil-structure interaction are described below :

Lysmer and Kuhlemeyer(1969)

They described a general method through which an infinite system may be approximated by a finite system with a special viscous boundary condition using finite element method. Previously unsolvable wave propagation problems in an infinite solid like axisymmetrical foundation vibration in an infinite soil mass are analysed and concluded that (a) the radiation of energy from the excited zone to the far field is properly accounted for, and (b) the concept of infinity is mathematically convenient represented.

Gupta and Schnobrich (1976)

Two prototype towers of heights 100m and 135m respectively were analysed to evaluate the response of towers subjected to El-Centro Earthquake time history (May 18,1940,N-S component) using axisymmetric finite element model. Hashish & Abu-sitta, 1971; Gould et al, 1967 also employed axisymmetric finite element model for seismic analysis of hyperbolic cooling tower. The following three methods of analysis were used :

(a) Direct step by step integration of the equations of motion
(b) Modal superposition method
(c) Response spectrum method

The following conclusions were derived from the study :

(i) Response spectrum method of analysis is of maximum practical use because it involves less computational time than time history analysis.

(ii) Designing the tower for one horizontal component of earthquake is adequate.

(iii) The design earthquake loads may be reduced if sufficient inelastic deformation capacity can be incorporated into the design. The inelastic deformation can be simulated either by use of ductility factors applied to the elastic design spectrum or by the use of substitute damping method. Soil-structure interaction may reduce the response of tower.

(iv) The design spectra are the site related and should be constructed based on the actual seismic survey of the site. The design spectrum specifies the desired strength of a structure and not its response to a given earthquake.

Hall and Kissenpfening (1976)

The state-of-the-art on soil-structure interaction has been presented. The basic principles of soil-structure interaction and advantages and limitations of the lumped parameter and finite element approaches have been discussed. The comparison between the exact frequency dependent and approximate frequency

independent soil-structure parameters have been obtained for nuclear containment vessel. The results are presented in terms of acceleration response spectra at three points of a reactor building, that is, top of the containment, the top of the internal structure, and the base of the slab. It was found that frequency independent parameters are adequate for soil-structure interaction earthquake response calculations. It has been found that frequency independent stiffness coefficients give accurate results, especially for translational modes of vibration. Kobatake et. al.(1985) observed that frequency dependent soil stiffness should be employed in seismic analysis of reactor building resting on soft soil.

Finite element method can solve relatively complex structural problems where the material properties are variable and boundary conditions are complex. The accuracy of finite element solution, in general, depends upon the size and shape of the elements used to represents the real system. The accuracy of the solution is not only dependent on the dimensions of the model, but also on the treatment of the boundary conditions, as artificial boundaries must be introduced so that infinite system is reduced to one of finite size. For the case of dynamic problems, additional complexities is introduced as a result of wave propagation characteristics of individual finite elements and reflections of waves at the artificial boundaries of the finite element model.

Hadjian (1976)

The two methods of analysis of soil-structure interaction, the lumped parameter and finite element methods, have been reviewed with regard to their capabilities to address the significant factors of the soil-structure interaction problem. The questions related to the reduction of the seismic motion with depth, scattering of incident waves, the three dimensionality of the real problem, soil damping, strain dependency of soil properties and the uncertainties associated with all of the above have been discussed in detail. It was observed that, although both methods as presently practiced have not yet completely solved the problem, the lumped parameter approach has come closer to addressing the more significant issues because of its simplicity and low cost and therefore this approach is the preferred engineering method for soil-structure interaction. However the use of finite element method in design should be limited to special cases only because of its three-dimensional representation of the problem.

Costantino and Miller (1976)

A significant number of two-dimensional finite element computations were made to compute the frequency dependent soil-structure interaction coefficients. The variations in the element size, mesh dimensions, boundary conditions, and soil hysteretic damping ratio to determine their influence on the computed interaction coefficients were made. It has been determined that the primary requirement of the mesh is a transmitting boundary formulation. For low damping conditions, roller support boundary conditions must be placed exceedingly far from the structure to ensure convergence of the results to the analytical solution. In addition, with such boundary conditions, the addition of artificial hysteretic soil damping could not be used to simulate radiation damping behaviour of the continuum. A frequency dependent criterion is also presented to determine minimum size of elements that must be used in any calculations.

Seed and Lysmer (1978)

The current capability for evaluating soil-structure interaction effects during earthquakes using finite element procedures has been summarized. It is suggested that finite element procedures provide a powerful tool for use in the design of nuclear plants, especially for embedded structures, and their applicability in this respect has been illustrated by comparing computed results with those recorded in a nuclear power plant during a strong motion earthquake. It was concluded that when the methods are used in conjunction with good engineering judgment and with full recognition of their limitations, they provide evaluations of response with a level of accuracy entirely adequate for engineering design.

Takemori et.al.(1979)

Dynamic soil-structure interaction analysis of PWR power plant facilities was performed using parameters of modulus of elasticity, soil dampings and three earthquake waves having different frequency characteristics, by the following two methods :

(a) Response analysis of the lumped mass model with swaying-rocking springs of soil, called swaying-rocking model (SRM)

(b) Deconvolution analysis by FEM model of soil

The PWR containment facilities consist of the outer shield wall(OSW), steel containment vessel(SCV) and inner concrete structure(IC). It was observed that the acceleration on and beneath the foundation is not so significantly amplified as compared with that at a point of same level in the free field due to radiation damping of SSI. This tendency was not clearly found by SRM but fairly well shown by FEM, particularly at small value of modulus of elasticity. Consequently it was found that when SRM is used in dynamic analysis for its simplicity, damping factors of swaying spring representing soil can be taken higher than that for FEM.

The observed accelerations at the foundation bottom of structure during earthquakes are influenced by the characteristics of earthquakes, structure themselves and soil. These are generally almost equal to those at the same level in free field. However, when accelerations as the control motions at the foundation bottom level of free fields are applied to the SSI lumped models, response accelerations are generally amplified around the foundation. In SRM, springs are generally estimated from the evaluation of the steady-state force displacement relationship of massless foundation supported on the elastic half space medium.

Waas and Weber (1979)

The interaction of partly embedded axisymmetric reactor building with the surrounding soil was analysed using,

(a) A plane strain finite element model
(b) An axisymmetric finite element model, and
(c) Lumped parameter model

Takemori et.al.(1979) also compared the soil-structure interaction effects by different models.

The structure weighs 1600 MN, 65 m high, 60 m dia, and very stiff; founded 18 m below ground level on alluvial deposits of several hundreds meters thick. The plain strain finite element analysis was carried out using the transmitting boundaries to account for radiation damping. The control motion was assumed at the ground surface in the free field. The seismic input at the base of the model is obtained from the control motion by one-dimensional deconvolution.

Reddy(1987) also carried out dynamic analysis of containment building of 500 MWe using axisymmetric model.

The axisymmetric finite element analysis with non-axisymmetric loading is similar to the plane strain analysis. It also uses the transmitting boundaries and the same input motion computed by deconvolution.

In the lumped parameter model, the flexibility and damping due to the subgrade was represented by soil springs and dashpots based on half space theory. The control motion was directly applied as support acceleration.

The lumped parameter model yields structural acceleration much larger than that of the finite element models listed above. However, results similar to those of the axisymmetric finite element analysis can be obtained by the lumped parameter model when the control motion is not directly used as support acceleration, but modified using one-dimensional deconvolution to account for the variation of the free field ground motion with depth. The structural responses have been computed in the time domain by modal analysis using frequency independent soil springs. Lumped model analysis is particularly suited for preliminary analysis and design as it is inexpensive, quick and thus permits extensive parametric studies.

Chen et.al.(1979)

A deeply embedded nuclear power plant structure has been analysed using finite element model and central explicit direct step by step integration method. The important parameters affecting seismic soil-structure interaction analysis, such as foundation embedment, soil material damping and soil layering are investigated. The following conclusions are drawn from this study :

(i)   The foundation embedment significantly increases the horizontal coupling, rocking stiffness and radiation dampings. The effect of soil layering introduces a marked frequency dependence.

(ii)   The amplitude of the horizontal input motion at the foundation base is significantly reduced due to the presence of the embedded rigid foundation, especially at high frequencies. The amplitude of the rocking input motion (which is zero for surface foundations) attains a significant fraction of the

free field amplitude as the result of the foundation embedment.

Cheron et.al.(1981)

Seismic analysis of Fast-breeder reactor(FBR) building has been carried out using a substructure approach based on modal condensation. Time history analysis of selected accelerations has been applied to reactor building on a soil with modulus of elasticity varying from 5.0×10^8 N/m^2 to 1.0×10^{10} N/m^2. Soil-structure interaction has been taken into account by springs and dampers based on half space theory.

It was concluded that this approach allows to reduce the large extent of problems, when performing linear seismic analysis and of particular interest for very large models which are expensive to run with usual finite element programs.

Benda and Johnson (1981)

The work carried out to quantify the variation in dynamic characteristics and seismic response of nuclear power plant structures caused by different modelling assumptions. The following four idealized mathematical models of the structure have been used :

(a) A detailed Finite Element Model (FEM).
(b) A detailed FEM Model with lumped mass at selected nodes.
(c) A detailed FEM Model with the constraint of rigid floors.
(d) An equivalent beam model.

The following conclusions were drawn from the study :

(i)   All the above four modelling approaches preserved total mass and rotational moment of Inertia.

(ii) The greater variation was found in the frequencies of the comparable mode, the coefficient of variation from 0.09 to 0.31. Hadjian et.al.(1977) recommended a coefficient of variation equal to 0.10 to define the dispersion of frequencies calculated for complex structures by experienced engineers.

(iii) Large variation in dynamic characteristics and response could be introduced by modelling assumptions when a need exists to reduce the number of dynamic degree of freedom.

Gantenbein and Aguilar (1983)

The seismic analysis of reactor building has been studied in two steps :

(a) **Study of building** : The equipment are integrated as mass only and the natural frequencies and the associated mode shapes, seismic response and floor spectra at various levels were computed.

(b) **Study of equipment** : Computation of natural frequencies, mode shapes and seismic response using floor spectra was done as in previous step. The parametric study of a typical PWR 900 MWe reactor building was done. The stresses in the building and floor spectra at several levels of the building have been investigated. They simplified the modelling of complex internal structure of reactor building and performed a parametric study of the seismic response of the complete structure.

With these results, it is possible to study the seismic response of equipment and one can also use the efforts obtained as input for computation of stresses in some part of the structure or equipment.

Satoh and Sasagawo (1983)

The study has been made to evaluate the soil-structure interaction effects on seismic response of the liquid metal fast breeder reactor(LMFBR) Pool type structure, especially focused on the effect of the embedment and the effect of the step mat configurations.

Lattice mathematical model technique is used to simulate the dynamic response characteristics of the structure and the surrounding soil in the one horizontal direction. Soil-structure interaction effects are also taken into account.

A single stick lumped mass model is used to model the reactor building and lattice pattern multi stick lumped mass model is used to model the surrounding soil.

An earthquake input motion applied to the base of the model is calculated by a deconvolution method based on wave propagation theory.

Three different layouts for a pool type FBR building at a site of hard rock are

subjected to earthquake (El-Centro, May 18,1940, NS component) ground motion at the free surface of the base stratum, and following conclusions were made :

(i) The participation factors are decreased due to existence of surface soil layer.

(ii) The decreasing effect in generating input earthquake from the basic earthquake ground motion was observed due to surface soil layer.

(iii) The decrease in structural response was found due to embedment effects.

Singhal (1985)

Two actual axisymmetric structures, namely, a natural draft hyperbolic cooling tower and a thermal power house chimney, have been analysed for their self weight and earthquake forces. Two types of analysis, i.e., axisymmetric finite element analysis and beam analysis, have been carried out and the results from the two types of analysis have been compared with those obtained from theoretical analysis. To verify the method of analysis and the assumption involved therein, the natural periods of vibration of the two structures have been measured by carrying out wind excited vibration tests on the structures at the site and the following conclusions were drawn :

(i) The experimentally observed fundamental periods for cooling tower and chimney exhibited a good agreement with the ones obtained theoretically.

(ii) The two types of analysis gave good comparison of periods, mode participation factors and stresses.

(iii) The stresses due to vertical component of earthquake for both the structures were found to be negligibly small.

(iv) The effect of higher modes on the total response of the cooling tower was found to be insignificant and concluded that first three mode must be considered in the seismic analysis of chimney.

Thakkar (1989)

The dynamic analysis of few reactor buildings, that is, Kakrapara atomic power plant on rocky foundation and Narora atomic power plant on deep alluvial soil under horizontal and vertical ground motion was carried out using axisymmetric finite element model. Both the structure and foundation were idealized by axisymmetric finite elements. Dynamic response of building due to earthquake motions was calculated by mode superposition method. The stresses caused due to ground motion have been computed at different locations in the structure and foundation. The comparison of time periods in horizontal and vertical vibration and bending moments obtained by both finite element and beam methods has been done. The following conclusions were drawn from the study :

(i) The finite element analysis throws more light on stress pattern which is not so accurately available through beam model.

(ii) The fundamental period in horizontal vibration by beam and finite element methods is in close agreement. The periods in higher modes differ by both the models. This shows that behaviour of structure predicted by beam model does not match with that predicted by finite element model.

(iii) The bending moment response obtained by the beam method is more as compared to the finite element method.

Several aspects of dynamic analysis of reactor building have been presented. The most difficult aspect of modelling in the axisymmetric analysis is for the reactor internal structure. The non-axisymmetric internal structure should be modelled into equivalent solid cylinder by matching its dynamic characteristics.

Ghoparah and Baumber(1992)

The work was carried out on the tall industrial chimneys with different heights and diameters when subjected to earthquake ground motion. Simple one dimensional lumped mass approach is used to model the chimneys. The flexural deformations are considered to dominate the response of the structure. The effects of shear and rotary inertia are neglected.

Failure of chimney is either at near the base or at the top one third of its height.

Failure near to base of chimney is due to strong participation of fundamental mode and failure at top one third height is observed due to participation of the second mode of vibration in the dynamic response. Rock foundation underneath the chimneys is assumed to be rigid with no structure -foundation interaction effects. The following conclusions are drawn from this study :

(i)   First five modes are sufficient to evaluate the dynamic response of masonry chimneys.

(ii) Strong participation of higher modes of vibration is observed in relatively flexible chimneys resting on rock, when subjected to near field ground motion.

Daming and Zhangzu (1992)

A perspex model (scale 1:67) of 210 m high R.C.C. smoke stack(Which is situated in eastern Guangdon Province, China) was prepared for static and excited vibration test. Warudkar et.al.(1984) also designed 140m tall R.C.C ventilation stack for Narora atomic power plant project under strong ground motion. Zhang & Zhangzhu(1992) also compared the seismic response of a smoke stack by test and analytical study. Free vibration of the model and the prototype(using similitude conditions) of smoke stack have been analysed by considering :

(a) Bending and shear deformation
(b) Only bending deformation

Also finite element model of smokestack was analysed analytically and compared the seismic response from that obtained by model testing. The mode superposition and direct step by step integration methods are used in seismic analysis of finite element model of smoke stack. The seismic response ,i.e., bending moment, shear force and axial force, obtained by above two methods has been compared. The following conclusions were drawn from the study :

(i)   Analytical response are consistent with the test value basically.

(ii) The shearing deformations must be taken into consideration when the high order mode shapes of vibration of smoke stack are calculated.

(iii) At least five mode must be considered in seismic analysis of 210 m high smoke stack.

(iv) Earthquake damage of smoke stack often appears in top one- third height.

The effect of vertical seismic motion on the smoke stack has been evaluated and found that axial forces are less than dead load, so the smoke stack does not possess the axial tension for the vertical seismic motion with peak acceleration equal to 0.13g.

Hirano K. et.al.(1993)

Forced vibration tests (with two 10 ton vibration generators) were performed on prototype Fast Breeder Reactor(FBR) power plant building of 280 MWe (Power Reactor and Nuclear fuel development corporation, Monju). The evaluation is based on an earthquake response analysis taking into account of the weight condition of the building during plant operation and the strain level during earthquake. Kato et.al.(1989) also carried out forced vibration tests on the reactor building of Tsuruge nuclear power station.

Analytical results of above tests are simulated analytically by performing earthquake analysis using a lumped mass model. Input artificial seismic waves are used for the design with maximum acceleration of $2.8m/s^2$. The following conclusions were derived :

(i) Seismic response ,i.e., bending moment and shear force, obtained analytically are less than the design values.

(ii) Natural frequency and damping ratio obtained from the tests were agreed with the design values.

(iii) At the base mat amplitudes are correctly simulated at the peak position, but in the low frequency range the amplitude is small, which shows that ground stiffness is a little high.

Setogawa et.al.(1993)

Forced vibration tests and numerical analysis were carried out on the reactor building at Ohi nuclear power station (ONPS), Japan.

For the forced vibration tests on Inner concrete structure(I/C); two vibration generators of 10 ton were symmetrically set on the operating floor and operated in 1-25 Hz frequency range. The forced vibration test is carried out on the prestressed concrete containment vessel (PCCV), a generator of 3 ton(exciting force capacity) was set on the top of the PCCV and operated in the 1-20 Hz frequency range.

Simulation analysis was carried out using the lumped mass model for design and a model based on FEM was applied to the I/C.

Dynamic modulus of elasticity of concrete has estimated through simultaneous elastic waves tests performed on the reactor building and the Young's modulus tests were performed on small concrete blocks collected from the actual PCCV and I/C. The following conclusions were drawn from this study :

(i)   The natural frequency of the I/C and the PCCV are clarified at the first and second modes of vibration i.e. calculated (by analytically simulation) and measured (test values) frequencies for the first and second mode are consistent.

(ii)   Vibration characteristics of the PCCV can be described satisfactorily using the lumped mass model for design.

(iii) As for the I/C, a model using FEM is effective to describe the complex vibration characteristics of the structure in case of exciting directly the I/C.

(iv) The lumped mass model is a reliable practical tool for earthquake resistant design of structure.

Saha et.al.(1993)

Seismic analysis of reactor building of Nuclear power plant of India has been performed idealising the system as a beam model and also an axisymmetric model (ASM). The results obtained by these two methods were compared. In both the cases the effect of Soil-structure interaction have been taken into account. In the axisymmetric model the structure was modelled as two noded shell element or 4 noded solid elements. The degree of descretization, boundary

limits and representation of non-axisymmetric internal structural subsystem into a dynamically equivalent axisymmetric sub system have been established by parametric studies and trial solutions. The supporting soil medium has been considered to be homogeneous, isotropic elastic half space. Since the lower boundary of the axisymmetric model was at a depth much lower than that of the Beam model, deconvolution of the specified Free-field motion(FFM) has been performed using time domain procedure applied at the base of the model. The analysis has been performed by direct step by step integration method which treats soil and the structure integrally and a consistent seismic motion on the support boundaries of the model needs to be known.

In the beam model, soil medium was considered in the form of lumped soil mass and frequency independent soil springs.

The shear forces and moments for axisymmetric model were calculated from the mean stress and the geometry of the section. This has been done in order to neutralize bending effect which is not manifested in the results of beam model. The result shows that responses from axisymmetric model are 30% lesser than that from beam model. The study demonstrates the effect of soil-structure interaction and also the conservative nature of results obtained by beam method which justifies the suitability of beam model in designing the reactor building containment structure.

Morisita et.al.(1993)

Forced vibration tests of the Hualien 1/4 scale R.C.C. cylindrical containment soil-structure interaction test model have been conducted before backfill (without embedment) and after backfill (with embedment) in the stiff site environment at Haulien, Taiwan, for the purpose of defining basic dynamic characteristics of the soil-structure system.

The responses of test model and the surrounding soil surface were measured using displacement meters. The vibration tests were performed by applying sinusoidal exciting force generated by an exciter installed either on the basement or on the roof slab. The following conclusions are derived:

31

(i)   The dynamic characteristics of the soil-structure interaction system is not axisymmetric due to inhomogeneity of soil conditions.

(ii)   The basic dynamic characteristics (natural frequencies, damping factors and mode shapes) of the soil-structure system without embedment are obtained for principal axis whose direction appeared correlate the observations of exposed soil conditions at the site.

Kakodkar(1995)

Some issues like mathematical modelling and soil-structure interaction in aseismic design of nuclear structures and components are discussed by Kakodkar.

The author investigated that, in dynamic analysis of nuclear structures, lumped mass method gives conservative response prediction and unable to evaluate the seismic response of complex structural geometries, so in such a case, one has to take resource of Finite Element Method(FEM) for modelling of important structures such as the containment building, which enables the generation of the detailed stress picture. The author modelled the two containments (outer and inner) of a reactor building using axisymmetric finite elements and that the non-axisymmetric reactor internals have been converted into an equivalent axisymmetric system by matching their dynamic characteristics for the first mode of vibration using the modal mass concept. Soil-Structure Interaction not only introduces flexibility in the overall system but also introduces damping in the form of radiation damping.

A detailed FEM model of the soil strata is used to evaluate the SSI effects and concluded as per American Society of Civil Engineers (ASCE) standards that, if the shear wave velocity of soil is more than 1100 m/s and the corresponding shear strain in the soil medium is less than 0.001 %, a fixed base condition may be assumed, but not necessary, because for a 220 MWe PHWR reactor building wherein it has been observed that for shear wave velocity of 1600 m/s, the building does not behave as a fixed base case, because sometimes stiffness of super structure become comparable or even more than that of the soil stiffness for a particular direction of vibration.

Codal provision should thus be used with caution and with full understanding of the subject matter.

The author accounted for the various uncertainties in the structural frequencies owing to variation in parameters such as material properties of the structure and the soil, damping values, soil-structure interaction effects and the approximations involved in modelling techniques. So, in the absence of detailed parametric study, the author recommended that variation should be taken as +15% around the peaks which are associated (as a compensation for uncertainties), with the structural frequencies(USNRC RG.1.122).

2.5 Concluding Remarks

A critical review of literature on seismic behaviour of axisymmetric structures, simplified beam method and sophisticated finite element model, mode superposition and direct step-by-step integration methods in time domain, soil-structure interaction effects, modelling of boundaries and modelling of reactor internal structure, etc., are summarized. Based on the review following points emerge :

(i)   The three dimensional dynamic analysis is required for axisymmetric structures subjected to earthquake excitation to capture the real behaviour using axisymmetric finite element model. The one-dimensional beam model can not depict the real behaviour of structure subjected to earthquake excitation.

(ii) For the massive embedded structures such as nuclear reactor building resting on loose to medium soil, soil-structure interaction effects should be considered in the seismic analysis of the structure. To take the soil-structure interaction into account, the soil should be modelled along with the structure.

(iii) There is not much literature available on the effects of modelling of non-axisymmetric internal structure of nuclear reactor building as equivalent axisymmetric body.

(iv) It is observed that not much work has been done to study the effect of viscous boundaries in place of fixed boundaries of soil-structure system on the seismic behaviour of axisymmetric structures.

DYNAMIC ANALYSIS OF AXISYMMETRIC STRUCTURES -FINITE ELEMENT METHODOLOGY

3.1 Introduction

The finite element method is capable, in principle, of dealing with any two or three dimensional situations in structural analysis. Nevertheless the cost of solution increases greatly with each dimension added. It is therefore always desirable to search for alternatives which may reduce the computational labour. In many civil, mechanical, nuclear and aerospace engineering problems like cylindrical tanks, containment vessels, rotors, shells, cooling towers, chimneys, etc., the situation is such that the geometry and material properties do not vary along the circumferential direction. However the 'load' terms may still exhibit a variation in that direction, preventing the use of such simplifying assumptions as those which, for instance, permitted a two dimensional plane strain analysis to be substituted for a full three-dimensional treatment. The structure which satisfy this property is known as axisymmetric structure, which forms a class of three-dimensional analysis problem. The distinction with the general three-dimensional problem is that a cylindrical rather than a rectangular coordinate system is used in the definition of all pertinent relationships.

The problem of stress analysis of axisymmetric structure under axisymmetric load like vertical inertia load, (Fig. 3.1), is two-dimensional. The displacements are confined to the radial and vertical (axial) directions. In the axisymmetric loading, any radial displacement would indicate a strain in the circumferential direction and the associated stress will have to be considered. This is the main difference between axisymmetric analysis under axisymmetric loads and the plane stress or plane strain analysis (Berger, 1975). There may be certain situations where the loading are not axisymmetric. The examples of non-axisymmetric loadings are the wind acting on chimney or other such structures and the horizontal inertia force arising from ground accelerations due to earthquake on these structures, as shown in Figure 3.2. This would again involve some additional components of strains and stresses (Nayak, 1974).
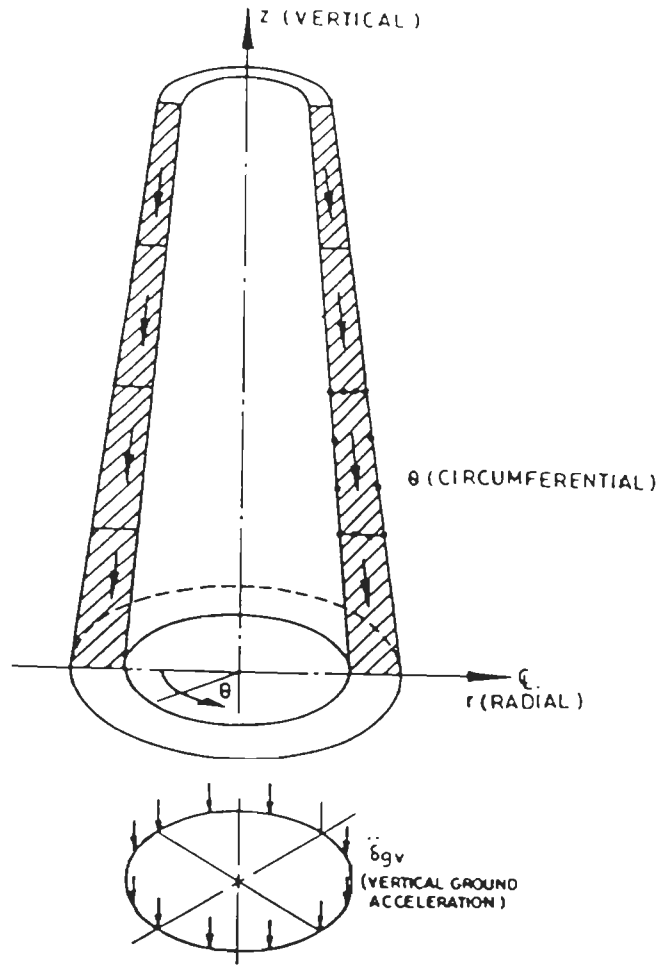
FIG.3·1 AXI-SYMMETRIC TOWER UNDER AXI-SYMMETRIC
LOAD (VERTICAL INERTIA LOAD)
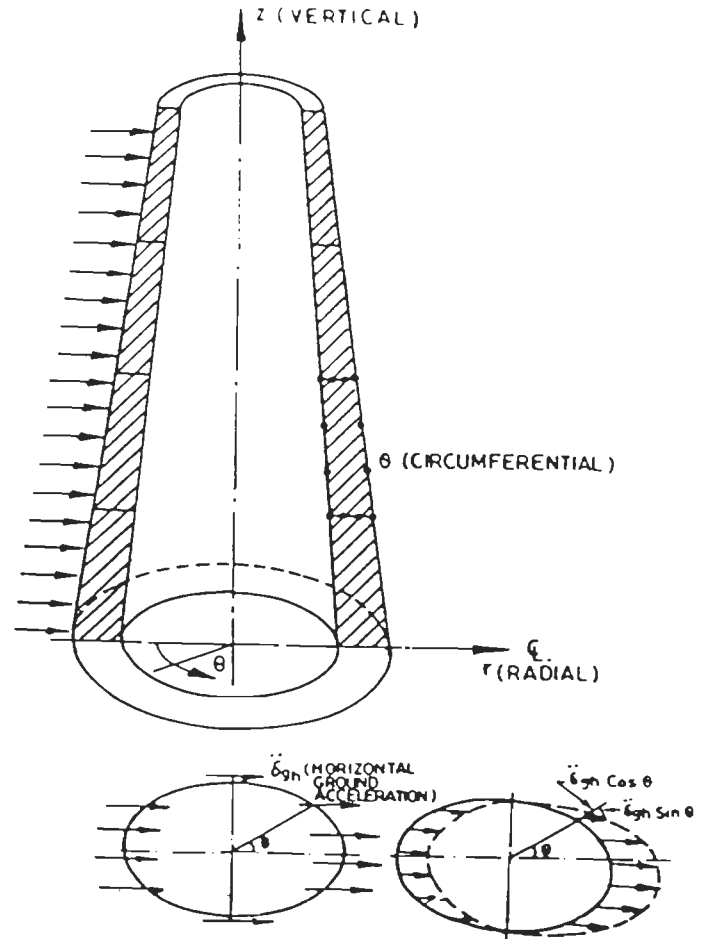
FIG.3·2 AXI-SYMMETRIC TOWER UNDER NON-AXI-SYMMETRIC
LOAD (HORIZONTAL INERTIA LOAD)

In cases where the geometry and elastic properties of axisymmetric bodies remain independent of circumferential co-ordinate 'θ' non-axisymmetric loading may be handled by the fourier series method. This involves expressing the given loading as a sum of several separate loadings and carrying out the analysis of each loading. Applying the principle of superposition the original problem thus can be solved by adding the solution of the component problems for each harmonic. Each separate analysis remain essentially two-dimensional, so that the original problem reduces to several uncoupled two-dimensional problems. This type of analysis is known as harmonic analysis.

3.2 Finite Element Formulation

In case of axisymmetric structures subjected to non-axisymmetric loads, not only the radial and axial displacements will have to be considered but also a tangential component associated with the angular direction 'θ' will be considered. The three displacement components, u, v and w in the radial, vertical and circumferential directions, respectively, can be expressed in cylindrical coordinates r, z and θ, as shown in Figure. 3.3.
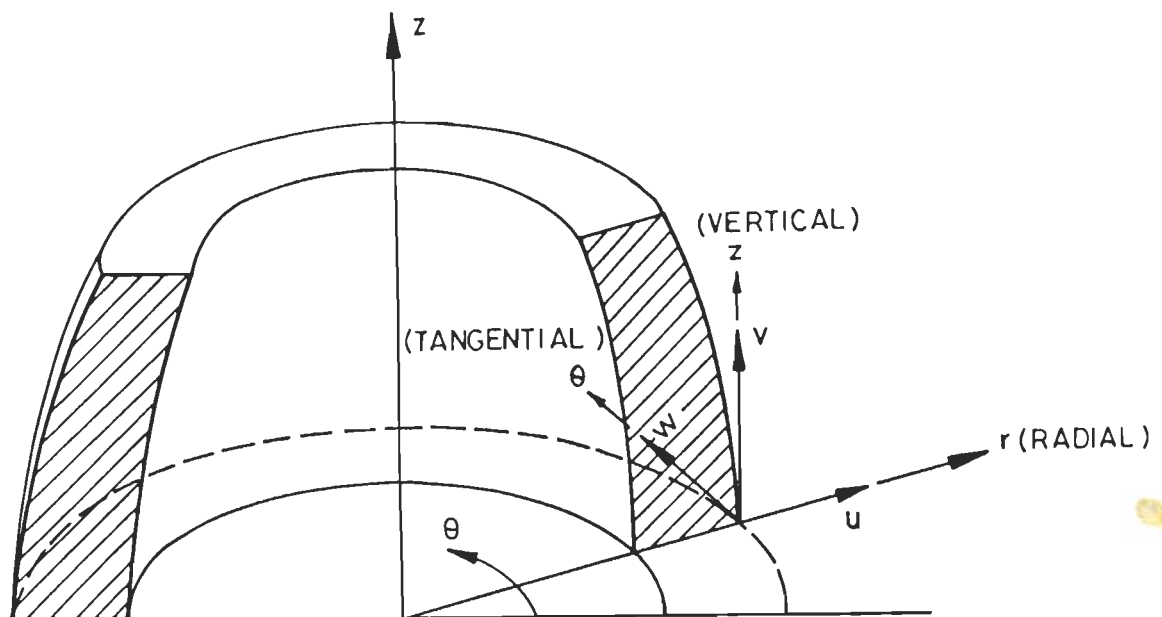
FIG. 3·3   AXISYMMETRIC BODY AND DISPLACEMENTS IN CYLINDRICAL COORDINATES (r, z, θ)

For the purpose of analysis, the non-axisymmetric loads are assumed to have been broken down into its radial (r), vertical (z) and tangential (θ) components; $P_r, P_z,$ and P_θ respectively. Now, following the standard procedure of Fourier series representation, *(Zienkiewicz,1977 and Gallagher, 1975)*, these can be written as

$$P_r(r,z,\theta) = \sum_{n=0}^{\infty} \left\{ P_{rn}^s(r,z)Cos\ n\theta + P_{rn}^a(r,z)Sin\ n\theta \right\}$$

$$P_z(r,z,\theta) = \sum_{n=0}^{\infty} \left\{ P_{zn}^s(r,z)Cos\ n\theta + P_{zn}^a(r,z)Sin\ n\theta \right\} \tag{3.1}$$

$$P_\theta(r,z,\theta) = \sum_{n=0}^{\infty} \left\{ P_{\theta n}^s(r,z)Sin\ n\theta - P_{\theta n}^a(r,z)Cos\ n\theta \right\}$$

where each term of above series is called a harmonic and the subscript, 'n', is the order of harmonic. The summations are on 'n' and extend over as many terms as are necessary for proper representation of circumferential variation of loading. Superscript 's' and 'a' refer to symmetric and antisymmetric components about $\theta = 0^o$ axis, respectively.

The resulting displacements have corresponding variation and can be written similarly as :

$$u(r,z,\theta) = \sum_{n=0}^{\infty} \left\{ u_n^s(r,z)Cos\ n\theta + u_n^a(r,z)Sin\ n\theta \right\}$$

$$v(r,z,\theta) = \sum_{n=0}^{\infty} \left\{ v_n^s(r,z)Cos\ n\theta + v_n^a(r,z)Sin\ n\theta \right\} \tag{3.2}$$

$$w(r,z,\theta) = \sum_{n=0}^{\infty} \left\{ w_n^s(r,z)Sin\ n\theta - w_n^a(r,z)Cos\ n\theta \right\}$$

For analysis of response to earthquake excitation including static stresses, only first two terms in the Fourier series survive and, therefore, only two separate two dimensional analysis are required; n=0 for static stresses and vertical component of earthquake ground motion, and n=1 for horizontal component of ground motion.

The generalized displacements and loads are functions of r and z only. Thus, what was originally a three-dimensional problem is reduced to a two-dimensional problem with substantial reduction in total degrees of freedom.

If the loading has symmetry with respect to some r-z plane, this plane may be defined as $\theta = 0^o$ plane and only the symmetric terms need be retained. The axially symmetric case is represented by the use of only the 'n=0' terms of the symmetric part, that is,

$$u(r,z,\theta) = u_0^s(r,z)$$

$$v(r,z,\theta) = v_0^s(r,z) \tag{3.2a}$$

$$w(r,z,\theta) = 0$$

Antisymmetric loading is represented by antisymmetric terms. Use of only the 'n = 0' terms of the antisymmetric part corresponds to pure torque and is given as:

$$u(r,z,\theta) = 0$$

$$v(r,z,\theta) = 0 \tag{3.2b}$$

$$w(r,z,\theta) = w_0^a(r,z)$$

The coupled translational and rocking variations are represented by the use of only 'n =1' terms of the symmetric parts, as given below :

$$u(r,z,\theta) = u_1^s(r,z) \cos\theta$$

$$v(r,z,\theta) = v_1^s(r,z) \cos\theta \tag{3.2c}$$

$$w(r,z,\theta) = -w_1^s(r,z) \sin\theta$$

Figure 3.4 shows the torsional, vertical, coupled translation and rocking vibrations of a rigid circular plate.

TORSION

$w = w_0^a$

$\theta = 0$

VERTICAL

$\theta = 0$

$v = v_0^s$

TRANSLATION

δ_H

θ

$\theta = 0$

$u = u_1^s \cos\theta$

$w = -w_1^s \sin\theta$

$u_1^s = w_1^s = \delta_H$

ROCKING

θ

δ_V

$v = v_1^s \cos\theta$

$(v_1^s = \delta_V)$
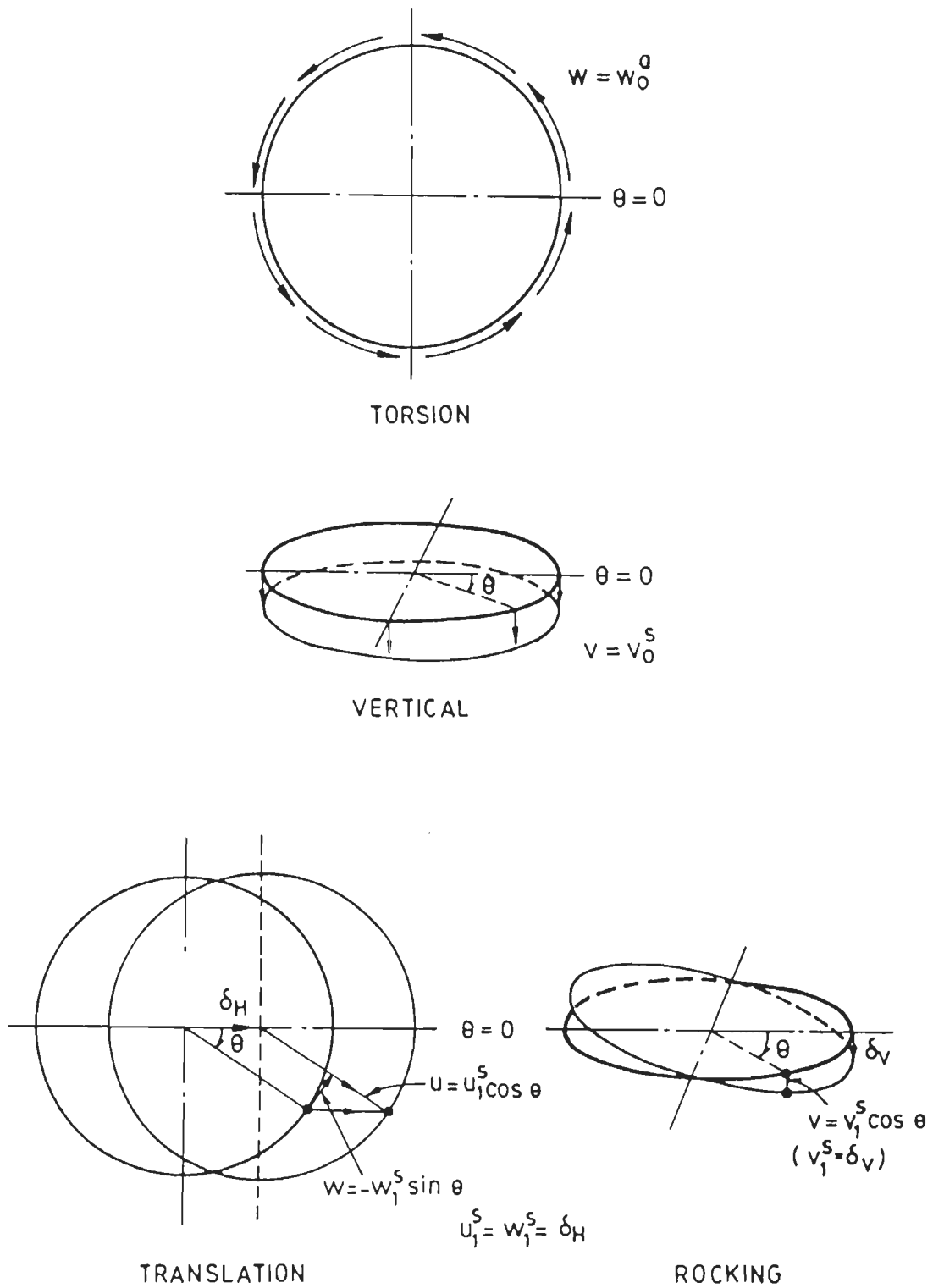
FIG.3·4 DISPLACEMENT FIELDS DUE TO THE RIGID BODY MOTIONS
OF THE CIRCULAR PLATE

39

3.2.1 Interpolation Functions

To represent the variation of displacement function within an element   in r-z plane, suitable interpolation functions are chosen. In an isoparametric formulation of the finite element method, the co-ordinates of any point within an element (Fig. 3.5) are interpolated as:

$$r = \sum_{i=1}^{Np} N_i\,(\xi,\eta)\,r_i$$

$$\text{(3.3)}$$

$$z = \sum_{i=1}^{Np} N_i\,(\xi,\eta)\,z_i$$

Where, r_i and z_i are the coordinates of nodes, i=1 to Np. The N_i 's are the interpolation or shape functions in the natural coordinate system (ξ,η) and 'Np' are the total number of nodes in a element.
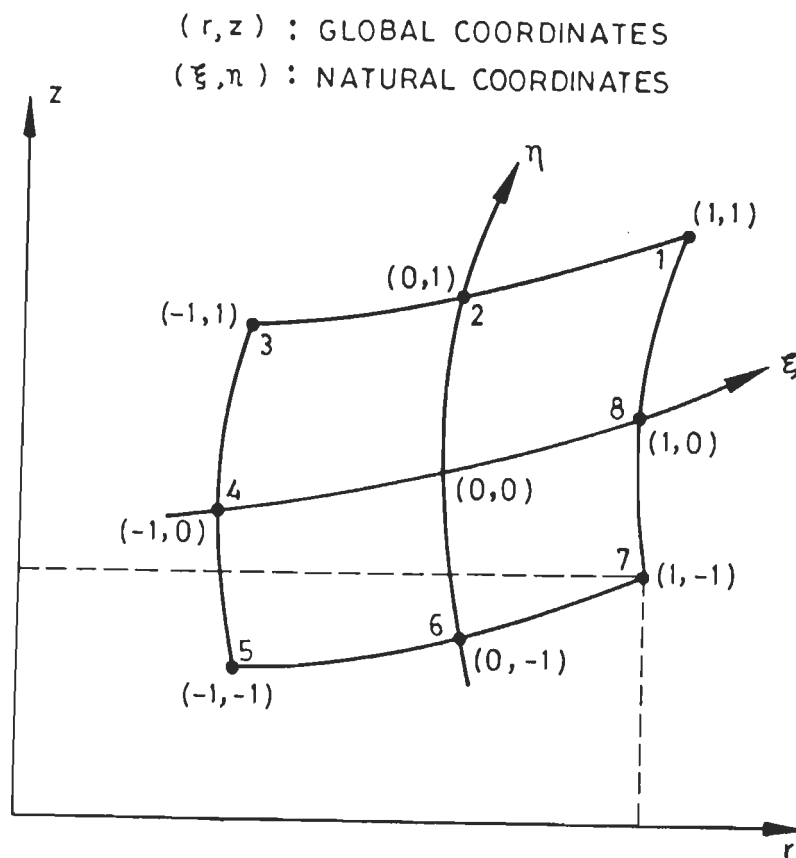
FIG.3·5   8-NODED ISOPARAMETRIC ELEMENT

The displacement field within an element is also approximated by the same interpolation functions. Therefore, combining Eqs. 3.2 and 3.3, one can obtain,

$$u(r,z,\theta) = \sum_{n=0}^{\infty}\sum_{i=1}^{Np} \left(N_i u_{in}^s \cos n\theta + N_i u_{in}^a \sin n\theta \right)$$

$$v(r,z,\theta) = \sum_{n=0}^{\infty}\sum_{i=1}^{Np} \left(N_i v_{in}^s \cos n\theta + N_i v_{in}^a \sin n\theta \right) \tag{3.4}$$

$$w(r,z,\theta) = \sum_{n=0}^{\infty}\sum_{i=1}^{Np} \left(N_i w_{in}^s \sin n\theta - N_i w_{in}^a \cos n\theta \right)$$

3.2.2 Stress-Strain Relationship

Figure 3.6 shows the components of stresses in an element. These stresses are related to the corresponding strain components by the following relationship:

$$\underline{\sigma} = \underline{D}\,\underline{\varepsilon} \tag{3.5}$$

where $\underline{\sigma}$ is the stress vector,

$$\underline{\sigma} = \left(\sigma_r, \sigma_z, \sigma_\theta, \tau_{rz}, \tau_{r\theta}, \tau_{\theta z} \right)^T \; ;$$

$\underline{\varepsilon}$ is the strain vector,

$$\underline{\varepsilon} = \left(\varepsilon_r, \varepsilon_z, \varepsilon_\theta, \gamma_{rz}, \gamma_{r\theta}, \gamma_{\theta z} \right)^T \; ;$$

and $\underline{D}$ is the elasticity matrix,

$$\underline{D} = \frac{2G}{(1-2\nu)} \begin{bmatrix} (1-\nu) & \nu & \nu & 0 & 0 & 0 \\ & (1-\nu) & \nu & 0 & 0 & 0 \\ & & (1-\nu) & 0 & 0 & 0 \\ & & & (0.5-\nu) & 0 & 0 \\ & -symmetric- & & & (0.5-\nu) & 0 \\ & & & & & (0.5-\nu) \end{bmatrix} \tag{3.5a}$$

where G = shear modulus, and
       ν = Poisson's ratio
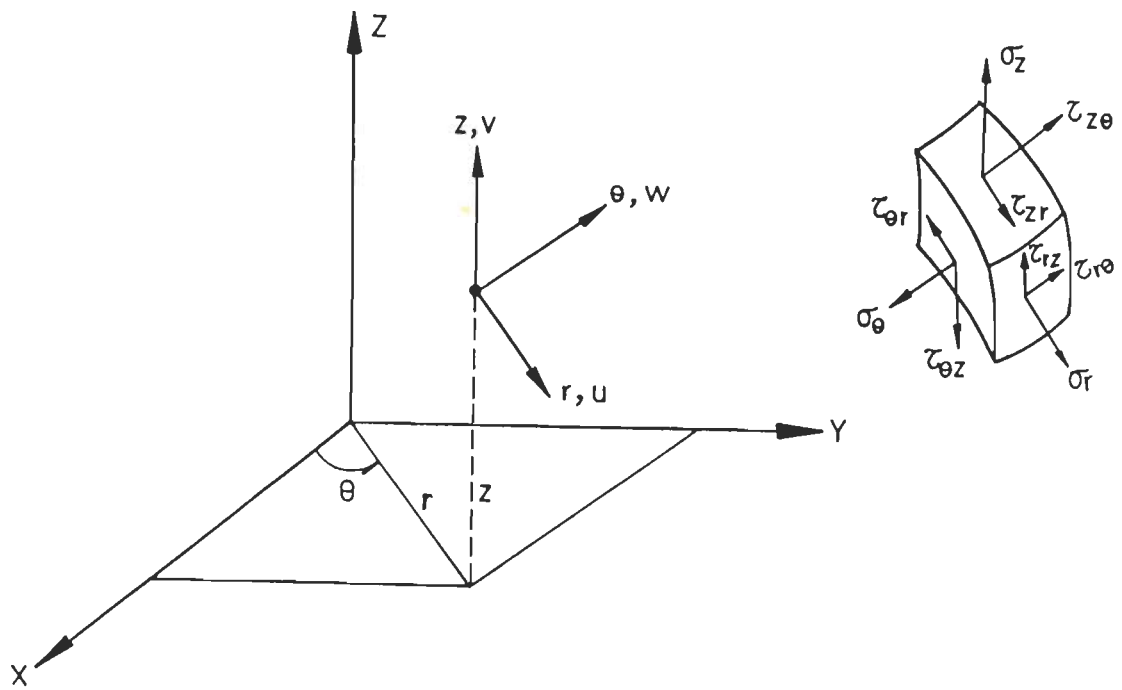
FIG. 3·6   STRESSES IN CYLINDRICAL COORDINATES (r, z, θ)

3.2.3 Strain Displacement Relationship

The strains are related to displacements by the relation

$$\underline{\varepsilon} = \underline{L}\,\underline{\delta} \tag{3.6}$$

where $\underline{\varepsilon}$ is the strain vector ;
$\underline{L}$ is partial derivative matrix, known as strain operator,

$$\underline{L} = \begin{bmatrix} \partial/\partial r & 0 & 0 \\ 0 & \partial/\partial z & 0 \\ 1/r & 0 & (1/r).\partial/\partial \theta \\ \partial/\partial z & \partial/\partial r & 0 \\ (1/r).\partial/\partial \theta & 0 & (\partial/\partial r)-(1/r) \\ 0 & (1/r).\partial/\partial \theta & \partial/\partial z \end{bmatrix} \tag{3.6a}$$

and, $\underline{\delta}$ is a displacement vector, $\underline{\delta} = (u, v, w)^{T}$.

Combining Eqs. 3.4 and 3.6, taking only symmetric terms of displacements; one can obtain,

$$\underline{\varepsilon} = \sum_{n=0}^{\infty} \sum_{i=1}^{Np} \underline{B}_{in}\,\underline{\delta}_{in}$$

(3.7)

where,

$$\underline{B} = \begin{bmatrix} \dfrac{\partial N_i}{\partial r}\cos n\theta & 0 & 0 \\[2ex] 0 & \dfrac{\partial N_i}{\partial z}\,Cos\,n\theta & 0 \\[2ex] \dfrac{1}{r}N_i\,Cos\,n\theta & 0 & \dfrac{n\,N_i}{r}\,Cos\,n\theta \\[2ex] \dfrac{\partial N_i}{\partial z}\,Cos\,n\theta & \dfrac{\partial N_i}{\partial r}\,Cos\,n\theta & 0 \\[2ex] -\dfrac{n\,N_i}{r}\,Sin\,n\theta & 0 & \left\{\dfrac{\partial N_i}{\partial r} - \dfrac{N_i}{r}\right\}Sin\,n\theta \\[2ex] 0 & -\dfrac{n\,N_i}{r}\,Sin\,n\theta & \dfrac{\partial N_i}{\partial z}\,Sin\,n\theta \end{bmatrix}$$

(3.7a)

$\underline{B}$ is the strain shape function matrix and expressed as,

$$\underline{B} = \underline{L}\,\underline{N}$$

(3.7b)

$\underline{N}$ is displacement shape function matrix.

Since the interpolation functions N_i 's are given in terms of natural coordinates (ξ, η) the partial derivatives $\partial N / \partial r$ and $\partial N / \partial z$ in Eq.3.7a are obtained by using the chain rule :

$$\begin{bmatrix} \dfrac{\partial}{\partial \xi} \\[2ex] \dfrac{\partial}{\partial \eta} \end{bmatrix} \begin{bmatrix} \dfrac{\partial r}{\partial \xi} & \dfrac{\partial z}{\partial \xi} \\[2ex] \dfrac{\partial r}{\partial \eta} & \dfrac{\partial z}{\partial \eta} \end{bmatrix} \begin{bmatrix} \dfrac{\partial}{\partial r} \\[2ex] \dfrac{\partial}{\partial z} \end{bmatrix} = [J]\begin{bmatrix} \dfrac{\partial}{\partial r} \\[2ex] \dfrac{\partial}{\partial z} \end{bmatrix}$$

(3.8)

Where, $[\underline{J}]$ is the Jacobian matrix, the elements of which can be obtained by differentiating Eq.3.3, that is,

$$\partial r / \partial \xi = \sum_{i=1}^{Np} \left(\partial N_i / \partial \xi \right).r_i \tag{3.8a}$$

Upon inversion of Eq. 3.8, one gets

$$\begin{bmatrix} \dfrac{\partial}{\partial r} \\ \dfrac{\partial}{\partial z} \end{bmatrix} = \dfrac{1}{|J|} \begin{bmatrix} \dfrac{\partial z}{\partial \eta} & \dfrac{-\partial z}{\partial \xi} \\ \dfrac{-\partial r}{\partial \eta} & \dfrac{\partial r}{\partial \xi} \end{bmatrix} \begin{bmatrix} \dfrac{\partial}{\partial \xi} \\ \dfrac{\partial}{\partial \eta} \end{bmatrix} \tag{3.8b}$$

Where $\quad |\underline{J}| = \dfrac{\partial r}{\partial \xi}.\dfrac{\partial z}{\partial \eta} - \dfrac{\partial r}{\partial \eta}.\dfrac{\partial z}{\partial \xi},$ $\tag{3.8c}$

is the determinant of the Jacobian matrix which must always be positive to satisfy Equation. 3.7. A non-positive Jacobian, $|\underline{J}|$, implies that the transformation from global (r, z) to natural (ξ, η) coordinates is not unique. This may be caused by the angle between adjacent side of the element being greater than $180°$ or by node sequencing errors during input. The Jacobian also represents the conversion of the volume differential from global to natural coordinates, as under:

$$dV = (r.d\theta).dr.dz = (r.d\theta)|J| d\xi.d\eta \tag{3.9}$$

3.2.4 Element Matrices

The element stiffness and mass matrices can be obtained using the principal of virtual displacements which can be stated as :

$$\int_V d\underline{\ddot{\delta}}^T \underline{\delta}\rho dV + \int_V d\underline{\varepsilon}^T \underline{\sigma} dV - \int_V d\delta^T \underline{P}_n dV = 0 \tag{3.10}$$

where $\quad \underline{\delta} = (u,v,w)^T$

Substituting Eqs. 3.4, 3.5 and 3.7 into Eq. 3.10, one gets for element 'e',

$$\sum_{m=0}^{\infty} d\,\underline{\delta}^{e^T}_{-m} \left[\sum_{n=0}^{\infty} \left(\int_{V^e} \rho \underline{N}^T_{-m} \underline{N}_{-n} dV \,\underline{\ddot{\delta}}^e_{-n} + \int_{V^e} \underline{B}^T_{-m} \underline{D}\,\underline{B}_{-n} dV \,\underline{\delta}^e_{-n} - \int_{V^e} \underline{N}^T_{-m} \underline{P}_{-n} dV \right) \right] = 0 \tag{3.10a}$$

44

or, $\quad \sum\limits_{m=0}^{\infty} d\, \delta^{e^T}_{-m} \left[\sum\limits_{n=0}^{\infty} \left(M^e_{-mn} \ddot{\delta}^e_{-n} + K^e_{-mn} \delta^e_{-n} - P^e_{-mn} \right) \right] = 0 \qquad \text{(3.10b)}$

which leads to coupled equations of motion, as :

$$M^e_{-mn} \ddot{\delta}^e_{-n} + K^e_{-mn} \delta^e_{-n} - P^e_{-mn} = 0 \qquad \text{(3.11)}$$

where,

$$M^e_{-mn} = \int\limits_{V^e} \rho N^T_{-m} N_{-n}\, r\, dr\, dz\, d\theta$$

$$K^e_{-mn} = \int\limits_{V^e} B^T_{-m} \underline{D}\, B_{-n}\, r\, dr\, dz\, d\theta \qquad \text{(3.11a)}$$

$$P^e_{-mn} = \int\limits_{V^e} N^T_{-m} P_{-n}\, r\, dr\, dz\, d\theta$$

M^e_{-mn}, K^e_{-mn} and P^e_{-mn} are the consistent mass matrix, stiffness matrix and load vector, respectively, for element 'e'. The above integrals for an element 'e' can be transformed to natural coordinate system using Eq. 3.9, as below :

$$M^e_{-mn} = |\underline{J}| \int\limits_{-1}^{1} \int\limits_{-1}^{1} \int\limits_{0}^{2\pi} \rho N^T_{-m} N_{-n}\, r\, d\xi\, d\eta\, d\theta$$

$$K^e_{-mn} = |\underline{J}| \int\limits_{-1}^{1} \int\limits_{-1}^{1} \int\limits_{0}^{2\pi} B^T_{-m} \underline{D}\, B_{-n}\, r\, d\xi\, d\eta\, d\theta \qquad \text{(3.12)}$$

$$P^e_{-mn} = |\underline{J}| \int\limits_{-1}^{1} \int\limits_{-1}^{1} \int\limits_{0}^{2\pi} N^T_{-m} \underline{P}_n\, r\, d\xi\, d\eta\, d\theta$$

in which ρ, is the mass density and r, can be expressed in terms of shape functions as given in Eq. 3.3.

In the above Equations. 3.12, integration in θ-directions can be carried out explicitly, giving rise to the following integrals :

$$I_1 = \int\limits_{0}^{2\pi} \cos m\theta \cos n\theta\, d\theta = 0,\ m \neq n$$

$$2\pi,\ m = n = 0 \qquad \text{(3.12a)}$$

$$\pi,\ m = n = 1$$

$$I_2 = \int_0^{2\pi} \sin m\theta \sin n\theta \, d\theta = 0, \; m \neq n$$

$$0, \; m = n = 0 \tag{3.12b}$$

$$\pi, \; m = n = 1$$

$$I = \int \sin m\theta \cos n\theta \, d\theta = 0 \text{ for all values of m and n.} \tag{3.12c}$$

Since the integrals are equal to zero for $m \neq n$, it follows that,

$$\underset{-mn}{M^e} = 0, \; \underset{-mn}{K^e} = 0, \; \underset{-mn}{P^e} = 0; \; for \; m \neq n \tag{3.12d}$$

Therefore Eq. 3.11 reduces to the uncoupled form as :

$$\underset{-n}{M^e} \, \underset{-n}{\ddot{\delta}^e} + \underset{-n}{K^e} \, \underset{-n}{\delta^e} = \underset{-n}{P^e} \tag{3.12e}$$

Integrals of Eq. 3.11 in the ξ and η directions, are evaluated numerically using the Gaussian quadrature. Typical integration grids are shown in Figure 3.7.

3.2.5 Harmonic coefficient

The harmonic coefficients for the antisymmetric and symmetric components of loadings in Eq. 3.1 can be expressed as:

For n =1

$$P_r^s = \frac{1}{\pi} \int_0^{2\pi} P_r \, Cos\,\theta d\theta \qquad\qquad P_r^a = \frac{1}{\pi} \int_0^{2\pi} P_r \, Sin\,\theta d\theta$$

$$P_z^s = \frac{1}{\pi} \int_0^{2\pi} P_z \, Cos\,\theta d\theta \qquad\qquad P_z^a = \frac{1}{\pi} \int_0^{2\pi} P_z \, Sin\,\theta d\theta \tag{3.13}$$

$$P_\theta^s = \frac{1}{\pi} \int_0^{2\pi} P_\theta \, Sin\,\theta d\theta \qquad\qquad P_\theta^a = \frac{-1}{\pi} \int_0^{2\pi} P_\theta \, Cos\,\theta d\theta$$

For n = 0

$$P_r^s = \frac{1}{2\pi} \int_0^{2\pi} P_r \, d\theta \qquad\qquad P_r^a = 0$$

$$P_z^s = \frac{1}{2\pi} \int_0^{2\pi} P_z \, d\theta \qquad\qquad P_z^a = 0 \qquad\qquad (3.13a)$$

$$P_\theta^s = 0 \qquad\qquad P_\theta^a = \frac{-1}{2\pi} \int_0^{2\pi} P_\theta \, d\theta$$
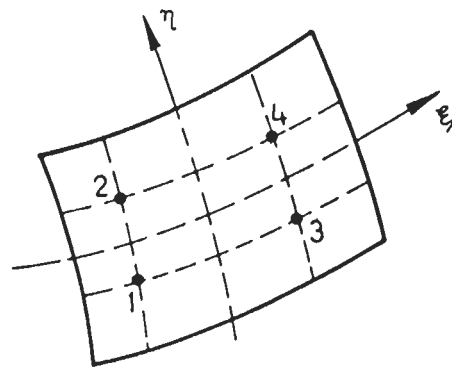
2×2 INTEGRATION POINTS
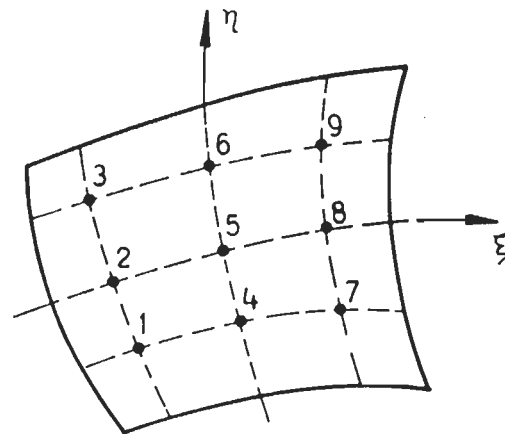
3×3 INTEGRATION POINTS

FIG.3·7 TYPICAL INTEGRATION GRIDS

Harmonics for earthquake loading

Variation of excitation due to horizontal and vertical components of earthquake ground motion of axisymmetric structures results in non-axisymmetric loading. The effective external loads associated with earthquake ground motion along $\theta = 0^o$ plane are :

$$P_r(r,z,\theta) = \rho(r,z)\,\ddot{\delta}_{gh}(t)\cos\theta$$

$$P_z(r,z,\theta) = \rho(r,z)\,\ddot{\delta}_{gv}(t) \tag{3.13b}$$

$$P_\theta(r,z,\theta) = -\rho(r,z)\,\ddot{\delta}_{gh}(t)\sin\theta$$

where $\ddot{\delta}_{gh}(t)$ *and* $\ddot{\delta}_{gv}(t)$, respectively, denote the horizontal and vertical components of ground motion, and ρ, is the mass density of the structural material.

Harmonics for horizontal components of ground motion

Harmonic coefficients in Eq. 3.1 for the loading in radial direction due to horizontal components of ground motion can be expressed as below :

For symmetric part of loading,

$$P_{rn}^s = \frac{1}{\pi}\int_0^{2\pi} P_r \cos n\theta\, d\theta$$

$$= \frac{1}{\pi}\int_0^{2\pi}\left[\rho\ddot{\delta}_{gh}(t)\cos\theta\right]\cos n\theta\, d\theta$$

$$= \rho\ddot{\delta}_{gh}(t),\ \textit{for}\ n = 1$$

$$= 0,\ \textit{for}\ n \neq 1$$

For antisymmetric part of loading,

$$P_{rn}^a = \frac{1}{\pi} \int_0^{2\pi} P_r \sin n\theta \, d\theta$$

$$= \frac{1}{\pi} \int_0^{2\pi} \left[\rho \ddot{\delta}_{gh}(t) \cos \theta \right] \sin n\theta \, d\theta$$

$$= 0, \text{ for all values of } n.$$

Similarly, the harmonic coefficients for the loading in circumferential direction can be expressed as :

$$P_{\theta n}^s = \frac{1}{\pi} \int_0^{2\pi} P_\theta \sin n\theta \, d\theta$$

$$= \frac{1}{\pi} \int_0^{2\pi} \left[-\rho \ddot{\delta}_{gh}(t) \sin \theta \right] \sin n\theta \, d\theta$$

$$= -\rho \ddot{\delta}_{gh}(t), \text{ for } n = 1$$

$$= 0, \text{ for } n \neq 1 \text{ and}$$

$$P_{\theta n}^a = \frac{-1}{\pi} \int_0^{2\pi} P_\theta \cos n\theta \, d\theta$$

$$= \frac{-1}{\pi} \int_0^{2\pi} \left[-\rho \ddot{\delta}_{gh}(t) \sin \theta \right] \cos n\theta \, d\theta$$

$$= 0, \text{ for all values of } n$$

From above, it is inferred that for horizontal components of earthquake loading, only the terms 'n = 1' of the Fourier series are required. Also, only symmetrical components of loading appear into analysis and the antisymmetric components vanish (Figure.3.8).

FINITE ELEMENT
IDEALIZATION

HORIZONTAL GROUND
ACCELERATION

RELATIVE DISPLACEMENT
OF NODAL CIRCLE i
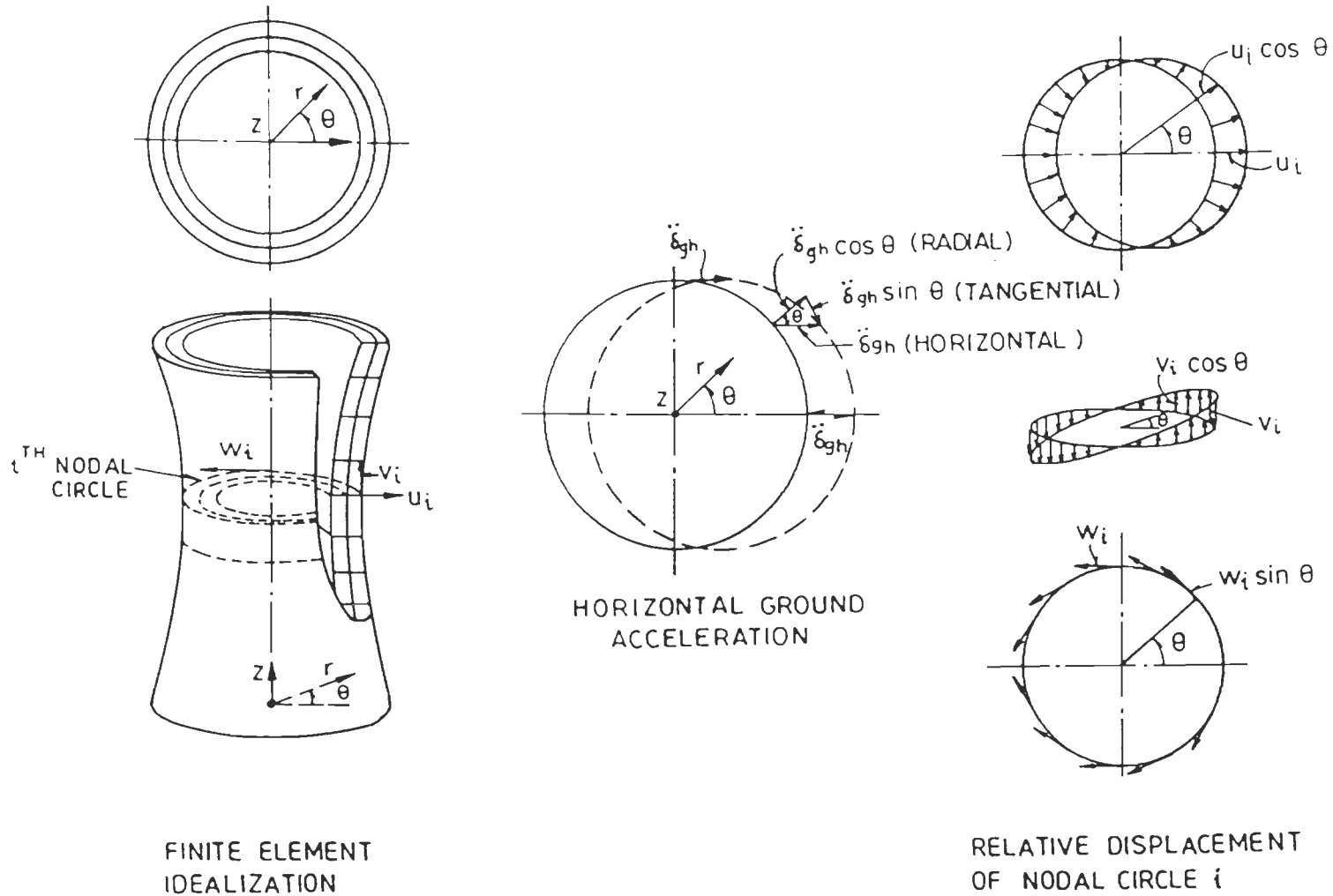
FIG. 3·8 AXISYMMETRIC STRUCTURE SUBJECTED TO HORIZONTAL GROUND MOTION

50

Harmonics for vertical component of ground motion

For vertical component of earthquake loading the harmonic coefficients are :

$$P_{zn}^s = \frac{1}{2\pi} \int_0^{2\pi} P_z \cos n\theta \, d\theta$$

$$= \frac{1}{2\pi} \int_0^{2\pi} \rho \ddot{\delta}_{gv}(t) \cos n\theta \, d\theta$$

$$= 0, \text{ for } n \geq 1$$

$$= \rho \ddot{\delta}_{gv}(t), \text{ for n = 0, and}$$

$$P_{zn}^a = 0, \quad \text{for } n = 0$$

Therefore ,the symmetric terms for n = 0 of the Fourier series are required for vertical component of earthquake and only symmetrical component of loading appears into analysis.

3.2.6 Equations of Motion

If a viscous form of damping (Rayleigh damping) is assumed, the force equilibrium equations for the linear elastic system subjected to ground motion may be expressed by the following equations, (Bathe, !976):

$$\underline{M}\,\ddot{\underline{\delta}}(t) + \underline{K}\,\underline{\delta}(t) + \underline{C}\,\dot{\underline{\delta}}(t) = -\underline{M}\,\{1\}\,\ddot{\delta}_g(t) \tag{3.14}$$

where,

$\underline{M}$ = mass matrix of the system,
$\underline{K}$ = global stiffness matrix of the system,
$\underline{C}$ = damping matrix of the system,
$\ddot{\underline{\delta}}(t)$ = nodal point acceleration (relative) vector, at any time, t,
$\dot{\underline{\delta}}(t)$ = nodal point velocity (relative) vector, at any time, t,
$\underline{\delta}(t)$ = nodal point displacement (relative) vector, at any time, t,

$\ddot{\delta}_g(t)$ = ground acceleration vector at any time, t,

{1}   = unit vector containing zeros and ones
      = {1,0,-1} for horizontal ground motion and
      = {0,1,0) for vertical ground motion.

Each one of these matrices are function of harmonic 'n'. In finite element discretization, these are expressed as :

$$\underline{M} = \int_V N^T \rho \underline{N} \, dV$$

$$\underline{K} = \int_V B^T \underline{D} B \, dV \qquad\qquad (3.14a)$$

where $\underline{N}$ = shape function matrix
      ρ = mass density of material
      B = strain matrix and
      $\underline{D}$ = elasticity matrix

The response of a structure to earthquake motion depends on its own characteristics and those of the ground motion used.

The three methods are normally employed for the solution of this set of ordinary differential equations, for each method convenient representation of the damping matrix is assumed. These are :

(i)   Timewise mode superposition method

(ii)   Direct step-by-step time integration method

(iii) Complex response method in frequency domain

In this study, only the first two methods are used for evaluating the maximum seismic response of a structure. Therefore, the basic theory of first two methods is described herein.

3.3 Mode Superposition Method

This method involves the solution of the characteristic value problem represented by the free vibration of the system followed by the transformation to the principal coordinate determined as the characteristic shapes of the system (Roesset & Whitman, 1973). This procedure uncouples the system of simultaneous equations, so that each equation may be evaluated independently of the others (Bathe, 1976).

This method is based on the assumption of linear structural behaviour and requires evaluation of the characteristic value problem and transformation to the principal coordinates.

3.3.1 Eigen Values and Eigen Vectors

The undamped natural frequencies and mode shape vector can be obtained from the following equation.

$$\underline{M}\,\ddot{\underline{\delta}} + \underline{K}\,\underline{\delta} = \underline{0} \tag{3.15}$$

let $\qquad \delta = \phi\, e^{i\omega t}$ $\hfill$ (3.16)

where, ω = circular frequency of vibration in radian/sec.

$\qquad \phi$ = column mode shape vector

Combining Equations 3.15 and 3.16 , one can gets,

$$\underline{K}\,\underline{\phi} = \omega^2\, \underline{M}\,\underline{\phi} \tag{3.17}$$

Equation 3.17 can be solved for ω^2 *and* $\underline{\phi}$ using matrix deflation method. Having obtained the frequencies and mode shape coefficients, the response can be obtained as follows :

3.3.2. Normal Co-ordinates

The displacement vector $\underline{\delta}$ can be transformed into normal co-ordinate, $\underline{z}$, through modal matrix $\underline{\phi}$ as a linear combination of response in various modes (Clough & Penzien, 1982). e.g.

$$\underline{\delta} = \underline{\phi}\,\underline{Z} \tag{3.18}$$

Substitution of Eq. 3.18 in Eq. 3.14 and mathematical transformation uncouples the equation of motion as,

$$M^{*}\,\ddot{Z} + C^{*}\,\dot{Z} + K^{*}\,Z = R^{*} \tag{3.19}$$

where,

$$M^{*} = \underline{\phi}^{T}\,M\,\underline{\phi}$$

$$C^{*} = \underline{\phi}^{T}\,C\,\underline{\phi} \tag{3.20}$$

$$K^{*} = \underline{\phi}^{T}\,K\,\underline{\phi}$$

$$R^{*} = -\underline{\phi}^{T}\,M\,\{1\}\,\ddot{\underline{\delta}}_{g}(t)$$

3.3.3. Participation Factors

The mode shape $\underline{\phi}$ can be normalized such that M is an identity matrix. Then the typical diagonal element of $\underline{c}$ and $\underline{K}$ are $2\omega_{j}\varsigma_{j}$ and ω_{j}^{2} respectively, where ς_{j} is the damping factor in the jth mode. The Equation 3.14 would then consists of equations of the form, as given below:

$$\ddot{\underline{Z}}_{j} + 2\omega_{j}\,\varsigma_{j}\,\dot{\underline{Z}}_{j} + \omega_{j}^{2}\underline{Z}_{j} = C^{j}\,\ddot{\underline{\delta}}_{g}(t) \tag{3.21}$$

where

$$\begin{aligned} C^{j} &= -\left(C_{r} - C_{0}\right) && \text{(for horizontal vibrations)} \\ &= C_{z} && \text{(for vertical vibrations).} \end{aligned} \tag{3.22}$$

C_r, C_0 and C_z are mode participation factors in $r, 0$ and z direction respectively. These can be expressed as :

$$C_r = \frac{\sum\limits_{i=1}^{Nd} m_i\, u_i}{\sum\limits_{i=1}^{Nd} m_i \left(u_i^2 + v_i^2 + w_i^2 \right)} \tag{3.23}$$

$$C_0 = \frac{\sum\limits_{i=1}^{Nd} m_i\, w_i}{\sum\limits_{i=1}^{Nd} m_i \left(u_i^2 + v_i^2 + w_i^2 \right)}$$

and, $$C_z = \frac{\sum\limits_{i=1}^{Nd} m_i\, v_i}{\sum\limits_{i=1}^{Nd} m \left(u_i^2 + v_i^2 + w_i^2 \right)}$$

where, 'Nd' is total number of nodes in finite element mesh of a system.

3.3.4. Timewise Mode Superposition

The uncoupled Eqs. 3.21 can be integrated time wise, using step by step integration, to obtain $\underline{Z}_j(t)$ in different modes of vibration. The total response at any level for horizontal vibration is obtained by time wise superposition, as below :

$$\underline{\delta}_i(t) = \sum\limits_{j=1}^{Ma} \underline{\phi}_{ji}\, \underline{Z}_{ji}(t) \tag{3.24}$$

where, Ma = Number of modes

3.3.5 .Weighted Modal Damping

The viscous damping of different materials in shells, and in soil is different. A weighted damping approach based on the strain energy is used to obtain a representative damping for each mode.

Strain energy $= \dfrac{1}{2}\underline{\delta}^T \left[\int_V B^T D\,B\,dV \right] \underline{\delta}$ $\tag{3.25}$

55

where symbols have their usual meaning, weighted damping in j^{th} mode can be expressed as :

$$\varsigma_j = \frac{\sum\limits_{k=1}^{Nm} \psi_k \varsigma_j}{\sum\limits_{k=1}^{Nm} \psi_k} \qquad (3.26)$$

where Nm = total number of materials in the structure.

ψ_k = strain energy in a particular structural component

ς_j = damping factor in a particular mode.

3.3.6 Stresses

The stresses in an element is computed from the vector of modal displacement $\underline{\delta}_m$,

$$\underline{\sigma}_m = \underline{D}\,\underline{B}\,\underline{\delta}_m \qquad (3.27)$$

where, $\underline{\sigma}_m$ is modal stress vector

For horizontal vibrations the dynamic stress can be obtained from the modal stresses, as follows

$$\underline{\sigma}_d = \underline{\sigma}_m \left(C_r - C_\theta\right) \underline{Z}_j(t) \qquad (3.27a)$$

The timewise superposition of stresses in different modes can then be obtained as below :

$$\underline{\sigma} = \sum_{j=1}^{Ma} \underline{\sigma}_d \qquad (3.28)$$

where, Ma = number of modes

Stress components computed from Eq. 3.28 are the amplitudes around the circumference (components along $\theta = 0^o$ plane), the variation being given as

$$\sigma_r(0,t) = \sigma_r(t)\cos\theta$$

$$\sigma_z(0,t) = \sigma_z(t)\cos\theta$$

$$\sigma_\theta(0,t) = \sigma_\theta(t)\cos\theta \qquad\qquad (3.28a)$$

$$\tau_{rz}(0,t) = \tau_{rz}(t)\cos\theta$$

$$\tau_{r\theta}(0,t) = \tau_{r\theta}(t)\sin\theta$$

$$\tau_{\theta z}(0,t) = \tau_{\theta z}(t)\sin\theta$$

Circumferential variation of the important stresses such as bending stress (σ_z) and shear stress $(\tau_{\theta z})$ is shown in Figure 3.9.

3.4 Direct Step-by-Step Time Integration Method

Many structures are subjected to time varying loads such as impulse, blast, impact or earthquake loading; although a form of mode superposition has been adopted in dynamic stress analysis, yet it is a general practice to use time stepping procedure. In direct step-by-step time integration method, the Equation 3.14 is integrated using a numerical step-by-step procedure, the term 'direct' means that prior to the numerical integration, no transformation of the equation into a different form is carried out. There are a number of step-by-step integration methods that can be employed for the calculation of dynamic response of a structure. Such direct integration schemes may be broadly classified as (Bathe, 1976):

(i)   Explicit methods

(ii) Implicit methods
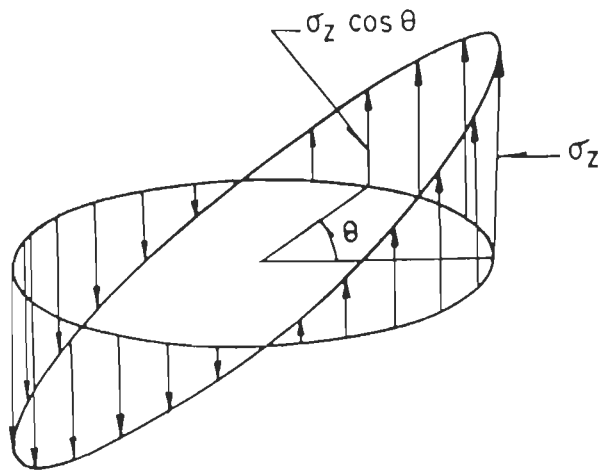
BENDING STRESS
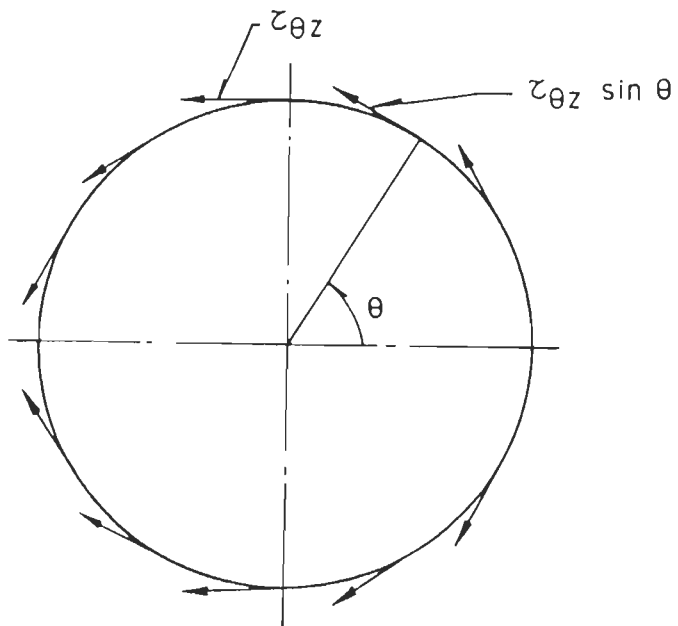
SHEARING STRESS

FIG.3·9 CIRCUMFERENTIAL VARIATION OF THE
IMPORTANT STRESS COMPONENTS

3.4.1 Explicit Methods

In an explicit scheme, the displacement at time $t+\Delta t$ ($\delta_{t+\Delta t}$) is obtained and the equation of equilibrium is considered at 't'. In these methods, relatively little computational effort is required for each time step since no formal matrix factorisation is necessary. Unfortunately, the method is conditionally stable and very small time steps are often needed and maximum time size is determined by the condition of stability. For example the central difference method.

3.4.2 Implicit Methods

In implicit scheme, the displacement ($\delta_{t+\Delta t}$) as well as equilibrium of equation is considered at $t+\Delta t$. In this scheme, a matrix factorisation is required which involve large computer core storage and more operations per time step than that required in explicit methods. This integration method is unconditionally stable if the solution for any initial conditions does not grow without bound for any step Δt, in particular when $\Delta t / T$ is large. Any errors in displacements, velocities and accelerations (for example due to round off in the computer) does not grow.

In the direct step-by-step integration method, the time scale is divided into a number of small steps of integration. With the knowledge of response at time t=0, the integration of equations proceed from one step to the next using time integration operator. Out of the available time integration operators implicit integration operators are considered most suitable for earthquake response of structural problems because of unconditional stability characteristics of these methods.

The Newmark's β and Wilson's θ methods provide an unconditionally stable time integration methods. The time step is normally considered $T_{min}/10$, where T_{min} is the time period of the last mode contributing in the total response.

In this thesis, Newmark's β method is used for the determination of displacements and stress histories . This method is based on the assumption that the acceleration changes linearly with time during a short period. This assumption provides linear relationship among displacements, velocities and accelerations; and has been known to be reasonable in solving numerically the

equation of motion of linear elastic system. In this method the difference equations for the displacements at the next time step $(t + \Delta t)$ involves the acceleration at the next time step $(t + \Delta t)$. Hence the solution is obtained by trial and error procedure involving iterations. The computational efficiency, stability and desired accuracy can be achieved by carefully choosing the numerical time stepping scheme and time step length Δt.

The incremental expressions of Newmark' β and Wilson' θ implicit integration methods are given as below,

Newmark's β Method

This is a general single step scheme and is popularly used in practice. This is derived in terms of two parameters; β and γ, which can be adjusted to yield different schemes.

In this method the expressions for velocity and displacement are written as :

$$\dot{\underline{\delta}}_{t+\Delta t} = \dot{\underline{\delta}}_t + \gamma \Delta t \, \ddot{\underline{\delta}}_{t+\Delta t} + (1 - \gamma) \Delta t \, \ddot{\underline{\delta}}_t \qquad (3.29)$$

$$\underline{\delta}_{t+\Delta t} = \underline{\delta}_t + \Delta t . \dot{\underline{\delta}}_t + (\Delta t)^2 (0.5 - \beta) \ddot{\underline{\delta}}_t + (\Delta t)^2 \beta \ddot{\underline{\delta}}_{t+\Delta t} \qquad (3.30)$$

where γ and β can be chosen to produce desired accuracy and stability. For $\gamma = 0.5$ and $\beta = 0.25$, we have constant average acceleration method which is an unconditionally stable method without numerical damping. For $\gamma = 0.5$ and $\beta = 1/6$, we have linear acceleration method.

The equilibrium equation at time $(t + \Delta t)$ can be written as :

$$\underline{M} \, \ddot{\underline{\delta}}_{t+\Delta t} + \underline{C} \, \dot{\underline{\delta}}_{t+\Delta t} + \underline{K} \, \underline{\delta}_{t+\Delta t} = \underline{R}_{t+\Delta t} \qquad (3.31)$$

The Eqs 3.29 and 3.30 are solved and obtained expressions for $\ddot{\delta}_{t+\Delta t}$ and $\dot{\delta}_{t+\Delta t}$, each in terms of the unknown displacements $\delta_{t+\Delta t}$ only. These two relations for $\ddot{\delta}_{t+\Delta t}$ and $\dot{\delta}_{t+\Delta t}$ are substituted into Eq 3.31 to solve for $\delta_{t+\Delta t}$, after which, using Eqs 3.29 and 3.30, $\ddot{\delta}_{t+\Delta t}$ and $\dot{\delta}_{t+\Delta t}$ can be calculated.

Solution of the formed differential equation gives $\Delta\underline{\delta}_t(\underline{\delta}_{t+\Delta t} - \underline{\delta}_t)$. Substitution of $\Delta\underline{\delta}_t$ in equations (3.29) and (3.30) produces,

$$\ddot{\underline{\delta}}_{t+\Delta t} = \frac{\Delta\underline{\delta}_t}{\beta(\Delta t)^2} - \frac{\dot{\underline{\delta}}_t}{\beta\Delta t} - \frac{\ddot{\underline{\delta}}_t}{2\beta} + \ddot{\underline{\delta}}_t \tag{3.32}$$

The resulting equation is,

$$\overset{\Theta}{\underline{K}}\,\underline{\delta}_{t+\Delta t} = \overset{\Theta}{\underline{R}}_{t+\Delta t} \tag{3.33}$$

Where, $\overset{\Theta}{\underline{K}} = \underline{K} + \left(1/\beta\Delta t^2\right)\underline{M} + (\gamma/\beta\Delta t)\,\underline{C}$

and $\overset{\Theta}{\underline{R}}_{t+\Delta t} = \underline{R}_{t+\Delta t} + \underline{M}\left(1/\beta\Delta t^2\right)\underline{\delta}_t + (1/\beta\Delta t)\dot{\underline{\delta}}_t + \left([1/2\beta]-1)\ddot{\underline{\delta}}_t\right) +$

$$\underline{C}\left\{(\gamma/\beta\Delta t)\underline{\delta}_t + ([\gamma/\beta]-1)\dot{\underline{\delta}}_t + ([\gamma/2\beta]-1)\Delta t\,\ddot{\underline{\delta}}_t\right)$$

Wilson's θ Method

It is also an extension of the linear acceleration method. The acceleration is assumed to be linear from time, t, to $t+\Delta t$, where $\theta \geq 1.0$. When $\theta = 1.0$, the method reduces to linear acceleration method. For unconditional stability, $\theta \geq 1.37$, usually $\theta = 1.40$. In this method the expressions for velocity and displacement are written as :

$$\dot{\underline{\delta}}_{t+\theta\Delta t} = \dot{\underline{\delta}}_t + \frac{\theta\Delta t}{2}\left(\ddot{\underline{\delta}}_{t+\theta\Delta t} + \ddot{\underline{\delta}}_t\right) \tag{3.34}$$

$$\underline{\delta}_{t+\theta\Delta t} = \underline{\delta}_t + \theta\Delta t.\dot{\underline{\delta}}_t + \left(\frac{\theta\Delta t}{6}\right)^2\left(2\ddot{\underline{\delta}}_t + \ddot{\underline{\delta}}_{t+\theta\Delta t}\right) \tag{3.35}$$

and, the equilibrium equation at $t + \theta\Delta t$ is,

$$\underline{M}\,\ddot{\underline{\delta}}_{t+\theta\Delta t} + \underline{C}\,\dot{\underline{\delta}}_{t+\theta\Delta t} + \underline{K}\,\underline{\delta}_{t+\theta\Delta t} = \underline{R}_{t+\theta\Delta t} \tag{3.36}$$

Where, $\underline{R}_{t+\tau} = \underline{R}_t + \theta\left(\underline{R}_{t+\tau} - \underline{R}\right), \tau = \theta\Delta t$ $\tag{3.36a}$

61

The resulting equation is,

$$\overset{\Theta}{\underset{-}{K}}\, \underline{\delta}_{t+\theta\Delta t} = \overset{\Theta}{\underset{-\ t+\theta\Delta t}{R}}$$

(3.37)

Where, $\overset{\Theta}{\underset{-}{K}} = K + \left[6/(\theta\Delta t)^2 \right] \underline{M} + [3/\theta\Delta t]\, \underline{C}$

and, $\overset{\Theta}{\underset{-\ t+\theta\Delta t}{R}} = \underline{R}_{t+\theta\Delta t} + \underline{M}\left(\left[6/(\theta\Delta t)^2 \right]\underline{\delta} + [6/(\theta\Delta t)]\,\dot{\underline{\delta}} + 2\ddot{\underline{\delta}} \right)$

$\qquad\qquad\qquad + \underline{C}\left([3/\theta\Delta t]\underline{\delta} + 2\dot{\underline{\delta}} + [\theta\Delta t/2]\,\ddot{\underline{\delta}} \right)$

SOIL-STRUCTURE INTERACTION EFFECTS

4.1 Introduction

It is a common practice to assume that the structure is attached to a rigid foundation and the influence of local properties of the ground on the response of the structure are ignored. The earthquake motions are assumed to be introduced of specified quantities at the support and are not influenced by the structure but in actual, the structure will interact with the surrounding soil. In many important cases such as earthquake excitation, the loading is applied to the soil region around the structure. Therefore, it is thus not permissible to analyse only the structure and the soil should be included in a model in some appropriate way. The soil is a semi-infinite medium, an unbounded domain; so the infinite extent of foundation is to be properly modelled.

The structural response may be affected or modified by the interaction with the soil as well as there may be feedback of energy from structure into the soil layer. Because of deformations within the soil immediately beneath the structure, the motion of the base of the structure may be different from the motion of the ground at some distance from the structure. If there is such a difference, there is soil-structure interaction. Soil-structure interaction generally affects both the horizontal and vertical motions of the base of the structure but perhaps the most important aspect of soil-structure interaction is to introduce rocking of the structure. The interaction phenomenon is affected by the following factors :

(i) The mechanism of energy exchange between the soil and structure,.

(ii) The local soil conditions,

(iii) The characteristics of the superimposed structure, and

(iv) The nature of excitation

4.2 Effects of Soil-structure Interaction

The important effects of taking soil-structure interaction into consideration are:

(i) The seismic input motion acting on the structure-soil system will change because of the amplification of the site (free-field response), the translational component will in many cases be larger than the control motion and, in addition, a significant rocking component will arise for an embedded structure. Each frequency component of the motion is affected differently. This amplification of the seismic motion is held responsible for the fact that structures founded on a deep soft-soil site have been damaged more severely in actual earthquake than have neighbouring structures founded on rock.

(ii) Increase in the natural time periods of the structure due to compressibility of foundation soil.

(iii) A change (usually increase) in its effective damping due to energy dissipated from the structure to the supporting soil by radiation and hysteretic action. The waves which are generated due to interaction effects do not get reflected back to the interface. This accounts for an energy loss due to radiation of waves and hence called a radiation damping.

(iv) It generally reduces the design forces in the structure as compared to those induced in the fixed base structure. The structure may, therefore, be designed conservatively without consideration of interaction. However, because of the contribution of foundation rocking, the horizontal displacements of the structure relative to the base may be larger than those to a fixed base condition. But at the same time, in case of flexible supported structure, a substantial part of its vibrational energy may be dissipated by the radiation of the waves into the supporting medium and by hysteretic action in the medium itself. The importance of later factor increases with increase in intensity of ground shaking. There is, of course, no counter-part of this effect of energy dissipation in a rigidly supported structure. The dissipation of vibrational energy by radiation of waves, termed as radiation

damping, increases the effective damping of the soil-structure system and thus causes reduction of stresses in the structure.

The consideration of all the above factors in dynamic analysis requires a detailed study of soil-structure problem in each individual case as below :

(i)   When a stiff structure rests on rocky foundation or stiff soil, the interaction effects are small and generally ignored.

(ii)   For the typical multi-storey structure which is generally rather flexible, while it rests on deformable ground (soft soil), soil-structure interaction effect becomes relatively unimportant.

(iii) For the stiffer structures, like the containment structure of nuclear power plant, resting on soft soil, interaction can have an influence on the response of structures to earthquakes. Hence, when a stiff structure rests on soft soil, the interaction effects are quite important and must be considered. In other words, evaluation of soil-structure interaction is important in the seismic analysis of massive and rigid structures supported on deformable ground.

(iv)   For a flexible structure resting on stiff soil, the interaction effect is unimportant.

4.3 Modelling of Soil-Structure System

An important limitation of the discretized model of the foundation medium is that such models necessarily have finite boundaries. Thus, a very important aspect to be considered in the modelling process is the extent of the foundation zone which must be included. As the model boundaries tend to retain the vibrational energy within the system and unless these are at great distances, it will inhibit radiation energy loss from the structure.

A realistic dynamic model of the soil requires the representation of the soil stiffness, material damping and radiation damping, allowing for strain dependence and variation of soil properties. For analyzing the problem of soil-

structure system (Fig. 4.1), the following two types of modelling techniques are in use :

(i)   Beam method

(ii) Finite element method

4.3.1 Beam Method

In this method, the structure is modelled by a numbers of two noded finite beam elements and the soil is assumed to be linearly elastic, isotropic and semi-infinite half space. The base of the structure is assumed to be supported by a system of frequency independent springs to simulate the soil-structure interaction effects (Fig. 4.2). In this study, the spring constants in horizontal, rocking and vertical degrees of freedom have been calculated using the formulae given by Novak(1972, 1973 and 1974). Such a model is a crude representation of actual structure as it treats the three-dimensional structure to one dimensional one. In such a model, the stresses in the shells, particularly at their junctions with the slab, cannot be properly estimated (Berdugo and Novak, 1972).
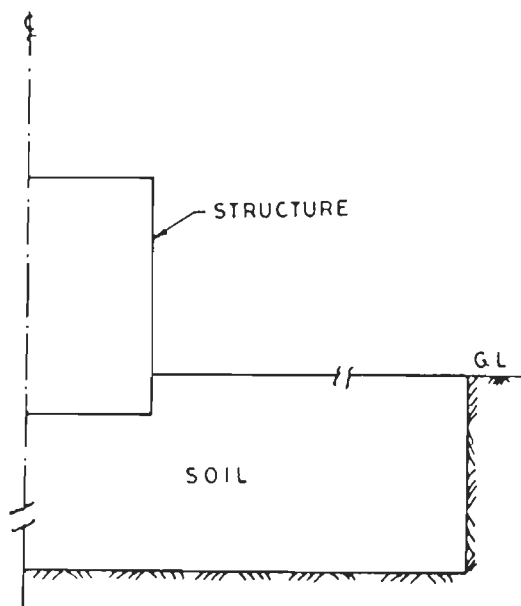
FIG. 4·1 SOIL- STRUCTURE SYSTEM   FIG. 4·2 BEAM MODEL OF SOIL- STRUCTURE SYSTEM
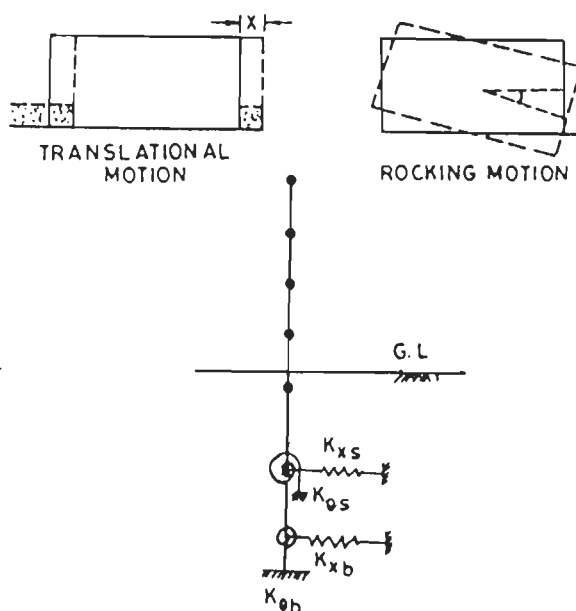
4.3.2 Finite Element Method (FEM)

Use of finite elements for modelling the foundation of a soil-structure system is the most comprehensive method available (Chu et.al., 1973 & Luco, 1974). Like the elastic half space model, it permits the radiation damping but has the major advantage of easily allowing changes of soil stiffness both horizontally and vertically to be explicitly formulated (Hadjian et.al., 1974 and 1988). The modelling of soil for such analysis depends on the geometry of the boundary and interfaces between different material properties as well as on the foundation system supporting the structure. Cheron et.al.(1981) and Singhal(1984) employed sub-structure method of axisymmetric finite element analysis in which structure and soil are considered as two sub systems. In this study, two dimensional soil model which has found considerable use in practical analysis of the axisymmetric system (soil and structure), has been used (Fig. 4.3). In this model, the soil boundaries are rotationally symmetric about the vertical axis, so that the radial and vertical coordinates are sufficient to define the geometry of the soil system as well as its finite element idealization. The axisymmetric structure is also rotationally symmetric about the same vertical axis. Luco & Westman(1971), Wass(1972), Kausel & Roesset(1974 & 1975) presented axisymmetric finite element two dimensional model for linear SSI problems of nuclear containment structures. Gassert(1983) and Singh(1973) described three dimensional FEM model of reactor building. Hwang et.al.(1975) employed a simplified three dimensional SSI study of axisymmetric structure.
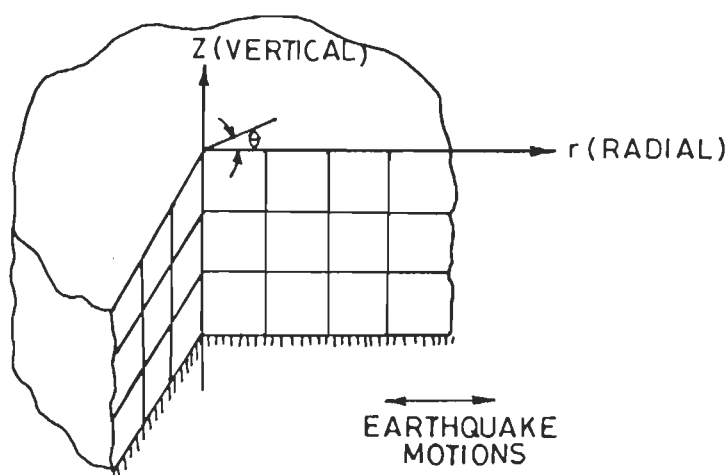
FIG. 4·3 AXISYMMETRIC FINITE ELEMENT MODEL OF FOUNDATION SYSTEM

4.4 Objectives

The main objectives of study in this Chapter are,

(i)   To examine the effect of extent of soil domain (mesh size of founding soil) on the seismic behaviour of the system.

(ii) To evaluate the significance of effects of soil-structure interaction on the seismic response of axisymmetric structures.

4.5 Assumptions in the Seismic Analysis of Axisymmetric Structures

(i)   The structure and the underlying soil are bonded and remain so throughout the period of ground shaking.

(ii) The motion of the foundation is assumed to be the same as the free-field ground motion.

(iii) The soil surrounding the structure is assumed to be linearly elastic and isotropic.

4.6 Ground Motions Used in the Study

The ground motion can be represented in many ways but the most comprehensive is the digitized earthquake time history. It is necessary to have some earthquake time histories acceleration record for vibrational analysis of structures.

In the present study, three different real earthquake ground motions (Krishna et.al. 1969 and 1994; Chandrasekaran & Das, 1992) have been selected (Table 4.1 and Figures through 4.4 to 4.6) and their influence on structural response has been studied.
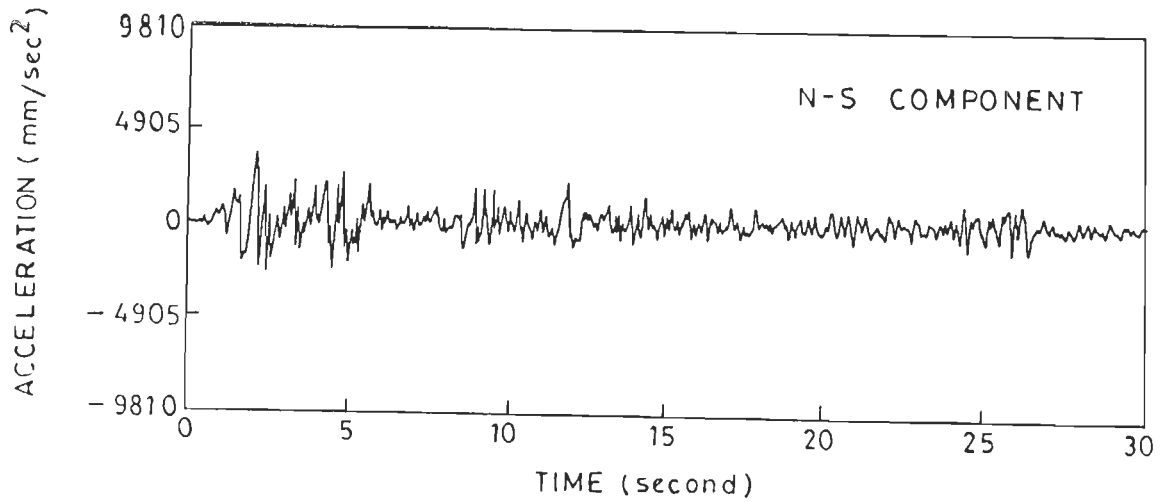
EL-CENTRO EARTHQUAKE ACCELERATION RECORD
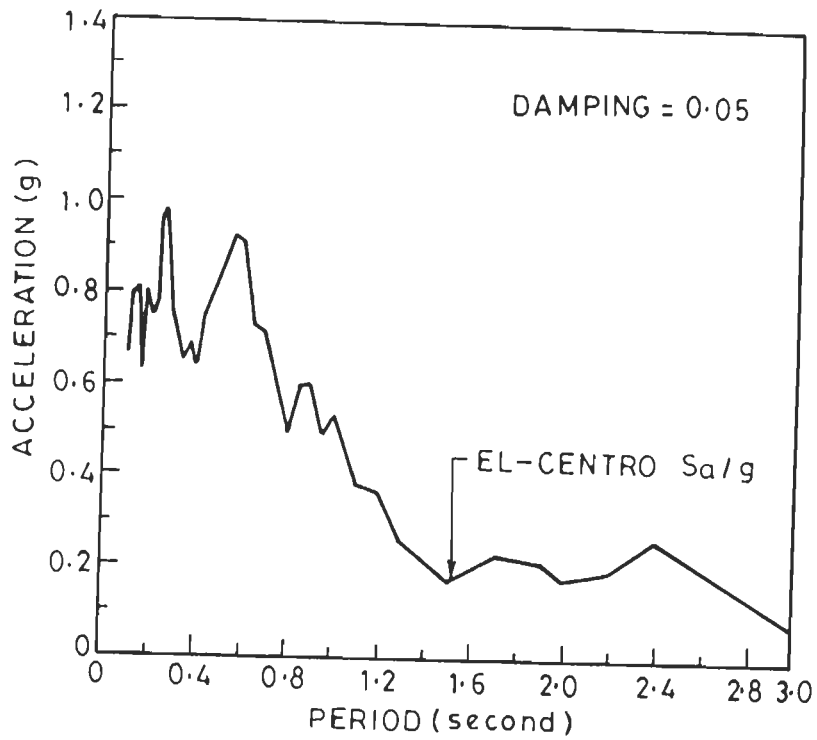
ACCELERATION RESPONSE SPECTRA OF EL-CENTRO
EARTHQUAKE

FIG. 4·4   ACCELERATION RECORD AND RESPONSE
SPECTRA OF EL-CENTRO EARTHQUAKE
(MAY 18,1940)
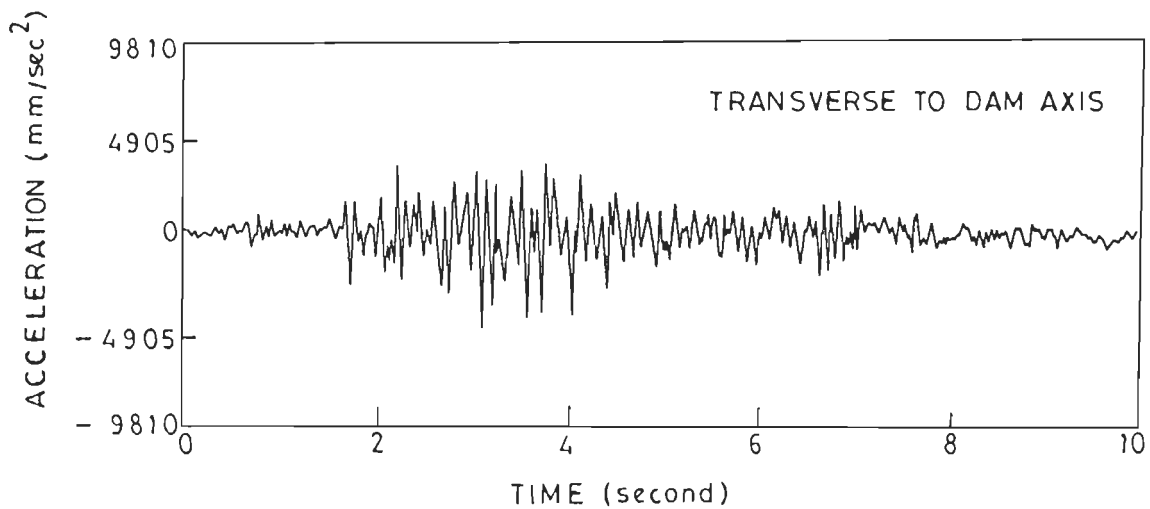
KOYNA EARTHQUAKE ACCELERATION RECORD
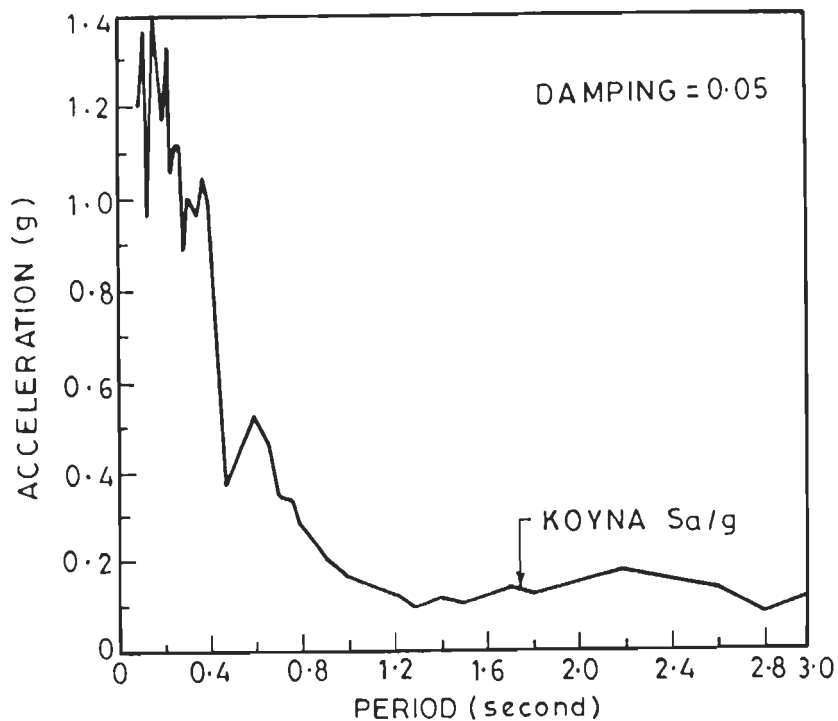
ACCELERATION RESPONSE SPECTRA OF
KOYNA EARTHQUAKE

FIG. 4·5 ACCELERATION RECORD AND RESPONSE
SPECTRA OF KOYNA EARTHQUAKE
(DEC. 11 , 1967)
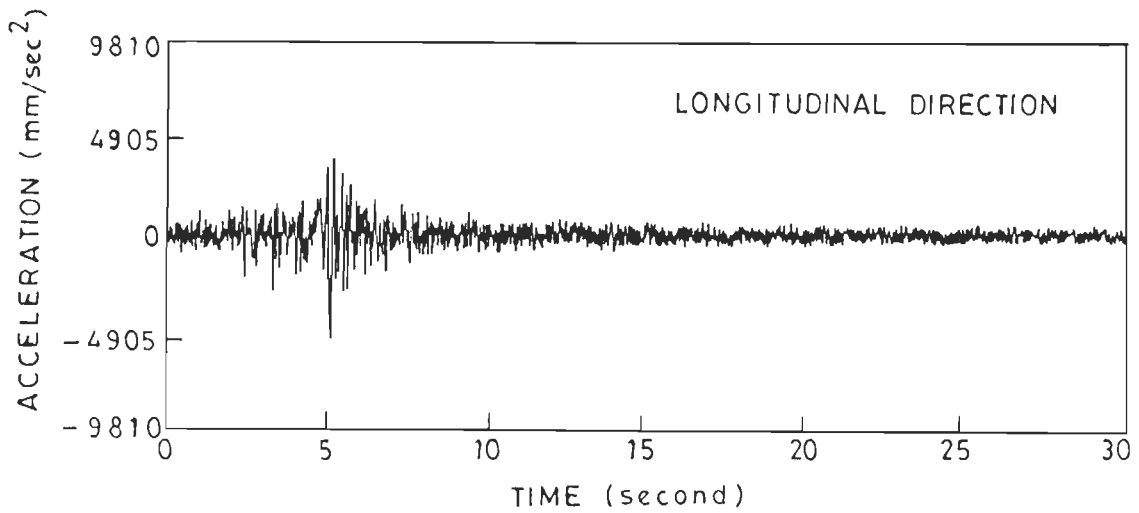
UTTARKASHI EARTHQUAKE ACCELERATION RECORD
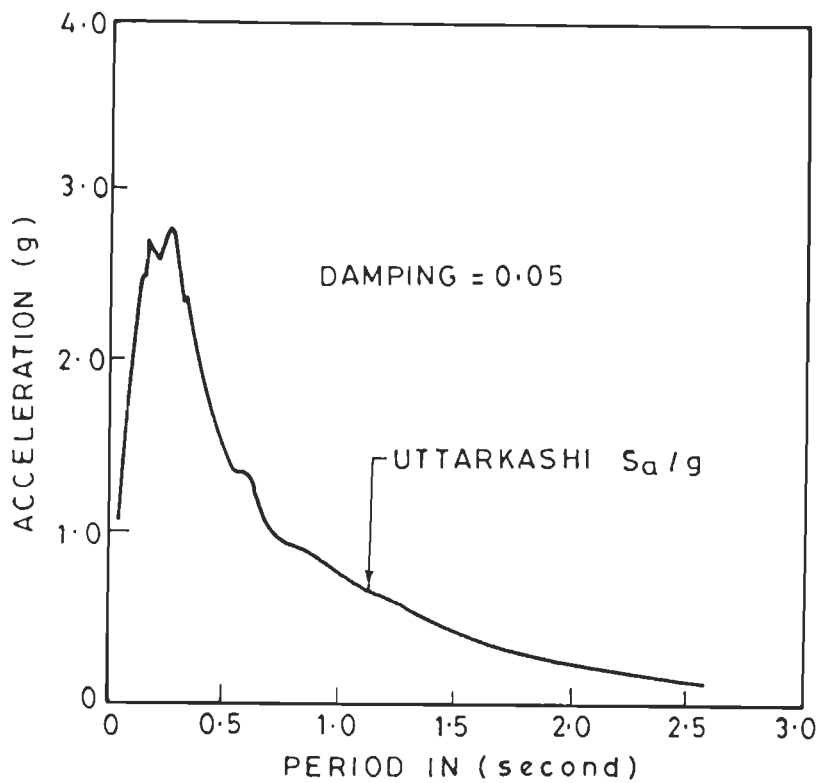
ACCELERATION RESPONSE SPECTRA OF
UTTARKASHI EARTHQUAKE

FIG. 4·6 ACCELERATION RECORD AND RESPONSE
SPECTRA OF UTTARKASHI EARTHQUAKE
(OCT. 20, 1991)

71

Table 4.1

Typical Details of Three Earthquake Time Histories

Location and date of occurrence	Component	Peak Value	Dominating time period range (sec)	Magnitude on Richter Scale	Approximate duration (sec)
El-Centro (California) May 18,1940 (Fig. 4.4)	N-S component	0.33 g	0.25-0.45	7.1	30.0
Koyna (India) Dec. 11,1967 (Fig.4.5)	Transverse to dam axis	0.49 g	0.10-0.18	6.5	10.3
Uttarkashi (India) Oct. 20,1991 (Fig. 4.6)	Longitudinal direction	0.53 g	0.17-0.34	6.1	37.1

g is the acceleration due to gravity.

4.7 Material Properties

The structures analysed in this study are made of reinforced cement concrete (R.C.C.) whose properties are given as under :

Properties of reinforced cement concrete

Modulus of elasticity (E) $= 3.0 \times 10^6 \, t/m^2$

Poisson's ratio (v) = 0.20

Mass density (ρ) $= 0.25 \, t-s^2/m^4$

Damping (ς) = 5% of critical

For carrying out the study of soil-structure interaction effects, the properties of soil have been assumed as follows :

Soil Properties

Shear wave velocity of soil (V_s) = 300, 600, 900, 1200 m/s

Poisson's ratio (v)	= 0.30
Mass density (ρ)	= $0.20 \; t - s^2/m^4$
Translational damping	= 20% of critical
Rocking damping	= 5% of critical

The modulus of elasticity(E) of soil was calculated with the relation,

$E = 2G(1 + v)$ and $G = \rho V_s^2$

where, G is the shear modulus of soil.

4.8 Results of Seismic Analysis

Following results of seismic analysis are computed :

Free vibration results :

(a)   Time periods of vibration (sec)
(b)   Weighted modal damping (% of critical damping)
(c)   Mode participation factor (m.p.f.)

Seismic response to horizontal ground motion :

(a) Displacements (mm)
     (i) Radial or horizontal displacement (u) in 'r' direction
     (ii) Vertical displacement (v) in 'z' direction
     (iii) Tangential displacement (w) in θ direction

Out of above three displacements, only horizontal displacement (u) is presented in the thesis.

(b) Stresses $\left(t/m^2 \right)$

       (i) Normal/ bending stresses :

σ_r, σ_z and σ_θ are three bending stresses in radial, vertical and tangential directions, respectively. Out of these three normal stresses, mostly σ_z (vertical normal stress or simply called as bending stress) is presented in the thesis.

(ii) Shear stresses

τ_{rz}, $\tau_{r\theta}$ and $\tau_{z\theta}$ are three shear stresses along rz, $r\theta$ and $z\theta$ planes respectively. Out of these three shear stresses, mostly τ_{rz} is presented in the thesis.

4.9 Seismic Analysis of Axisymmetric Structures

A few numerical examples have been solved with the computer program to compare the dynamic characteristics obtained by beam method, finite element method and results of other investigators.

Numerical Example 1

For the purpose of study, a reactor containment structure (Fig.4.7a) which is similar to that given by Wolf(1985), has been taken. The structure is symmetrical with respect to vertical axis. It consists of a cylindrical shell capped with a spherical dome. The shell and dome are made of reinforced concrete. The shell has been discretized by using

(i)   2-noded elements in beam model (Fig. 4.7b). and

(ii)   8-noded isoparametric parabolic elements in finite element model (Fig. 4.7c)

The undamped free vibration analysis of fixed base containment shell has been performed to calculate the first three natural time periods by Finite element method (FEM) and Beam method. Time periods obtained by the above two methods are compared with those of shell model given by Wolf(1985) and shown in Table 4.2. Maximum difference in values of time periods by Wolf and Beam model is 8.0% while between Wolf and finite element model is 3.7%. This difference is due to different types of elements and the modelling methods (Hadjian, 1973).

ELEMENTS = 22
NODES = 23

8-NODED ELEMENT
x - GAUSS POINT NUMBER
• NODE NUMBER
ⓝ ELEMENT NUMBER
⬚ MATERIAL NUMBER

ELEMENTS = 22
NODES = 113

FIXED BASE

(a) CONTAINMENT SHELL   (b) BEAM MODEL   (c) FINITE ELEMENT MESH

NOTE: ALL DIMENSIONS ARE IN m
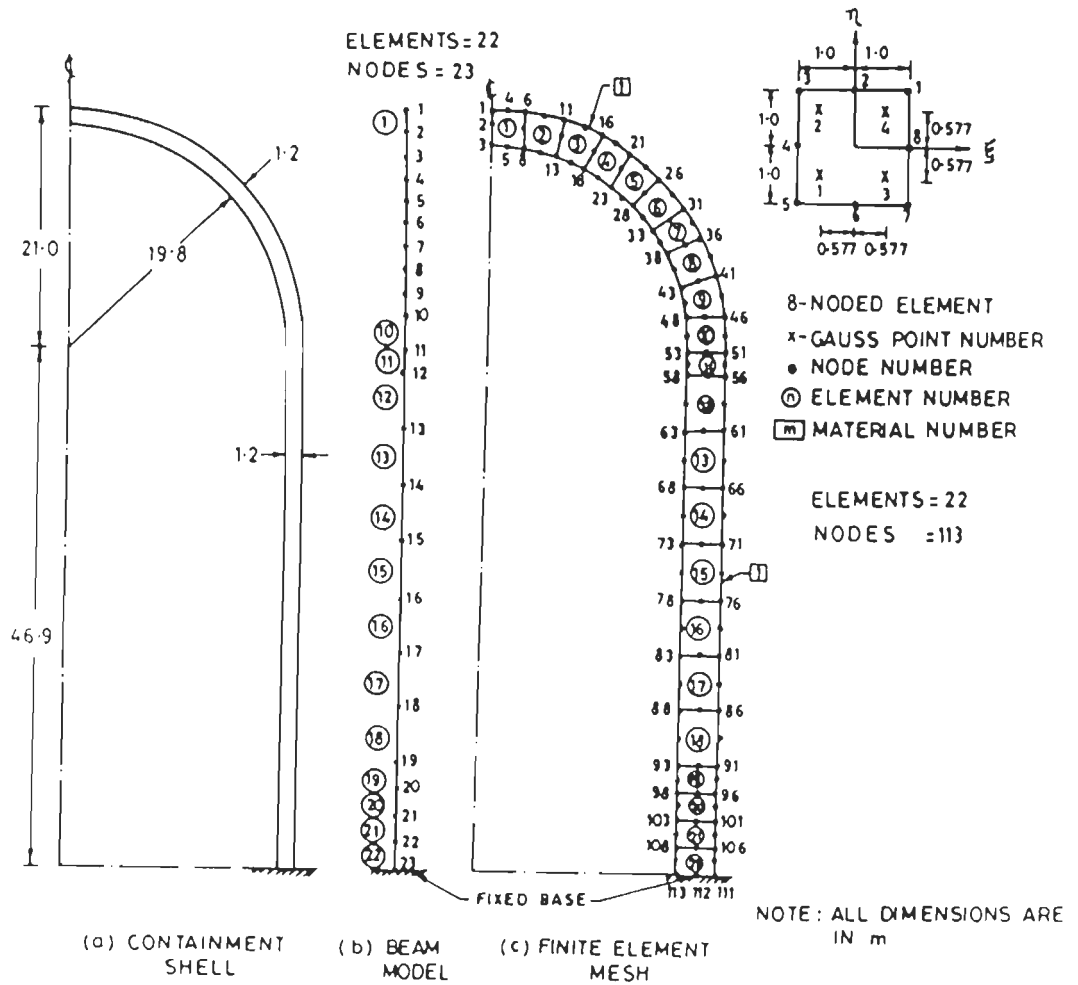
FIG. 4·7   BEAM MODEL AND FINITE ELEMENT MESH OF CONTAINMENT SHELL (FIXED BASE CONDITION)

Table 4.2
Periods of Vibration of Containment Structure, (Fig. 4.7)

Mathematical model	Time periods (sec)		
	Mode 1	Mode 2	Mode 3
FEM (Wolf(1985))	0.228	0.075	0.046
Beam Model (present study)	0.210	0.070	0.042
FEM (present study)	0.237	0.077	0.046

Numerical Example 2

San Bernardino intake tower(Fig. 4.8a) has been selected for study. The tower is made of reinforced cement concrete and is situated in southern California. It is cylindrical with circular plan having outside diameter of 18m. The dimensions of the tower have been taken from Liaw and Chopra(1973). Also the base of the tower was considered fixed for comparing the seismic response (due to May 18, 1940, El-Centro earthquake, E-W component) obtained from the present study to that of Singhal(1984) and Liaw & Chopra(1973). The effect of water and surrounding soil was not considered. The tower has been discretized by 8 noded isoparametric parabolic elements in finite element idealization (Fig. 4.8b).

Free vibration analysis of the tower has been carried out and its first three natural time periods are calculated. These time periods are compared with those obtained by Singhal (1984) and Liaw & Chopra (1973) and presented in Table 4.3.

Table 4.3

Periods of Vibration of Intake Tower, (Fig. 4.8)

Mathematical model	Time periods (sec)		
	Mode 1	Mode 2	Mode 3
Present study	0.454	0.087	0.038
Singhal (1984)	0.446	0.087	0.038
Liaw and Chopra (1973))	0.415	0.082	0.037

There is a negligible difference in the values of time period obtained from present study and that of other investigators.

(a) INTAKE TOWER

(b) FINITE ELEMENT IDEALIZATION OF TOWER

ELEMENTS = 27
NODES = 126

NOTE: ALL DIMENSIONS ARE IN m
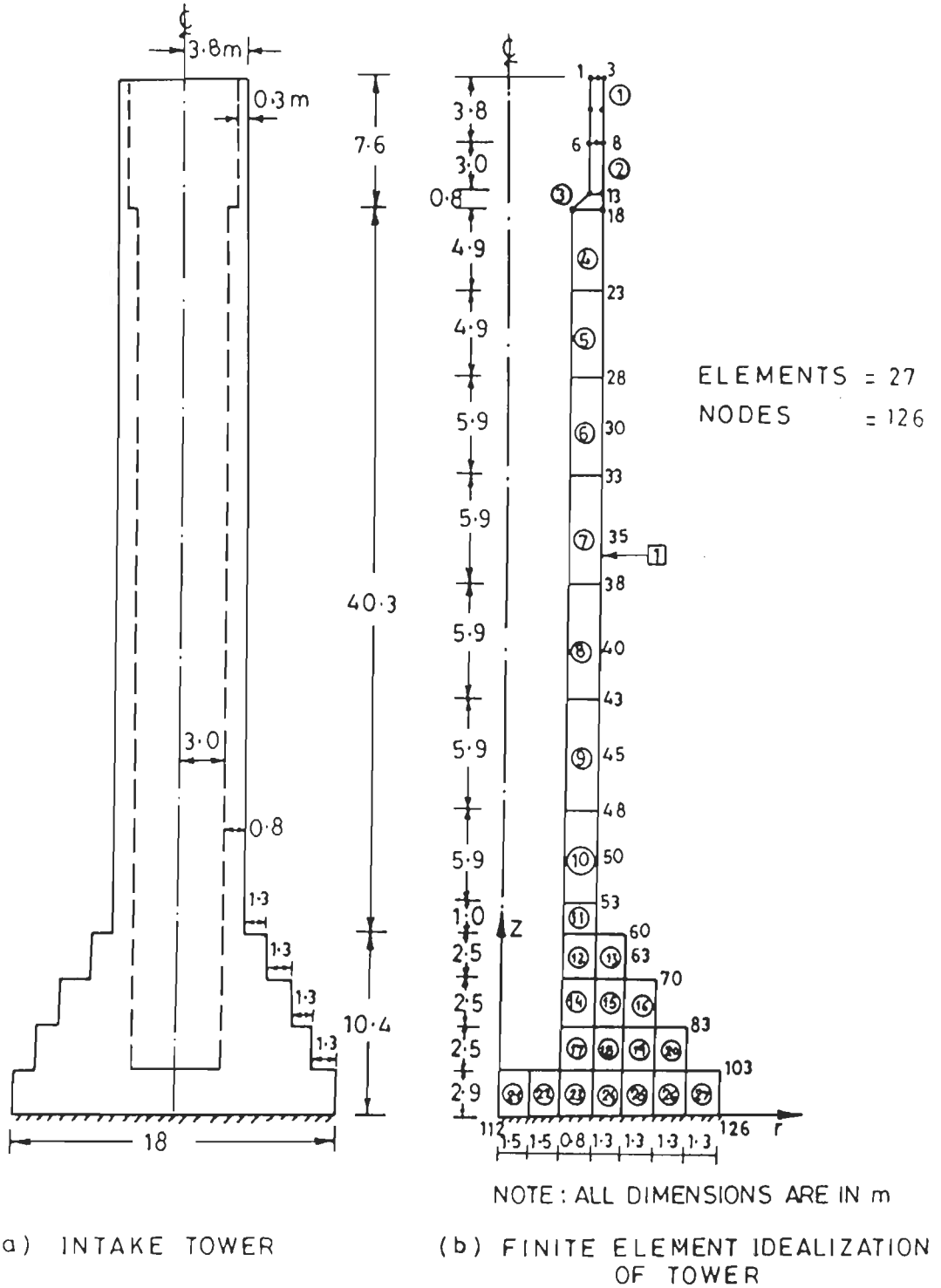
FIG. 4·8 INTAKE TOWER AND ITS AXISYMMETRIC FINITE ELEMENT IDEALIZATION

Table 4.4 presents some of the important results of earthquake response analysis using timewise mode superposition method, considering first three modes in the analysis. The maximum bending and shear stresses are computed at $\theta = 0^\circ$ plane (Albasiny and Martin, 1967).

Table 4.4
Maximum Seismic Response of Intake Tower, (Fig.4.8b)

Mathematical Model	Bending stress $\sigma_z \left(t/m^2 \right)$ (element 11,G.P.3)	Shear stress $\tau_{z\theta} \left(t/m^2 \right)$ (element 10, G.P.2)	Tip displacement (mm) (node 1)
Present Study	854.8	94.10	4.81
Singhal (1984)	830.0	92.00	4.73

There is a little difference in the values of maximum stresses and displacements between this study and that due to Singhal(1984). The small difference is because of the different element taken in the analysis (Abu-Sitta, 1970). In this study 8-noded isoparametric elements are taken while 6-noded paralinear elements were taken by Singhal(1984).

4.10 Parametric Study of SSI Effects on Seismic Behaviour of Containment Structure

The containment structure resting on raft (Fig. 4.9a) is considered to study the effects of soil-structure interaction. This structure including surrounding soil, called as soil-structure system, whose key diagram is shown in Fig. 4.9b, has been analysed by using,

(i)   8- noded parabolic elements in finite element method (Fig. 4.10a), and

(ii)   2-noded elements in beam model (Fig. 4.10b).

The parameters considered in the dynamic study of this soil-structure system are described in Table 4.5.

A — WIDTH OF FOUNDATION SOIL
B — DEPTH OF FOUNDATION SOIL
D — EMBEDMENT DEPTH
R — RADIUS OF RAFT
H — HEIGHT OF STRUCTURE

(a) REACTOR CONTAINMENT SHELL

(b) SOIL-STRUCTURE SYSTEM
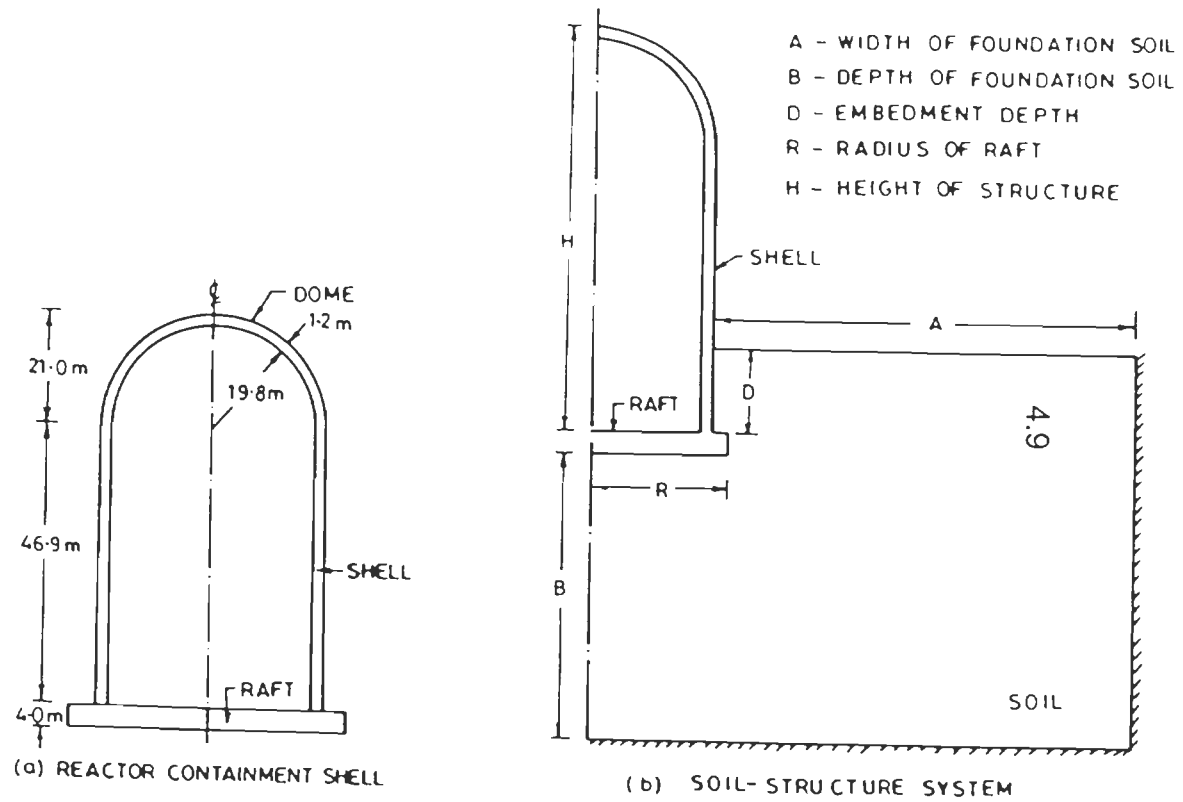
FIG. 4·9 REACTOR CONTAINMENT SHELL AND SOIL-STRUCTURE SYSTEM

ELEMENTS : 90
NODES : 345
MATERIALS : 2

(a) AXISYMMETRIC FINITE ELEMENT MODEL

(b) BEAM MODEL

ELEMENTS = 19
NODES = 20

R - RIGID LINK
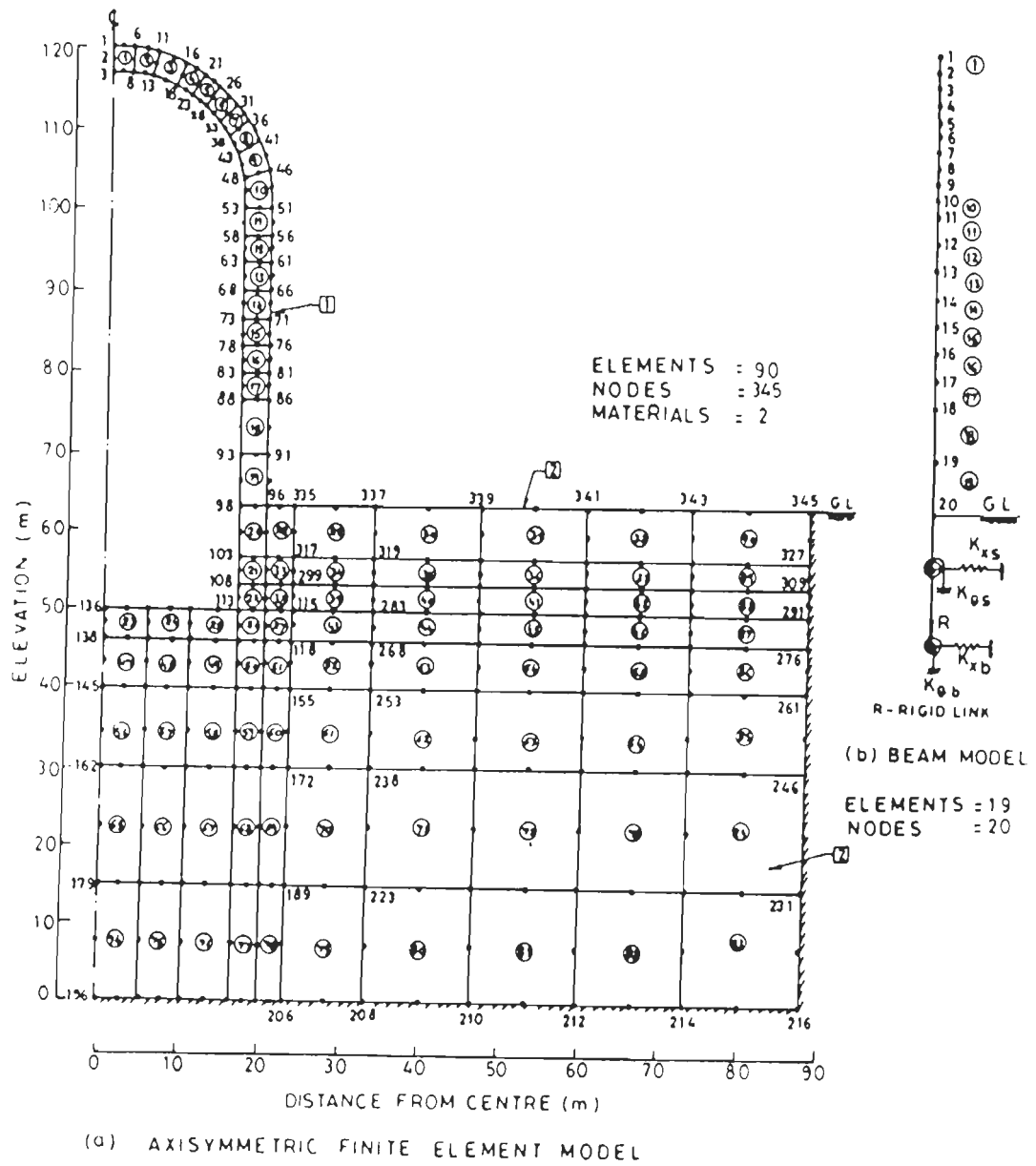
FIG. 4·10 AXISYMMETRIC FINITE ELEMENT AND BEAM MODELS
OF SOIL-STRUCTURE SYSTEM

80

Table 4.5

Parameters for Seismic Response Study of Containment Structure

Sr. no.	Parameters	Variations
1.	Mesh Size (AxB) of founding soil	A = 2R, 3R, 4R; B = R, 2R, 3R A = Horizontal dimension (soil width) B = Vertical dimension (soil depth) R = Radius of raft
2.	Shear wave velocity of founding soil (m/s)	300, 600, 900, 1200
3.	Boundary conditions	(a) Fixed base (b) Flexible base
4.	Depth of embedment (D)	Zero, H/16, H/8, H/6, H/4 H = Height of structure
5.	Type of earthquakes	El - centro, Koyna, Uttarkashi (Ref. Table 4.1 and Figures 4.4 to 4.6)
6.	Number of modes	3, 6, 9
7.	Soil damping (a) rocking (b) translational	 5%, 7% 20%, 35%

4.10.1 Effect of Mesh Size and Mass of Soil on the Seismic Behaviour

The dimensions of the structure are finite while the soil around the structure is of infinite extent in horizontal as well as in vertical directions. Therefore it is necessary to determine the approximate dimensions of the soil for dynamic analysis of the whole soil-structure system by using finite degrees of freedom.

These soil dimensions can be determined by making a parametric study of the depth and the width of the soil. To arrive at these soil dimensions, seismic response analysis of the system has been carried out. The results include the first three time periods and the corresponding weighted modal damping and mode participation factors, maximum bending stress at outer gauss points in some key elements along the height of the structure and maximum displacement at the top node of the element in the structure (tip displacement). The maximum

seismic responses are computed at $\theta = 0^o$ plane of axisymmetric structures using timewise mode superposition method and included first six modes in the finite element dynamic analysis throughout the parametric study in this chapter.

To find out the effect of soil mass on the seismic response of the structure, the surrounding soil has been treated in two ways as below :

(a) Soil-mass neglected
(b) Soil-mass included

Effect of depth of mesh size

The horizontal extent of soil was kept equal to three times the raft radius and varied the soil depth with the following parameters :

Soil width (A)	: 3 R
Soil depth (B)	: R, 2R, 3R
Embedment depth (D)	: 8m
Shear wave velocity of soil	: 900 m/s.
Earthquake motion	: Dec. 11, 1967, Koyna Earthquake, Transverse component

Tables 4.6 shows the result of free vibration analysis using axisymmetric finite element model. The results include the first three time periods (T), the associated weighted modal damping (ς) and mode participation factor (m.p.f.) for different depths of foundation soil below raft without and with the consideration of soil mass in the analysis.

It is observed from Table 4.6 that with the increase of soil depth from R to 2R, the time period in first mode increases from 0.275s to 0.281s in 'soil-mass neglected' case while in case of 'soil-mass included', the corresponding value increases from 0.280s to 0.292 s. For further increase of soil depth from 2R to 3R, the value of first time period remains almost constant in 'soil mass neglected' case while that value further increases from 0.292s to 0.322s in case of 'soil-mass included'. Similar pattern of variation of time period values with soil depth is observed in higher modes.

Table 4.6

Effect of Soil Depth on Dynamic Characteristics, (Soil Width = 3R)

Depth of soil in F.E. mesh (m)	Mode	Soil mass neglected			Soil-mass included		
		T(s)	ς (%)	m.p.f.	T(s)	ς (%)	m.p.f.
R	1	0.275	7.98	1.40	0.280	9.23	1.89
	2	0.080	6.85	0.73	0.095	10.21	1.71
	3	0.048	5.35	0.02	0.070	7.43	0.96
2R	1	0.281	8.32	1.45	0.292	10.60	2.11
	2	0.086	7.08	0.76	0.134	13.10	1.48
	3	0.052	5.86	0.06	0.086	8.93	1.05
3R	1	0.281	8.32	1.44	0.322	11.52	3.15
	2	0.086	7.08	0.77	0.198	15.12	2.10
	3	0.052	5.87	0.06	0.105	9.56	1.86

The other results of free vibration analysis, i.e. weighted modal damping and mode participation factor also show a good convergence for the 'soil-mass neglected' case while a large divergence is seen in the above values for 'soil-mass included' case (Table 4.6).

Table 4.7 shows the results of horizontal excitation of soil-structure system using finite element model (Fig. 4.10a). The results include the maximum bending stress at the outer gauss points in some key elements along the height of the structure and maximum tip displacement for different depths of foundation soil.

It is found from Table 4.7 that the stresses at different locations in 'soil-mass neglected' case are increased with increase of soil depth from R to 2R and for further increase of soil depth from 2R to 3R, these stresses are almost unaffected, while in case of 'soil-mass included', the values of stress at different elevations of the structure are increased with increase of soil depth from R to 3R. It shows that stresses do not converge with increase of soil depth from 2R to 3R for 'soil-mass included' case.

Tip displacement (node 1, Fig. 4.10a) increases with increase of soil depth in both the cases but the values are more in case of 'soil-mass included'.

Table 4.7
Effect of Soil Depth on Horizontal Seismic Response, (Soil Width = 3R)
(Fig. 4.10a)

Depth of soil in F.E. mesh(m)	Bending stress along the height				Tip displacement node 1 (mm)
	83.4 m	66.8 m.	60.8 m	50.4 m	
	$\sigma_z (\times 100) \, t/m^2$				
	(Soil-mass neglected)				
R	1.11	1.12	0.90	0.18	8.10
2R	1.42	1.34	1.04	0.23	9.45
3R	1.53	1.50	1.12	0.29	11.15
	(Soil-mass included)				
R	1.95	1.79	1.23	0.38	11.05
2R	2.17	2.00	1.72	0.44	12.31
3R	3.28	3.15	2.23	1.85	15.12

Therefore, the depth of foundation soil below raft can be fixed as two times the radius of the raft for evaluating maximum seismic response of a structure and mass of the interacting soil should not be considered in the analysis.

Effect of width of mesh size

Having established the depth of soil, a similar parametric study was carried out to determine the effective width of soil medium. The same model was subjected to horizontal excitation to find out the effect of soil width on the dynamic behaviour of the system. The different widths of soil equal to 2R, 3R and 4R were considered and the following parameters were taken :

Soil width (A)   : 2R, 3R, 4R

Soil depth (B)   : 2R

Embedment depth (D)   : 8m

Shear wave velocity of soil   : 900 m/s.

Earthquake motion   : Dec. 11, 1967, Koyna Earthquake,
                                    Transverse component

Table 4.8 shows the results of free vibration analysis which include the time periods (T) of first three modes, the associated weighted modal damping (ζ) and mode participation factor (m.p.f.) for different widths of foundation soil.

Table 4.8

Effect of Soil Width on Dynamic Characteristics, (Soil Depth = 2R)

Width of soil in F.E. mesh (m)	Mode	Soil mass neglected			Soil-mass included		
		T(s)	ζ (%)	m.p.f.	T(s)	ζ (%)	m.p.f.
2R	1	0.281	8.30	1.43	0.287	9.01	1.80
	2	0.086	7.00	0.70	0.120	7.86	1.05
	3	0.050	5.80	0.04	0.056	6.12	0.93
3R	1	0.281	8.32	1.45	0.292	10.60	2.11
	2	0.086	7.08	0.76	0.134	13.10	1.48
	3	0.052	5.86	0.06	0.086	8.93	1.05
4R	1	0.282	8.33	1.46	0.315	12.30	3.12
	2	0.087	7.10	0.80	0.198	14.56	2.10
	3	0.052	5.86	0.07	0.100	10.12	1.95

It is observed from Table 4.8 that in the case of 'soil-mass neglected', the values of time period, weighted modal damping and mode participation factor practically converge after a distance (soil width) of 3R. On the contrary, in the 'soil-mass included ' case, these values show a divergence pattern.

Table 4.9 shows the results of horizontal excitation of soil-structure system which include the maximum bending stress at the outer gauss points in some key elements along the height of the structure and maximum tip displacement for different widths of foundation soil. The results show convergence even after a soil widths of 2R in the 'soil-mass neglected' case while there is no convergence of stresses for the case of 'soil-mass included'.

Table 4.9
Effect of Soil Width on Horizontal Seismic Response,(Soil Depth = 2R)
(Fig. 4.10a)

Soil width in F.E. mesh (m)	Bending stress along the height				Tip displacement node 1 (mm)
	83.4 m	66.8 m. $\sigma_z (\times 100) t/m^2$	60.8 m	50.4m	
	(Soil-mass neglected)				
2R	1.48	1.41	1.10	0.28	10.10
3R	1.42	1.34	1.04	0.23	9.45
4R	1.40	1.31	1.00	0.22	9.12
	(Soil-mass included)				
2R	2.56	2.19	1.98	0.59	14.20
3R	2.17	2.00	1.72	0.44	12.31
4R	1.49	1.38	1.06	0.24	10.12

Tip displacement (Table 4.9) decreases with increase of soil width in both the cases but the values are more in case of soil-mass included.

Therefore, it can be inferred that width of soil medium can be taken to be equal to three times the radius of the structure at its base (raft radius) from the edge of the structure and mass of the interacting soil should not be considered.

It is concluded from the above study that (i) the depth of soil medium below the raft and the width of soil from the outer edge of the structure can be taken to be at distances of 2R and 3R, respectively, where R, is the radius of the raft, and (ii) the mass of the interacting soil should not be included in the analysis of soil-structure system

4.10.2 Effect of Shear Wave Velocity of Soil on Dynamic Behaviour

The soil-structure system (Fig. 4.9b) subjected to horizontal excitation, was analysed by Finite element model (Fig. 4.10a) as well as beam model (Fig. 4.10b). Also, the containment structures with fixed base of raft (Fig. 4.11a) has been analysed by using finite element model (Fig. 4.11b) as well as beam model (Fig. 4.11c). The study has been made for different shear wave velocities of founding soil with following parameters of soil-structure system,

Soil width (A)	: 3R
Soil depth (B)	: 2R
Embedment depth (D)	: 8 m
Shear wave velocity of soil	: 300, 600, 900, 1200 m/s
Earthquake motion	: Dec.11, 1967, Koyna Earthquake Transverse component

Table 4.10 shows the results of free vibration study of the structure with fixed base and flexible base having different shear wave velocities, using (i) axisymmetric finite element model, and, (ii) beam model. The results include the period of vibration in three modes obtained by beam and finite element analysis, and the associated weighted modal damping and mode participation factor by finite element method.

Effect of mathematical models on time period

Time period values by beam analysis are lesser than those obtained by finite element analysis (Table 4.10). This is due to the finite element model being 3-dimensional model, depicting greater flexibility as compared to beam model (Agrawal, 1973).

Effect of Shear Wave Velocity on Dynamic Characteristics (Table 4.10)

Time Period

Table 4.10 shows that, as shear wave velocity of soil increases, more stiffness introduced to the soil-structure system; so the value of time period decreases considerably for first mode and almost insignificant variation occurs for higher
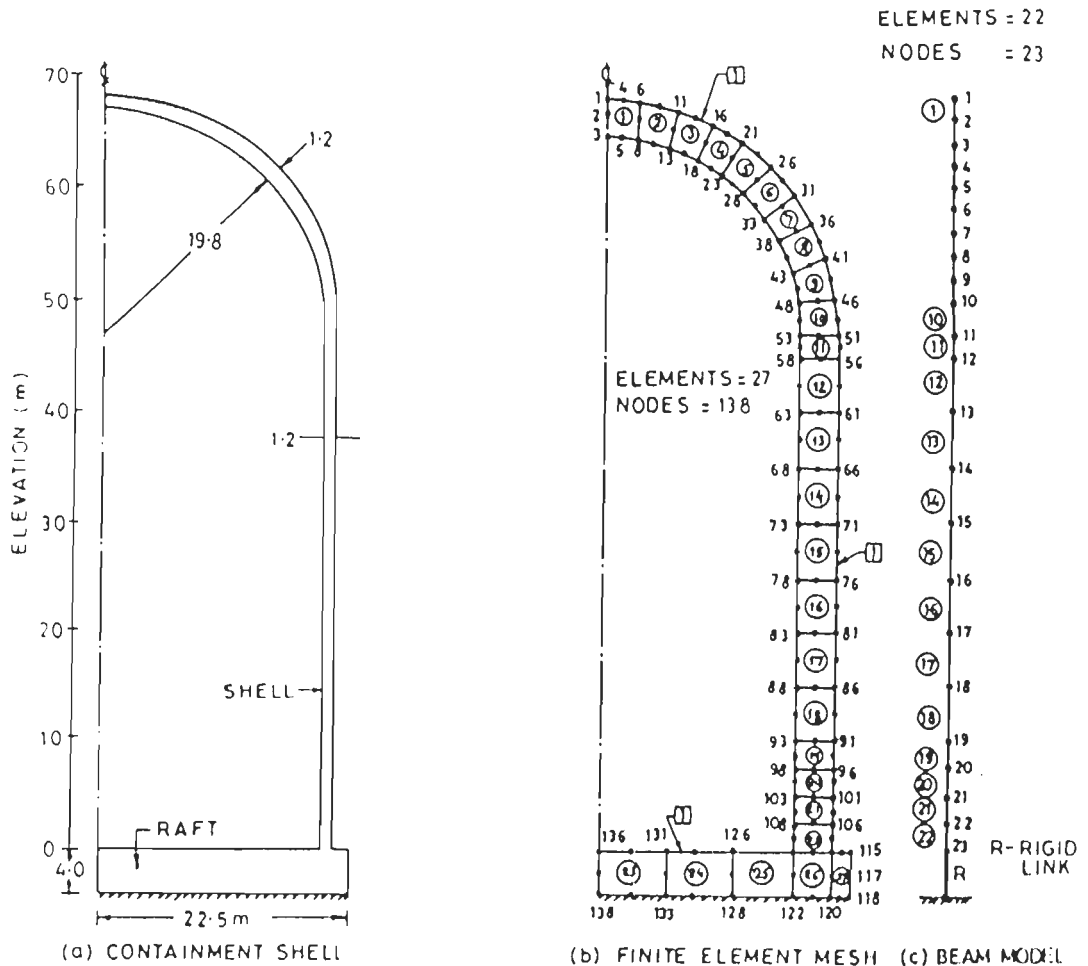
FIG. 4·11 CONTAINMENT SHELL AND ITS FINITE ELEMENT AND BEAM
MODELS (FIXED AT BASE OF RAFT)

modes, that is, with increase of shear wave velocity from 300 to 1200 m/s, the fundamental time period decreases from 0.481 s to 0.266 s; second mode period from 0.107s to 0.083s and third mode period is almost insensitive to the variation of shear wave velocity. It is also observed that decrease in time period is more between shear wave velocity of 300 to 600 m/s and this effect of decrease in time period is reduced for further increase of shear wave velocity from 600 to 900 m/s. The variation in values of time period is insensitive beyond shear wave velocity of 1200 ms. This shows that near fixity condition is achieved when shear wave velocity approaches 1200 m/s.

Table 4.10

Effect of Shear Wave Velocity of Soil on Dynamic Characteristics

Shear wave velocity,m/s	Mode	Time periods,sec		Weighted modal damping(%)	m.p.f.
		Beam	FEM		
300	1	0.475	0.481	16.10	1.47
	2	0.083	0.107	10.90	0.89
	3	0.070	0.074	8.80	0.11
600	1	0.289	0.318	12.20	1.46
	2	0.070	0.094	10.20	0.86
	3	0.056	0.058	7.50	0.12
900	1	0.235	0.281	8.32	1.45
	2	0.070	0.086	7.08	0.76
	3	0.051	0.052	5.86	0.06
1200	1	0.220	0.266	7.60	1.44
	2	0.070	0.083	6.50	0.71
	3	0.050	0.051	5.50	0.08
Fixed base	1	0.215	0.243	5.00	1.39
	2	0.070	0.080	5.00	0.68
	3	0.045	0.048	5.00	0.07

Weighted modal damping (Table 4.10) :

Weighted modal damping decreases with increase of shear wave velocity for first mode and a very small variation occurs in higher modes. With the increase of

shear wave velocity of soil, the more stiffness is added to soil-structure system which causes the reduction in displacement and strain energy. The weighted modal damping is based on the strain energy of various subsystems. So weighted modal damping decreases with increase of shear wave velocity. As the shear wave velocity increases from 300 to 1200 m/s, weighted modal damping for fundamental mode decreases from 16.1 % to 7.6 % and not much affected in higher modes. Also, the variation is more between shear wave velocity of 300 to 600 m/s and thereafter becomes almost constant for shear wave velocity beyond 1200 m/s.

Mode participation factor(m.p.f.)

Mode participation factor decreases with increase of shear wave velocity in first and second mode. Mode participation factor values in third mode are not following any pattern.

Table 4.11 shows the variation of maximum bending stress at outer gauss points in some key elements along the height of the structure and tip displacement due to horizontal excitation for different shear wave velocities of the soil.

Table 4.11

Effect of Shear Wave Velocity of Soil on Seismic Response
(Fig.4.10a)

Shear wave velocity of soil (m/s)	Bending stress along the height						Tip displacement node-1 (mm)
	110.2m	100.6m	83.4m σ_z $(\times 100)$ t/m^2	66.8m	60.8m	50.4m	
300	0.09	0.39	1.52	1.52	1.94	0.30	20.20
600	0.16	0.70	1.64	1.78	2.03	0.47	12.31
900	0.18	0.90	1.70	1.90	2.30	0.53	9.45
1200	0.28	1.02	1.87	2.10	2.79	0.68	9.32
Fixed base	0.29	1.12	1.90	2.20	2.95	0.78	9.38

Maximum bending stress :

It is observed from Table 4.11 that the bending stress at various levels in the structure increases with increase of shear wave velocity. It is also observed that stresses at various locations in the structure for shear wave velocity of 1200 m/s have approached to that of fixed base structure (Parkash, 1994).

Maximum tip displacement :

The tip displacement decreases with increase of shear velocity which is obvious due to increase in stiffness of foundation soil (Table 4.11).

Therefore it is concluded from the seismic analysis of soil-structure system, that, (i) if the shear wave velocity of soil is 1200 m/s and above, a fixed base condition may be assumed, (ii) stresses are reduced in the structure founded on soft soil as compared to the structure with fixed base or the structure founded on stiff soil, and, (iii) deformations are increased in the structure founded on soft soil as compared to that of structure founded on stiff soil.

4.10.3 Effect of Depth of Embedment on Seismic Behaviour

An earthquake response analysis of the same containment structure including surrounding soil (Fig. 4.9) for a horizontal ground motion has been carried out using finite element model. The study has been made for different depths of embedment with the following parameters

Soil width (A)	: 3R
Soil depth (B)	: 2R
Depth of embedment	: 0m, 4m, 8m, 12m, 16 m
Shear wave velocity of soil	: 600 m/s
Earthquake motion	: Dec. 11, 1967, Koyna earthquake, Transverse component

Table 4.12 shows time period, weighted modal damping and mode participation factor (m.p.f.) in first three modes for different depths of embedment.

Table 4.12
Effect of Depth of Embedment on Dynamic Characteristics

Depth of embedment (m)	Mode	Time Period (Sec)	Weighted modal damping (%)	m.p.f.
0.0	1	0.468	16.10	1.50
	2	0.156	10.90	0.90
	3	0.068	8.80	0.14
4.0	1	0.323	13.00	1.49
	2	0.099	10.50	0.88
	3	0.064	8.01	0.13
8.0	1	0.318	12.20	1.46
	2	0.094	10.20	0.86
	3	0.058	7.50	0.12
12.0	1	0.266	9.32	1.45
	2	0.070	7.81	0.75
	3	0.048	6.43	0.09
16.0	1	0.266	8.92	1.45
	2	0.070	7.52	0.75
	3	0.048	6.41	0.09

Time period (Table 4.12)

As the depth of embedment increases time period decreases. This is because of increase of stiffness due to increase of embedment depth. This effect of decrease in time period with increase of embedment depth is faster when embedment depth increases from 0m to 4m and slower from 4m to 12m and thereafter almost constant.

Weighted modal damping (Table 4.12)

Weighted modal damping decreases with increase of depth of embedment. It is due to increased rigidity of structure with increase of embedment depth which results in reduced deformation and strain energy. However, the decrease in

modal damping is insignificant for second and third modes. Also, the variation is insensitive for increase in embedment depth from 12m to 16m.

Mode participation factor (Table 4.12)

Mode participation factor decreases with increase of depth of embedment for fundamental mode and insignificant variation occurs in higher modes.

The maximum seismic response of the structure subjected to horizontal excitation for three depths of embedment (4, 8, 12m) is computed. The variation of stress and displacement response in the structure is shown in Figure 4.12.

Maximum bending stress

Figure 4.12a shows the variation of maximum bending stress on bottom gauss points of the raft with different depths of embedment. It is observed that bending stresses on the outer one third part of the raft reduce significantly with increase in the depth of embedment.

Figure 4.12b shows the variation of maximum bending stress along the height of containment structure with different depths of embedment. It shows that the stresses in the lower portion of shell are reduced significantly with the increase of embedment depth and a very small variation occurs in the upper and middle portion of the shell (Anderson, 1972).

Maximum shear stress

Figure 4.12c shows the shear stress distribution along the height of containment with different depths of embedment. It is observed that the shear stress in the lower part of the structure is reduced considerably with the increase of embedment depth and insignificant variation occurs in the middle and upper part of the structure.

Maximum horizontal displacement

Figure 4.12d shows the variation of displacement along the height of the containment with different embedment depths.
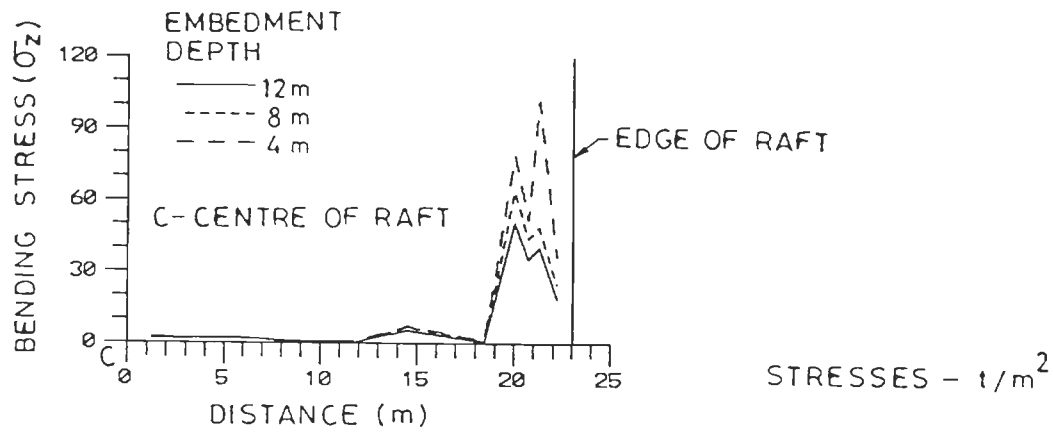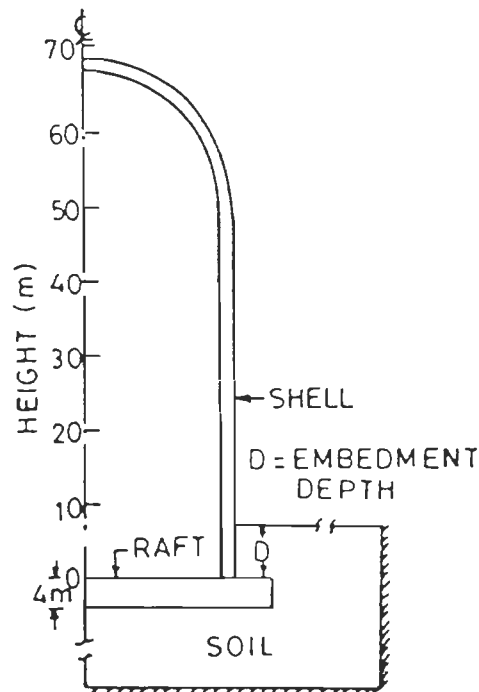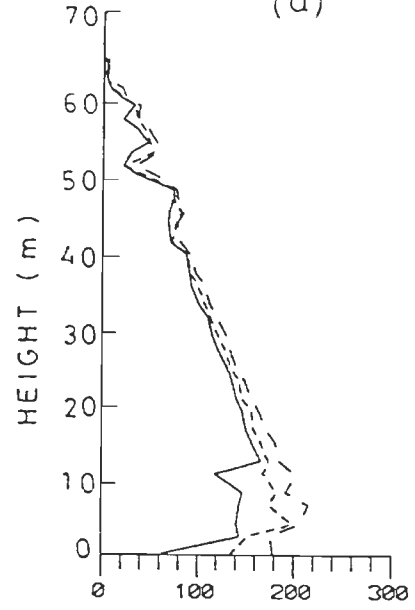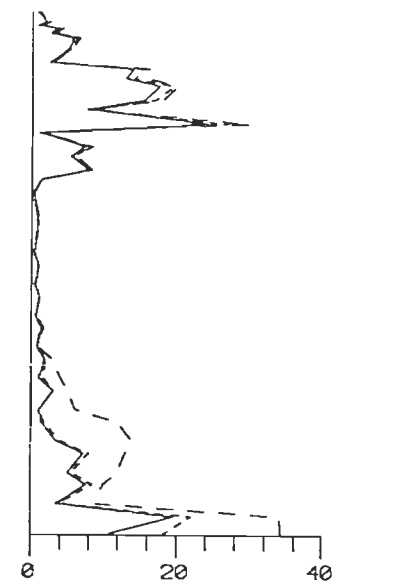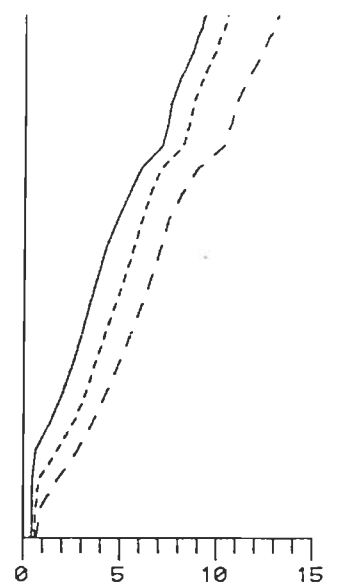
FIG. 4·12 MAXIMUM STRESS/DISPLACEMENT RESPONSE OF SHELL FOR DIFFERENT DEPTHS OF EMBEDMENT (KOYNA EARTHQUAKE, DEC.11,1967, TRANSVERSE)

It is observed that the displacements are reduced considerably throughout the height of the structure with the increase of depth of embedment.

Therefore, it is concluded that most suitable depth of embedment for minimum seismic response of the structure is 12m, that is, about one sixth of the height of the structure.

4.10.4 Effect of Type of Earthquake on Seismic Response

To compare the maximum seismic response (bending stress at some levels and tip displacement) of the above containment structure including surrounding soil (Fig. 4.9), three earthquake time histories have been taken, namely, Koyna, El-Centro and Uttarkashi, shown in Figures 4.4 to 4.6. Theses have been normalized to common peak value acceleration equal to 0.49g (peak value of Koyna earthquake). The salient data of these time histories are given in Table 4.1. The finite element dynamic analysis using timewise mode superposition method has been carried out with following foundation parameters :

Soil width (A)	: 3R
Soil depth (B)	: 2R
Embedment depth (D)	: 8m
Shear wave velocity of soil	: 600 m/s.

Figure 4.13 shows the maximum response obtained as a result of finite element seismic analysis of soil-structure system (Fig. 4.10a) due to the above three normalized time histories. The fundamental time period of containment structure with fixed base is 0.243 sec (Table 4.10) which lies between the dominating time period range of Uttarkashi earthquake (Table 4.1).

Maximum bending stress

Figure 4.13a shows the variation of bending stress on bottom gauss points of raft due to three earthquakes. It is observed that stresses at the end one third portion of the raft are significantly higher due to Uttarkashi earthquake as compared to the other two earthquakes and variation of stress in the central part of the raft is insensitive to the type of earthquake.

Figure 4.13b shows the variation of maximum bending stress along the height of containment structure due to these three earthquakes. It shows that stresses along the height of structure are much higher in case of Uttarkashi earthquake as compared to other two earthquakes. The stresses are almost equal for Koyna and El-centro earthquakes, slightly higher in case of Koyna as compared to El-centro earthquake.

Maximum shear stress

Figure 4.13c shows the shear stress distribution along the height of containment due to these three earthquakes. It shows that in the lower portion of the shell, stresses are significantly higher due to Uttarkashi earthquake as compared to other two. The shear stresses in upper part of the shell are slightly more due to Uttarkashi earthquake as compared to other two while the shear stresses in the middle part of shell are almost equal for these three earthquakes.

Maximum horizontal displacement

Figure 4.13d shows the variation of displacement along the height of containment due to these three earthquakes. It is clear that the displacement throughout the height of the structure are significantly higher for Uttarkashi earthquake as compared to the other two earthquakes. The displacements are almost equal for Koyna and El-centro earthquakes.

Therefore, it is concluded that seismic response of a structure not only depends upon the peak acceleration but also depends upon the frequency content of an earthquake.

4.10.5 Effect of Number of Modes on Seismic Response

The study has been made for soil-structure system (Fig. 4.9) subjected to horizontal excitation with following foundation parameters,

Soil width (A)   : 3R
Soil depth (B)   : 2R
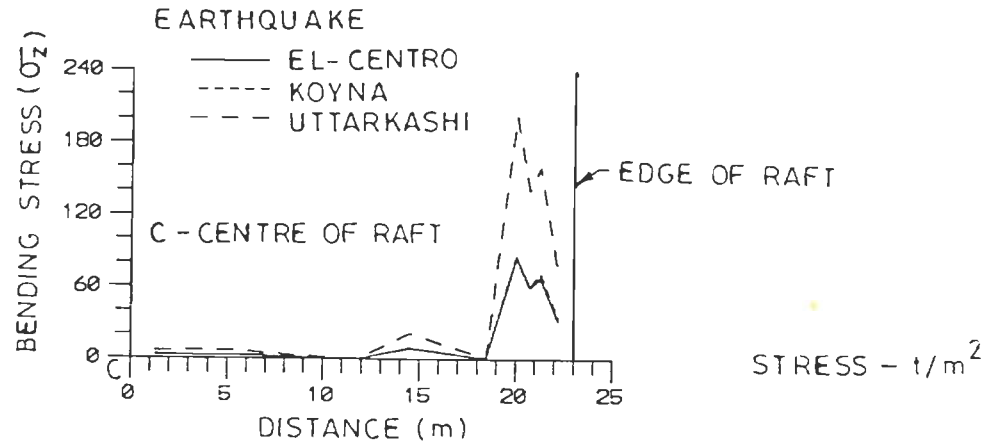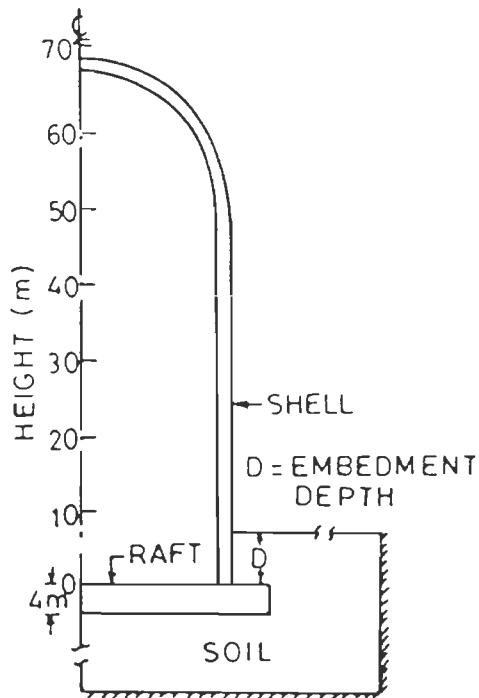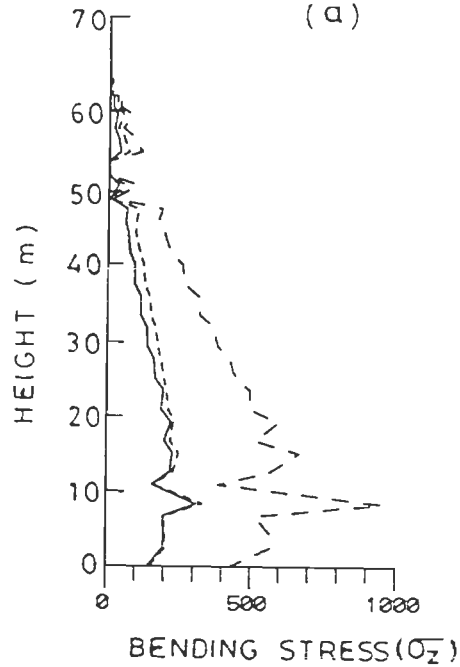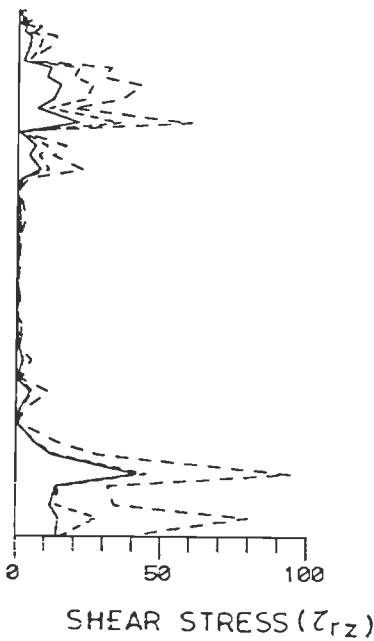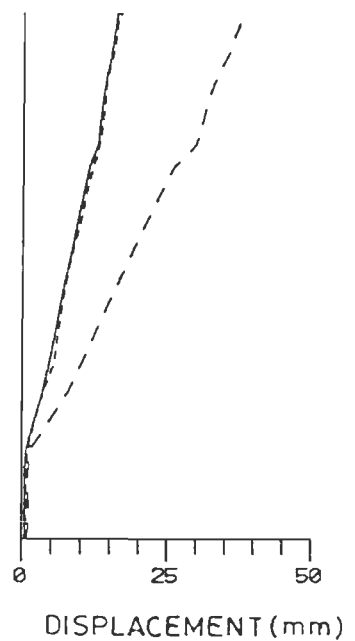
FIG. 4·13 COMPARISON OF MAXIMUM STRESS / DISPLACEMENT
RESPONSE OF SHELL TO THREE EARTHQUAKE

Embedment depth (D)   : 8m
Shear wave velocity of soil   : 600 m/s.
Earthquake motion   : Dec. 11, 1967, Koyna Earthquake,
                                   Transverse component

Table 4.13 shows the maximum bending stress at some locations in the structure due to horizontal excitation using timewise mode superposition method considering different number of modes in the analysis.

Table 4.13

Effect of Number of Modes on Seismic Response (Fig.4.10a)

Number of modes	Bending stress along the height						Tip displacement node-1 (mm)
	110.2m	100.6m	83.4m	66.8m	60.8m	50.4m	
	$\sigma_z \, (\times 100) \, t/m^2$						
3	0.18	0.62	1.34	1.40	1.07	0.24	11.15
6	0.20	0.70	1.52	1.45	1.10	0.27	12.31
9	0.20	0.70	1.52	1.45	1.10	0.27	12.32

It is observed from Table 4.13 that there is insignificant change in stresses after six modes in the finite element seismic analysis because only first few modes participate in overall seismic response of a structure. So, the consideration of first six modes is sufficient for evaluating maximum seismic response of this structure.

4.10.6 Effect of Soil Damping on Seismic Response

The study has been made for soil-structure system (Fig.4.9) subjected to horizontal excitation for two different sets of soil damping with following foundation parameters :

        Soil width (A)   : 3R
        Soil depth (B)   : 2R
        Embedment depth (D)   : 8m

Shear wave velocity of soil   : 600 m/s.

Earthquake motion   : Dec. 11, 1967, Koyna Earthquake, Transverse component

Maximum bending stress at some location and tip displacement obtained are given in Table 4.14.

Table 4.14
Effect of Damping of Soil on Seismic Response, (Fig.4.10a)

Damping (%)	Bending stress along the height				Tip displacement node 1 (mm)
	83.4m	66.8m $\sigma_z (\times 100) \, t/m^2$	60.8m	50.4m	
Rocking 5% Translational 20%	1.52	1.45	1.10	0.27	12.31
Rocking 5% Translation 35%	1.35	1.27	0.97	0.20	8.31

It is observed from Table 4.14 that there is a small decrease in stresses and displacement with increase of soil damping (Tsai, 1974; Veletsos & Wei, 1971).

4.11 Earthquake Analysis of Complete Reactor Building

The design philosophy of conventional structures differs from that of nuclear power plant facilities. In conventional structures, the emphasis is placed on the survivability of the building when subjected to an earthquake, and inelastic deformation and some damages are accepted. In fact, the buildings are designed to be ductile and possess energy absorption capability. For nuclear power plant facilities, the primary purpose of the seismic analysis and design is to ensure that the structural systems, and equipment necessary for nuclear safety remain functional during an earthquake. It is substantially more difficult to verify a system's functional ability by analysis or test when inelastic deformation occurs. To do so it has generally been required of a system to behave elastically during the horizontal seismic event (Luco, 1982; Whitman, 1972).

Reactor building and its mathematical model

For the purpose of study, a nuclear reactor building which is similar to that given by Kati(1973) has been selected (Fig. 4.14). The main structure is symmetrical with respect to its vertical axis. The structure consists of two co-axial cylindrical shell, a dome, a circular slab and an internal structure, all resting on a massive raft foundation, all made of reinforced concrete. The external shell is capped by a spherical dome while the internal shell carries a circular slab.
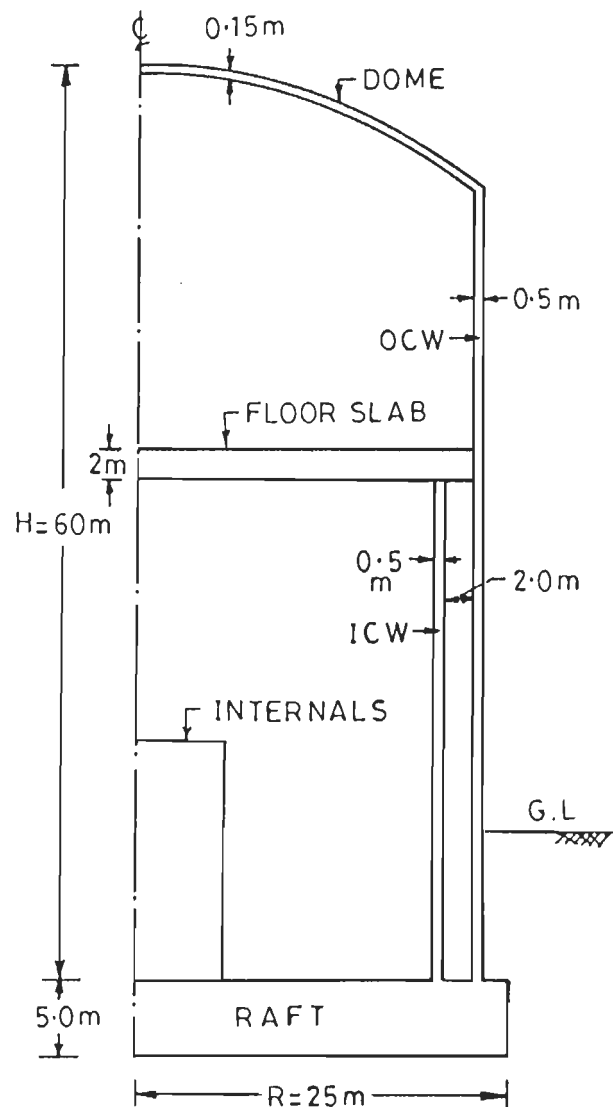
FIG. 4·14 REACTOR BUILDING

The building has been analyzed using the axisymmetric finite element model. The external and internal shells being mainly axisymmetric, have been modelled by axisymmetric finite elements. The internal structure cannot be truly represented by an axisymmetric model (Benda, 1981). Therefore the internals has been represented by an equivalent solid cylinder. By such representation, it has been shown that the stresses in the external and internal shell will be little effected [Chandrasekaran and Paul (1978)]. The modelling of internal structure of reactor building and its effects on outer and inner shell has been studied in chapter 7.

The internal structure is relatively rigid one and, therefore, a high value of modulus of elasticity has been assigned to the element representing the internal structure. The side soil and base soil have been treated as a part of reactor building but having no mass. In the discretization of whole system (soil and structure), isoparametric 8-noded parabolic elements have been used. The parameters considered in this study are described in Table 4.15.

Table 4.15
Parameters for Seismic Response Study of
Axisymmetric Reactor Structure

Sr.No.	Parameters	Variations
1	Boundary conditions	(a) Fixed base (b) Flexible base
2	Shear wave velocity of founding soil (m/s)	300, 600, 900, 1200
3	Depth of embedment	Zero, H/12, H/6, H/4 H = Height of structure
4	Type of Earthquake	El-Centro, Koyna, Uttarkashi (Ref. Table 4.1, Fig. 4.4 to 4.6)

Reactor Building Fixed at the Base of the Raft

Finite element analysis of reactor building (Fig. 4.14) subjected to horizontal excitation (Dec. 11, 1967, Koyna Earthquake, Transverse component) has been

carried out . Figure 4.15 shows the finite element mesh of this reactor building with fixed base of the raft. First six modes of vibration have been considered and six mode shapes are plotted as shown in Figure 4.16.
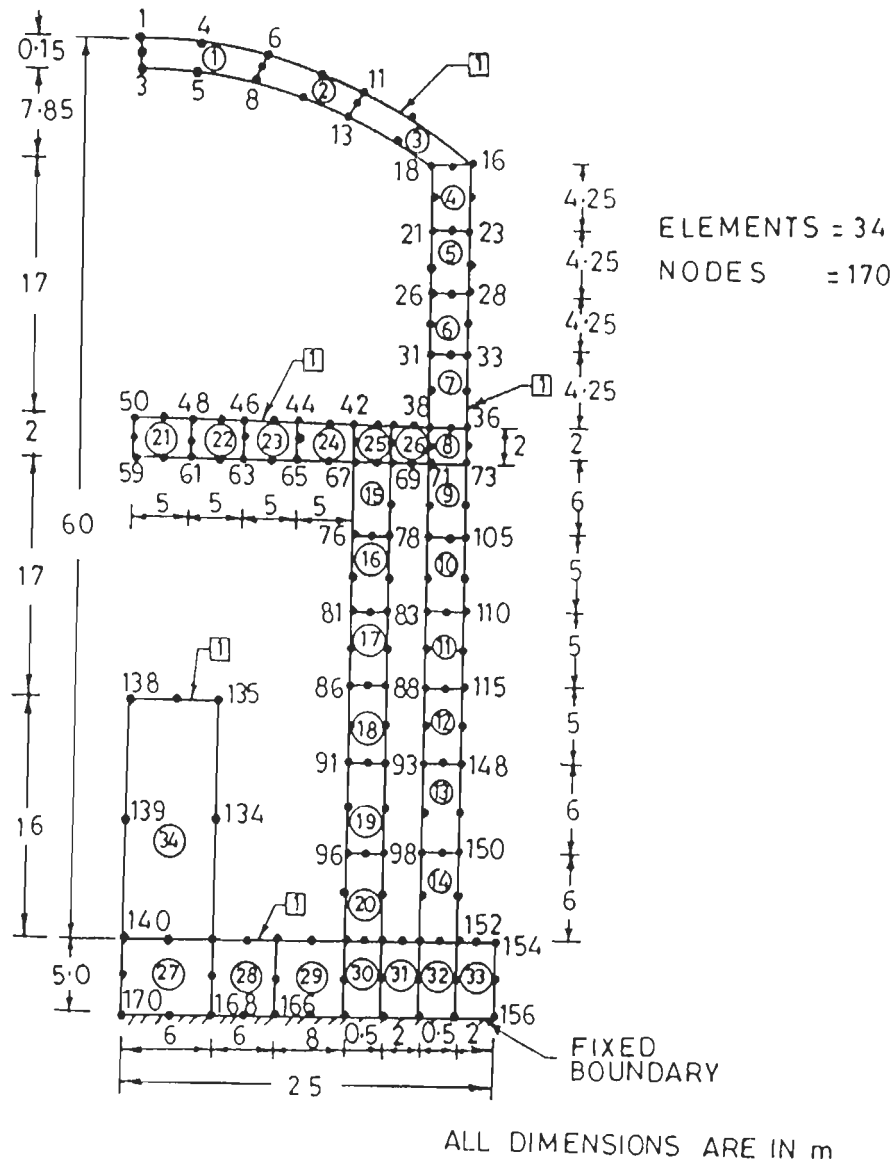
FIG. 4·15 FINITE ELEMENT MESH OF
REACTOR BUILDING (FIXED BASE)

Table 4.16 shows the time periods and mode participation factors for first six modes of the reactor building with fixed base.

Table 4.16
Dynamic Characteristics of Fixed Base Reactor Building

Mode	Time period (sec)	Mode participation factor
1	0.2172	1.68
2	0.1327	1.30
3	0.0780	0.29
4	0.0720	1.78
5	0.0520	1.27
6	0.0421	1.05

Structural behaviour during earthquake

The structural behaviour during earthquake can be explained with the aids of modes of vibration of a structure. A simple cantilever structure resting on elastic medium such as soil can have different modes of vibration as rocking mode, translational mode, structural bending mode and mixed mode, that is, combination of two or more basic modes (Thakkar, 1987). The rocking and translational modes are due to elasticity of soil, the structure behaving as rigid body ; these modes do not cause deformation in the structure, they cause deformation in the soil (Thakkar, 1983). The bending mode causes deformation in the structure and thus producing stresses in the structure. There can be higher structural modes of vibration. The nuclear reactor building is a structure composed of different substructures representing outer shell, inner shell, dome, reactor internal, floor slab etc. There can be modes in which outer shell alone vibrates, dome alone vibrates, two or more substructures can also vibrate together (Chandrasekaran, 1985). The type of modes of vibration would depend on relative stiffness and mass of different subsystems of structure and soil (Thakkar, 1989).

Figure 4.16 shows that first mode of vibration is a combination of vibration of outer shell, dome, inner shell and floor slab of reactor building. Second mode is a vibration of the reactor internal alone which is a pure bending mode. Third and fourth modes are combination of vibration of outer shell, inner shell and floor
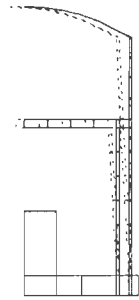
First Mode   T = 0.2172 Sec
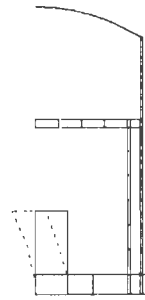
Second Mode   T = 0.1327 Sec
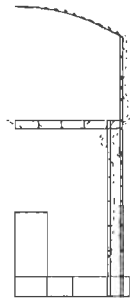
Third Mode   T = 0.0780 Sec
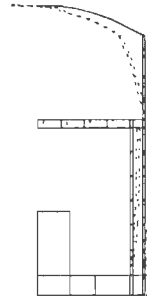
Fourth Mode   T = 0.0720 Sec
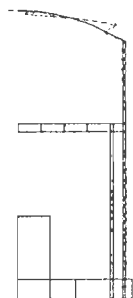
Fifth Mode   T = 0.0520 Sec
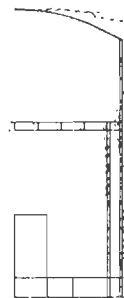
Sixth Mode   T = 0.0421 Sec

FIG. 4·16   FIRST SIX MODE SHAPES OF REACTOR
BUILDING

slab. Fifth mode is a mixed mode of vibration of outer shell and dome. Sixth mode is a combination of vibration of outer shell, inner shell, dome and floor slab. It is observed that the seismic response of a structure is mostly contained in first few modes of vibration. The response due to modes higher than six is generally small and is neglected. It should also be noted that the major response in a system is primarily due to vibration of its subsystems.

Further the study has been made for horizontal excitation due to Koyna earthquake (Fig. 4.5) of this fixed base reactor building (Fig. 4.14) and all the six stresses obtained (along the plane $\theta = 0^o$) are plotted along the height of outer shell, as shown in Figure 4.17.

It is observed from Figure 4.17 that the stress pattern is significantly changed at the junction points such as junction of shell and dome, junction of raft and shell, junction of inner shell and floor slab etc.; this phenomenon can not be predicted by simplified beam analysis and hence the necessity of axisymmetric analysis to locate such points of stress concentration. Also, the beam analysis can not predict the other stress components like σ_r and σ_θ which are evident in the axisymmetric analysis (Descleve, 1985).

Reactor building with flexible base

4.11.1 Effect of Shear Wave Velocity on Overall Seismic Response

The study has been made for horizontal excitation of above reactor building (Fig. 4.14) including surrounding and base soil, with different shear wave velocities. Figure 4.18 shows the finite element mesh of reactor building with founding soil. The following foundation parameters are taken,

Soil width (A)	: 3R
Soil depth (B)	: 2R
Depth of embedment	: 12 m
Earthquake motion	: Dec. 11, 1967, Koyna Earthquake, Transverse component
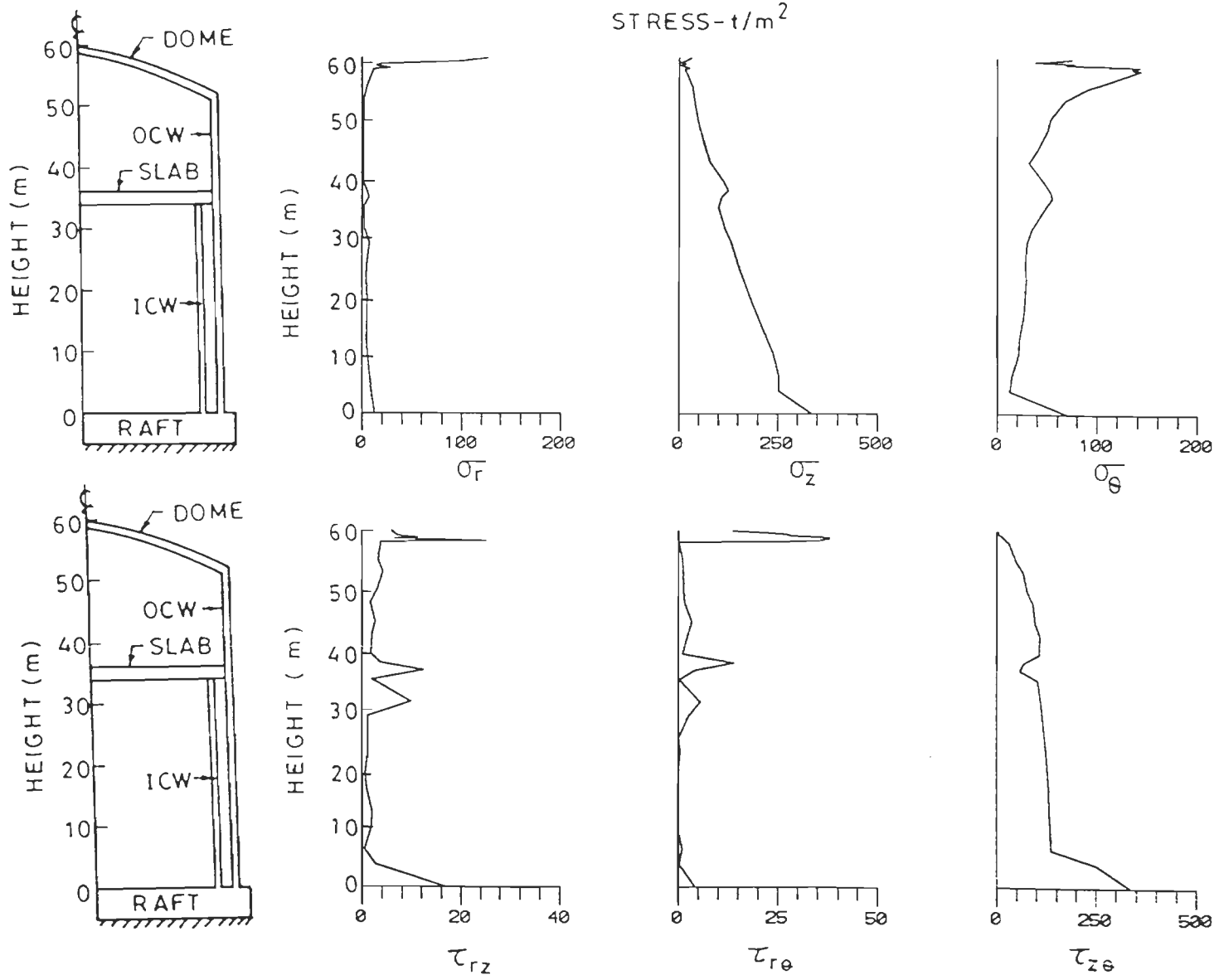
FIG. 4·17 SIX STRESS COMPONENTS ALONG THE HEIGHT OF OCW OF REACTOR BUILDING
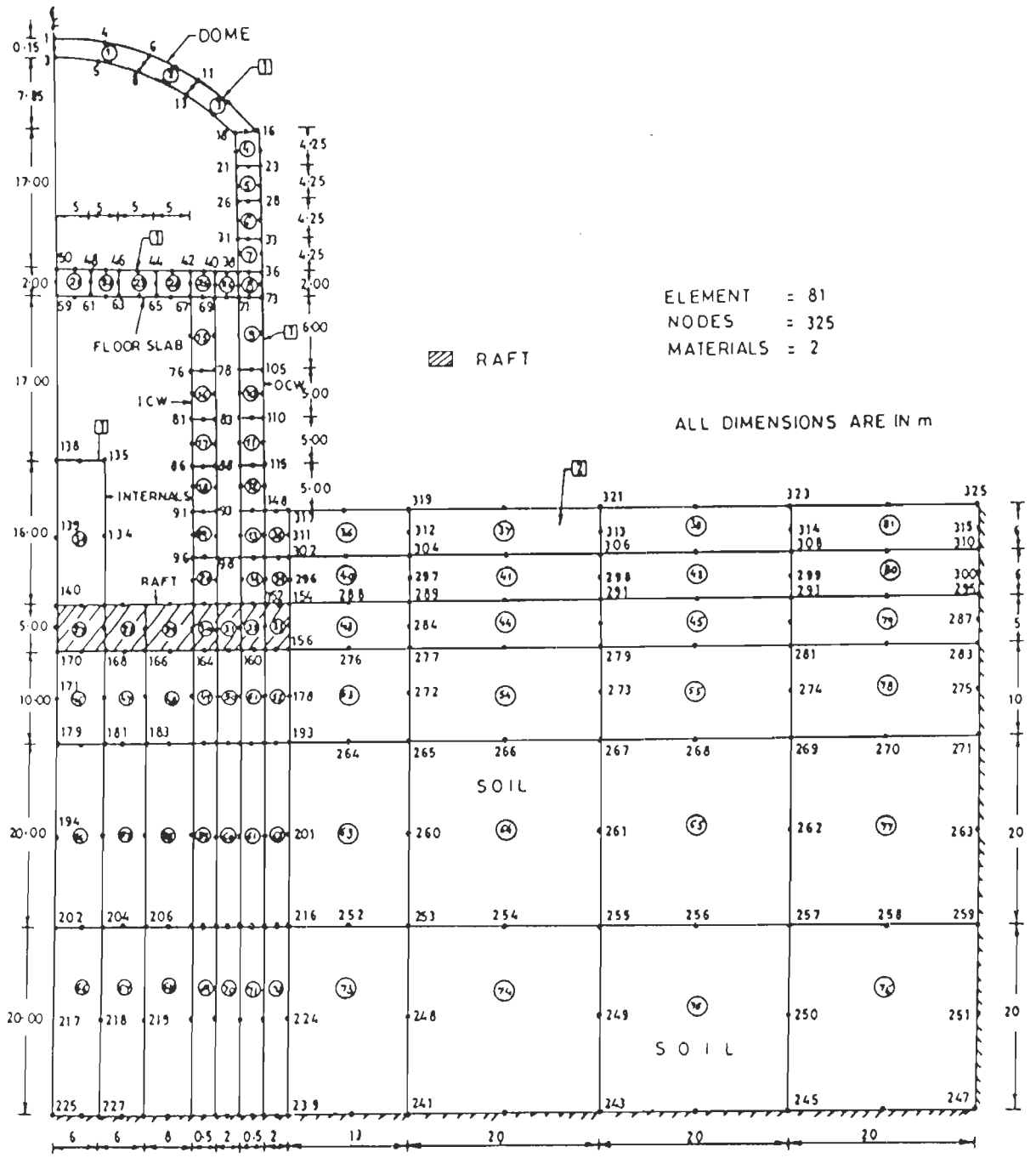
FIG. 4·18 – FINITE ELEMENT MESH OF REACTOR BUILDING AND FOUNDING SOIL

Tables 4.17 through 4.25 present the results of parametric study on the reactor building for different shear wave velocities of soil. These results include the first six mode periods, the associated mode participation factor and weighted modal damping, bending and shear stresses at gauss points and horizontal displacements at nodes.

Effect of shear wave velocity on dynamic characteristics (Table 4.17)

Time period

It is observed from Table 4.17 that as the shear wave velocity increases from 300 to 1200 m/s, the fundamental time period decreases from 0.411 s to 0.220 s; second mode period from 0.244 s to 0.178 s and third mode period from 0.169 s to 0.088 s etc. It is also observed that decrease in time period is more between shear wave velocity of 300 to 600 m/s and this effect of decrease in time period is reduced for further increase of shear wave velocity from 600 to 900 m/s. The variation in values of time periods is insensitive after shear wave velocity of 900m/s.

Weighted modal damping

As the shear wave velocity increases from 300 to 1200 m/s, weighted modal damping for fundamental mode decreases from 16.14 % to 9.32 % and very small variation occurs in higher modes. Also, the variation is faster between shear wave velocity of 300 to 600 m/s and this effect is almost insensitive after shear wave velocity of 900 m/s (Singhal, 1983).

Mode participation factor(m.p.f.)

The values of mode participation factor in six modes do not follow any pattern with increase of shear wave velocity.

Table 4.17
Effect of Shear Wave Velocity on Dynamic Characteristics

Shear wave velocity, m/s	Mode	Time period	Weighted modal damping (%)	Mode participation factor
300	1	0.411	16.14	1.96
	2	0.244	10.16	0.71
	3	0.169	15.52	0.69
	4	0.108	5.12	0.15
	5	0.077	5.85	0.20
	6	0.064	6.80	0.03
600	1	0.267	12.51	1.98
	2	0.210	8.20	0.43
	3	0.089	14.80	1.25
	4	0.087	5.80	0.94
	5	0.077	6.25	1.30
	6	0.064	9.23	0.81
900	1	0.224	10.17	2.05
	2	0.189	8.54	0.64
	3	0.089	5.54	0.98
	4	0.083	8.10	1.50
	5	0.074	8.72	1.55
	6	0.063	7.02	1.54
1200	1	0.220	9.32	1.96
	2	0.178	9.20	1.11
	3	0.088	6.32	1.38
	4	0.082	6.63	1.33
	5	0.069	7.71	1.10
	6	0.049	8.53	0.76
Fixed base	1	0.217	5.00	1.68
	2	0.133	5.00	1.30
	3	0.078	5.00	0.29
	4	0.072	5.00	1.78
	5	0.052	5.00	1.27
	6	0.042	5.00	1.05

Effect of shear wave velocity on seismic response of OCW

Maximum bending stress

Table 4.18 shows the variation of maximum bending stresses at outer gauss points in different elements of OCW for different shear wave velocities and compared with that of fixed base case.

Table 4.18
Effect of Shear Wave Velocity on Bending Stress (σ_z) in OCW

Element G.P. number (Fig.4.18)		σ_z $\left(t/m^2\right)$ for shear wave velocity (m/s)			
		300	600	900	Fixed Base
1	4	14.54	70.65	70.83	71.47
	3	9.91	51.00	52.45	53.10
2	4	7.61	28.31	35.35	36.47
	3	5.99	35.98	36.76	37.16
3	4	5.20	8.24	10.89	15.08
	3	9.69	45.54	45.59	46.05
4	4	5.13	32.76	33.63	35.53
	3	18.88	41.15	43.36	44.30
5	4	19.40	47.61	48.01	48.10
	3	22.83	52.81	55.19	55.94
6	4	29.24	58.22	62.64	63.87
	3	36.46	70.17	75.18	78.34
7	4	43.98	80.11	85.58	89.35
	3	64.37	130.89	131.21	133.16
8	4	72.24	141.26	142.14	145.62
	3	53.67	115.56	122.27	128.75
9	4	51.00	105.76	111.31	120.70
	3	95.45	135.10	147.93	148.55
10	4	103.34	146.83	161.98	163.63
	3	125.02	170.19	189.79	191.14
11	4	144.76	186.93	207.91	214.90
	3	142.26	187.94	214.00	224.75
12	4	97.46	169.90	206.21	210.57
	3	240.66	314.22	356.23	362.86

It is observed that bending stresses at various points are increased with increase of shear wave velocity. It is also observed that stresses are largest for fixed base structure as compared to the structure resting on soil.

Maximum shear stress

The variation of maximum shear stresses at outer gauss points in different elements of OCW for different shear wave velocities is presented in Table 4.19 and compared with that of fixed base structure. It is observed that the shear stresses at various points are increased with increase of shear wave velocity from 300 to 900 m/s. It is also found that the shear stresses are maximum for fixed base structure as compared to the flexible base structure (Bycroft, 1977).

Table 4.19
Effect of Shear Wave Velocity on Shear Stress (τ_{rz}) in OCW

Element G.P. number (Fig.4.18)		$\tau_{rz} \left(t/m^2 \right)$ for shear wave velocity (m/s)			
		300	600	900	Fixed Base
1	4	1.46	12.89	13.35	16.06
	3	1.45	13.98	14.05	16.78
2	4	5.33	24.84	25.44	27.16
	3	3.71	29.19	30.01	30.26
3	4	3.74	13.45	14.46	16.68
	3	9.69	48.60	49.50	54.96
4	4	3.16	4.43	4.52	5.72
	3	1.34	5.63	6.22	6.23
5	4	1.20	6.12	7.16	8.10
	3	1.23	4.27	4.87	5.03
6	4	0.86	1.82	2.64	2.71
	3	1.29	3.08	3.97	4.64
7	4	1.03	3.13	3.14	3.30
	3	1.35	2.12	2.18	4.90
8	4	2.69	4.91	5.61	13.66
	3	10.63	12.42	15.54	17.41
9	4	1.27	2.86	3.83	4.03
	3	8.01	11.41	12.36	12.86
10	4	0.30	1.20	1.32	2.17
	3	2.14	2.28	2.72	3.20
11	4	2.40	3.42	3.70	3.84
	3	2.03	2.89	2.58	4.69
12	4	3.99	4.40	5.85	5.98
	3	18.71	17.02	18.14	22.03

Maximum horizontal displacement

Table 4.20 shows the variation of maximum lateral displacement at outer nodes of OCW for different shear wave velocities and compared with the fixed base case. There is a significant decrease in the values of displacement at various nodes with increase of shear wave velocity from 300 to 900 m/s and the values of displacement are least for the fixed base structure.

Table 4.20

Effect of Shear Wave Velocity on Displacement in OCW

Node number (Fig. 4.18)	Maximum horizontal displacement (mm) For shear wave velocity (m/s)			
	300	600	900	Fixed Base
1	26.87	11.05	10.28	10.03
6	26.58	10.75	9.92	9.71
11	25.42	9.45	9.36	9.34
14	24.93	10.33	9.64	9.21
16	24.15	10.35	9.55	8.97
20	23.18	9.72	9.00	8.51
23	22.22	9.01	8.41	7.82
28	20.45	7.93	7.49	6.86
33	18.56	6.84	6.52	5.82
36	16.72	5.98	5.92	5.54
73	14.10	4.95	4.92	4.31
105	11.61	3.37	3.33	3.04
110	9.58	2.17	2.11	2.00
115	4.93	0.70	0.55	0.49
148	4.62	0.49	0.14	0.13

Effect of shear wave velocity on seismic response of ICW

Maximum bending stress

The maximum bending stress distribution in various elements along the height of

ICW for different shear wave velocities is presented in Table 4.21 and compared with that of fixed base structure. It can be seen from this table that bending stresses are increased with increase of shear wave velocity and the maximum bending stresses are found for the fixed base structure.

Table 4.21

Effect of Shear Wave Velocity on Bending Stress (σ_z) in ICW

Element number (Fig.4.18)	G.P.	$\sigma_z \left(t/m^2 \right)$			
		For shear wave velocity (m/s)			
		300	600	900	Fixed Base
15	4	19.62	60.70	61.03	62.62
	3	44.65	68.04	75.68	85.48
16	4	50.24	77.46	85.85	99.74
	3	58.28	88.29	99.37	119.17
17	4	66.07	108.36	112.19	136.05
	3	76.91	111.56	128.15	159.68
18	4	84.81	121.29	140.43	177.18
	3	96.37	133.34	156.45	201.82
19	4	105.30	143.15	169.60	220.80
	3	109.50	168.67	179.89	238.40
20	4	104.17	165.65	178.87	239.05
	3	184.53	219.96	232.84	319.50

Maximum shear stress

The values of maximum shear stress at the outer gauss points in the different elements of ICW are given in Table 4.22. The maximum shear stress values at the same points for fixed base structure are also presented in this table. It is observed that the shear stresses are increased with the increase of shear wave velocity and these values are largest for the fixed base structure.

Table 4.22

Effect of Shear Wave Velocity on Shear Stress (τ_{rz}) in ICW

Element number (Fig.4.18)	G.P.	τ_{rz} (t/m^2) For shear wave velocity (m/s)			
		300	600	900	Fixed Base
15	4	2.29	4.24	5.65	5.75
	3	2.41	3.46	3.72	4.38
16	4	2.59	3.00	3.05	3.77
	3	2.71	3.64	3.75	4.00
17	4	3.08	3.73	3.98	4.93
	3	3.13	3.37	3.93	4.46
18	4	3.77	3.84	3.98	4.66
	3	2.25	4.35	4.89	5.85
19	4	4.53	5.85	6.47	7.73
	3	1.42	1.61	1.66	2.82
20	4	1.27	4.40	4.56	5.43
	3	8.01	16.96	19.47	24.78

Maximum horizontal displacement

The maximum lateral displacement values at outer nodes of ICW for different shear wave velocities are listed in Table 4.23. Also, the displacement at these nodes are tabulated for the fixed base structure. The displacements decrease significantly with increase of shear wave velocity from 300 to 600 m/s and negligible decrease in displacements occurs with further increase of shear wave velocity from 600 to 900 m/s. It is also observed that the displacements are minimum for fixed base structure.

Effect of Shear Wave Velocity on Seismic Response of the Raft

Table 4.24 shows the variation of maximum bending stress on bottom gauss points in various elements of the raft for different shear wave velocities and compared with the fixed base case.

Table 4.23

Effect of Shear Wave Velocity on Displacement in ICW

Element number (Fig.4.18)	Maximum horizontal displacement (mm) For shear wave velocity (m/s			
	300	600	900	Fixed Base
69	16.09	5.47	5.50	5.48
78	12.24	4.64	4.26	4.19
83	10.38	3.86	3.30	3.11
88	8.58	3.15	2.45	2.11
93	6.85	2.53	1.58	1.24
98	4.95	1.71	1.41	1.05

Table 4.24

Effect of Shear Wave Velocity on Bending Stress (σ_z) in raft

Element number (Fig.4.18)	GP	$\sigma_z \left(t/m^2 \right)$ For shear wave velocity (m/s)			
		300	600	900	Fixed Base
27	1	10.16	16.21	17.83	65.63
	3	28.40	31.25	32.29	79.58
28	1	16.61	25.35	28.85	72.13
	3	10.83	16.37	20.23	65.67
29	1	18.91	22.05	24.89	57.34
	3	18.43	22.26	25.94	65.69
30	1	25.38	32.70	32.75	54.02
	3	21.73	27.77	29.68	59.73
31	1	20.61	25.17	26.09	26.43
	3	4.65	8.96	10.48	23.28
32	1	41.43	62.27	102.72	266.64
	3	4.19	5.22	7.54	8.37
33	1	3.90	14.78	34.76	110.82
	3	12.74	51.57	106.16	383.44

It is observed that the bending stresses increase with increase of shear wave velocity from 300 to 900 m/s and stresses are largest for the fixed base structure.

Effect of Shear Wave Velocity on Seismic Response of the Slab

The variation of maximum bending stress on bottom gauss points in different elements of slab for various shear wave velocities is presented in Table 4.25 and the stresses are compared with the fixed base structure.

Table 4.25
Effect of Shear Wave Velocity on Bending Stress (σ_z) in Slab

Element number (Fig.4.18)	GP	$\sigma_z \left(t/m^2\right)$ For shear wave velocity (m/s)			
		300	600	900	Fixed Base
21	1	0.81	1.01	1.57	1.71
	3	0.28	0.35	0.45	0.48
22	1	0.52	1.42	1.98	2.86
	3	0.62	1.26	1.36	1.51
23	1	0.73	1.77	1.83	2.24
	3	0.67	1.21	1.28	2.17
24	1	2.32	4.35	4.66	5.52
	3	4.44	6.55	7.15	7.38
25	1	14.98	17.84	20.29	24.13
	3	10.66	26.01	26.60	27.79
26	1	6.11	7.86	9.06	9.99
	3	13.33	19.41	19.88	20.50

It is observed that stresses at different points increase with increase of shear wave velocity from 300 to 900 m/s. It is also found that stresses are largest for fixed base structure.

4.11.2 Effect of Embedment Depth on Overall Seismic Response

The same reactor building (Fig. 4.14) is considered to see the effect of different depths of embedment on over all seismic response of the reactor building. Satosh & Sasagawa (1982) studied the dynamic response characteristics of reactor building with different depths of embedment. Figure 4.18 shows the finite

element mesh of reactor building including foundation soil. The following parameters are considered :

Soil width (A)	: 3R
Soil depth (B)	: 2R
Embedment depth (D)	: 0m, 6m, 12m, 8m
Shear wave velocity of soil	: 600 m/s
Earthquake motion	: Dec.11, 1967, Koyna Earthquake, Transverse component

Table 4.26 shows time period, weighted modal damping and mode participation factor (m.p.f.) in first three modes for different depths of embedment.

Table 4.26
Effect of Embedment Depth on Dynamic Characteristics

Depth of embedment (m)	Mode	Time period (sec)	Weighted modal damping (%)	m.p.f.
0.0	1	0.267	11.55	1.50
	2	0.210	9.10	0.90
	3	0.089	11.82	0.13
6.0	1	0.256	10.50	1.49
	2	0.191	8.90	0.88
	3	0.089	8.60	0.14
12.0	1	0.247	10.23	1.46
	2	0.191	8.81	0.86
	3	0.088	6.40	0.12
18.0	1	0.224	10.17	1.45
	2	0.189	8.54	0.75
	3	0.088	5.54	0.09

Time period (Table 4.26) :

The fundamental time period decreases from 0.267 to 0.224 sec. with the depth of embedment varying from 0.0 m to 18.00 m and very small variation of time period occurs for higher modes with the increase of embedment depth. It is also observed that this effect of decrease in time period with increase of embedment depth is more when the embedment depth increases from 0.0 m to 12.00 m.

Weighted modal damping (Table 4.26) :

Weighted modal damping decreases with increase in depth of embedment. It is due to increased rigidity of structure with increase of embedment depth which results in reduced deformation and strain energy. However the decrease in modal damping is insignificant for second and third modes. Also, the variation is insensitive for increase in embedment depth from 12m to 18m.

Mode participation factor (Table 4.26) :

Mode participation factor decreases with increase of depth of embedment for fundamental mode and insignificant variation occurs in higher modes.

Figures 4.19 through 4.22 show the results of parametric study on the reactor building for different depths of embedment. The seismic response is obtained as a result of finite element analysis of soil-structure system under horizontal ground motion using mode superposition method, considering first six modes in the analysis.

Effect of embedment depth on seismic response of OCW

Maximum bending stress

Figure 4.19a shows the variation of bending stress along the height of outer shell (OCW and dome) with and without embedment of the reactor building. The depth of embedment is taken as 12m. It is found that stresses in the lower part of the shell are significantly reduced for embedded structure as compared to unembedded one.

Maximum shear stress

Figure 4.19b shows the variation of shear stress along the height of shell for embedment depth of 0m and 12m respectively. It is observed that stresses in the shell are not much reduced for embedded structure as compared to unembedded one.
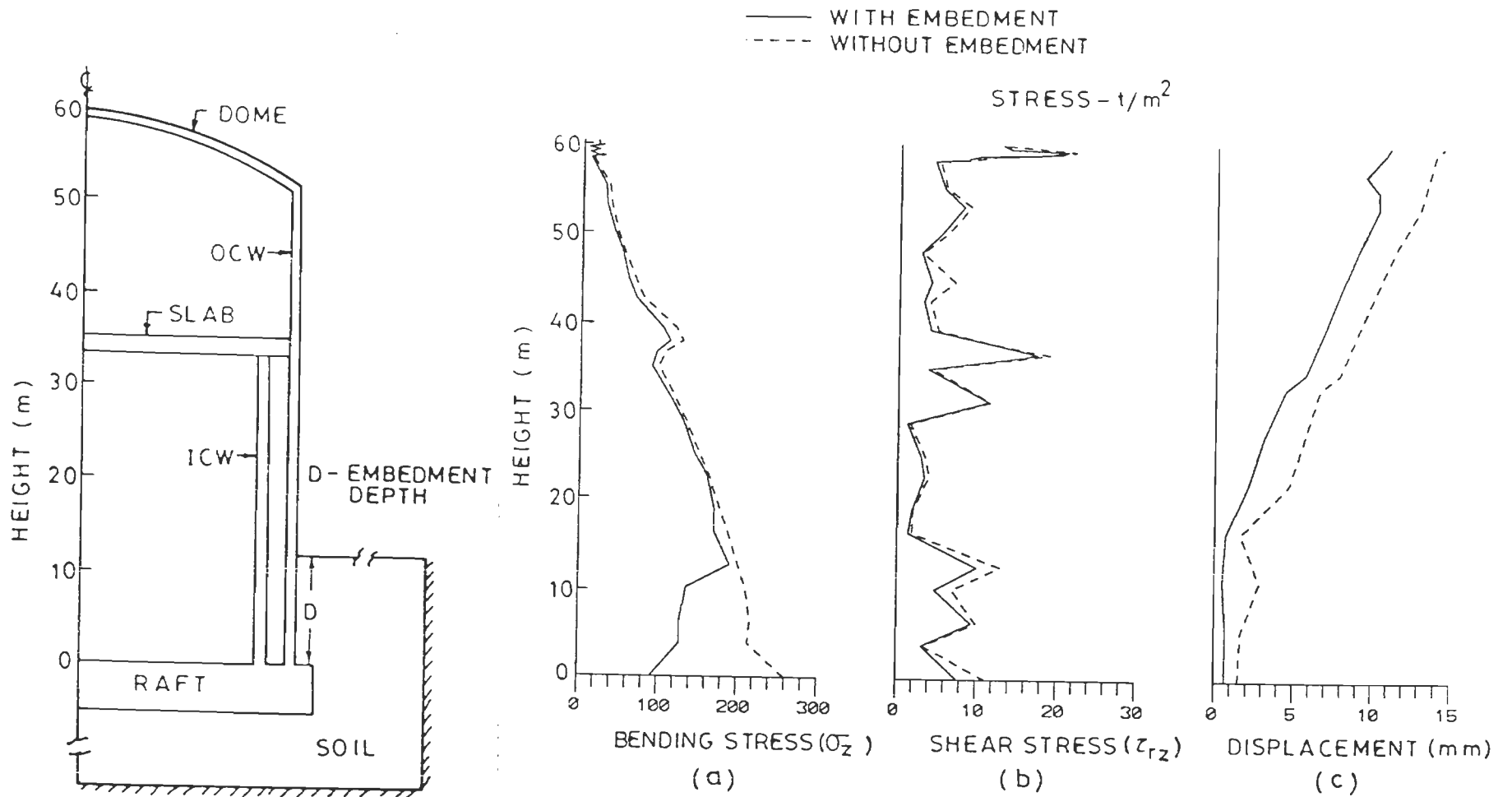
FIG. 4·19 MAXIMUM STRESS/DISPLACEMENT RESPONSE OF OCW WITH AND WITHOUT EMBEDMENT OF BUILDING (KOYNA EARTHQUAKE, DEC. 11, 1967, TRANSVERSE)
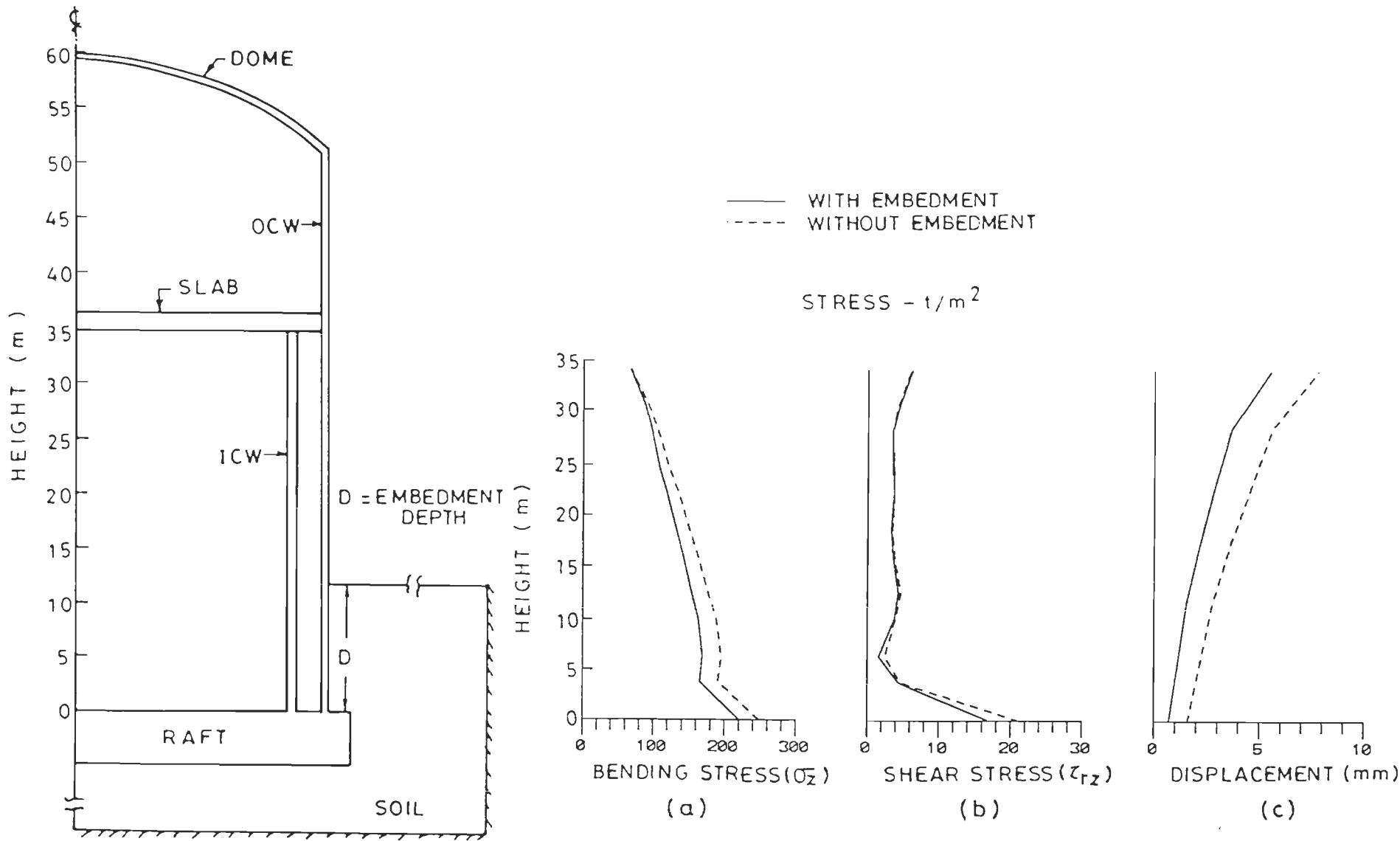
FIG. 4·20 MAXIMUM STRESS/DISPLACEMENT RESPONSE OF ICW WITH AND WITHOUT EMBEDMENT OF BUILDING (KOYNA EARTHQUAKE, DEC. 11, 1967, TRANSVERSE)
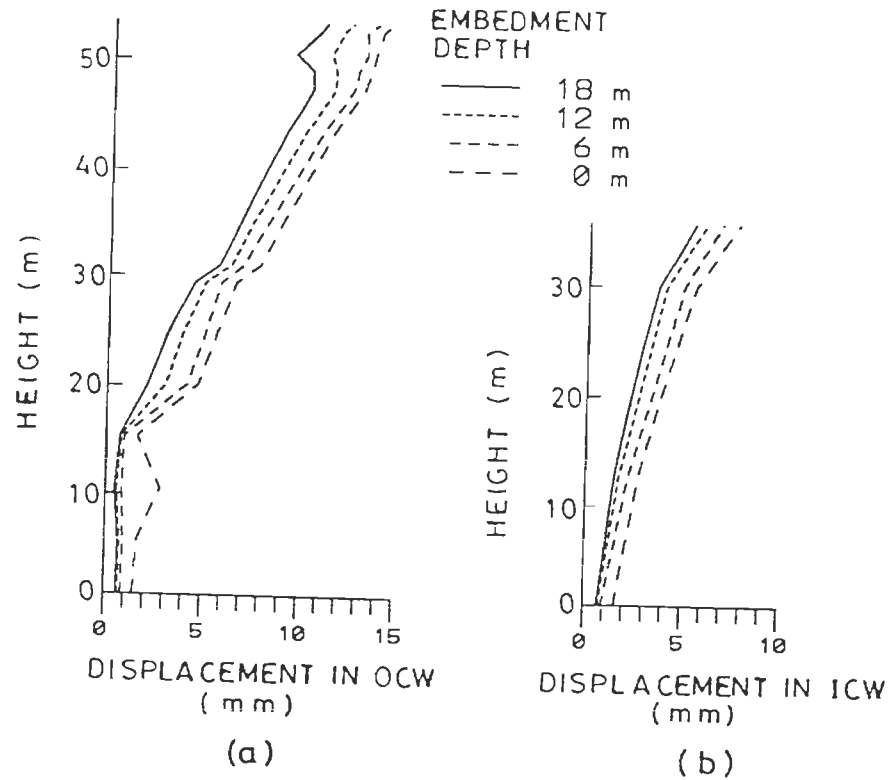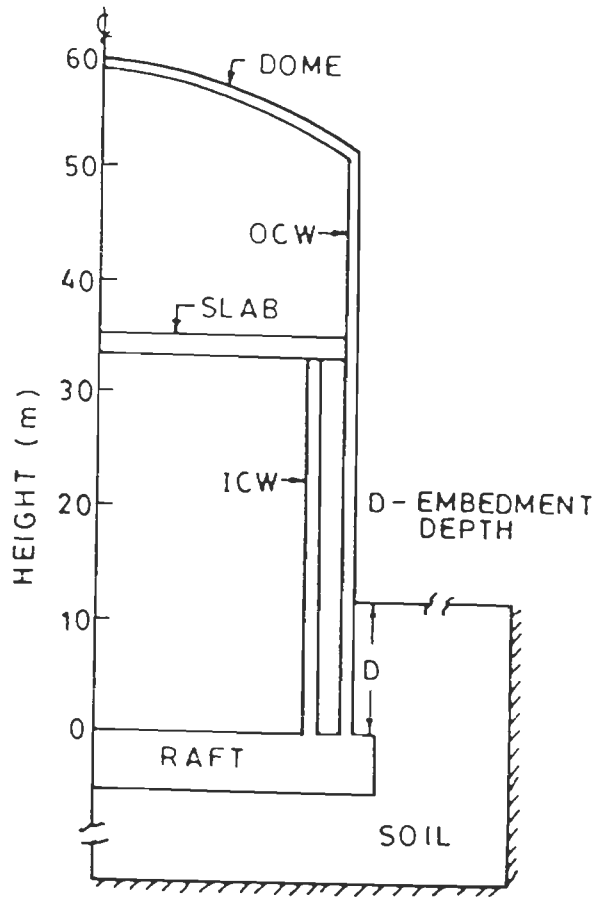
FIG. 4·21 MAXIMUM DISPLACEMENT RESPONSE OF OCW AND ICW FOR DIFFERENT DEPTHS OF EMBEDMENT (KOYNA EARTHQUAKE, DEC. 11,1967 TRANSVERSE)
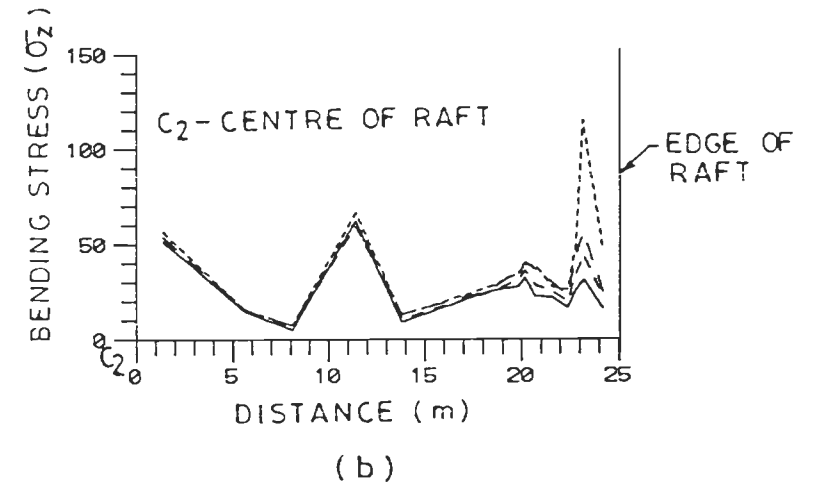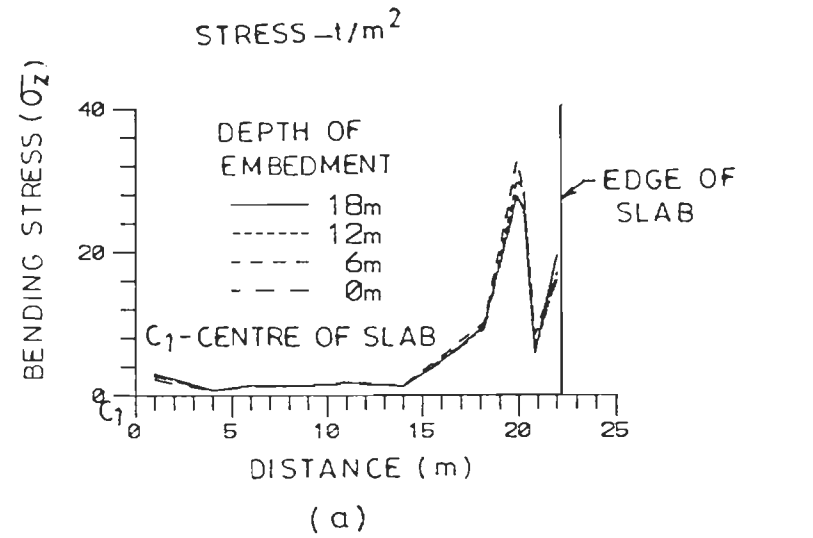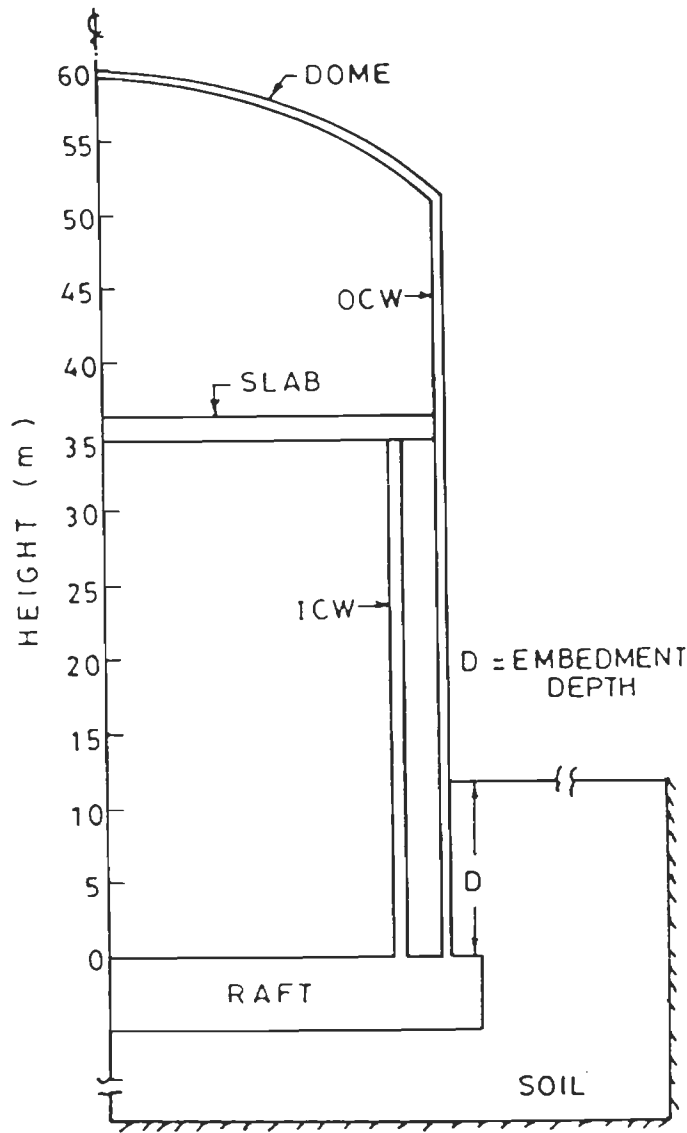
FIG. 4·22 MAXIMUM STRESS RESPONSE OF SLAB AND RAFT FOR DIFFERENT DEPTHS OF EMBEDMENT (KOYNA EARTHQUAKE, DEC. 11, 1967, TRANSVERSE)

Maximum horizontal displacement

The variation of horizontal displacement along the height of OCW for the depths of embedment of 0m and 12m is shown in Fig. 4.19c. It is clear that displacements are significantly reduced throughout the height of OCW for embedded structure as compared to unembedded one.

Effect of embedment depth on seismic response of ICW

Maximum bending stress

Figure 4.20a shows the variation of bending stress along the height of ICW for embedment depths of 0m and 12m. It is observed that stresses in the lower part of shell are significantly reduced for embedded structure as compared to unembedded structure.

Maximum shear stress

Figure 4.20b shows the variation of shear stress along the height of ICW for embedment depths of 0m and 12m respectively. It is observed that shear stresses are not much affected with increase in depth of embedment.

Maximum horizontal displacement

Figure 4.20c shows the variation of horizontal displacement along the height of shell for the depths of embedment of 0m and 12m. The displacements throughout the height of ICW are considerably reduced for embedded structure.

Variation of maximum lateral displacement along the heights of OCW and ICW for different depths of embedment

The variation of lateral displacement along the heights of OCW and ICW for embedment depths of 0.0m, 6.0m, 12.0m and 18.0m is shown in Figures 4.21a and 4.21b, respectively. It is observed that the displacements are reduced significantly with increase of embedment depth from 0m to 12m and for further

increase in depth of embedment, there is a small decrease in the values of the lateral displacement along the heights of OCW and ICW.

Effect of embedment depth on seismic response of floor slab

Figure 4.22a shows the variation of maximum bending stress on bottom gauss points of slab for different depths of embedment. It is observed that stresses are reduced considerably on end one third portion of slab with increase of embedment depth and almost insignificant variation occurs in the central part of slab for different depths of embedment.

Effect of embedment depth on seismic response of the raft

The variation of maximum bending stress on bottom gauss points of raft for different depths of embedment is shown in Fig. 4.22b. It is found that stresses are reduced significantly on end one third part of the raft with increase of embedment depth.

Therefore, it is concluded that most suitable depth of embedment for minimum seismic response of structure is 12m, that is, about one fifth of the height of the structure.

4.11.3 Effect of Type of Earthquake on Seismic Response

For comparing the maximum seismic responses of axisymmetric reactor structure founded on soil and subjected to horizontal excitation, three time histories (Figures 4.4 to 4.6) have been normalized to 0.49g (peak value of Koyna earthquake) as a common peak acceleration. Salient characteristics of these time histories are given in Table 4.1. The study has been made for soil-structure system (Fig. 4.18) with following foundation parameters,

Soil width (A)	: 3R
Soil depth(B)	: 2R
Embedment depth (D)	: 12m
Shear wave velocity of soil	: 600 m/s.

Figures 4.23 to 4.25 show the results of parametric study on the reactor building for these three earthquake time histories.
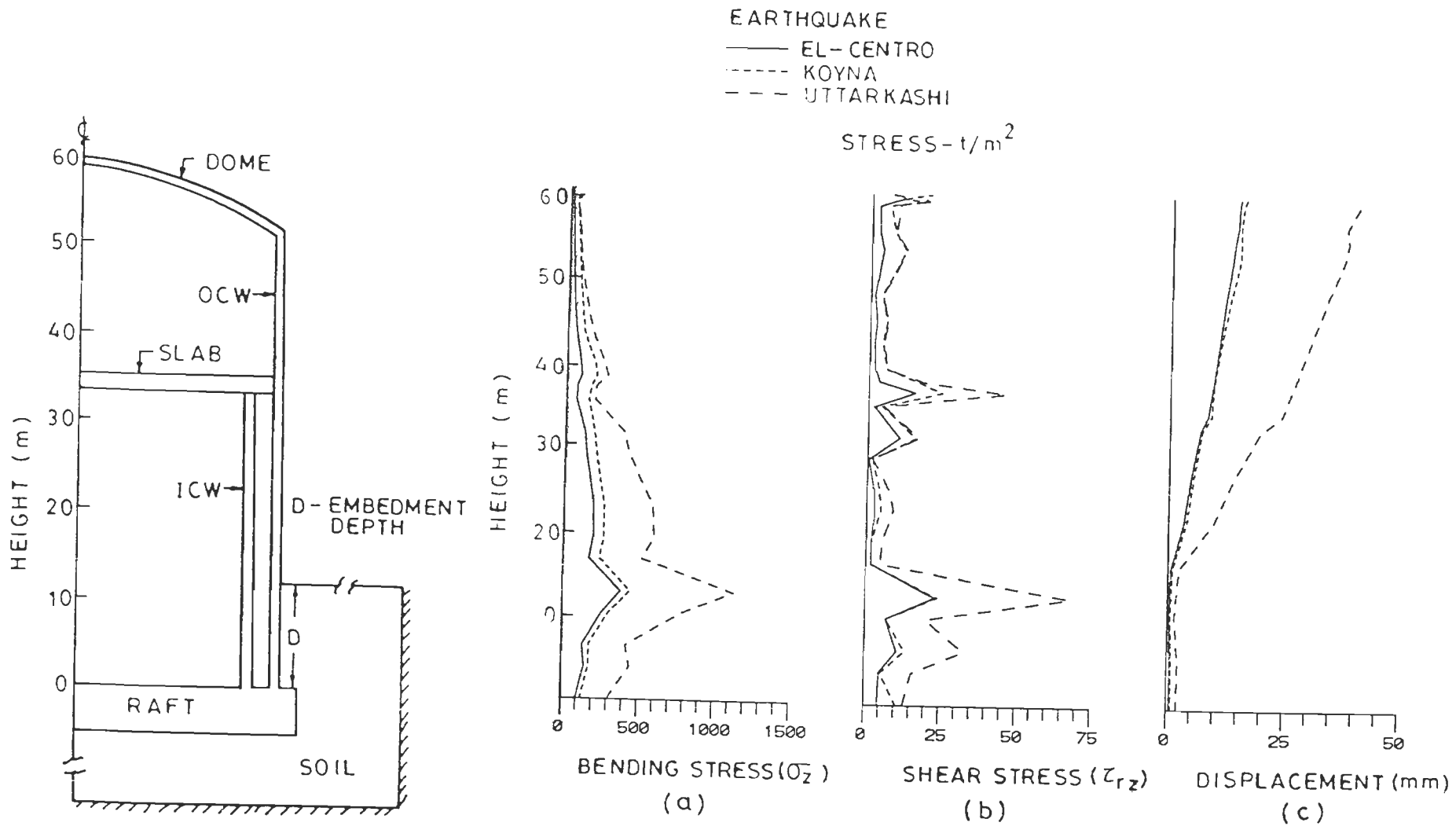
FIG. 4·23 COMPARISON OF MAXIMUM STRESS/DISPLACEMENT RESPONSE OF OCW TO THREE EARTHQUAKES
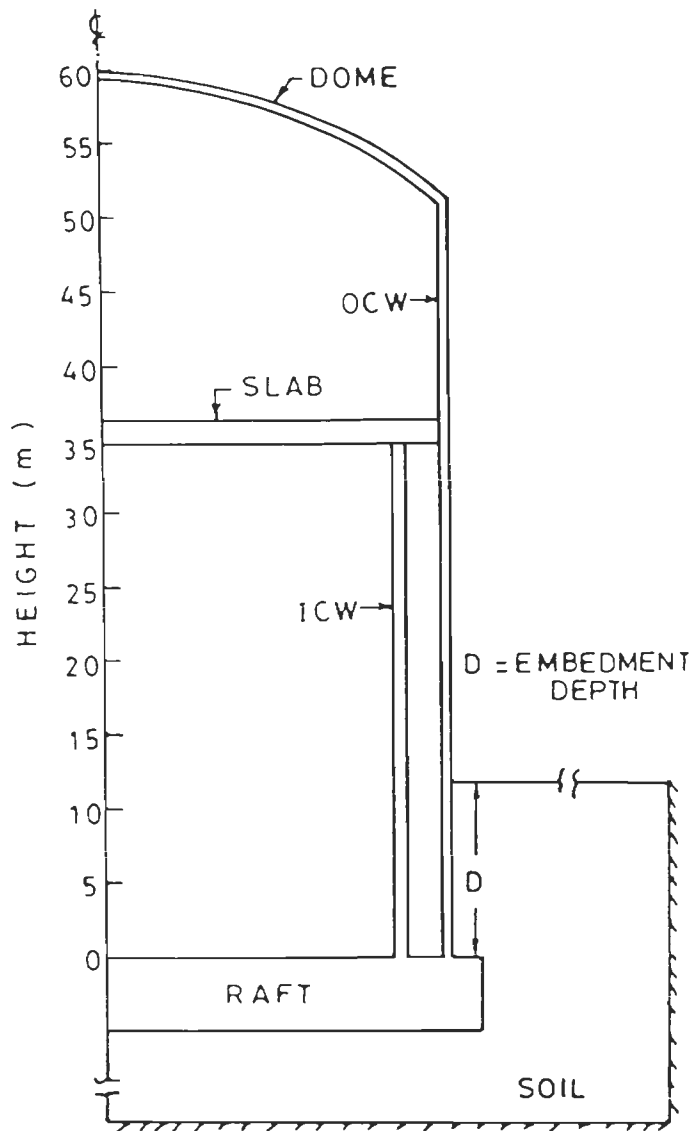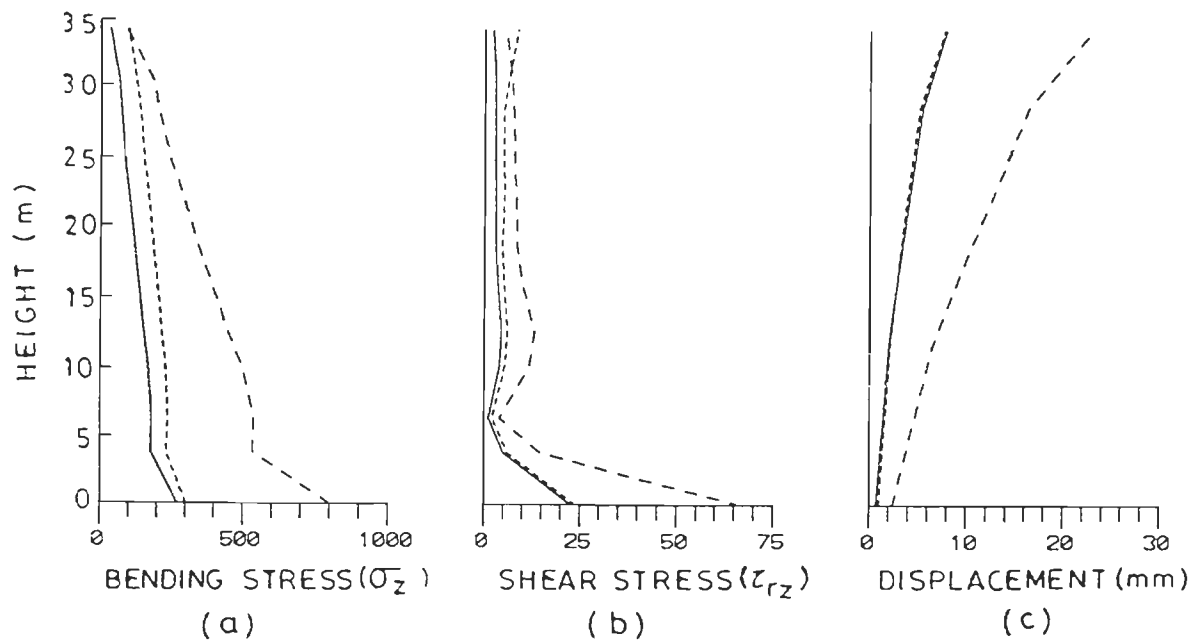
FIG. 4·24 COMPARISON OF MAXIMUM STRESS / DISPLACEMENT RESPONSE OF ICW TO THREE EARTHQUAKE
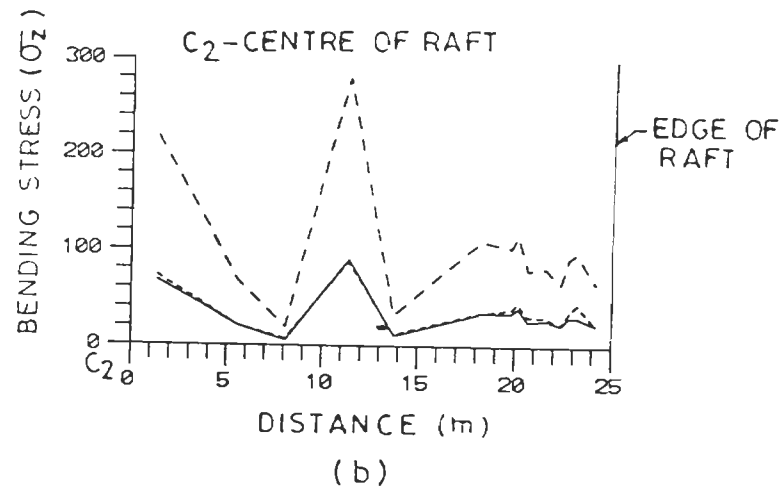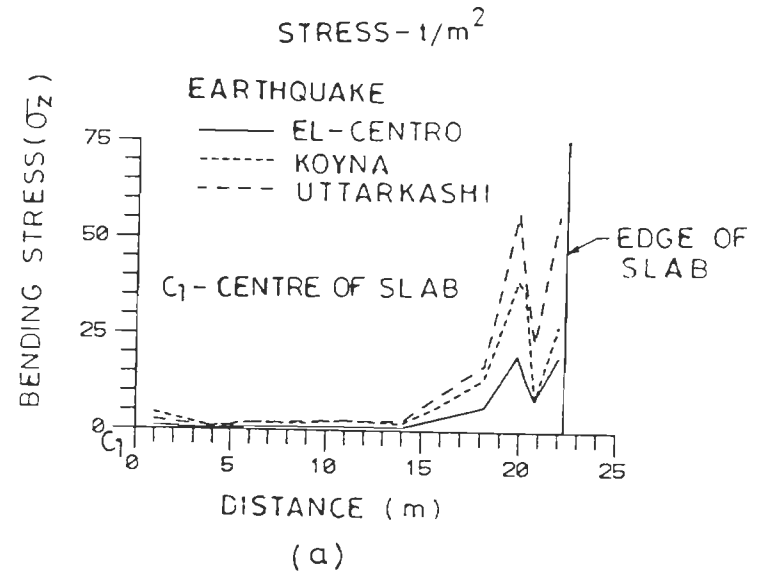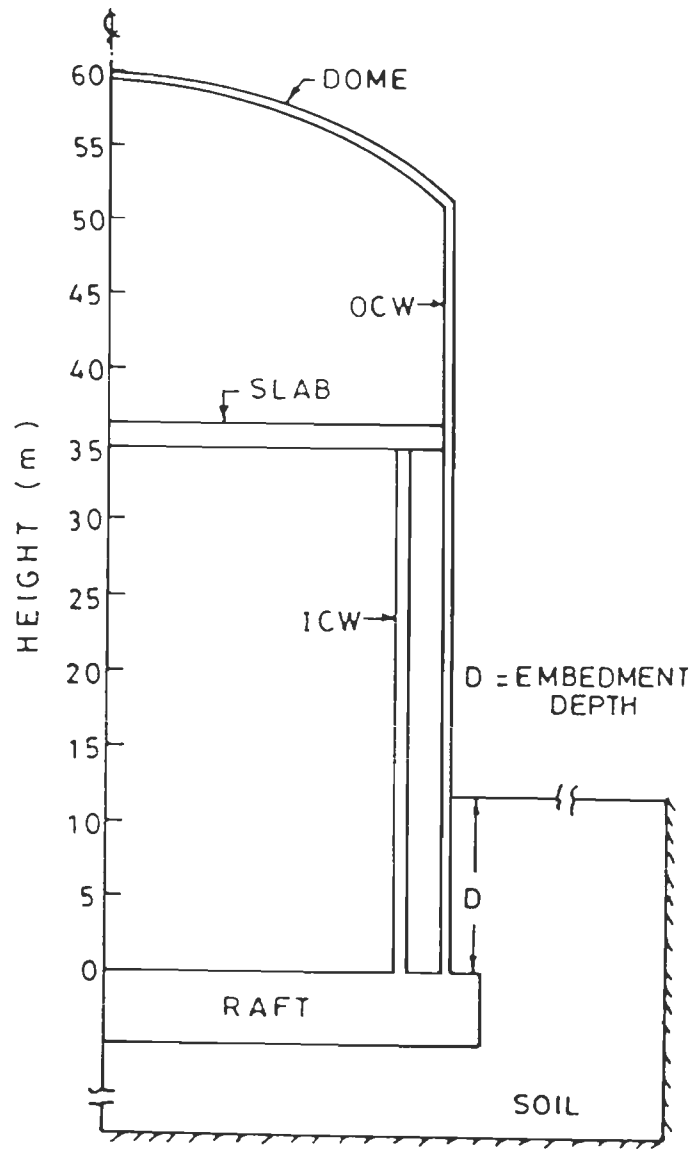
FIG. 4·25   COMPARISON OF MAXIMUM STRESS RESPONSE OF SLAB AND RAFT
TO THREE EARTHQUAKE

Effect of type of earthquake on the response of OCW

Maximum bending stress

Figure 4.23a shows the variation of bending stress along the height of outer shell for these three earthquake time histories. The stresses in the lower and middle parts of wall are significantly larger due to Uttarkashi earthquake as compared to other two. The difference is small in the upper part of the shell for these three earthquakes.

Maximum shear stress

The variation of shear stress along the height of outer shell for these three earthquake time histories are shown in Fig. 4.23b. It is found that the stresses in the lower and upper part of shell are larger for Uttarkashi earthquake as compared to other two. There is a small change of stress distribution in the middle part of wall for these three normalized earthquakes.

Maximum horizontal displacement

The horizontal displacement distribution along the height of outer shell for these three earthquake time histories is shown in Fig. 4.23c. It is observed that the displacements are significantly larger due to Uttarkashi earthquake as compared to other two. The displacements are almost equal for Koyna and El-Centro earthquakes.

Effect of type of earthquake on seismic response of ICW

Maximum bending stress

The variation of bending stress along the height of ICW for these three earthquake time histories is shown in Fig. 4.24a. It is observed that stresses in the lower and middle parts of wall are significantly larger due to Uttarkashi earthquake as compared to other two. The difference is small in the upper part of wall for three earthquakes.

Maximum shear stress

Figure 4.24b shows the shear stress distribution along the height of wall for these three earthquake time histories. It is observed that stresses in the lower part of wall are larger for Uttarkashi earthquake as compared to other two. The difference is small in the middle and upper parts of wall for these three normalized earthquakes.

Maximum horizontal displacement

Figure 4.24c shows the variation of horizontal displacement along the height of wall for theses three earthquake time histories. It is observed that displacements are significantly larger due to Uttarkashi earthquake as compared to other two. The displacements are almost equal for Koyna and El-Centro earthquakes.

Effect of type of earthquake on seismic response of floor slab

Figure 4.25a shows the variation of maximum bending stress on bottom gauss points of slab for these three earthquake time histories. It is observed that stresses are considerably larger on end one third portion of slab for Uttarkashi earthquake as compared to other two and almost insignificant change occurs in the central part of slab for these three earthquakes.

Effect of type of earthquake on seismic response of the raft

Figure 4.25b shows the variation of maximum bending stress on bottom gauss points of the raft for these three earthquake time histories. It is found that stresses are considerably larger on central two third portion of the raft for Uttarkashi earthquake as compared to other two and a small difference occurs in the end part of raft for these three earthquakes.

As the fundamental time period of reactor building is 0.2172 sec.(Table 4.16) and dominating time period range of Uttarkashi earthquake is 0.17-0.34 sec (Table 4.1). Therefore it is clear that fundamental time period of structure lies between the dominating time period range of Uttarkashi earthquake which

results in higher deformations and stresses due to possible quasi-resonance condition.

4.12 Effect of Vertical Earthquake on Seismic Response

Morishita et.al.(1992) examined the vertical response characteristics of a reactor building and its neighbouring soil based on the records of forty-six observed earthquakes and found that the vertical response characteristics of the building do not change even excluding the contribution of the rocking on the vertical response of the building, the effect of vertical component of earthquake on seismic response of reactor building is considered to be negligible. Other investigators have also found the insignificant effect of vertical ground motion on overall seismic response of reactor building. Therefore, the vertical earthquake motion is not considered in the dynamic analysis of axisymmetric structures in this thesis.

4.13 Comparison of Seismic Responses of Containment Structure and Complete Reactor Building

As the parametric study of soil-structure interaction (SSI) effects on seismic behaviour of (a) containment structure without internal structures, and (b) complete reactor building including internal structure, double containment wall, raft, dome and slab; has been carried out, the following conclusions on structural behaviour of these two structures are derived from this comparative study :

(a) The near fixity condition of containment structure is achieved for shear wave velocity of 1200 m/s while in case of complete reactor building this condition is achieved for shear wave velocity of even 900 m/s.

(b) The minimum seismic response on containment structure is observed at the depth of embedment equal to one-sixth of the height of containment structure while in case of complete reactor building the minimum seismic response is observed at the depth of embedment equal to about one-fifth of the height of the reactor building.

130

4.14 Concluding Remarks

For complicated and important structures such as nuclear reactor building, sophisticated finite element method is suggested for better assessment of stress and displacement response. The finite element seismic analysis of few axisymmetric structures have been carried out and following conclusions on soil-structure interaction effects have been drawn :

(i) For all practical purposes, the horizontal extent of foundation soil from the outer surface of the wall and vertical extent of soil below raft can be taken as three times and two times of the radius of the raft, respectively.

(ii) With the inclusion of soil mass in the analysis, the results do not converge. Therefore, soil mass should not be considered in the seismic analysis of a reactor building, only flexibility of founding soil needs to be considered.

(iii) The near fixity condition of containment structure alone is achieved for shear wave velocity of 1200 m/s while this condition is achieved even at shear wave velocity of 900 m/s in complete reactor building. It is also concluded that the stresses are reduced in soil-structure system as compared to fixed base structure.

(iv) For achieving minimum seismic response of a structure, the most suitable depth of embedment should be equal to about 1/6th of the height of the structure for containment shell alone and 1/5th height of structure for complete reactor building.

(v) The structure whose fundamental time period lies in the range of dominating time periods of an earthquake, shows greater deformations and stresses.

(vi) The first six modes are sufficient for evaluating the overall maximum seismic response of a reactor building.

SEISMIC RESPONSE FROM MODE SUPERPOSITION AND DIRECT INTEGRATION METHODS

5.1 Introduction

The procedure of solving the set of force equilibrium equations for the linear elastic system subjected to ground motion has been presented in Chapter 3. The following two methods of solution have been employed in this study :

(i)   Timewise mode superposition method, and

(ii)   Direct step-by-step time integration method

Although, the two techniques may at first sight appear to be quite different, in fact, they are closely related, and the choice of one method over the other method is determined only by their numerical effectiveness.

5.2 Timewise Mode Superposition Method

This method has the following characteristics :

1.   It involves the solution of the characteristic value problem represented by the free vibration of the system, followed by the transformation to the principal coordinates determined as the characteristic shapes (mode shapes) of the system.

2.   This procedure uncouples the system of simultaneous equations, so that each equation may be evaluated independently of the others.

3.   The response of a system to an earthquake is largely expressed by the first few modes of vibration. Therefore, a good accuracy can be obtained by involving only a few of the principal coordinates in an analysis while all other coordinates must be retained by the direct integration of the equilibrium equations.

4. Modal analysis requires Rayleigh type of damping for uncoupling the equations of motion.

5. This method is based on the assumption of linear structural behaviour. So the method is generally most effective for linear analysis of earthquake response of structures.

6. In the conventional modal analysis the response from the modal values is computed using SRSS (square root of sum of squares) or some similar methods, this procedure would give all positive values of stresses, that is, all stresses would represent the compression as well as tension. The timewise mode superposition method takes care of proper sign of stresses.

7. It permits better visualization of participation of different modes of vibration to the total response.

5.3 Direct Step-by-Step Time Integration Method

This method has following characteristics :

1. The evaluation of the characteristic value problem (eigen value problem) and transformation to the principal coordinates are major computational effort not required in this procedure.

2. This method directly integrates the system of simultaneous equations without uncoupling.

3. In this method, all modes are supposed to be included. This depends upon the choice of time increment (Δt) used in the method. Generally this time increment is taken as one-tenth of the smallest time period value contributing to the seismic response of a structure.

4. In this method, explicit construction of damping matrix consists of either proportional to mass matrix or stiffness matrix or combination of both mass and stiffness matrices. These proportional coefficients are calculated using two modal values of damping and corresponding time periods.

5. This approach is easily extended to non-linear problems by modifying the stiffness matrix at each successive step of integration.

6. The accuracy and stability of results obtained by this method depend upon amplitude decay (numerical damping), period elongation, mesh size of finite elements etc.

In this study, implicit Newmark's constant average acceleration scheme ($\beta = 0.25$, $\gamma = 0.50$) has been used which is unconditionally stable, having zero numerical damping and no mesh grading effect. This is most effective method because of the smallest numerical integration error and unconditional stability.

5.4 Elastic Earthquake Analysis

The elastic time history analysis of few axisymmetric structures subjected to horizontal ground motion (Koyna earthquake Dec. 11, 1967, Transverse component) is carried out using above two methods. The seismic response of the structures obtained by these two methods is compared. The suitability and effectiveness of these methods in seismic response computation is also determined.

5.4.1 Containment Structure With Fixed Base

The containment shell resting on raft and fixed base (Fig. 4.11a), is considered for study. Figure 4.11b shows the finite element mesh of this structure in which there are 27 elements and 138 nodes in the finite element mesh. The containment structure is subjected to horizontal ground motion due to Koyna (India) Earthquake (Fig. 4.5). The maximum responses are obtained using above two approaches and presented through Tables 5.1 to 5.3.

Table 5.1 lists the bending and shear stresses at outer gauss points in selected elements along the height of containment structure obtained by these two methods of analysis, i.e,. mode superposition and direct integration methods.

It is observed from Table 5.1 that the bending and shear stresses in the upper part of the shell are larger in response obtained by direct integration method as

compared to that by mode superposition method while in the lower part of the structure the bending and shear stresses obtained by these two methods are comparing reasonably well.

Table 5.1

Maximum Stresses at Outer G.P. of Elements in Shell, (Fig. 4.11b)

Element number	G.P.	Bending stress $\left(\sigma_z - t / m^2 \right)$		Shear stress $\left(\tau_{rz} - t / m^2 \right)$	
		Mode superposition	Direct integration	Mode superposition	Direct integration
1	4	0.91	3.03	1.18	3.51
	3	0.20	1.04	0.77	2.12
2	4	0.41	1.47	0.86	3.20
	3	0.43	2.25	1.93	3.94
4	4	3.09	6.56	5.20	9.31
	3	4.63	7.15	5.27	9.39
6	4	18.12	29.94	12.98	21.50
	3	18.86	30.98	14.01	22.68
8	4	47.00	77.36	24.51	39.88
	3	36.48	58.24	7.62	12.03
10	4	7.62	10.52	8.48	12.33
	3	39.33	60.65	5.35	8.94
11	4	70.42	114.43	0.44	1.27
	3	76.00	121.82	1.39	2.32
13	4	99.18	137.00	0.45	1.49
	3	95.06	119.49	0.74	2.20
15	4	135.67	162.64	0.76	2.30
	3	129.62	155.11	1.00	2.94
17	4	170.24	197.50	0.80	2.48
	3	160.76	185.46	0.97	2.87
19	4	197.32	220.33	0.87	2.34
	3	190.22	206.51	1.33	2.33
21	4	219.72	224.28	2.21	2.78
	3	226.36	234.22	1.98	2.41
22	4	295.90	308.62	31.93	33.51
	3	191.88	211.91	14.79	17.31

This difference of response results obtained by these two methods is due to incorporation of different damping effects in these two methods of analysis. The mass proportional damping is employed in direct integration method and the

proportional constant is computed to consider the effect of first mode only which implies decreasing damping effect in higher modes. The damping value is given modewise in mode superposition method which results in higher damping effects. It shows that the damping effect is more in mode superposition method as compared to direct integration method. Therefore, the response obtained by direct integration method is more than that by mode superposition method.

Table 5.2 shows values of maximum bending and shear stresses at bottom gauss points in the elements from centre to edge of the raft. A small deference in the values of stresses is observed in the central part of the raft by these two methods while negligible difference is seen in the edge portion of the raft.

Table 5.2

Maximum Stresses at Bottom G.P. of Elements in Raft, (Fig. 4.11b)

Element number	G.P	Bending stress $\left(\sigma_z - t/m^2\right)$		Shear stress $\left(\tau_{rz} - t/m^2\right)$	
		Mode superposition integration	Direct integration	Mode superposition	Direct
23	1	0.48	1.25	0.56	2.96
	3	0.54	1.42	0.57	3.35
24	1	3.98	4.41	4.23	4.96
	3	3.76	4.48	1.90	3.78
25	1	29.41	31.32	13.52	15.18
	3	33.02	33.32	8.60	9.22
26	1	134.15	134.85	6.30	7.10
	3	78.45	78.62	29.32	33.51
27	1	11.87	12.46	7.63	9.91
	3	92.26	94.67	12.16	11.82

The maximum horizontal displacements at different nodes along the height of the structure obtained by the two methods are presented in Table 5.3. This shows a good comparison of displacements computed by using these two methods of

solution.

Table 5.3

Maximum Displacement in Containment Structure, (Fig. 4.11b)

Node number	Maximum horizontal displacement (mm)	
	Mode superposition	Direct integration
1	9.29	9.44
4	9.26	9.40
6	9.23	9.37
11	9.10	9.22
16	8.90	9.00
21	8.66	8.73
26	8.32	8.37
31	7.97	8.00
36	7.57	7.61
41	7.35	7.44
46	7.07	7.14
51	6.04	5.89
56	5.51	5.54
61	4.86	5.08
66	4.25	4.61
71	3.81	4.19
76	3.40	3.84
81	3.00	3.56
86	2.55	3.30
91	2.03	2.35
96	1.37	2.00
101	0.62	0.97
106	0.46	0.63
115	0.04	0.04
117	0.04	0.04
118	0.00	0.00

5.4.2 Containment Structure With Soil Base

The same containment structure is considered but resting on soil instead of fixed base. The finite element mesh of the structure including founding soil is shown in Figure 4.10a. There are total 90 elements (27 structural elements and 63 soil elements) and 345 nodes in the finite element mesh.

The soil-structure system is subjected to horizontal ground motion due to Koyna

Earthquake and the following parameters are taken :

Soil width (A)	: 3R
Soil depth (B)	: 2R
Embedment depth (D)	: 12m
Shear wave velocity of soil	: 600 m/s

The maximum responses are computed using above two approaches and are presented through Tables 5.4 to 5.6.

Table 5.4
Maximum Stresses at Outer G.P. of Elements in Shell, (Fig.4.10a)

Element number	G.P.	Bending stress $\left(\sigma_z - t/m^2 \right)$		Shear stress $\left(\tau_{rz} - t/m^2 \right)$	
		Mode superposition	Direct integration	Mode superposition	Direct integration
1	4	0.88	2.58	1.08	2.78
	3	0.12	0.58	0.75	1.95
2	4	0.40	1.20	0.77	2.56
	3	0.33	1.62	1.91	3.73
4	4	3.05	1.20	5.11	8.39
	3	4.60	6.86	5.64	8.84
6	4	18.00	23.42	12.88	20.47
	3	18.20	24.39	13.98	21.00
8	4	46.70	70.10	24.41	39.55
	3	35.65	48.89	7.55	11.09
10	4	7.28	9.86	7.87	11.83
	3	37.21	51.67	5.30	8.55
11	4	68.27	108.07	0.43	1.19
	3	72.55	114.07	1.32	2.27
13	4	91.87	127.06	0.37	1.22
	3	88.35	117.91	0.66	2.18
15	4	125.52	156.49	0.70	2.20
	3	118.30	140.53	0.90	2.85
17	4	153.00	170.21	0.71	2.08
	3	146.72	158.21	0.90	2.95
19	4	165.69	172.65	0.44	1.79
	3	177.52	183.91	0.47	1.72
21	4	140.50	140.72	1.55	1.75
	3	143.52	149.20	1.62	1.93
22	4	107.54	108.73	10.08	12.13
	3	143.58	146.05	14.61	15.93

Table 5.4 shows the bending and shear stresses at outer gauss points in some elements along the height of containment structure obtained by these two methods.

It is observed from Table 5.4 that the bending and shear stresses in the upper part of the shell are larger in response obtained by direct integration method as compared to those obtained by mode superposition method. It is also seen that, in the lower part of the structure, the bending and shear stresses obtained by these two methods compare well. It is due to different methods of consideration of damping effects in these two methods of analysis.

The maximum bending and shear stresses at bottom gauss points in the elements from centre to edge of the raft are presented in Table 5.5. It is observed there is a small difference in the values of stresses in the central part of the raft by these two methods and a negligible difference of these values is found in the edge portion of the raft.

Table 5.5

Maximum Stresses at Bottom G.P. of Elements in Raft, (Fig.4.10a)

Element number	G.P.	Bending stress $\left(\sigma_z - t/m^2 \right)$		Shear stress $\left(\tau_{rz} - t/m^2 \right)$	
		Mode superposition	Direct integration	Mode superposition	Direct integration
23	1	0.19	0.22	0.50	2.87
	3	0.42	0.78	0.47	2.21
24	1	2.19	2.64	4.03	4.06
	3	3.41	7.62	1.04	2.06
25	1	19.01	19.31	12.52	14.18
	3	11.30	11.37	8.34	8.63
26	1	55.65	56.09	5.30	6.10
	3	23.67	23.60	6.92	7.00
27	1	10.08	11.46	4.63	8.91
	3	36.12	36.89	10.16	10.82

The maximum horizontal displacements at different nodes along the height of the structure obtained by the two methods are presented in Table 5.6. This shows a

good comparison of displacements computed by using these two methods of solution.

Table 5.6

Maximum Displacement in Containment Structure, (Fig. 4.10a)

Node number	Maximum horizontal displacement (mm)	
	Mode superposition	Direct integration
1	9.80	10.15
4	9.77	10.11
6	9.75	10.08
11	9.64	9.93
16	9.48	9.72
21	9.28	9.45
26	9.00	9.05
31	8.70	8.65
36	8.33	8.22
41	8.11	8.03
46	7.86	7.74
51	6.95	7.01
56	6.44	6.75
61	5.79	6.35
66	5.17	5.87
71	4.56	5.31
76	3.94	4.74
81	3.33	4.14
86	2.75	3.50
91	2.22	2.85
96	1.71	2.21
101	1.17	1.51
106	0.56	0.69
115	0.04	0.04
117	0.04	0.04
118	0.00	0.00

5.4.3 San Bernardino Intake Tower

The San Bernardino Intake tower fixed at the base and without considering the water inside or outside (Fig. 4.8a), is analysed for its seismic response. Figure 4.8b shows the finite element mesh of intake tower. There are 27 elements and

126 nodes in the finite element mesh. The tower is subjected to horizontal ground motion due to Koyna (India) Earthquake (Fig. 4.5). The seismic response is computed by using above two method and listed in Tables 5.7 and Table 5.8.

Table 5.7

Maximum Stresses at Outer G.P. of Elements in the Tower, (Fig. 4.8b)

Element number	G.P.	Bending stress $\left(\sigma_z - t/m^2 \right)$		Shear stress $\left(\tau_{rz} - t/m^2 \right)$	
		Mode superposition	Direct integration	Mode superposition	Direct integration
1	4	13.80	49.25	0.71	2.79
	3	12.86	31.63	1.98	7.19
2	4	33.66	68.74	2.18	7.36
	3	55.56	120.78	0.75	2.78
3	4	54.82	105.39	0.75	1.57
	3	57.83	112.18	2.57	6.94
4	4	58.26	116.62	1.24	1.50
	3	85.24	158.23	0.44	1.30
5	4	123.60	216.10	1.02	2.18
	3	177.04	291.53	0.64	1.91
6	4	219.60	342.52	0.85	2.44
	3	286.64	428.46	1.25	3.39
7	4	330.15	474.03	1.24	4.28
	3	385.26	526.42	1.60	4.12
8	4	418.38	545.93	1.55	4.89
	3	460.56	555.46	1.65	3.85
9	4	494.32	558.80	1.77	4.27
	3	564.81	569.08	7.55	7.67
10	4	575.59	569.25	7.96	8.40
	3	694.19	777.05	8.79	10.94
11	4	848.25	977.35	50.54	62.33
	3	1028.60	1207.00	170.72	207.15
16	4	3.66	6.10	1.18	1.74
	3	101.96	138.63	43.83	59.10
20	4	2.81	4.42	1.06	1.54
	3	61.18	87.32	25.61	36.48
27	4	2.33	3.77	1.07	1.69
	3	39.84	59.07	13.11	19.26

Table 5.7 compares the bending and shear stresses at outer gauss points in some elements along the height of tower obtained by these two methods.

It is observed from Table 5.7 that the bending and shear stresses in the upper part of the tower are larger in direct integration method as compared to those obtained by mode superposition method while in the lower part of the structure the bending and shear stresses obtained by these two methods compare reasonably well. This difference of response obtained by two methods is due to different damping effects included in the two methods of analysis.

The maximum horizontal displacements at different nodes along the height of the tower obtained by the two methods are presented in Table 5.8. There is a good comparison of displacements obtained from the two methods of solution.

Table 5.8

Maximum Displacement Along the Height of Intake Tower, (Fig. 4.8b)

Node number	Maximum horizontal displacement (mm)	
	Mode superposition	Direct integration
3	48.66	51.69
8	43.58	45.62
13	39.56	40.80
18	38.48	39.51
23	32.00	31.85
30	21.95	21.81
35	15.50	16.61
40	9.96	11.31
43	7.45	8.73
45	5.16	6.25
48	3.22	4.05
50	1.67	2.20
63	0.18	0.30
126	0.00	0.00

5.5 Concluding Remarks

The horizontal seismic response of two axisymmetric structures, namely,

Containment shell (Wolf,1985) and Intake tower (Liaw & Chopra, 1973), has been computed using time wise mode superposition and direct step-by-step time integration approaches. A comparison is made between maximum seismic responses obtained by these two methods and following conclusions are derived from this study :

1. A good comparison is observed in maximum horizontal displacement obtained by the two methods of analysis.

2. The maximum bending and shear stresses in the structures, obtained by mode superposition and direct integration methods, compare reasonably well except at some points. It is due to incorporation of different damping effects in the two methods of analysis.

3. The mode superposition method is most effective in accommodating different values of material damping.

4. Out of many direct step-by-step time integration schemes, the Newmark's β scheme is most effective in computation of elastic earthquake response of a structure because it is unconditionally stable and has least numerical error. However it has following demerits as compared to timewise mode superposition method : (a) more computational time is required, and (b) problem of consideration of different material damping.

5. Therefore, it is recommended that timewise mode superposition method is more suitable method as compared to direct step-by-step time integration method in elastic analysis of earthquake response.

6. The analysis of structures by two methods places more confidence to the analyst and also provides understanding of total number of modes participating in overall seismic response of the structures.

EFFECT OF VISCOUS BOUNDARIES ON SEISMIC RESPONSE

6.1 Introduction

The finite element method has been widely used in recent years for dynamic soil-structure interaction studies. The finite element analysis of dynamic foundation problems requires the use of viscous boundaries for eliminating the reflection of wave energy at the fixed boundaries of the finite element model of soil-structure system. With the values of material damping in soil, such as encountered in earthquake analysis, the waves reflected at the fixed boundaries are partly absorbed before they return to the foundation. It is, however, desirable that the incoming waves are mostly absorbed at the boundary and any reflection of waves occurring get absorbed through the material damping of the foundation. The wave reflection problem at the fixed boundaries in finite element model of soil-structure system, has not been completely resolved so far. A study has been performed here to investigate the effectiveness of viscous boundaries in respect of absorption of incoming waves and for minimizing their reflection.

A general method through which an infinite system may be approximated to a finite system with a viscous boundaries condition, is described herein. The resulting model may be analyzed by ordinary numerical methods but is handled with particular ease by the finite element method (Corsanego, 1983). The three-dimensional effect of energy dissipation into the soil mass is taken into account in an approximate manner by the use of a viscous boundaries in connection with an essentially two-dimensional axisymmetric models for the soil-structure interaction system (Kuhlemeyer & Lysmer, 1973).

6.2 Background of Viscous Boundaries

The use of viscous boundaries to simulate the propagation of wave energy into an infinite soil mass is based on an analogy between the dynamic response of a uniformly loaded elastic half space and a viscous dashpot [Lysmer and Richart(1966)], as shown in Fig. 6.1.
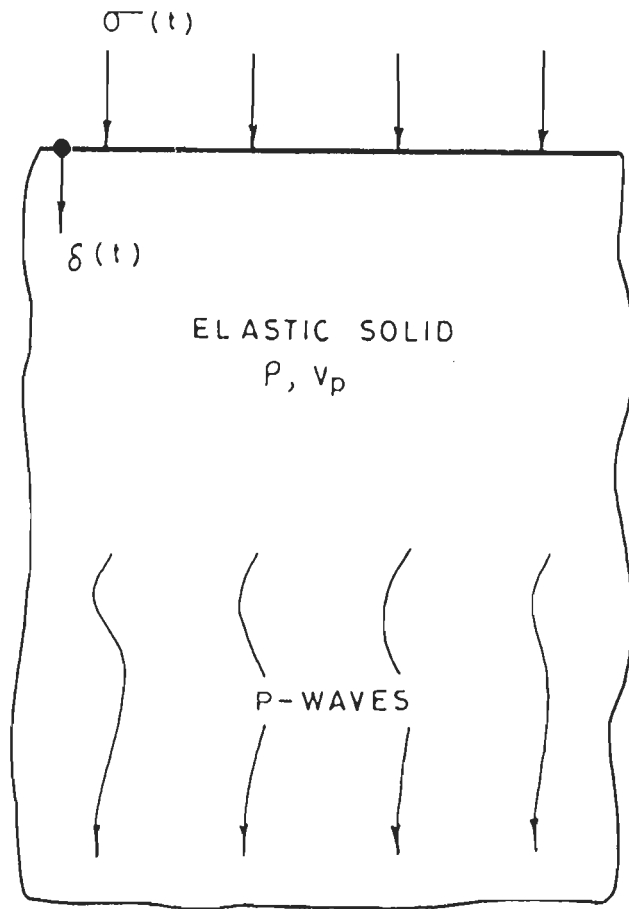
(a) ELASTIC HALF SPACE
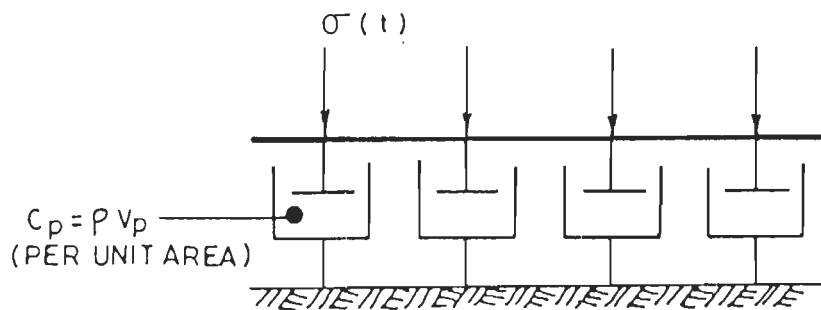
(b) DASHPOT ANALOG

FIG. 6·1 ANALOGS FOR VERTICALLY LOADED HALF SPACE

According to this analogy the surface displacement, $\delta(t)$, of an elastic half space loaded with a uniform normal stress, $\sigma(t)$ (Fig.6.1a), is identical to that of a dashpot, (Fig. 6.1b),with the damping coefficient for P-waves, C_p, as under:

$$C_P = \rho V_P \qquad (1)$$

where ρ is the mass density and V_p is the P-wave velocity of the medium.

The relationship between the stress and displacement, δ, is,

$$\sigma(t) = C_p \, \dot{\delta}(t) \qquad (2)$$

which is the equation for the normal stress in a plane P-wave propagating in one direction only (into the half space).

The term $\dot{\delta}(t)$ is the time derivative of displacement, i.e., $d\delta/dt$.

The above analogy can be directly extended to the case of a half space excited by a uniform shear stress, $\tau(t)$ as shown in Fig. 6.2. The corresponding equations are :

$$C_s = \rho V_s \qquad (3)$$

$$\tau(t) = C_s \, \dot{\delta}(t) \qquad (4)$$

where V_s , is the shear wave velocity, C_s is the damping coefficient for S-waves and $\delta(t)$ is the tangential surface displacement of the medium.

The significance of the above analogies is that the analysis of an infinite system (the half space) can be reduced to an analysis of a finite system (the dashpot). However, more complicated situations have been investigated by Lysmer and Kuhlemeyer (1969) who showed that the above viscous boundaries, with both dashpots applied simultaneously, can absorb both P-waves and S-waves over a large range of incidence angles. This made it possible to solve foundation vibration problems by the finite element method using models of the type, as shown in Fig. 6.3.
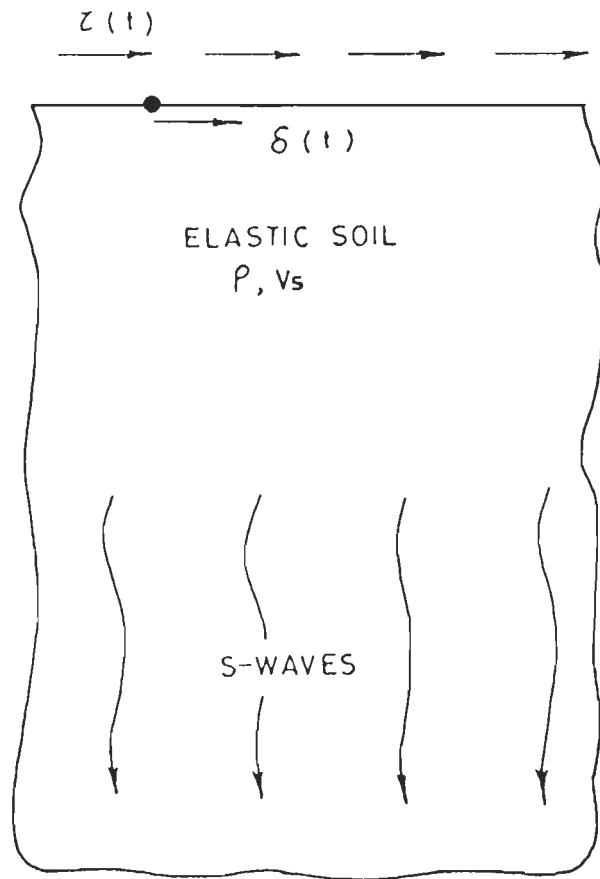
(a) ELASTIC HALF SPACE
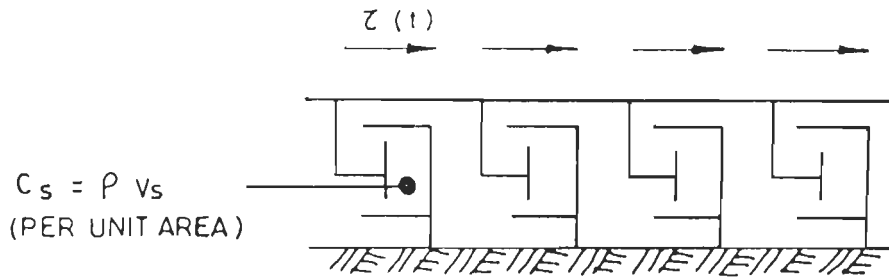
(b) DASHPOT ANALOG

FIG. 6·2 ANALOGS FOR HORIZONTALLY LOADED HALF SPACE

The velocity of P-wave is related to that of S-wave as,

$$V_p = V_s / s, \quad where \ s^2 = (1 - 2 v)/(2 - 2 v), \quad v \ \text{is Poisson's ratio.}$$
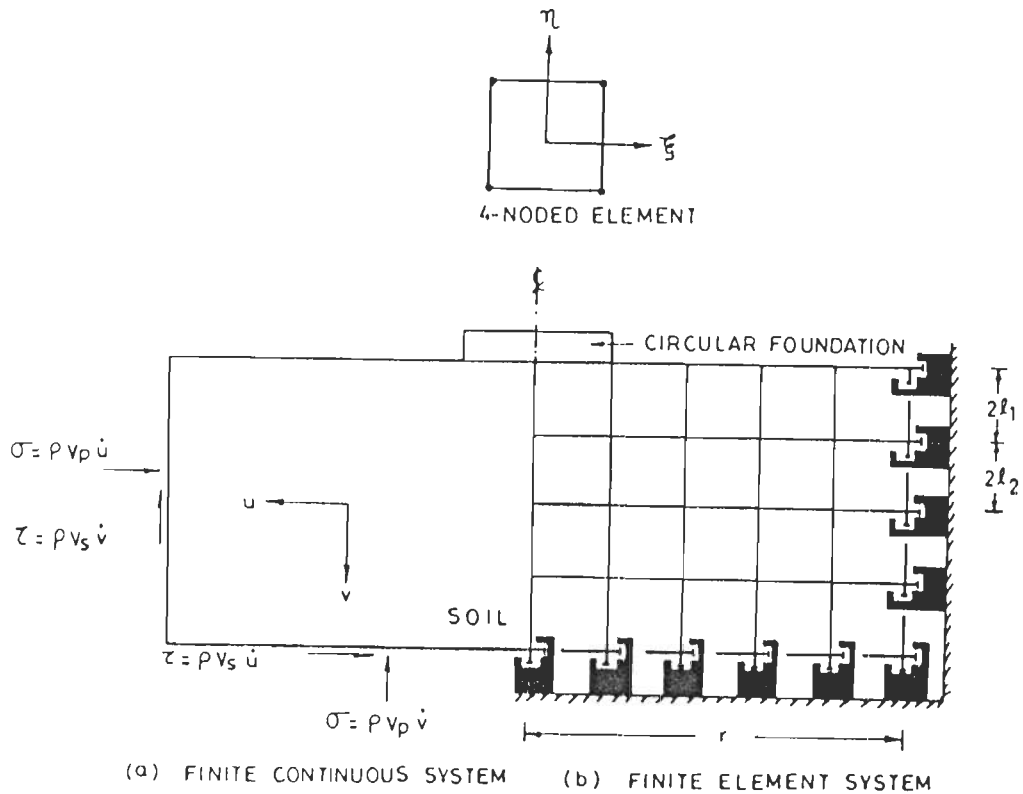
FIG. 6·3 FINITE ELEMENT MODEL FOR SOIL MEDIUM

6.3 Computation of Damping Coefficients at Nodes in Finite Element Mesh

As the force equilibrium equation for the linear elastic system subjected to ground motion is,

$$\underline{M}\,\ddot{\delta}(t) + \underline{C}\,\dot{\delta}(t) + \underline{K}\,\delta(t) = -\,\underline{M}\{1\}\,\ddot{\delta}_g(t)$$

In this equation damping matrix $\underline{C}$ consists of the coefficients of velocity term $[\dot{\delta}(t)]$ and have the dimension of force per unit velocity while the above coefficients C_p and C_s have the dimension of stress per unit velocity. Therefore, these coefficients are multiplied by the area, 'a', for lumping the damping values at the nodes of boundary elements (in the form of horizontal and vertical dashpots). The area, 'a', is calculated as :

$$a = 2\pi r \left(l_1 + l_2 \right)$$

148

Where, r, is the distance from centre of the soil-structure system to the node of viscous boundary elements and l_1, l_2 are the half of the distances between the node of lumped damping value and the adjacent nodes of the finite elements at outer planer surface of soil boundary (Fig. 6.3).

6.4 Problems Considered for the Study of Effect of Viscous Boundaries

For the purpose of study, a reactor containment structure (Fig.4.9) has been taken. The structure is symmetrical with respect to vertical axis. It consists of a cylindrical shell capped with a spherical dome and resting on a raft. The containment structure is founded on base and surrounding soil. The following parameters are considered in the seismic analysis of this structure including foundation soil (Fig. 4.9b).

Embedment depth (D)   : 8m
Shear wave velocity of soil   : 800 m/s

The material properties of structure and founding soil used in the analysis are presented in table 6.1

Table 6.1
Material Properties of Structure and Founding Soil

Description of structure	Modulus of elasticity $\left(\times 10^6 \, t/m^2\right)$	Poisson's ratio	Mass density $\left(t - s^2/m^4\right)$	Damping (percent of critical)
Shell, Dome and Raft	3.00	0.20	0.25	5%
Founding soil	0.29	0.30	0.00 (soil mass is not considered)	20%

The elastic time history seismic analysis of the above axisymmetric soil-structure system (Fig. 4.9b) is carried out using fixed and viscous boundaries in lateral and vertical directions. In order to evaluate the effectiveness of viscous boundaries in absorbing the incoming waves in relation to fixed boundaries, the following

problems (as shown in Table 6.2) are considered :

Table 6.2

Problems Considered for the Study of Effect of Viscous Boundaries

Sr.No.	Boundaries in the Problem	Variations (Fig. 4.9b)	Case
1	Fixed	A = 3.0 R and B = 2.0 R	Case 1 or Case A
2	Viscous	A = 3.0 R and B = 2.0 R	Case 2
2	Viscous	A = 1.5 R and B = 2.0 R	Case 3
2	Viscous	A = 0.5 R and B = 2.0 R	Case 4
2	Viscous	A = 1.5 R and B = 1.5 R	Case B
2	Viscous	A = 1.5 R and B = 1.0 R	Case C
2	Viscous	A = 1.5 R and B = 0.5 R	Case D

6.5 Method of Dynamic Analysis and Ground Motion Used

The finite element analysis of above soil-structure interaction problems subjected to horizontal ground motion is carried out using direct step-by-step time integration method. The shell along with the surrounding soil has been discretized by 8-noded parabolic axisymmetric finite elements (Fig.4.10a).

The horizontal ground motion of Koyna Earthquake (Dec. 11, 1967, Transverse component) is considered. The maximum seismic response is computed for above problems. Some of the important results of seismic analysis of above problems are discussed in the coming sections. However a brief description of these response is given as under (Figures 4.10a and 6.4) :

(i) Effect of Horizontal Mesh Size of Soil

The results of the problems of Case 1 to Case 4 are as under :

Structural Response :

(a) The maximum bending stress (σ_z) at outer gauss points (G.P.) of the

elements along the height of the shell.

(b) The maximum shear stress (τ_{rz}) at outer gauss points of the elements along the height of the shell.

(c) The maximum horizontal displacement (u) at outer nodes along the height of the shell.

(d) The maximum bending stress (σ_z) at bottom gauss points of the elements in the raft.

Soil response along the Plane $Y_1 = Y_2$ (Fig. 6.4)

(a) The maximum bending stress (σ_z)

(b) The maximum shear stress (τ_{rz})

Soil response along the Plane $X_1 = X_2$ (Fig. 6.4)

(a) The maximum bending stress (σ_z)

(b) The maximum shear stress (τ_{rz})

(II) Effect of vertical mesh size of soil

The results of the problems of Case A to Case D are as under:

Structural response :

(a) The maximum bending stress (σ_z) at outer gauss points of the elements along the height of the shell

(b) The maximum shear stress (τ_{rz}) at outer gauss points of the elements along the height of the shell

(c) The maximum horizontal displacement (u) at outer nodes along the height of the shell.
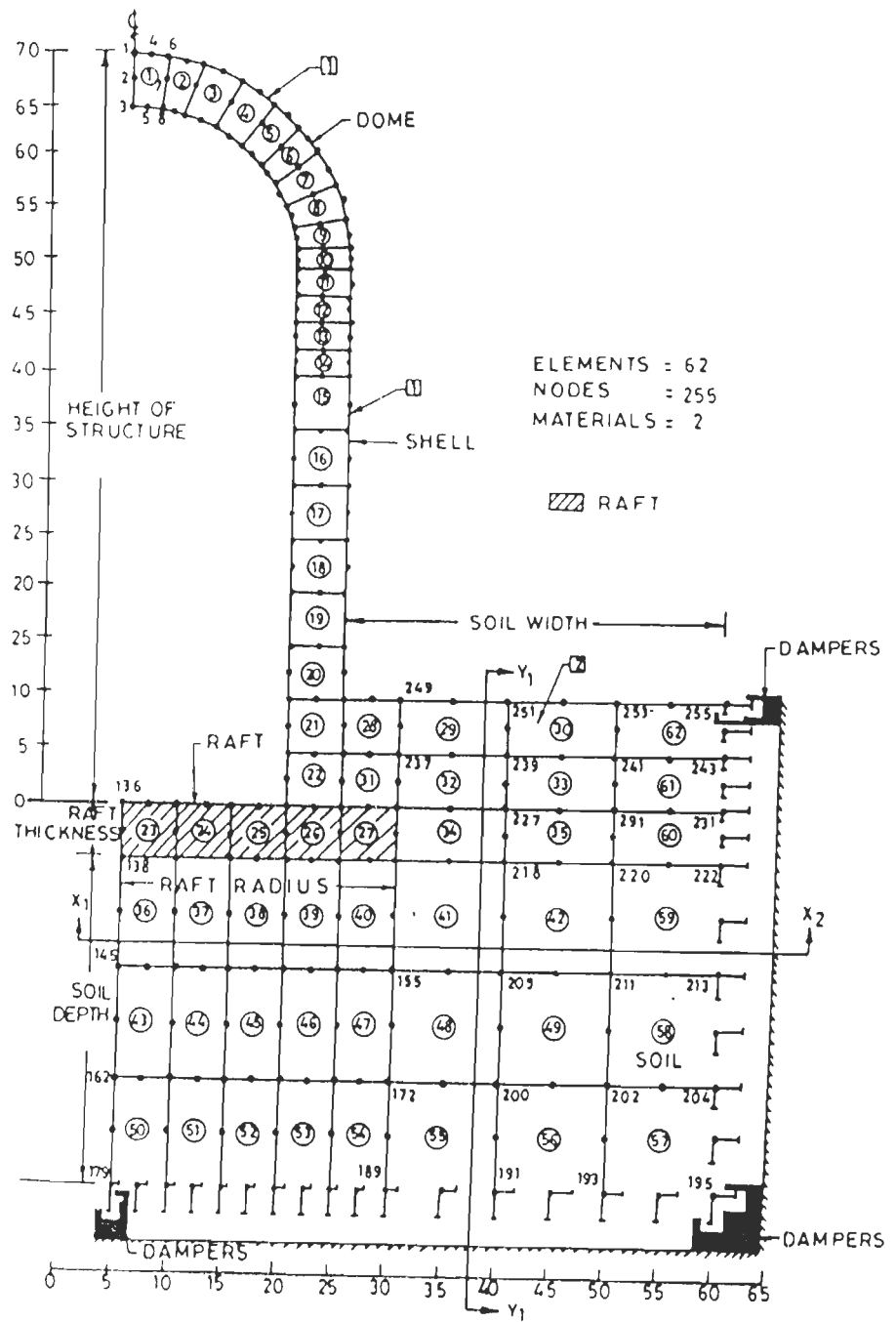
FIG. 6·4   FINITE ELEMENT MESH OF SOIL-STRUCTURE
SYSTEM WITH VISCOUS BOUNDARIES

(d) The maximum bending stress (σ_z) at bottom gauss points of the elements in the raft.

6.6 Effect of Horizontal Mesh Size of Soil With Viscous Boundary

To obtain the effective horizontal mesh size (A) of soil where the viscous boundary in the form of dashpots is introduced, the vertical mesh size of soil is kept constant (equal to two times the raft radius) and vary the horizontal mesh size of soil with viscous boundaries on outer plane slice of soil, (Fig. 4.9b). The following parameters are considered :

      Soil width (A)   : 3.0R, 1.5R, 0.5R
      Soil depth (B)   : 2.0R
      Shear wave velocity of soil   : 800 m/s

This parametric study is treated in the following four cases :
Case 1 : fixed boundaries   at   A = 3.0R and B = 2.0R
Case 2 : viscous boundaries at A = 3.0R and B = 2.0R
Case 3 : viscous boundaries at A = 1.5R and B = 2.0R
Case 4 : viscous boundaries at A = 0.5R and B = 2.0R

Discussion of Results

Structural Response

The structural response for the problems of Case 1 to Case 4 is presented through Tables 6.3 to 6.6.

Table 6.3 presents the maximum bending stress (σ_z) at outer gauss points in the elements along the height of the structure (from top to bottom) for the above four cases. It is observed from Table 6.3 that,

(a) The stresses obtained in the shell for Case 1 and Case 2 compare well, a little less stresses are observed for Case 2 as compared to Case 1. It shows that comparable stresses are obtained by introducing the fixed and the viscous boundaries at the same greater lateral distance (equal to 3R).

Table 6.3

Bending Stress at Outer G.P. Along the Height of Shell, (Fig.4.10a)

Element number	G.P.	Maximum bending stress, $\sigma_z \left(t/m^2 \right)$			
		Case 1	Case 2	Case 3	Case 4
1	4	2.58	2.42	2.21	2.44
	3	0.78	0.74	0.71	0.76
2	4	1.25	1.23	1.21	1.24
	3	1.92	1.91	1.87	1.91
4	4	8.58	7.23	7.46	7.83
	3	9.58	8.32	7.99	8.32
6	4	33.42	31.40	29.19	29.24
	3	34.39	32.31	29.33	29.50
8	4	80.10	75.51	65.80	66.31
	3	58.89	55.60	50.55	54.72
10	4	15.58	11.50	11.50	11.80
	3	61.67	58.18	52.32	53.73
11	4	118.07	111.11	99.30	103.52
	3	128.07	116.77	104.17	108.64
13	4	137.06	129.79	118.36	122.85
	3	119.08	112.42	104.24	107.81
15	4	166.58	150.06	138.47	145.39
	3	142.09	135.20	125.63	132.67
17	4	170.58	162.27	152.62	160.10
	3	158.58	151.45	142.49	143.25
19	4	175.58	169.17	157.89	157.95
	3	183.91	177.21	168.23	168.26
21	4	140.58	136.02	130.38	131.12
	3	149.20	144.00	134.65	135.91
22	4	108.73	104.44	98.68	100.60
	3	160.50	141.07	133.70	133.85

(b) The stresses in the shell for Case 3 are less as compared to Case 2. It shows that stresses in the shell for the case of placing viscous boundary at a smaller lateral distance are almost equal to that of fixed boundary at a greater lateral distance, that is, most of the incoming waves are absorbed by viscous boundary (damper) placed at even smaller lateral distance (equal to 1.5R) as compared to fixed boundary at a greater lateral distance (equal to 3.0R).

(c) The stresses in the shell for Case 4 are more than that of Case 3. Also, the stresses at some gauss points in the shell for case 4 are even more than that of Case 2 but less than that of Case 1.

(d) The stresses in the shell for Case 3 are the least as compared to other cases. Therefore, the viscous boundary placed at a horizontal distance equal to 1.5R is effective in obtaining minimum stresses in the shell due to absorption of most of the incoming waves and minimizes the reflection.

The maximum shear stress (τ_{rz}) at outer gauss points in the elements along the height of the structure for the above four cases are presented in Table 6.4. It is observed from Table 6.4 that,

Table 6.4

Shear Stress at Outer G.P. Along the Height of Shell, (Fig.4.10a)

Element number	G.P.	Maximum shear stress, $\tau_{rz}\left(t/m^2\right)$			
		Case 1	Case 2	Case 3	Case 4
1	4	2.78	2.61	2.20	2.21
	3	1.95	1.83	1.18	1.94
2	4	2.96	2.70	2.64	2.96
	3	3.87	3.71	3.62	3.87
4	4	11.39	10.70	10.44	11.13
	3	11.84	11.11	10.95	11.53
6	4	24.47	23.00	21.43	21.52
	3	25.00	23.50	21.46	21.55
8	4	40.55	38.27	34.40	34.48
	3	12.09	10.98	10.54	10.68
10	4	12.83	12.15	11.42	11.44
	3	9.55	8.95	7.94	8.54
11	4	1.18	1.07	0.99	1.18
	3	2.27	2.17	2.02	2.27
13	4	1.82	1.61	1.36	1.66
	3	2.58	2.32	2.08	2.38
15	4	2.20	2.00	1.98	2..20
	3	2.85	2.78	2.76	2.78
17	4	2.68	2.46	2.41	2..62
	3	3.95	3.72	3.64	3.84
19	4	3.79	3.60	3.46	3.49
	3	1.72	1.61	1.30	1.37
21	4	5.75	5.27	4.74	4.91
	3	8.93	8.72	8.13	8.14
22	4	12.13	11.06	9.27	9.74
	3	20.93	20.29	18.40	18.87

(a)   The shear stresses along the height of shell are observed little higher for Case 1 in comparison of Case 2. It shows that the almost similar stresses are obtained by providing fixed and viscous boundaries at the same greater horizontal distance.

(b)   The shear stresses in the shell for Case 3 are less as compared to Case 2. It shows that shear stresses in the shell get reduced in case of viscous boundary as compared to those due to fixed boundary.

(c)   The shear stresses in the shell for Case 4 are more than that of Case 3. Also, the shear stresses at some gauss points in the shell for case 4 are even more than that of Case 2. It shows that the shear stresses in the shell are increased due to further decrease of lateral position of viscous boundary from 1.5R to 0.5R.

(d)   The shear stresses in the shell for Case 3 are the minimum as compared to other cases. Therefore the viscous boundary placed at a horizontal distance equal to 1.5R is effective in obtaining minimum shear stresses in the shell.

The maximum horizontal displacement at outer nodes along the height of the shell for the above four cases is given Table 6.5 The following observations are made from this Table :

(a)   The displacements obtained at different locations in the shell for Case 1 and Case 2 compare well. It shows that comparable displacements are obtained by introducing fixed and the viscous boundaries at the same greater lateral distance.

(b)   The displacements in the shell for Case 3 are less as compared to Case 2. It shows that displacements in the shell   decrease with decrease of lateral distance of viscous boundary.

(c)   The displacements in the shell for Case 4 are more than that of Case 3 and less than that of Case 2 and Case 1. It shows that displacements in the shell are increased due to further decrease of the lateral position of viscous boundary from 1.5R to 0.5R.

(d) The displacements in the shell for Case 3 are the least as compared to other cases. Therefore the viscous boundary placed at a horizontal distance equal to 1.5R is effective in obtaining minimum displacements.

Table 6.5
Displacement at Outer Nodes Along the Height of Shell
(Fig.4.10a)

Node number	Maximum horizontal displacements, (mm)			
	Case 1	Case 2	Case 3	Case 4
1	9.44	9.27	8.93	8.96
4	9.40	9.24	8.89	8.92
6	9.37	9.21	8.87	8.89
11	9.22	9.07	8.74	8.76
16	9.00	8.86	8.56	.8.58
21	8.73	8.61	8.32	8.32
26	8.37	8.26	7.98	7.99
31	8.00	7.91	7.63	7.66
36	7.61	7.51	7.24	7.28
41	7.44	7.33	7.05	7.10
46	7.14	7.04	6.78	6.82
51	5.89	5.75	5.63	5.64
56	5.54	5.33	5.00	5.01
61	5.08	4.88	4.71	4.71
66	4.61	4.56	4.38	4.39
71	4.19	4.16	3.98	3.99
76	3.84	3.80	3.68	3.68
81	3.56	3.55	3.31	3.35
86	3.30	3.25	2.92	2.94
91	2.83	2.76	2.38	2.43
96	1.99	1.91	1.52	1.60
101	0.97	0.90	0.63	0.65
106	0.73	0.68	0.47	0.51
111	0.71	0.66	0.46	0.52
117	0.69	0.64	0.44	0.50
118	0.65	0.60	0.41	0.46

Table 6.6 presents the maximum bending stress (σ_z) at bottom gauss points in the elements of the raft (from centre to edge). It is observed from Table 6.6 that,

(a) The stresses obtained in the raft for Case 1 and Case 2 compare well,

However the stresses in the shell for Case 2 are observed little less as compared to Case 1.

(b) The stresses in the raft for Case 3 are less as compared to Case 2. It shows that stresses in the raft decrease with decrease of lateral position of viscous boundary.

(c) The stresses in the raft for Case 4 are more than that of Case 3 and less than that of Case 2 and Case 1. It shows that the stresses in the raft are increased due to further decrease of lateral position of the viscous boundary from 1.5R to 0.5R.

(d) The stresses in the shell for Case 3 are the least as compared to other cases. Therefore, the viscous boundary placed at a horizontal distance equal to 1.5R is effective in obtaining minimum stresses in the raft.

Table 6.6
Bending Stress at Bottom G.P. in the Elements of the Raft, (Fig.4.10a)

Element number	G.P	Maximum bending stress, $\tau_{rz}\left(t/m^2\right)$			
		Case 1	Case 2	Case 3	Case 4
23	1	3.21	3.09	2.67	2.73
	3	3.03	2.75	2.37	2.44
24	1	1.02	0.99	0.97	0.98
	3	0.46	0.45	0.43	0.44
25	1	5.35	5.23	5.01	5.03
	3	0.52	0.51	0.45	0.46
26	1	51.07	49.32	46.88	47.06
	3	35.28	34.09	32.48	32.59
27	1	40.26	38.87	37.25	37.55
	3	18.55	17.78	16.94	17.17

Soil response :

The response in the soil is listed through Tables 6.7 to 6.10 along the two planes

defined as under :

(i) Plane $Y_1 - Y_2$ at a horizontal distance of 38.0 m from the centre line of soil-structure system (Fig. 6.4).

(ii) Plane $X_1 - X_2$ at a vertical distance of 12.0 m from the bottom of the raft (Fig. 6.4).

Soil response along the plane $Y_1 - Y_2$

Tables 6.7 and 6.8 present the soil response along the plane $Y_1 - Y_2$.

The maximum bending stress along the plane $Y_1 - Y_2$ (from Y_1 to Y_2) passing through outer gauss points of soil elements for the above four cases.

It is observed from Table 6.7 that,

(a) The stresses in the soil elements are significantly lower for Case 2 as compared to Case 1.

(b) The stresses in the soil decrease with decrease of lateral position of viscous boundary from 3.0R (Case 2) to 1.5R (Case 3).

(c) The stress at some of the gauss points in soil elements along this plane is further decreased in Case 4 but at few points stresses are more in Case 4 as compared to Case 3. Also, at some points stresses in Case 4 are even more than that of Case 2. Therefore it is found that, the relatively less stresses, at different depths of soil strata, are obtained when viscous boundary is placed at a lateral distance equal to 1.5R.

The maximum shear stress (τ_{rz}) in soil elements along the plane $Y_1 - Y_2$ are presented in Table 6.8 for the above four cases.

It is observed from Table 6.8 that,

(a) The shear stresses in the soil elements at different depths of soil strata are

decrease by introducing viscous boundary in place of fixed boundary.

Table 6.7

Bending Stress at G.P. of Soil Elements Along the Plane $Y_1 - Y_2$.(Fig.6.4)

Element number	G.P	Maximum bending stress, $\sigma_z \left(t/m^2 \right)$			
		Case 1	Case 2	Case 3	Case 4
55	3	17.11	8.85	7.73	6.45
	4	17.41	11.24	8.60	6.70
48	3	25.44	20.18	17.43	17.49
	4	22.50	17.44	15.62	16.25
41	3	43.17	39.33	41.57	38.66
	4	31.17	27.39	27.04	24.80
34	3	75.97	73.00	72.16	74.50
	4	27.47	25.42	24.20	22.87
32.	3	62.28	60.06	59.38	59.23
	4	37.67	35.00	34.62	32.52
29	3	45.89	43.93	42.21	41.81
	4	12.81	11.64	11.02	10.97

(b) The shear stresses in the soil are further reduced due to decrease of lateral position of viscous boundary from 3.0R (Case 2) to 1.5R (Case 3).

(c) The shear stress at some of the gauss points in soil elements along this plane are further decreases with decrease of lateral position of viscous boundary from 1.5R to 0.5R. But at few points the increase in stresses are observed with decrease of the horizontal distance of viscous boundary.

So, the viscous boundary at a lateral distance of 1.5R is effective in absorption of most of the incoming waves.

Table 6.8

Shear stress at G.P. of soil elements along the plane $Y_1 - Y_2$ (Fig.6.4)

Element number	G.P.	Maximum shear stress, $\tau_{rz} \left(t/m^2 \right)$			
		Case 1	Case 2	Case 3	Case 4
55	3	7.43	6.00	2.81	1.65
	4	7.80	7.10	5.42	4.23
48	3	11.27	10.89	7.12	6.90
	4	11.20	10.32	8.78	7.63
41	3	18.90	16.83	16.39	15.04
	4	17.66	16.83	16.71	16.62
34	3	42.70	39.67	36.96	39.36
	4	34.51	31.97	31.12	28.47
32	3	59.89	57.45	54.98	55.41
	4	29.87	27.78	26.21	25.91
29	3	60.00	56.37	56.17	55.74
	4	33.98	32.32	32.12	32.45

Soil Response Along the Plane $X_1 - X_2$

Tables 6.9 and 6.10 present the soil response along the plane $X_1 - X_2$

.
Table 6.9 lists the maximum bending stress (σ_z) along the plane $X_1 - X_2$ (from X_1 to X_2), passing through bottom gauss points of soil elements for the four cases.

It is observed from Table 6.9 that,

(a) The stresses in the soil elements are less for Case 2 as compared to Case 1. It shows that stresses in the soil elements at different points of a horizontal soil layer are decreased by introducing viscous boundary (Case 2) in place of fixed boundary (Case 1).

(b) The stresses in the soil are further decreased with the decrease of lateral position of viscous boundary from 3.0R (Case 2) to 1.5R (Case 3).

(c) The stress at most of the gauss points in soil elements along this plane are further decreased in Case 4 but at few points stresses are more in Case 4 as compared to Case 3 and at some points stresses in Case 4 are even more than that of Case 2. Therefore it is found that, the relatively less stresses in soil elements (at different points of a horizontal soil layer) are obtained when viscous boundary is placed at a lateral distance equal to 1.5R.

Table 6.9

Bending Stress at G.P. of Soil Elements Along the Plane $X_1 - X_2$
(Fig.6.4)

Element number	G.P.	Maximum bending stress, $\sigma_z \left(t/m^2\right)$			
		Case 1	Case 2	Case 3	Case 4
36	1	4.00	3.67	3.24	3.45
	3	3.76	3.43	3.42	3.47
37	1	19.05	17.74	17.50	17.22
	3	22.75	21.18	20.90	20.67
38	1	65.50	62.49	61.20	60.70
	3	65.36	61.88	60.83	60.58
39	1	136.64	130.92	128.21	127.78
	3	105.66	101.40	100.23	100.50
40	1	154.88	148.52	146.12	145.17
	3	115.02	109.56	108.65	109.09
41	1	93.91	90.60	89.59	91.20
	3	75.95	73.00	72.16	74.50

Table 6.10 lists the maximum shear stress (τ_{rz}) along the plane $X_1 - X_2$ passing through bottom gauss points of soil elements for the above four cases.

It is observed from Table 6.10 that,

(a) The stresses in the soil elements are less for Case 2 as compared to Case 1. It shows that stresses in the soil elements at different points of a

horizontal soil layer are decreased by introducing viscous boundary (Case 2) in place of fixed boundary (Case 1).

(b) The stresses in the soil are further decreased due to decrease of lateral position of viscous boundary from 3.0R (Case 2) to 1.5R (Case 3).

(c) The stress at most of the gauss points in soil elements along this plane are further decreased in Case 4 but at few points stresses are more in Case 4 as compared to Case 3.

Therefore, it is found that, the relatively less stresses in soil elements at different points of a horizontal soil layer are obtained when viscous boundary is placed at a lateral distance equal to 1.5R.

Table 6.10

Shear Stress at G.P. of Soil Elements Along the Plane $X_1 - X_2$
(Fig.6.4)

Element number	G.P.	Maximum shear stress, τ_{rz} (t/m^2)			
		Case 1	Case 2	Case 3	Case 4
36	1	45.82	42.90	32.10	28.93
	3	39.26	36.81	29.46	26.45
37	1	41.04	38.65	32.12	29.35
	3	38.60	36.14	30.78	27.91
38	1	53.46	49.74	39.24	38.65
	3	43.94	40.89	32.69	30.63
39	1	41.41	39.06	30.49	28.23
	3	30.01	28.27	20.91	17.86
40	1	44.78	42.19	33.33	28.49
	3	28.02	25.16	21.37	19.43
41	1	59.10	56.13	52.76	53.70
	3	42.70	39.67	36.96	39.36

The following conclusions are derived from the study of effect of horizontal mesh size of soil using viscous boundaries :

(a) The response of structure (shell, dome and raft) is decreased by introducing viscous boundary at a smaller lateral dimension in relation to fixed boundary at a greater lateral dimension

(b) The response of soil (at different soil depths and at different points in a horizontal soil layer) is decreased significantly by introducing viscous boundary at a smaller lateral dimension in relation to fixed boundary at a greater lateral dimension

(c) The viscous boundary is found to be effective for minimum seismic response of soil-structure system when it is placed at a lateral distance (from the outer edge of the wall) equal to one and half times the radius of the raft.

6.7 Effect of Vertical Mesh Size of Soil With Viscous Boundary

Having established horizontal mesh size of soil with viscous boundaries (equal to 1.5R), similar parametric study is carried out to determine the effective depth of soil medium (vertical dimension of soil mesh) at which viscous boundaries (both dashpots) can be introduced for minimum seismic response of the structure.

Therefore, horizontal dimension of soil mesh is kept constant equal to 1.5R and vary the vertical mesh size of soil with viscous boundaries on outer planer slice of soil boundaries (Fig. 4.9b), as follows :

    Soil width (A)   : 1.5R
    Soil depth (B)   : 1.5R, 1.0R, 0.5R

This parametric study is described as following four cases :

Case A :   fixed boundaries   at   A = 3.0R and B = 2.0R
Case B :   viscous boundaries at A = 1.5R and B = 1.5R
Case C :   viscous boundaries at A = 1.5R and B = 1.0R
Case D :   viscous boundaries at A = 1.5R and B = 0.5R

The structural response for the problems of above four cases (Case A to Case D) is presented through Tables 6.11 to 6.14.

Table 6.11 presents the maximum bending stress (σ_z) at outer gauss points in the elements along the height of shell for the above four cases. It is observed from Table 6.11 that,

(a) The stresses obtained in the shell for Case A and Case B compare well, little less stresses are observed in Case B as compared to Case A due to absorption of energy.

(b) The stresses in the shell for Case C are less as compared to Case B. It shows that stresses in the shell are less in case of placing viscous boundary at a smaller vertical distance as compared to fixed boundary at a greater vertical distance, that is, most of the incoming waves are absorbed by viscous boundary (damper) placed at even smaller vertical distance (equal to 1.0R) as compared to fixed boundary at a greater vertical distance (equal to 2.0R).

(c) The stresses in the shell for Case D are more than that of Case C and at some gauss points stresses in the shell for case D are even more than that of Case B but less than that of Case A. It shows that Case D (in which viscous boundary is provided at a vertical distance equal to 0.5R) is not much effective because stresses are increased as compared to Case C.

(d) The stresses in the shell for Case C are the least as compared to other cases. Therefore the viscous boundary placed at a vertical distance equal to 1.0R is effective in obtaining minimum stresses in the shell due to absorption of most of the incoming waves and minimizes the reflection.

Table 6.12 presents the maximum shear stress (τ_{rz}) at outer gauss points in the elements along the height of shell for the above four cases. It is observed from Table 6.12 that,

(a) The stresses obtained in the shell for Case A and Case B compare well, little less stresses are observed in Case B as compared to Case A due to

absorption of energy.

Table 6.11

Bending Stress at Outer G.P. Along the Height of Shell, (Fig.4.10a)

Element number	G.P.	Maximum bending stress, $\sigma_z \left(t/m^2\right)$			
		Case 1	Case 2	Case 3	Case 4
1	4	2.58	2.48	2.41	2.42
	3	0.78	0.71	0.64	0.76
2	4	1.25	1.21	1.09	1.16
	3	1.92	1.87	1.52	1.75
4	4	8.58	8.41	8.38	8.49
	3	9.58	9.09	9.03	9.08
6	4	33.42	33.30	33.07	33.41
	3	34.39	34.01	33.52	33.68
8	4	80.10	77.71	76.56	77.19
	3	58.89	57.21	56.87	58.02
10	4	15.58	14.71	14.04	14.47
	3	61.67	58.21	57.72	58.63
11	4	118.07	117.21	108.79	111.05
	3	124.07	119.77	114.36	116.77
13	4	137.06	134.71	131.90	132.76
	3	119.08	117.91	116.89	118.98
15	4	166.58	164.71	158.84	165.64
	3	142.09	139.01	138.85	141.85
17	4	170.58	168.71	162.66	167.90
	3	158.58	152.21	151.52	155.82
19	4	175.58	169.71	164.90	170.67
	3	183.91	178.21	177.71	181.13
21	4	140.58	136.71	135.41	138.02
	3	149.20	144.21	140.51	144.83
22	4	108.73	106.71	105.12	105.24
	3	160.50	151.07	139.66	143.39

(b) The stresses in the shell for Case C are less as compared to Case B. It shows that stresses in the shell are less in case of placing viscous boundary at a smaller vertical distance as compared to fixed boundary at a greater lateral distance, that is, most of the incoming waves are absorbed by viscous boundary (damper) placed at even smaller vertical distance (equal

to 1.0R) as compared to fixed boundary at a greater vertical distance (equal to 2.0R).

Table 6.12

Shear Stress at Outer G.P. Along the Height of Shell
(Fig.4.10a)

Element number	G.P.	Maximum shear stress, $\tau_{rz}\left(t/m^2\right)$			
		Case A	Case B	Case C	Case D
1	4	2.78	2.71	2.18	2.20
	3	1.95	1.94	1.82	1.83
2	4	2.96	2.66	2.40	2.56
	3	3.87	3.72	3.51	3.62
4	4	11.39	10.78	10.54	11.00
	3	11.84	11.71	11.00	11.41
6	4	24.47	24.01	23.20	23.90
	3	25.00	24.43	23.45	24.67
8	4	40.55	39.67	38.45	39.02
	3	12.09	11.07	10.84	11.01
10	4	12.83	12.70	11.93	11.99
	3	9.55	9.01	8.77	8.98
11	4	1.18	1.16	1.07	1.09
	3	2.27	2.20	2.11	2.17
13	4	1.82	1.77	1.67	1.80
	3	2.58	2.49	2.30	2.41
15	4	2.20	2.12	2.00	2.16
	3	2.85	2.79	2.75	2.80
17	4	2.68	2.61	2.50	2.58
	3	3.95	3.87	3.74	3.80
19	4	3.79	3.68	3.54	3.59
	3	1.72	1.66	1.55	1.67
21	4	5.75	5.61	5.44	5.55
	3	8.93	8.82	8.71	8.77
22	4	12.13	12.01	11.94	11.99
	3	20.93	20.63	19.87	20.01

(c) The stresses in the shell for Case D are more than that of Case C and at some gauss points stresses in the shell for case D are even more than that of Case B but less than that of Case A. It shows that Case D (in which viscous boundary is provided at a vertical distance equal to 0.5R) is not much effective because stresses are increased as compared to Case C.

(d) The stresses in the shell for Case C are the least as compared to other cases. Therefore the viscous boundary placed at a vertical distance equal to 1.0R is effective in obtaining minimum stresses in the shell due to absorption of most of the incoming waves and minimizes the reflection.

Table 6.13 presents the maximum horizontal displacement at outer nodes along the height of shell for the above four cases. It is observed from Table 6.13 that,

(a) The displacements obtained in the shell for Case A and Case B compare well, little less displacements are observed in Case B as compared to Case A due to absorption of energy.

(b) The displacements in the shell for Case C are less as compared to Case B. It shows that displacements in the shell are less in case of placing viscous boundary at a smaller vertical distance as compared to fixed boundary at a greater lateral distance, that is, most of the incoming waves are absorbed by viscous boundary (damper) placed at even smaller vertical distance (equal to 1.0R) as compared to fixed boundary at a greater vertical distance (equal to 2.0R).

(c) The displacements in the shell for Case D are more than that of Case C and less than that of Case B and Case A. It shows that Case D (in which viscous boundary is provided at a vertical distance equal to 0.5R) is not much effective because displacements are increased as compared to Case C.

(d) The displacements in the shell for Case C are the least as compared to other cases. Therefore the viscous boundary placed at a vertical distance equal to 1.0R is effective in obtaining minimum stresses in the shell due to absorption of most of the incoming waves and minimizes the reflection.

Table 6.14 presents the maximum shear stress (τ_{rz}) at bottom gauss points in the elements from centre to edge of the raft for the above four cases. It is observed from Table 6.14 that,

(a) The stresses obtained in the raft for Case A and Case B compare well, little less stresses are observed in Case B as compared to Case A due to absorption of energy.

Table 6.13

Displacement at Outer Nodes Along the Height of Shell
(Fig.4.10a)

Node number	Maximum horizontal displacements (mm)			
	Case A	Case B	Case C	Case D
1	9.44	9.38	9.01	9.04
4	9.40	9.32	9.00	9.02
6	9.37	9.27	8.97	9.00
11	9.22	9.20	8.81	8.92
16	9.00	8.99	8.71	8.82
21	8.73	8.63	8.49	8.62
26	8.37	8.26	8.10	8.23
31	8.00	7.88	7.77	7.87
36	7.61	7.52	7.43	7.51
41	7.44	7.35	7.18	7.30
46	7.14	7.10	7.01	7.09
51	5.89	5.78	5.71	5.72
56	5.54	5.41	5.28	5.34
61	5.08	5.00	4.91	4.95
66	4.61	4.58	4.43	4.44
71	4.19	4.17	4.08	4.14
76	3.84	3.81	3.71	3.80
81	3.56	3.55	3.45	3.50
86	3.30	3.27	3.00	3.19
91	2.83	2.78	2.59	2.71
96	1.99	1.93	1.80	1.90
101	0.97	0.93	0.73	0.89
106	0.73	0.70	0.65	0.68
111	0.71	0.68	0.66	0.67
117	0.69	0.66	0.55	0.60
118	0.65	0.62	0.49	0.51

(b) The stresses in the raft for Case C are less as compared to Case B. It shows that stresses in the raft are less in case of placing viscous boundary at a

smaller vertical distance as compared to fixed boundary at a greater vertical distance.

(c) The stresses in the shell for Case D are more than that of Case C and less than that of Case B and Case A. It shows that Case D (In which viscous boundary is provided at a vertical distance equal to 0.5R) is not much effective because stresses are increased as compare to Case C.

(d) The stresses in the shell for Case C are the least as compared to other cases. Therefore the viscous boundary placed at a vertical distance equal to 1.0R is effective in obtaining minimum stresses in the shell due to absorption of most of the incoming waves and minimizes the reflection.

Table 6.14

Bending Stress at Bottom G.P. in the Elements of the Raft, (Fig.4.10a)

Element number	GP	Maximum bending stress, $\sigma_z \left(t/m^2 \right)$			
		Case A	Case B	Case C	Case D
23	1	3.21	3.17	2.91	3.01
	3	3.03	2.98	2.87	2.91
24	1	1.02	1.00	0.98	0.99
	3	0.46	0.45	0.43	0.44
25	1	5.35	5.30	5.26	5.28
	3	0.52	0.51	0.48	0.49
26	1	51.07	50.43	48.78	49.53
	3	35.28	34.87	33.43	33.95
27	1	40.26	39.43	38.57	39.01
	3	18.55	18.01	17.45	17.87

The following conclusions are derived from the parametric study of the effect of vertical mesh size using viscous boundaries :

(a) The almost same seismic response of the structure (shell, dome and raft)

are obtained by introducing viscous boundaries at a smaller vertical dimension as compared to fixed boundaries at a greater vertical dimension

(b) The viscous boundary is effective to obtain minimum seismic response when it is placed at a vertical distance (from the bottom of the raft) equal to the radius of the raft.

6.8 Concluding Remarks

The finite element seismic analysis of an axisymmetric soil-structure system has been carried out using fixed and viscous boundaries in lateral and vertical directions . The effectiveness of viscous boundaries has been studied in relation to fixed boundaries . A parametric study has been carried out to evaluate the effect of horizontal and vertical mesh size of soil with viscous boundaries in comparison to fixed soil boundaries. The conclusions derived from this study are as under :

(i) The viscous boundaries have been found to be effective in absorbing the wave energy at the boundary and minimize wave reflections.

(ii) The almost same seismic response of the structure resting on soil is obtained by providing viscous boundaries at a smaller lateral dimension as compared to fixed boundaries at a greater lateral dimension.

(iii) The almost same seismic response of soil (at different depths of soil strata and at various points in a horizontal soil layer) is obtained by providing viscous boundaries at a smaller lateral dimension as compared to fixed boundaries at a greater lateral dimension.

(iv) The almost same structural response is obtained by providing viscous boundaries at a smaller vertical dimension as compared to fixed boundaries at a greater vertical dimension.

(v) It is recommended that viscous boundaries in the form of dampers could be placed at a horizontal dimension of one and half times the raft radius and at a vertical dimension equal to radius of the raft for the absorption of the energy at the boundaries and minimize the reflection of waves from the boundaries.

EFFECT OF MODELLING OF NON-AXISYMMETRIC INTERNAL STRUCTURE

7.1 Introduction

The dynamic response of a nuclear reactor building is sensitive to the method of modelling of its internal structure. As reactor internal structure is not axisymmetric while outer containment wall (OCW), inner containment wall(ICW), outer containment dome(OCD) and inner containment dome(ICD) are axisymmetric. The reactor internal structure being non-axisymmetric poses problem in its idealization. So in order to model the complete reactor building as axisymmetric solid, the internal structure is to be modelled as equivalent solid cylinder which enables one to carry out axisymmetric analysis of the complete reactor building as axisymmetric structure.

The objective of the study in this chapter is to evaluate the effect of modelling of non-axisymmetric portion of nuclear reactor building as equivalent axisymmetric body, on overall seismic response of the building.

In order to achieve this objective, two complete reactor buildings of different size and type are selected as under :

(i)   A hypothetical reactor building of a power plant on a rocky foundation is considered herein (Fig. 4.18). The foundation-structure interaction is relatively less in this case, however, a portion of foundation has been considered in the finite element idealization.

(ii)   Another hypothetical reactor building of different size and type of a power plant is considered fixed at base (Fig. 7.1), obviously, in this case foundation structure interaction is not considered.

7.2 Structural Configuration of a Reactor Building

The structure consists of two axisymmetric containments, namely, inner and outer shells. The outer containment wall (OCW) is covered by a spherical

dome. The inner containment wall (ICW) is covered by a floor slab in first building while it is covered by a spherical dome and floor slab in second building (two reactor buildings (i) and (ii) are described in section 7.1). The ICW and OCW are connected at floor slab level in first building while only ICW is connected at floor slab in second building. The height to diameter ratio of containments is almost unity. There is a clear gap of 2m between the containments. The reactor internals are enclosed inside the ICW and resting on raft. The internals consist of the frame structure and have two solid shear walls of different stiffness in perpendicular directions. The calandria vault is resting on the internal frame structure over a heavy hollow concrete block. It is rectangular in shape. It is made of heamatite concrete and is treated as a cantilever structure supported on heavy hollow concrete block. The circular foundation raft 4m to 5m thick supports both the containments and reactor internals. The OCW is partly embedded in soil to a depth of about one-fifth of overall height of building. The building is completely closed from outside and is a massive and stiff structure.

7.3 Method of Dynamic Analysis and Ground Motion Used

The seismic response of above two buildings to earthquake motion is obtained by timewise mode superposition method and first six modes are considered in the analysis. The maximum stresses at gauss points and displacements at nodes are obtained as a result of finite element seismic analysis of the buildings. The complete reactor building including equivalent solid cylinder representing internal structure is modelled by 8-noded isoparametric parabolic solid finite elements.

The horizontal ground motion of Koyna Earthquake (Dec. 11, 1967, Transverse component) is considered.

7.4 Methods Considered for Modelling of Reactor Internals

The reactor internal structure is modelled as equivalent solid cylinder by four alternate methods as under (Thakkar, 1989):

Case 1. Single mass of internal structure lumped at the centre of gravity of internals connected by rigid element with the raft.

Case 2. Simulating equivalent EI value of reactor internal structure, the mass of internal structure is uniformly distributed.

Case 3. Simulating fundamental natural frequency of internal structure, by suitably adjusting the diameter of equivalent solid cylinder.

Case 4. Mass of the internal structure is distributed on the raft.

The above cases of modelling of reactor internals are simulated by adjusting the size and material properties of equivalent solid cylinder. In Case 1, the total mass of the internals is lumped at the centre of gravity of internal structure and is connected by rigid element with the raft. The rigidity of the element is simulated by giving high value of modulus of elasticity to this element. In Case 2, the mass is uniformly distributed over the equivalent solid cylinder and simulating equivalent EI value of internals. In finite element analysis, EI value of internal is simulated by varying the value of E only to the element representing equivalent solid cylinder. In Case 3, the first natural frequency of internal is matched with that of equivalent solid cylinder. The diameter of equivalent solid cylinder is adjusted in such a way that the total mass of the internals has been preserved. In Case 4, the internal is represented by mass only and this total mass of internals is uniformly distributed on the raft.

7.5 Analysis of First Reactor Building (Fig. 4.18)

Figure 4.18 shows the finite element idealization of reactor building including base and surrounding soil. There are total 81 elements (34 structural elements and 47 soil elements) and 325 nodes in the finite element mesh.

Table 7.1 gives the material properties of structure and foundation soil.

Simulation of First Frequency of Reactor Internals

The finite element free vibration analysis of equivalent solid cylinder with fixed base is carried out by suitably distributing the mass of the internals in such a way that at least first frequency of this cylinder matches with that of reactor internals. The balance mass is placed on the raft. Table 7.2 shows the first three frequencies of equivalent solid cylinder and fundamental frequency of reactor internals.

Table 7.1

Material Properties of Structure and Founding Soil, (Fig. 4.18)

Description of structure	Modulus of elasticity $(\times 10^6 \ t/m^2)$	Poisson's ratio	Mass density $(t-s^2/m^4)$	Damping (percent)
Outer and Inner walls, Raft and Floor slab	2.500	0.200	0.250	5%
Founding soil	1.200	0.233	0.000	20% (translational) 5% (rocking)

Table 7.2

Frequencies of Equivalent Solid Cylinder and of Reactor Internals, (Fig. 4.18)

Mode	Frequencies (Hertz)	
	Reactor internals	Equivalent solid cylinder
1	8.70	8.70
2	----	28.57
3	----	55.56

The equivalent diameter of solid cylinder simulating the internal structure is obtained corresponding to the above four cases. The properties of this cylinder in the four cases are given in Table 7.3.

Results and Discussions :

The results of seismic analysis of reactor building include the time periods of vibration in first six modes and corresponding weighted modal damping, the maximum stresses (bending and shear) and displacements. The results of analysis are described below :

The time periods (T) in first six modes and corresponding weighted modal damping values (ς) are presented in Table 7.4.

Table 7.3

Material Properties of Equivalent Solid Cylinder, (Fig. 4.18)

Case	Modulus of elasticity $\left(\times 10^6 \ t/m^2\right)$	Poisson's ratio	Damping (percent)	Equivalent diameter of solid cylinder (m)
1	10000.0	0.200	5%	14.00
2	2.0	0.200	5%	14.00
3	2.5	0.200	5%	12.00
4	The internals are represented by mass alone, distributed on raft			

Table 7.4

Effect of Modelling of Internals on Dynamic Characteristics,(Fig. 4.18)

Mode	Time periods of vibration (sec)				Weighted modal damping factors			
	case 1	case 2	case 3	case 4	case 1	case 2	case 3	case 4
1	0.2326	0.2215	0.2277	0.2195	0.1140	0.0972	0.1044	0.0930
2	0.1962	0.1500	0.1968	0.0893	0.0857	0.1024	0.0759	0.1010
3	0.0879	0.0880	0.0880	0.0872	0.0536	0.0551	0.0578	0.0960
4	0.0815	0.0820	0.0825	0.0779	0.0684	0.0745	0.0888	0.0700
5	0.0742	0.0693	0.0713	0.0776	0.0544	0.0956	0.0849	0.0544
6	0.0518	0.0561	0.0509	0.0561	0.0930	0.0743	0.0917	0.1290

Time periods

It is observed from Table 7.4 that, (a) time period in second mode is quite different in four cases, (b) time periods in first and third mode are almost equal in four cases, and (c) time periods in 4 to 6 modes are not much different in four cases. Since in the Case 3, first frequency of internals is simulated, therefore the overall response of the reactor building would be more realistic as compared to other cases.

Weighted modal damping

The values of weighted modal damping in six modes are quite different in four cases (Table 7.4). It shows that weighted modal damping is also sensitive to the type of modelling of internals.

Effect of modelling of internals on seismic response of OCW

Tables 7.5 and 7.6 list the maximum stresses and displacements in various elements of OCW, obtained as a result of seismic analysis of complete reactor building in four methods of modelling of its internal structure.

Maximum bending stress

It is observed from Table 7.5 that bending stresses (σ_z) at outer gauss points in elements along the height of OCW are maximum in case 4 and are minimum in case 3.

Maximum shear stresses

Table 7.5 also compares the maximum shear stresses (τ_{rz}) at outer gauss points in elements of OCW for the four cases of modelling of reactor internal. It is observed that, although the shear stresses are almost equal in all the cases, yet the stresses are relatively high in Case 4 and low in Case 3.

Maximum horizontal displacements :

Table 7.6 presents the maximum horizontal displacements at outer nodes along the height of OCW. It is found from this table that displacements are minimum in Case 3 and maximum in Case 4.

Effect of modelling of internals on seismic response of ICW

Tables 7.7 and 7.8 list the maximum stresses and displacements in various elements of ICW, obtained as a result of seismic analysis of complete reactor building in four methods of modelling of internal structure.

Maximum bending stress

It is observed from Table 7.7 that bending stresses at outer gauss points in elements along the height of ICW are maximum in Case 4 and are minimum in Case 3.

Maximum shear stresses

Table 7.7 also compares the maximum shear stresses at outer gauss points in elements of OCW for the four cases of modelling of internals. It is observed that shear stresses are almost equal in Cases 1, 3 and 4.

Table 7.5
Maximum Stresses at Outer G.P. in Elements of OCW, (Fig. 4.18)

Element number	GP	Bending stress $\left(\sigma_z - t/m^2\right)$				Shear stress $\left(\tau_{rz} - t/m^2\right)$			
		Case 1	Case 2	Case 3	Case 4	Case 1	Case 2	Case 3	Case 4
4	4	12.22	12.17	7.78	12.67	3.22	3.83	3.17	3.44
	3	32.11	32.36	18.73	32.77	3.70	3.25	1.66	2.78
5	4	36.38	36.14	17.99	36.85	4.19	4.31	2.92	4.47
	3	45.58	46.03	21.88	46.19	3.03	3.06	1.56	3.61
6	4	53.35	54.01	27.16	54.40	1.71	1.72	1.01	1.79
	3	67.61	68.55	35.73	68.94	2.65	2.65	1.44	2.74
7	4	78.64	78.55	44.18	79.04	2.04	1.97	1.15	2.06
	3	113.65	112.91	58.44	114.05	1.98	1.90	1.18	2.08
8	4	125.75	125.48	65.14	126.47	3.89	3.83	2.25	3.89
	3	106.90	109.28	56.13	109.96	12.57	12.13	9.92	13.07
9	4	98.66	101.41	56.14	99.86	1.99	2.13	1.37	2.23
	3	118.20	118.70	91.04	120.28	9.83	9.86	7.17	9.88
10	4	132.96	132.93	100.20	133.53	1.16	1.19	0.33	1.27
	3	150.54	151.40	122.14	156.20	1.22	1.21	0.90	1.26
11	4	164.20	165.21	137.61	172.80	1.25	1.25	0.57	1.31
	3	184.19	185.29	159.96	193.85	0.69	0.69	0.36	0.69
12	4	200.02	201.14	176.98	210.05	0.97	0.99	0.65	0.99
	3	222.36	223.47	201.98	232.38	2.02	2.04	1.80	2.17
13	4	238.15	239.28	219.22	248.41	1.97	1.98	1.77	2.11
	3	251.41	252.52	236.05	261.26	0.58	0.54	0.58	0.58
14	4	252.43	253.54	239.33	261.70	2.70	2.73	2.51	2.92
	3	336.69	337.23	330.52	342.90	16.92	16.92	16.86	17.14

Table 7.6

Maximum Horizontal Displacements Along the Height of OCW, (Fig. 4.18)

Node number	Maximum horizontal displacement (mm)			
	Case 1	Case 2	Case 3	Case 4
1	12.04	12.04	10.63	12.14
6	11.74	11.73	10.14	11.84
11	11.37	11.33	10.79	11.70
14	11.22	11.22	10.13	11.22
16	10.97	10.98	10.04	10.90
20	10.41	10.42	9.61	10.38
23	9.83	9.93	9.18	9.81
28	8.87	8.87	8.47	8.86
33	7.83	7.84	7.72	7.84
36	6.74	6.75	6.74	6.96
73	6.49	6.49	6.46	6.71
105	5.38	5.38	5.34	5.58
110	4.24	4.24	4.19	4.48
115	3.16	3.16	3.12	3.38
148	2.19	2.18	2.15	2.35
150	1.29	1.29	1.27	1.37
152	0.04	0.04	0.04	0.04

Table 7.7

Maximum Stresses at Outer G.P. in Elements of ICW, (Fig. 4.18)

Element number	G.P.	Bending stress $\left(\sigma_z - t/m^2\right)$				Shear stress $\left(\tau_{rz} - t/m^2\right)$			
		Case 1	Case 2	Case 3	Case 4	Case 1	Case 2	Case 3	Case 4
15	4	61.69	62.86	28.91	65.51	5.61	5.76	2.41	5.77
	3	86.50	84.81	58.50	86.97	3.41	3.31	1.51	3.35
16	4	100.68	99.13	70.98	100.76	2.79	2.71	1.42	2.76
	3	119.42	118.54	91.69	121.09	3.04	2.95	1.50	3.02
17	4	136.30	135.44	109.61	138.70	2.97	2.86	1.49	2.93
	3	159.95	159.13	135.24	162.59	2.53	2.37	1.27	2.45
18	4	177.47	176.69	154.24	180.39	2.72	2.58	1.67	2.66
	3	202.14	201.43	182.19	205.20	3.85	3.83	3.19	3.87
19	4	221.12	220.47	203.14	224.38	2.65	2.64	2.02	2.62
	3	238.69	238.15	224.81	242.08	5.12	2.56	2.55	2.94
20	4	239.12	238.72	227.64	242.05	3.32	3.33	2.87	3.44
	3	320.08	319.61	318.07	322.05	26.58	26.64	25.70	26.34

Maximum horizontal displacements :

Table 7.8 presents the maximum horizontal displacements at outer nodes along the height of ICW. It is found from this table that displacements are almost equal in all the cases.

Table 7.8

Maximum Horizontal Displacements Along the Height of ICW
(Fig. 4.18)

Node number	Maximum horizontal displacement (mm)			
	Case 1	Case 2	Case 3	Case 4
69	6.50	6.72	6.47	6.50
78	5.32	5.54	5.30	5.32
83	4.19	4.45	4.17	4.19
93	2.11	2.29	2.12	2.10
98	1.24	1.33	1.23	1.24
127	0.06	0.04	0.04	0.04

Effect of modelling of internals on seismic response of raft

Table 7.9 gives the maximum bending stresses at bottom gauss points in elements from centre to edge of the raft. It is observed from this table that the stresses are maximum in Case 1 and minimum in Case 4 in the central 2/3rd portion of the raft. In the 1/3rd portion of the raft near the end, though the stresses are equal in all the cases yet the stresses are relatively maximum in Case 4 and minimum in Case 3. Therefore, it is concluded that (a) method of modelling of reactor internals does not affect bending stresses in the end 1/3rd part of the raft. (b) The realistic stresses are obtained in Case 3 in the central 2/3rd portion of the raft due to simulation of first natural frequency of reactor internals.

Table 7.9

Maximum Bending Stresses at Bottom G.P. in Elements of Raft
(Fig. 4.18)

Element number	G.P.	Bending stress $\left(\sigma_z - t/m^2\right)$			
		Case 1	Case 2	Case 3	Case 4
27	1	180.83	77.00	8.92	0.18
	3	797.67	273.45	42.46	0.76
28	1	656.64	185.49	36.67	36.67
	3	82.16	7.27	5.72	5.72
29	1	79.46	14.15	7.17	5.37
	3	25.00	24.57	24.51	24.15
30	1	55.88	55.09	54.88	56.45
	3	60.66	60.09	59.62	61.50
31	1	58.05	57.84	57.39	58.83
	3	65.42	65.56	64.58	66.21
32	1	71.77	71.66	70.36	72.13
	3	65.23	65.17	63.76	65.64
33	1	65.12	65.02	63.54	65.41
	3	78.77	78.55	76.78	78.70

Effect of modelling of internal on seismic response of floor slab

Table 7.10 lists the maximum bending stresses at bottom gauss points in elements from centre to edge of slab. It is observed from this table that stresses are almost equal in all the four cases except in Case 3 which gives least stresses. It shows that the method of modelling of internals does not very much affect the response in the slab.

7.6 Analysis of Second Reactor Building

Figure 7.1 shows the finite element idealization of building in N-S direction. There are total 89 elements and 421 nodes in the finite element mesh.

Table 7.11 gives the material properties of structure.
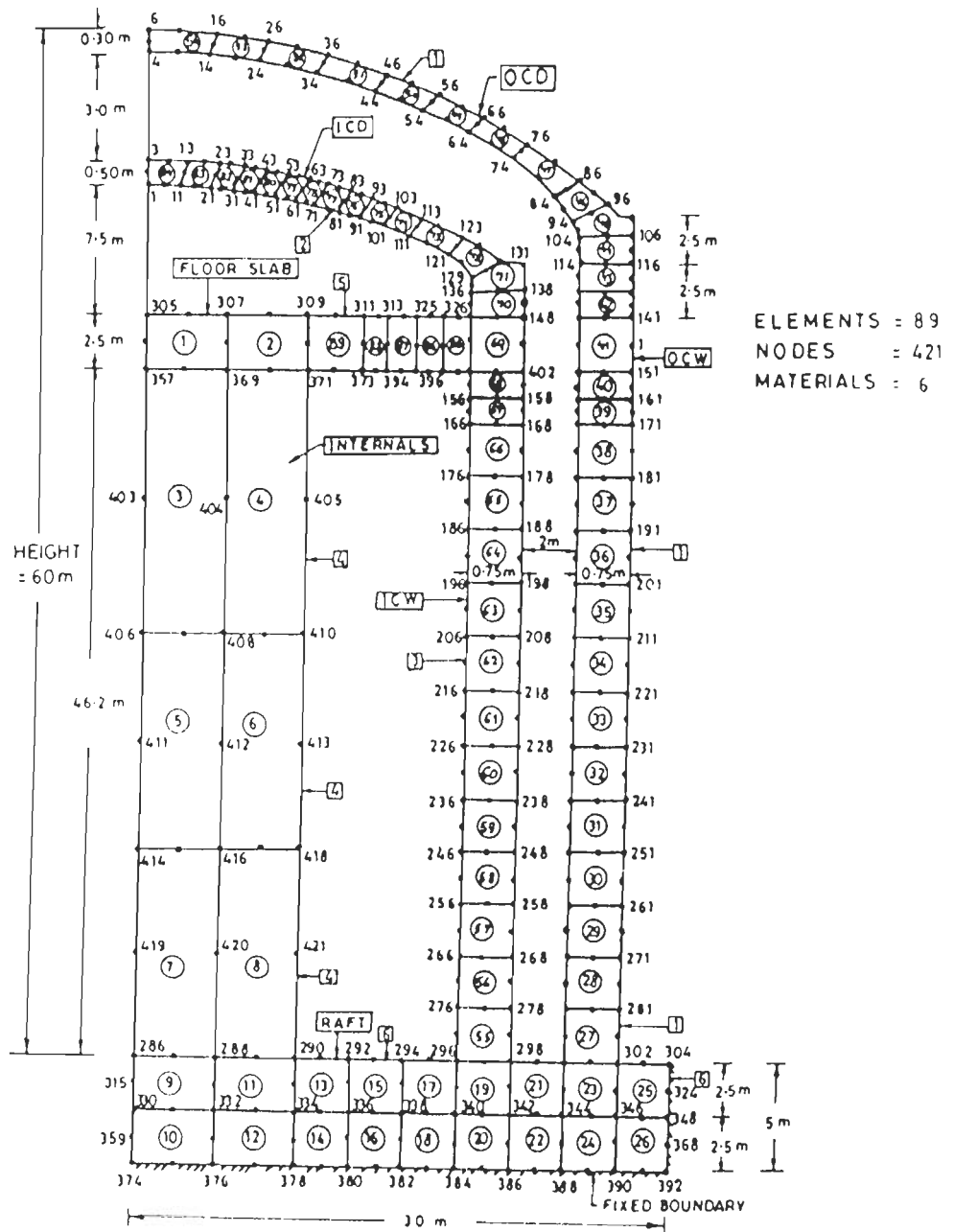
FIG. 7·1   FINITE ELEMENT MESH OF REACTOR BUILDING
FIXED AT BASE OF RAFT – NS DIRECTION

Table 7.10

Maximum Bending Stresses at Bottom G.P. in Elements of Slab (Fig. 4.18)

Element G.P. number		Bending stress $\left(\sigma_z - t / m^2\right)$			
		Case 1	Case 2	Case 3	Case 4
21	1	1.70	1.73	0.42	1.62
	3	0.49	0.48	0.20	0.48
22	1	0.88	0.85	0.37	0.82
	3	1.03	0.99	0.61	1.00
23	1	1.28	1.21	0.64	1.22
	3	1.17	1.17	0.62	1.17
24	1	3.58	3.46	2.19	3.49
	3	7.47	7.20	4.89	6.85
25	1	24.39	23.83	14.23	23.98
	3	24.63	24.81	11.07	19.65
26	1	6.76	7.42	6.60	6.66
	3	15.71	15.29	13.49	14.92

Table 7.11

Material Properties of Second Reactor Building, (Fig. 7.1)

Description of structure	Modulus of elasticity $\left(\times 10^6 \, t / m^2\right)$	Poisson's ratio	Mass density $\left(t - s^2 / m^4\right)$	Damping (percent)	Material number
OCW and OCD	2.600	0.210	0.250	7%	1
ICD	3.380	0.210	0.250	5%	2
ICW	3.000	0.210	0.250	5%	3
Internals	3.000	0.210	0.290	7%	4
Slab	4.100	0.210	0.200	6%	5
Raft	3.000	0.260	0.250	7%	6

Simulation of First Frequency of Reactor Internals

The finite element free vibration analysis of equivalent solid cylinder with fixed

base is carried out by suitably distributing the mass of the internals so that at least first frequency of this equivalent solid cylinder matches with that of reactor internals. The balance mass is placed on the raft. Table7.12 shows the first three frequencies of equivalent solid cylinder and first frequency of reactor internals.

Table 7.12

Frequencies of Equivalent Solid Cylinder and of Reactor Internals, (Fig. 7.1)

Mode	Frequencies (Hertz)	
	Reactor internals	Equivalent solid cylinder
1	2.35	2.35
2	----	11.00
3	---	23.81

The equivalent diameter of solid cylinder simulating the internal structure is obtained corresponding to the above four cases (Case 1 to 4 are described in section 7.4). The properties of this cylinder in the four cases are given in Table 7.13.

Table 7.13

Material Properties of Equivalent Solid Cylinder, (Fig. 7.1)

Case	Modulus of elasticity $\left(\times 10^6 \ t/m^2\right)$	Poisson's ratio	Damping (percent)	Equivalent diameter of solid cylinder (m)
1	10000.0	0.200	7%	18.00
2	2.4	0.200	7%	18.00
3	3.0	0.200	7%	16.00
4	The internals are represented by mass alone, distributed on raft			

Results and discussions

The results of seismic analysis of reactor building include the time periods of vibration in first six modes and corresponding weighted modal damping, the maximum bending and shear stresses and displacements. The results of analysis are described below :

The time periods (T) in first six modes and corresponding weighted modal damping values (ς) are presented in Table 7.14.

Table 7.14

Effect of Modelling of Internals on Dynamic Characteristics,(Fig. 7.1)

Mode	Time periods of vibration (sec)				Weighted modal damping factors			
	Case 1	Case 2	Case 3	Case 4	Case 1	Case 2	Case 3	Case 4
1	0.2237	0.2239	0.2507	0.2239	0.0700	0.0700	0.0625	0.0700
2	0.1752	0.1970	0.2238	0.1356	0.0646	0.0628	0.0700	0.0580
3	0.0858	0.0857	0.1157	0.0858	0.0700	0.0696	0.0621	0.0700
4	0.0738	0.0797	0.0854	0.0744	0.0520	0.0524	0.0690	0.0518
5	0.0623	0.0648	0.0757	0.0635	0.0628	0.0566	0.0542	0.0690
6	0.0521	0.0494	0.0622	0.0611	0.0655	0.0622	0.0596	0.0659

Time periods

It is observed from Table 7.14 that time periods in six modes differ from each other in four cases. The time periods in six modes are highest in Case 3 as compared to other cases . It shows that Case 3 in which first frequency of internals is simulated would represent the relatively flexible behaviour of the building. Therefore, the overall response of the building would be least in Case 3 as compared to other methods of modelling of internals.

Weighted damping

The weighted damping factor values in six modes for four cases (Table 7.14) do

not follow any pattern. Therefore, the weighted modal damping is sensitive to the type of modelling of internals.

Effect of modelling of internals on seismic response of OCW

Tables 7.15 and 7.16 list the maximum stresses and displacements in various elements of OCW, obtained as a result of seismic analysis of complete reactor building in four methods of modelling of its internals.

Maximum bending stress

It is observed from Table 7.15 that bending stresses (σ_z) at outer gauss points in elements along the height of OCW are maximum in Case 4 and are minimum in Case 3.

Maximum shear stresses

Table 7.15 also compares the maximum shear stresses (τ_{rz}) at outer gauss points in elements of OCW for the different four cases of modelling of reactor internals. It is observed that shear stresses are almost equal in all the four cases, little less values are found in Case 3 as compared to other cases.

Maximum horizontal displacements

Table 7.16 presents the maximum horizontal displacements at outer nodes along the height of OCW including OCD. It is found from this table that displacements are almost same in all the cases and little lesser values of displacement are found in Case 3.

Effect of modelling of internals on seismic response of ICW

Tables 7.17 and 7.18 list the maximum stresses and displacements in various elements of ICW including ICD, obtained as a result of seismic analysis of complete reactor building in four methods of modelling of internals.

Table 7.15

Maximum Stresses at Outer G.P. in Elements of OCW, (Fig. 7.1)

Element number	G.P.	Bending stress $\left(\sigma_z - t/m^2\right)$				Shear stress $\left(\tau_{rz} - t/m^2\right)$			
		Case 1	Case 2	Case 3	Case 4	Case 1	Case 2	Case 3	Case 4
54	4	2.24	2.31	2.33	2.86	2.07	1.80	1.05	1.81
	3	10.29	9.67	6.79	13.66	1.59	1.29	1.26	1.45
51	4	1.41	1.05	0.47	1.88	6.78	5.47	2.11	4.70
	3	2.87	2.91	2.50	2.97	4.72	4.32	3.44	4.19
48	4	9.47	11.17	8.41	10.77	9.59	8.38	3.89	8.36
	3	6.84	5.15	5.13	7.11	8.27	4.85	4.18	4.85
45	4	7.89	7.85	7.34	8.03	7.54	7.49	6.96	7.65
	3	7.83	7.88	7.49	8.11	8.19	8.14	7.53	8.30
44	4	60.95	60.57	56.02	61.68	14.59	14.39	13.40	14.69
	3	6.78	6.66	6.25	6.79	10.05	9.95	9.27	10.17
42	4	32.03	32.67	31.14	32.77	0.48	0.54	0.44	0.51
	3	33.49	34.37	32.39	34.21	1.53	1.47	1.29	1.43
39	4	79.69	81.03	76.53	81.50	0.64	0.65	0.54	0.62
	3	69.83	70.56	66.24	70.65	0.62	0.60	0.55	0.63
36	4	123.37	125.10	118.51	125.28	0.53	0.52	0.47	0.53
	3	116.46	117.76	111.41	118.19	0.48	0.42	0.35	0.42
33	4	165.12	168.2	158.94	169.83	0.47	0.46	0.43	0.46
	3	156.05	158.69	150.15	159.17	0.46	0.43	0.37	0.43
30	4	172.99	176.66	167.70	177.67	6.62	6.80	6.45	6.49
	3	196.44	200.70	190.54	201.53	1.21	1.23	1.21	1.17
27	4	99.18	103.14	91.58	104.58	2.96	3.00	2.13	2.97
	3	144.76	149.18	138.89	150.05	7.66	7.76	7.59	7.71

Maximum bending stress

It is observed from Table 7.17 that bending stresses at outer gauss points in elements along the height of ICW are maximum in Case 4 and are minimum in Case 3.

Maximum shear stresses

Table 7.17 also compares the maximum shear stresses at outer gauss points in elements of OCW for the four cases of modelling of internals. It is observed that shear stresses are almost equal in Cases 1, 3 and 4 . The shear stresses are least in Case 3 as compared to other cases.

Table 7.16

Maximum Horizontal Displacements Along the Height of OCW, (Fig. 7.1)

Node number	Maximum horizontal displacement (mm)			
	Case 1	Case 2	Case 3	Case 4
6	8.66	8.65	8.41	8.57
26	8.60	8.57	8.32	8.50
56	7.86	7.86	7.82	7.85
86	7.59	7.70	7.40	7.49
106	7.76	7.83	7.54	7.66
116	7.88	7.93	7.68	7.81
126	7.19	7.22	7.05	7.14
151	5.97	6.03	5.94	5.95
171	4.64	4.77	4.63	4.72
191	3.60	3.72	3.61	3.65
211	2.49	2.58	2.47	2.51
231	1.85	1.91	1.80	1.82
261	0.33	0.36	0.32	0.35
271	0.18	0.22	0.17	0.20
281	0.16	0.19	0.15	0.17
302	0.01	0.01	0.01	0.01

Maximum horizontal displacements :

Table 7.18 presents the maximum horizontal displacements at outer nodes along the height of ICW including ICD. It is found from this table that displacements are minimum in case 3 as compared to other cases.

Effect of modelling of internals on seismic response of raft

Table 7.19 gives the maximum bending stresses at bottom gauss points in elements from centre to edge of the raft. It is observed from this table that the stresses are maximum in Case 1 and minimum in Case 4 in the central 2/3rd portion of the raft. In the 1/3rd portion of the raft near the end, the stresses are almost equal in all the cases. Therefore, it is concluded that (a) method of modelling of reactor internals does not affect bending stresses in the end 1/3rd part of the raft. (b) The realistic stresses are obtained in Case 3 in the central 2/3rd portion of the raft due to simulation of first natural frequency of reactor

internals.

Table 7.17

Maximum Stresses at Outer G.P. in Elements of ICW

(Fig. 7.1)

Element number	G.P.	Bending stress $(\sigma_z - t/m^2)$				Shear stress $(\tau_{rz} - t/m^2)$			
		Case 1	Case 2	Case 3	Case 4	Case 1	Case 2	Case 3	Case 4
84	4	1.46	1.10	0.51	2.09	4.76	3.73	1.51	3.17
	3	2.11	1.34	0.67	2.19	1.69	1.31	0.47	1.18
81	4	9.16	7.71	3.97	9.71	27.07	23.12	10.22	19.70
	3	7.06	5.99	2.52	7.05	24.32	20.60	8.74	17.40
78	4	4.44	4.97	2.77	4.98	3.71	2.95	2.58	4.58
	3	2.92	2.83	1.28	3.20	3.61	5.16	3.42	5.30
75	4	67.18	69.38	39.89	69.59	13.40	13.16	6.95	11.12
	3	96.00	96.37	52.63	98.37	52.38	50.74	26.33	42.83
72	4	135.05	146.05	102.84	146.25	14.83	15.63	10.02	13.25
	3	99.93	107.95	74.44	108.02	14.42	15.14	9.12	12.77
71	4	72.79	78.70	47.39	79.11	4.77	4.93	4.07	4.82
	3	126.63	138.95	101.96	139.63	7.42	8.05	5.80	6.94
70	4	79.35	78.81	47.66	81.71	15.47	15.66	12.54	19.55
	3	55.64	55.01	14.13	63.97	8.29	8.20	7.24	9.90
69	4	43.57	71.46	21.97	92.77	18.74	14.00	2.57	14.45
	3	65.98	62.05	34.22	70.14	22.18	19.01	9.85	14.33
67	4	162.64	193.04	142.25	204.35	0.28	0.47	0.25	0.50
	3	156.61	186.20	137.35	202.22	0.82	1.15	0.25	0.73
64	4	197.93	238.75	156.97	250.42	0.83	0.82	0.47	0.79
	3	189.80	229.30	152.68	240.25	0.74	0.60	0.60	0.62
61	4	247.95	293.39	181.78	312.95	0.95	0.94	0.72	0.84
	3	236.74	281.57	176.78	299.15	0.77	0.70	0.44	0.66
58	4	262.96	302.49	179.17	331.53	10.96	10.87	6.01	12.06
	3	295.70	341.22	202.13	372.38	1.78	1.79	1.13	2.11
55	4	141.70	171.22	103.28	180.92	5.20	6.00	4.82	4.08
	3	213.89	248.62	145.51	271.34	12.27	13.13	7.20	15.04

Table 7.18

Maximum Horizontal Displacements Along the Height of ICW

(Fig. 7.1)

Node number	Maximum horizontal displacement (mm)			
	Case 1	Case 2	Case 3	Case 4
3	11.10	12.03	7.09	13.28
23	10.76	11.66	6.71	13.00
53	10.10	10.96	6.05	12.35
73	10.05	10.70	6.16	11.98
93	10.12	10.80	6.47	11.90
103	9.86	10.53	6.29	11.63
113	9.58	10.23	6.09	11.35
123	9.13	9 74	5.73	10.90
131	9.00	9.60	5.62	10.78
148	6.46	6.97	3.16	8.56
168	5.86	6.51	3.21	7.32
188	4.75	5.39	2.77	5.55
208	3.45	3.94	2.08	3.72
228	2.60	2.95	1.58	2.70
258	0.44	0.56	0.27	0.31
268	0.21	0.29	0.17	0.17
278	0.21	0.27	0.15	0.15
298	0.01	0.01	0.01	0.01

Table 7.19

Maximum Bending Stresses at Bottom G.P. in Elements of Raft

(Fig. 7.1)

Element number	G.P.	Bending stress $\left(\sigma_z - t/m^2\right)$			
		Case 1	Case 2	Case 3	Case 4
10	1	515.97	362.87	165.89	135.16
	3	179.62	125.71	55.53	47.33
12	1	956.32	639.41	289.32	229.53
	3	837.60	573.89	265.53	211.41
16	1	23.62	15.96	7.79	5.74
	3	45.95	29.74	12.52	9.71
20	1	29.85	34.70	19.25	39.73
	3	8.50	8.10	6.52	11.40
26	1	11.25	10.93	10.51	12.03
	3	24.91	23.77	22.68	27.09

Effect of modelling of internals on seismic response of floor slab

Table 7.20 lists the maximum bending stresses at bottom gauss points in elements from centre to edge of slab. It is observed from this table that stresses are least in Case 3 as compared to other cases.

Table 7.20
Maximum Bending Stresses at Bottom G.P. in Elements of Slab,(Fig. 7.1)

Element number	G.P.	Bending stress $\left(\sigma_z - t / m^2\right)$			
		Case 1	Case 2	Case 3	Case 4
1	1	46.62	19.48	3.65	5.27
	3	154.23	51.37	11.38	12.31
2	1	98.89	164.27	23.39	57.02
	3	32.16	3.90	3.28	19.97
89	1	303.32	211.26	70.50	88.78
	3	777.00	291.46	91.26	96.52
88	1	106.99	86.93	28.10	54.97
	3	436.04	141.90	42.89	77.83
87	1	57.59	41.56	15.71	45.13
	3	38.76	72.46	21.87	44.20
86	1	22.31	23.94	17.46	35.29
	3	31.72	18.35	8.62	20.19
85	1	25.15	22.49	16.60	24.00
	3	24.97	22.66	6.36	18.10

7.7 Concluding Remarks

The non-axisymmetric internal structures of two reactor buildings of different size and type have been modelled as equivalent axisymmetric body (solid cylinder) by four different methods. The complete reactor building including equivalent internal structure subjected to horizontal ground motion have been analysed using finite element method. The maximum seismic response of overall reactor building (on OCW, ICW, raft and slab) are computed using mode superposition method. The effects of modelling of reactor internal on overall seismic response of building have been studied. The following conclusions are derived from this study :

(i) The seismic response of reactor buildings is sensitive to the method of

modelling of reactor internals.

(ii) The model in which the fundamental time period or frequency of reactor internal matches with the equivalent solid cylinder leads to higher time periods of vibration as compared to other methods of modelling of internal structure. It shows that the relatively flexible behaviour of complete reactor building reduces the response in OCW, ICW, raft and slab.

(iii) The stresses obtained in the central 2/3rd portion of the raft where observed to be minimum when the fundamental frequency of the equivalent axisymmetric replacement for the internal parts was equal to the fundamental frequency of the original system of the internal component.

(iv) It is recommended that the realistic seismic response of a reactor building is obtained by simulation of first natural frequency of its internal structure when modelling non-axisymmetric internals into equivalent axisymmetric body.

SUMMARY AND CONCLUSIONS

8.1 Introduction

The main aim of the thesis is to study the seismic behaviour of axisymmetric structures with particular emphasis on the reactor buildings. The design philosophy of these important structures differ from that of conventional buildings. In conventional structures, the emphasis is placed on the survivability of the building when subjected to an earthquake. Also, inelastic deformations and some damages are accepted. In fact, the conventional buildings are designed to be ductile and possess energy absorption capability. The primary purpose of the seismic analysis and design of such type of structures is to ensure that structure including equipment, for nuclear safety, remain functional during an earthquake. To do so, it is generally required that the structure should behave elastically during the horizontal seismic event. In this thesis, the seismic response study of few axisymmetric structures, such as intake tower and containment shell, has been carried out but emphasis is made on reactor building.

During the course of the study, the effects of soil-structure interaction, the utility of viscous boundaries in relation to fixed boundaries, and the validity of the assumptions of modelling of non-axisymmetric internal structure of reactor building to an equivalent axisymmetric body; on overall seismic response of the structure have been examined. An attempt has been made in this study to compare the seismic response of an axisymmetric structure obtained by timewise mode superposition and direct step-by-step time integration methods of analysis and the suitability of the method has been determined for seismic response computation of axisymmetric structures.

The significant conclusions based on the present study are summarised in the following sections :

8.2 Literature Review

A critical review of literature on seismic behaviour of axisymmetric structures, mathematical models, finite element formulation of axisymmetric structures, computation of maximum seismic response of structures using timewise mode superposition and direct step-by-step time integration methods, soil-structure interaction effects, modelling of infinite extent of soil and modelling of reactor internals are summarized. Based on the review following points emerge:

(i) The three dimensional dynamic analysis is required for axisymmetric structures subjected to earthquake excitation to capture the real behaviour. One-dimensional beam model cannot depict the real behaviour of structure subjected to strong ground motion.

(ii) For the massive embedded structures, such as reactor building, resting on loose to medium soil, soil-structure interaction effects should be considered in the seismic analysis of the structure. To take the soil-structure interaction into account, the soil should be modelled along with the structure.

(iii) There is not much literature available on the effects of modelling of non-axisymmetric internal structure of nuclear reactor building as equivalent axisymmetric body on the overall seismic response.

(iv) It is observed that not much work has been done to study the effect of viscous boundaries in place of fixed boundaries of soil-structure system on the seismic behaviour of axisymmetric structures.

8.3 Soil-Structure Interaction

The soil-structure interaction studies have been carried out for a containment shell alone and a complete reactor building with internals. For preliminary study, free vibration analysis of containment shell is carried out using beam method. As the soil is semi-infinite medium, an unbounded domain, so in order to capture the realistic behaviour of soil-structure system, three dimensional modelling of the system is required. The axisymmetric finite element method enables to take into account 3-D nature of the soil-structure system and is employed to carry out

a detailed parametric study of axisymmetric structures. The following parameters are considered to study soil-structure interaction effect on the seismic behaviour of the structure :

(i) Mesh size, i.e., horizontal and vertical extent of founding soil in finite element idealization ;

(ii) The effect of considering the mass of the founding soil ;

(iii) Variations in shear wave velocity of soil ;

(iv) Variations in damping of founding soil ;

(v) Depth of embedment ; and

(vi) The effect of earthquakes having different frequency characteristics.

The following conclusions on seismic response of the structure have been drawn as a result of this study :

(i) The horizontal extent of founding soil from the outer surface of the structure and vertical extent of soil below bottom of the structure, can be taken as three times and two times of the radius of the structure respectively, for minimizing the effect of reflection of waves from the fixed soil boundaries.

(ii) The mass of the founding soil can be neglected in the seismic analysis of soil-structure system.

(iii) The response of the above two structures, that is, containment shell and complete building for horizontal ground motion has been computed for (a) fixed base, and (b) flexible base having different shear wave velocities of soil. The near fixity condition for the analysis of containment shell alone is achieved for shear wave velocity of 1200m/s while this condition is achieved even at shear wave velocity of 900 m/s in complete building. Also, the soil-structure interaction results in the reduction of the stresses in the structure as compared to fixed base structure.

(iv) For obtaining minimum seismic response, the most suitable depth of embedment should be equal to about 1/6th of the height for containment shell alone, and about 1/5th the height for complete building.

(v) Three real earthquakes are considered, these are normalized to common peak ground acceleration and their effects on response of these two structures are studied. It is observed that (a) the structural response not only depends upon the peak ground acceleration of an earthquake but also depends upon its frequency content, and (b) the structure whose fundamental time period lies in the range of dominating time period of an earthquake shows greater deformations and stresses.

8.4 Seismic Response by Mode Superposition and Direct Integration Methods

A finite element seismic analysis of few axisymmetric structures with fixed base and with flexible base has been carried out using mode superposition and direct step-by-step time integration methods. A comparison has been made of maximum seismic response obtained by these two methods of analysis. The objective of the study is to determine the suitability of one method over the other and to study the response results due to different methods of considerations of damping in these methods. The following significant conclusions have been drawn from the study :

(i) The maximum seismic response, that is, stresses and displacements at various locations in the structure obtained by these two methods compare reasonably well except at some sections. Also the structural response is found more from direct integration method as compared to mode superposition method. It is due to incorporation of different damping effects in the two method of analysis. In mode superposition method, higher damping effects are incorporated due to damping value assigned to each mode while in direct integration method mass proportional damping was used and proportional constant was computed to consider the effect of first mode only. This type of damping implies decreasing damping effect in higher modes.

(ii)   The Newmark's β implicit scheme of direct step-by-step time integration method is most accurate in comparison to other schemes of integration, because of least numerical error. In this study, Newmark's constant average acceleration method is employed in both mode superposition and direct integration methods. However, relatively less computational effort is required in mode superposition method and damping can be prescribed modewise.

Therefore, it is found from the study that timewise mode superposition method is more suitable as compared to direct step-by-step time integration method for elastic earthquake analysis of the structures. However, the analysis of the structure by two method gives more confidence to the analyst.

8.5 Effects of Viscous Boundaries

In the finite element dynamic soil-structure interaction studies, the reflection of the incoming waves at the fixed soil boundaries strike at the base of the structure and change the dynamic response of the structure. However the waves are partly absorbed in the soil medium due to its damping characteristics. The problem of modelling of boundaries always poses questions on the effect of reflection of waves. The dampers at the boundaries are required to absorb the incoming waves and minimizes their reflection. A study has been performed to investigate the effectiveness of viscous boundaries in the form of horizontal and vertical dampers to absorb P and S waves in relation to fixed boundaries. An elastic earthquake time history analysis of an axisymmetric soil-structure system, that is, containment structure resting on soil has been done using step-by step time integration method. A parametric investigation has been carried out to evaluate the effects of viscous boundaries in different lateral and vertical directions in comparison to fixed boundaries.

The following conclusions on effect of viscous boundaries on seismic response has been drawn from this study :

(i)   The viscous boundaries are found to be effective in absorption of incoming waves and minimise wave reflections.

197

(ii) The almost same structural response in shell and raft of containment is obtained by providing viscous boundaries at a smaller lateral distance as compared to fixed boundaries at a greater lateral distance.

(iii) The soil response at different depths of soil strata and at various sections in horizontal soil layer is reduced significantly by using the viscous boundaries.

(iv) The vertical mesh size of the soil medium in soil-structure system with viscous boundaries does not affect much in the seismic response of the structure compared to mesh with fixed boundaries at a greater vertical distance.

It is found from the above study that the most of the incoming waves are absorbed and their reflection is minimum when viscous boundaries are placed at a horizontal distance equal to 1.5 times the raft radius and at a vertical distance equal to the radius of the raft.

8.6 Effect of Modelling of Non-Axisymmetric Internal Structure

The design philosophy of reactor building differs from that of conventional structure. The rational evaluation of forces and displacements in various portion of reactor building and foundation during strong ground motion is most important for safe performance and economic design of the reactor building. The accuracy of the results of the dynamic analysis is dependent upon the type of mathematical model employed. The axisymmetric finite element modelling of the reactor building is most suitable due to consideration of three dimensional behaviour of the building. The internal structure of a reactor building is non-axisymmetric while its other subsystems are axisymmetric. It poses problem when complete reactor building is modelled as axisymmetric structure. Therefore, internal structure has to be modelled as equivalent axisymmetric body. The study has been carried out here to evaluate the effects of modelling of non-axisymmetric internals as equivalent solid cylinder on overall seismic response of the reactor building.

Two hypothetical reactor buildings of different size and shape are selected and their internals are modelled as equivalent solid cylinder by different methods of

modelling. The finite element seismic analysis of the complete reactor building including equivalent internal structure has been performed. The following conclusions are derived from the study :

(i) The seismic response of a reactor building is sensitive to the method of modelling of its internal structure.

(ii) The stresses obtained in the central 2/3rd portion of the raft are minimum in case of simulation of fundamental frequency of internals.

(iii) The model in which first frequency of internals matches with the equivalent solid cylinder would represent more realistic seismic response of a building as compared to other methods of modelling of internals.

8.7 Conclusions

In this thesis several aspects of seismic response study of axisymmetric structures with particular emphasis on reactor building have been made. The important conclusions made from this study are following :

(i) The near fixity condition of containment structure alone is achieved for shear wave velocity of soil of 1200 m/s while this condition is achieved even at shear wave velocity of 900 m/s for complete reactor building.

(ii) For minimum seismic response, the most suitable depth of embedment should be equal to about 1/6th of the height of the containment shell alone and about 1/5th of the height of the reactor building.

(iii) The structure whose fundamental time period lies in the range of dominating time periods of an earthquake shows greater deformations and stresses.

(iv) The timewise mode superposition method is more suitable as compared to direct step-by-step time integration method for elastic earthquake analysis.

(v) Viscous boundaries are found to be effective in absorbing incoming waves and minimize wave reflections and it is recommended that viscous

boundaries could be placed at horizontal dimension of one and half times the radius of the raft and at vertical dimension of equal to the radius of the raft.

(vi) On the basis of various methods of modelling of reactor internals, it is found that the model in which fundamental frequency of reactor internals matches with the equivalent axisymmetric body is most suitable.

Agrawal, P.K. et.al.(1973), Comparative study of soil spring and finite element models for seismic soil structure interaction analysis, Proceedings of the First ASCE specialty conference on structural design of Nuclear power plant facilities, Chicago, Dec., Vol.II, pp.(63-82).

Anderson, J.C.(1972), Seismic response effects on embedded structures, Bulletin of the Seismological society of America, Vol.62, No.1, Feb., pp.(177-194).

Abu-Sitta, S.H. and A.G. Daveport(1970), Earthquake Design of cooling towers-Probabilistic view point, J. of ASCE, Str. Engg. Div.

Albasiny, E.L. and D.W. Martin(1967), Bending and membrane equilibrium in cooling towers, Proc. ASCE, Engg. Mech. Div., Vol.93, No.EM3, pp.(1-17).

Benda, B.J. and J.J. Johnson(1981), Uncertainty in mathematical models of a typical nuclear reactor power plant structure, SMiRT-6, Vol.k(b), Paper No. 16/8.

Bycroft, G.N.(1977), Soil-structure interaction at higher frequency factors, Int. J. of Earthquake Engg. and Str. Dyn., Vol.5, pp.(235-248).

Bathe, K.J. and E.L. Wilson(1976), Numerical Methods in Finite Element Analysis, Prentice Hall.

Berger, E. et.al.(1975), ALUSH- A computer program for seismic response analysis of axisymmetric soil-structure interaction systems, EERC Report NO.75-31, Nov., University of California, Berkeley, USA.

Berger, E. et.al.(1975), Comparison of plane strain and axisymmetric soil-structure interaction analysis, Proceedings of the second ASCE specialty conference on structural design of Nuclear plant facilities, New Orleans, Dec., Vol. I-A, pp.(809-825).

Berdugo, Y.O. and M. Novak (1972), Coupled Horizontal and Rocking vibrations of embedded footings, Canadian Geotech. Journal, Vol.9, No.4, pp.(477-497).

Chandrasekaran, A. R. and J.D. Das(1992), Analysis of strong motion accelerograms of Uttarkashi Earthquake of Oct. 20, 1991, Bulletin of Indian Society of Earthquake Technology, Paper No. 315, Vol. 29, No. 1, pp.(35-55).

Cook, R.D. et.al.(1989), Concepts and Applications of Finite Element Analysis, John Wiley & sons, Inc.

Chandrasekaran, A.R. and S.K. Thakkar(1985), Seismic analysis of reactor building on rocky site, Proc. of Int. Conf. on Finite Element on Computational Mechanics, Bombay (India), 2-6 Dec.

Corsanego, A. et.al.(1983), On the Simulation of Infinite regions in Seismic soil-structure interaction models, Proc. 7th Int. Conf. on SMiRT, Chicago, USA.

Clough, R.W. and J. Penzien(1982), Dynamics of Structures, McGraw-Hill Book Co., Int. Ed.

Cheron, P. et.al.(1981), A substructuring method based on modal condensation for linear seismic analysis -Application to seismic parametric analysis for design of a LMFBR standard plant, SMiRT-6, Vol.k, paper No. 7/3.

Chen, W.W.W. et.al.(1979), Comparison of Soil-structure interaction by different ground models, SMiRT-5, Berlin, West Germany, Aug., Vol.k(a), paper No. 5/5.

Chandrasekaran, A.R. and D.K. Paul(1978), Merits of sub system approach in a nuclear power plant analysis, Proc. of 5th Japan Earthquake Engineering Symposium.

Costantino, C.J. and C.A. Miller(1976), Soil-structure interaction parameters from finite element analysis, Int. J. of Nuclear Engg. and Design, Vol. 38, pp.(289-302).

Chu, S.L. et.al.(1973), Finite Element treatment of SSI problems for Nuclear power plants under seismic excitation, Second SMiRT, Berlin, Vol.2, paper no. k2/4.

Carter, R.L. et.al.(1969), Free vibrations of Hyperboloidal shells of revolution, J. of ASCE, Engg. Mech. Div., Oct.

Clough, R.W. and Y.R. Rashid(1965), Finite Element Analysis of Axisymmetric solids, J. of ASCE, Engg. Mech. Div., Vol.91, No. EM1 pp.(71-86).

Deek, A.J. and M.F. Rondolph(1994), Axisymmetric time domain transmitting boundaries, J. of Engg. Mech., ASCE , Vol.120, No.1, pp.(25-42).

Daming, Z. and W. Zhangzhu(1992), Experimental and analytical studies of a smokestack, 10th WCEE, Madrid, Spain. pp.(5037-5041).

Descleve, P. et.al.(1985), Comparison between a beam and shell model for seismic analysis of reactor vessel, SMiRT-8, Vol.k, No.9/11, pp.(455-460).

Dobry, R. and G. Gazetas(1985), Dynamic Stiffness and Damping of Foundations using simple methods, Proc. Symp. on Vibration problems in Geotech. Engg., ASCE, pp.(75-107).

Ghosh, R. et.al.(1994), Effect of soil-structure interaction on structural response, 10th Symp. on earthquake engg., Nov., Roorkee (India).

Ghoparah, A. and T.A. Baumber(1992), Seismic behaviour of tall industrial masonry chimneys, 10th WCEE, Madrid, Spain, pp.(5043-5048).

Goyal, A. and A.K. Chopra(1989), Earthquake analysis and response of Intake-Outlet towers, EERC Report No. 89-04.

Gonez, A.(1984), Seismic SSI by the superposition method, Journal of Nuclear Engg.& design, Vol.78, No.1, pp.(37-52).

Gassert, W.(1983), Floor-response spectra calculation with a 3-D Building-Model comparison with an Axisymmetric Analysis, SMiRT-7, Vol.k, paper No. 5/2, pp.(321-328).

Ganteinbein, F. and J. Aguilar(1983), Seismic Analysis of PWR 900 Reactor: Study of Reactor building with SSI and evaluation of floor spectra, SMiRT-7, U.S.A.

Gupta, A.K. and W.C. Schnabrich(1976), Seismic analysis and Design of Hyperbolic cooling towers, International Journal of Nuclear Engg and Design,

Vol.36, No.2, pp.(251-260).

Gallagher, R.H.(1975), Finite Element Analysis-Fundamentals, Prentice Hall Inc., Englewood, New Jersey.

Gould, P.L. and S.L. Lee(1967), Hyperbolic cooling towers under seismic load, Int. J. of ASCE, Str. Engg. Div., June.

Ghosh, S. and E.L. Wilson(1969), Dynamic stress analysis of axisymmetric structures under arbitrary loading, EERC Report No.69-10, University of California, Berkeley, U.S.A..

Hirano, K. et.al.(1993), Forced vibration tests on the reactor building of the prototype FBR Monju, SMiRT-12, Vol. k, paper 12/1, pp.(319-323).

Hadjian, A.H. et.al.(1986), Modelling for finite element soil-structure interaction analysis, ASCE proceedings of 3rd Conf. by Engg. Mech. Div.

Hadjian, A.H. et.al.(1977), Variability in Engg. Aspects of structural modelling, 6th WCEE, New Delhi, India.

Hadjian, A.H.(1976), Soil-structure interaction - An Engineering Evaluation, Int. J. of Nuclear Engg. and Design, Vol. 38, pp.(267-272).

Hal, J.R. and J.F. Kissenpfenning(1976), Special topics on soil-structure interaction, Int. J. of Nuclear Engg. and Design, Vol. 38, pp.(273-287).

Hwang, R.N. et.al.(1975), A simplified 3-dimensional soil-structure interaction study, Proceedings of the second ASCE specialty conference on structural design of Nuclear plant facilities, New Orleans, Dec, Vol.I-A, pp.(786-808).

Hadjian, A.H. et.al.(1974), SSI : Continuum or finite element, Int. J. of Nuclear Engg. and Design, Vol.31, pp.(151-167).

Hashish, M.G. and S.H. Abu-Sitta(1971), Free Vibrations of Hyperbolic Cooling Towers, Int. J. of ASCE, Engg. Mech. Div.

Isenberg, J. and S.A. Adham(1972), Interaction of soil and power plants in Earthquakes, Journal of the Power Div., ASCE, Oct., Vol.98, No.02, pp.(273-291).

Julio, E. et.al.(1977), Seismic SSI effects at Humboldt Bay power plant, Int. J. of ASCE, Geotech. Engg. Div.

Kakodkar, A.(1995), Some issues in Aseismic Design of Nuclear structures and components, Bulletin of Indian society of earthquake technology, paper No. 352, Vol. 32, No. 4, Dec., pp.(97-126).

Krishna, J., A.R. Chandrasekaran and B. Chandra(1994), Elements of Earthquake Engineering, 2nd Ed., South Asian Publishers, New Delhi, India.

Kato, M. et.al.(1989), Forced Vibration tests on the Reactor Building of Tsuruge unit No. 2, Nuclear power station, Int. J. of Nuclear Engg. and Design, Vol.111, pp.(327-340).

Kobatake, M. et.al.(1985), Influence of flexible foundation slab on seismic response of Nuclear reactor Building, SMiRT-8, Vol. k, paper No. 7/5, pp.(299-304).

Kausel, E. and J.M. Roesset(1975), Dynamic Stiffness of circular foundations, Int. J. of ASCE, Engg. Mech. Div., Dec.

Kausel, E. and J.M. Roesset(1975), Dynamic Analysis of circular footings on layered media, Int. J. of ASCE, Engg. Mech. Div.,Oct.

Kausel, E. and J.M. Roesset(1974), Soil-structure interaction problems for nuclear containment structures, presented at the specially conference-ASCE, Power Div., Denver, Colorado, U.S.A., Aug. 12-14.

Kuhlemeyer, R.L. and J. Lysmer(1973), Finite element method accuracy for wave propagation problems, J. of soil mech.& fdn. div., ASCE, Vol.99, No.SM5, May, pp.(421-427).

Kati, S.L.(1973), Conceptual Design of the Modified 200 MWe Reactor for Narora, Proc. Symp. on Nuclear Science and Engg., Bhabha Atomic Research Centre, Trombay, India.

Krishna, J. et.al.(1969), Analysis of Koyna Accelerogram of Dec. 11, 1967, Bulletin of the Seismological Society of America, Vol. 59, No. 4, pp.(1719-1731)

Luco, J.E.(1982), Linear SSI : A Review, Int. J. of ASME, Applied Mech. Div., Vol. 53, pp.(41-57).

Lysmer, J. et.al.(1975), FLUSH - A computer program for approximate 3-dimensional SSI Problems, EERC Report No.75-30, University of California, Berkeley, U.S.A..

Lysmer, J. et.al.(1975), Efficient Finite Element Analysis of Seismic Structure-soil-structure interaction, Second ASCE specialty conference on structural division of Nuclear plant facilities, New Orleans.

Lysmer, J. et.al.(1975), Efficient Finite Element Analysis of Seismic Structure-soil-structure interaction, EERC Report No. 75-34, University of California, Berkeley, U.S.A..

Liaw, C.Y. and A.K. Chopra(1975), Dynamic properties of San-Bernardino Intake Tower, EERC Report No. 75-7, University of California, Berkeley, U.S.A..

Luco, J.E. and A.H. Hadjian(1974), Two-dimensional approximations to the Three-dimensional SSI problems, Journal of Nuclear Engg. and Design, Amsterdam, Dec.31, Vol.31, No.2, pp.(195-203).

Luco, J.E.(1974), Impedance functions for a rigid foundation on a layered medium, Int. J. of Nuclear Engg. and Design, Vol.31, pp.(204-217).

Lysmer, T. et.al.(1974), LUSH- A computer program for complex response analysis of soil-structure system, EERC Report No.74-4, April, University of California, Berkeley, U.S.A.

Liaw, C.Y. and A.K. Chopra(1973), Earthquake response of Axisymmetric Tower structures surrounded by water, EERC Report No.73-25, University of California, Berkeley, U.S.A.

Luco, J.E. and R.A. Westman(1971), Dynamic response of circular footings, Int. J. of Engg. Mech. Div., ASCE, Oct., Vol. 97, No.EM-5, pp.(1381-1403).

Lysmer, J. and R.L. Kuhlemeyer(1969), Finite Dynamic model for infinite media, J. of Engg. Mech. Div., ASCE, Aug., Vol.95, No.EM-4, pp.(859-877).

Lysmer, J. and F.E. Richart(1966), Dynamic Response of footings to vertical loadings, J. of soil mech. & fdn. div., ASCE, Jan., Vol.92., No. SM-1, pp.(65-91).

Morishita, H. et.al.(1993), Forced vibration test of the Hualien large scale SSI model, SMiRT-12, Vol.k, paper 02/1, pp.(37-42).

Morishita, H. et.al.(1992), Vertical response characteristics of a nuclear reactor building during earthquakes, Proc. of 10th WCEE, Madrid, Spain, Vol. 9, pp.(4927-4932)

Ma, S.M. et.al.(1981), Limitations of Modal Analysis for SSI problems of high radiation damping, SMiRT-6, Vol.k, paper No.4/1.

Medina, F.(1980), Modelling of Soil-structure interaction by finite and infinite elements, EERC Report NO. 80-43, University of California, Berkeley, U.S.A.

Nayak, G.C. and V.K. Jain(1974), An Economic Harmonic Analysis of Axisymmetric Solids subjected to Non-Axisymmetric loads, Proc. Conf. on Finite Elements in Engg., University of New South Wales.

Novak, M.(1974), Effect of soil on structural response to wind and earthquake, Int. J. of Earthquake Engg. and Str. Dyn., Vol. 3, pp.(79-96).

Novak, M. and K. Sache(1973), Torsional and Coupled vibrations of embedded footings, Int. J. of Earthquake Engg. & Str. Dyn., Vol.2, No.1, pp.(11-33).

Novak, M. and Y.O. Beredugo(1972), Vertical Vibrations of Embedded footings, Int. J. of Soil Mech. & fdn. engg. div., ASCE, Dec., Vol.98, No.SM-12, pp.(1291-1309).

Parkash, S., S.K. Thakkar and N.C. Singhal(1994), Soil-structure interaction effects on seismic response of containment shell, 10th Symposium on Earthquake Engg., University of Roorkee, Roorkee (India).

Reddy, G.R. et.al.(1987), Dynamic analysis of containment building of 500 MWe PHWR using Axisymmetric model, SMiRT-9, Vol.k, Laussane, Switzerland.

Roesset, J.M. and R.V. Whitman(1973), Modal Analysis of Structures with Foundation Interaction, J. of Str. Engg. Div., ASCE, March, Vol.99, No.ST-3.

Richart, F.E. et.al.(1970), Vibrations of soils and foundations, Prentice Hall, Inc., New Jersey.

Saha, s. et.al.(1993), Seismic response analysis of reactor containment structures-Axisymmetric model with modified ground motion, SMiRT-12, Vol.k, paper 04/5, pp.(127-131).

Setogawa, S. et.al.(1993), Forced vibration test on the reactor building of a PWR type nuclear power station, SMiRT-12, Vol.k, paper 12/2, pp.(325-330).

Stojko, S.N.(1989), Soil-structure interaction analysis in the time domain, SMiRT-10, Vol.k1, pp.(109-114).

Singhal, N.C.(1984), Dynamic Behaviour of Axisymmetric structures, Ph.D. Thesis, Dept. of Earthquake Engg., University of Roorkee, Roorkee (India).

Singhal, N.C. and A.R. Chandrasekaran(1983), Analysis of a Nuclear reactor Containment Structure, SMiRT-7, Chicago, USA, Aug. 22-26.

Satoh, M. and K. Sasagawa(1983), A study of the dynamic response characteristics of the embedded reactor building for pool type LMFBR, SMiRT-7, Vol.k, paper No.5/11, pp.(381-388).

Satoh, M. and K. Sasagawa(1982), A study on the dynamic response characteristics of embedded reactor building, SMiRT-7, Vol.k, paper No.5/10.

Seed, H.B. and J. Lysmer(1978), SSI Analysis by finite elements-State-of-the - art, Int. J. of Nuclear Engg. & Design, Vol.46, pp.(349-365).

Seed, H.B. and J. Lysmer(1977), SSI analysis by FEM-State-of-the-art, Proceedings of 4th SMiRT, San Fransisco, Vol.k, pp.(1-11).

Seed, H.B. et.al.(1975), Soil-structure Interaction Analysis for evaluating seismic response, Journal of the Geotech. Engg. Div., ASCE, May, Vol.101, No.GT5, pp.(439-457).

Seed, H.B. et.al.(1974), Soil-structure Interaction Analysis for evaluating seismic response, EERC Report No.74-6, University of California, Berkeley, U.S.A.

Szilard, R.(1974), Theory and analysis of plates, Prentice Hall Inc., Englewood

cliffs, New Jersey.

Smith, W.D.(1974), A non-reflecting plane boundary for wave propagation, J. of computer Physics, Vol.15, pp.(492-503).

Singh. S. et.al.(1973), Three Dimensional soil-structure seismic analysis using finite elements, First ASCE specialty conference on structural design of Nuclear plant facilities, Chicago, Dec., Vol. II, pp.(43-62).

Seed, H.B. and I.M. Idriss(1973), Soil-structure interaction analysis of massive embedded structures during earthquakes, Fifth WCEE, Rome, Paper No. 233.

Schnabel, P.B. et.al.(1972), SHAKE-A computer program for Earthquake response analysis of Horizontally layered sites, EERC Report No.72-12, University of California, Berkeley, USA.

Seed, H.B. and I.M. Idriss(1970), Soil Moduli and damping factors for dynamic response analysis, EERC Report NO. 70-10, Dec., University of California, Berkeley, USA.

Seed, H.B. and I.M. Idriss(1969), Influence of soil conditions on ground motions during earthquakes, Journal of the Soil Mech. & Foundations Div., ASCE, Vol.95, No.M1, January, pp.(99-137).

Thakkar, S.K. and R.N. Dubey(1989), Dynamic analysis of reactor containment building using axisymmetric finite element model, SMiRT-10, Vol.k1, pp.(443-448).

Thakkar, S.K.(1989), Analysis of nuclear reactor building subjected to earthquake forces, Transactions of Conference of Indian Science Congress, Madurai (India).

Thakkar, S.K. et.al.(1987), Seismic response of a reactor building on rocky foundation, SMiRT-9, Lausanne, Switzerland, Vol.k.

Thakkar, S.K. and A.R. Chandrasekaran (1987), Finite element analysis of reactor containment structure-case study of NAPP and KAPP, Workshop on structures for nuclear power reactor technology, Feb. 25-28.

Thakkar, S.K. and A.K. Dinkar(1983), Seismic response of a reactor building on alluvial soil by direct implicit integration, SMiRT-7, Chicago (Illinois), Vol.k, paper 10/7.

Tzung, F.K. et.al.(1981), A New Transmitting boundary representation for Time domain analysis of SSI problems, SMiRT-6, Vol.k, paper No. 4/4.

Takemori. T. et.al.(1979), Comparison of SSI by different ground models, SMiRT-5, Vol.k(a), paper No. 5/5.

Tsai, N.C. (1974), Modal Damping for Soil-structure interaction, J. of Engg. Mech Div., ASCE, Vol. 100, No. Em-2.

Udaka et.al.(1981), SSI Analysis for varying seismic environment and boundary conditions, SMiRT-6, Vol.k, paper No. 3/1.

Van, M. et.al.(1984), The use of boundary elements to represents the far field in SSI, J. of Nuclear Engg. and design, Vol.79, No.2, pp.(161-198).

Valera et.al.(1977), Seismic soil-structure interaction effects at Humbolt Bay power plant, J. of Geotech. Engg. Div., ASCE, Vol.113, No.GT-10, pp.(1143-1161).

Vaish, A.K. and A.K. Chopra(1974), Earthquake Finite element analysis of structure-foundation system, J. of Engg. Mech. Div., Vol.100, pp. (1101-1116).

Vaish, A.K. and A.K. Chopra(1973), Earthquake Analysis of Structure Foundation Systems, EERC Report NO. 73-09, May, University of California, Berkeley, USA.

Veletsos, A.S. and V.T. Wei(1971), Lateral and Rocking vibrations of footings, Int. J. of Soil Mech & fdn engg div., ASCE, Vol.97, No.SM-9, pp.(1227-1246).

Wolf, J.P.(1987), Soil-structure interaction analysis in time domain, Prentice-Hall, Inc.

Wolf, J.P.(1985), Dynamic soil-structure interaction, Prentice-Hall, Inc.

Warudkar, A.S. et.al.(1984), Design of 140m Tall R.C.C. ventilation stack for Narora atomic power plant project, Seminar on Tall structures and use of

prestressed concrete in hydraulic structures, Srinagar (India).

Wass, G. and W. Weber(1979), SSI analysis by different methods, SMiRT-5, Vol.k, No.6/1.

White, W. et.al.(1974), Unified boundary for Finite Dynamic Models, J. of Engg. Mech. Div., ASCE, Vol.103, No.EM-5, pp.(949-964).

Wass, G.(1972), Linear 2-dimensional analysis of soil dynamics problems in semi-infinite layered media, Ph.D. Thesis, University of California, Berkeley, U.S.A.

Whitman, R.V. (1972), Soil-structure interaction in seismic design of Nuclear power plants Analysis, Edited by Robert J. Hansen, MIT press, England.

Wilson, E.(1965), Structural Analysis of Axisymmetric Shells, Journal of the American Institute of Aeronautics and Astronautics, Vol.3, No.12, Dec., pp.(2269-2274).

Zhang, D. and Wu Zhangzhu(1992), Experimental and Analytical studies of a smokestack, 10th WCEE.

Zienkiewicz, O.C.(1977), The finite element method, 3rd Ed., McGraw Hill Co..

Zienkiewicz O.C.(1972), Finite Element Methods in the analysis of Reactor Vessels, Journal of Nuclear Engg. & Design, Vol.20, pp.(507-541).